FLUORESCOPIC EVALUATION OF PROTEIN-LIPID RELATIONS IN CELLULAR SIGNALLING

Everard H.W. Pap

40951

Promotoren: Dr. C. Veeger
                hoogleraar in de Biochemie
                Landbouwuniversiteit Wageningen

                Dr. K.W.A. Wirtz
                hoogleraar in de Biochemie
                Rijksuniversiteit Utrecht

Copromotor: Dr. A.J.W.G. Visser
                universitair hoofddocent
                Vakgroep Biochemie
                Landbouwuniversiteit Wageningen

Everard H.W. Pap

FLUORESCOPIC EVALUATION OF PROTEIN-LIPID RELATIONS IN CELLULAR SIGNALLING

Proefschrift
ter verkrijging van de graad van
doctor in de landbouw- en milieuwetenschappen,
op gezag van de rector magnificus,
Dr. C.M. Karssen,
in het openbaar te verdedigen
op 14 oktober 1994
des namiddags te half twee in de Aula
van de Landbouwuniversiteit te Wageningen

NN08201. , 1840

STELLINGEN

1   Een aantal onderzoekers realiseert zich nog steeds niet dat de sigmoidiale afhankelijkheid van binding van eiwitten en componenten in membraansystemen niet een gevolg is van coöperativiteit maar van een reductie van dimensie.

Hannun, Y.A. & Bell, R.M. (1990) *J. Biol. Chem.* 265, 2962-2972.
Bazzi, M.D. & Nelsestuen, G.L. (1991) *Biochemistry, 30,* 7961-7969.
Orr J.W. & Newton A.C. (1991) *Biophys J.* 59, 401a
Orr J.W. & Newton A.C. (1992) *Biochemistry, 31,* 4661-4673.

2   De door Lassing en Lindberg gepostuleerde regulerende rol van fosfatidylinositol 4,5-bifosfaat in de functie van profiline en gelsoline kan, op grond van hun eigen experimenten waarin zij aantonen dat profiline alleen met vesikels coëlueert wanneer deze tenminste 35 mol % PIP$_2$ bevatten, als hoogst onwaarschijnlijk worden aangemerkt.

Lassing, I. & Lindberg, U. (1988) *J. Cell. Biochem.* 37, 255-267.

3   Het sterk negatief geladen fosfatidylinositol 4,5-bifosfaat is in staat door interactie met basische aminozuren alle cellulaire processen, die afhankelijk zijn van electrostatische eiwit-eiwit interacties, te beïnvloeden.

4   De experimenten van F.L. Huang en K. Huang waarbij binding van ongelabelde fosfoinositiden aan proteïne kinase C de intrinsieke tryptofaan fluorescentie van dit eiwit tot 40 % reduceert is hoogst opmerkelijk en in tegenspraak met de waarnemingen beschreven in dit proefschrift.

Huang F.L. & Huang K (1991) *J. Biol. Chem.* 266, 14 8727-8733
Dit proefschrift, hoofdstukken 5 en 6.

5   De uitdrukking "bioanorganische chemie" is een *contradictio in terminus* vergelijkbaar met een uitdrukking als "asexuele geslachtelijke voorplanting" en kan meestal vervangen worden door de term biometallochemie.

6   De stelling van Winter en Milstein dat men voor de produktie van hoge affiniteits-antilichamen het beste gebruik kan maken van hypergemuteerde genen van een geïmmuniseerde muis, wordt door Griffiths ontkracht.

Winter C. & Milstein G. (1991) Nature 349, 293-299.
Griffiths G.A. et al. (1994) EMBO J 13, 3245-3260.

7   De verhoogde efficiëntie die gestroomlijnde computerfaciliteiten teweegbrengen in het arbeidsproces wordt deels teniet gedaan doordat deze verleiden tot het verminderen van andere essentiële werkzaamheden.

8   De waarneming dat congresgangers tijdens hun bijeenkomsten wel eens aan sex denken is alleen opmerkelijk wanneer de rest van de bevolking dat niet doet.

De Volkskrant, maandag 1 augustus 1994.

9   De kleurloze bezuinigingsoverwegingen van het kabinet om de studieduur van het hoger onderwijs te verminderen contrasteert sterk met de paarse signatuur.

10   Ondanks de sterke aandrang van de bedrijfsschap Horeca om café's rookvrij te maken, is het vinden van een rookvrij café net zo moeilijk als het vinden van een café zonder bier.

Stellingen behorende bij het proefschrift
 "Fluorescopic evaluation of protein-lipid relations in cellular signalling"

E.H.W. Pap.
Wageningen, 14 oktober 1994

STELLINGEN

1   Een aantal onderzoekers realiseert zich nog steeds niet dat de sigmoidiale afhankelijkheid van binding van eiwitten en componenten in membraansystemen niet een gevolg is van coöperativiteit maar van een reductie van dimensie.

Hannun, Y.A. & Bell, R.M. (1990) *J. Biol. Chem.* 265, 2962-2972.
Bazzi, M.D. & Nelsestuen, G.L. (1991) *Biochemistry, 30,* 7961-7969.
Orr J.W. & Newton A.C. (1991) *Biophys J.* 59, 401a
Orr J.W. & Newton A.C. (1992) *Biochemistry, 31,* 4661-4673.

2   De door Lassing en Lindberg gepostuleerde regulerende rol van fosfatidylinositol 4,5-bifosfaat in de functie van profiline en gelsoline kan, op grond van hun eigen experimenten waarin zij aantonen dat profiline alleen met vesikels coëlueert wanneer deze tenminste 35 mol % PIP$_2$ bevatten, als hoogst onwaarschijnlijk worden aangemerkt.

Lassing, I. & Lindberg, U. (1988) *J. Cell. Biochem.* 37, 255-267.

3   Het sterk negatief geladen fosfatidylinositol 4,5-bifosfaat is in staat door interactie met basische aminozuren alle cellulaire processen, die afhankelijk zijn van electrostatische eiwit-eiwit interacties, te beïnvloeden.

4   De experimenten van F.L. Huang en K. Huang waarbij binding van ongelabelde fosfoinositiden aan proteïne kinase C de intrinsieke tryptofaan fluorescentie van dit eiwit tot 40 % reduceert is hoogst opmerkelijk en in tegenspraak met de waarnemingen beschreven in dit proefschrift.

Huang F.L. & Huang K (1991) *J. Biol. Chem.* 266, 14 8727-8733
Dit proefschrift, hoofdstukken 5 en 6.

5   De uitdrukking "bioanorganische chemie" is een *contradictio in terminus* vergelijkbaar met een uitdrukking als "asexuele geslachtelijke voorplanting" en kan meestal vervangen worden door de term biometallochemie.

6   De stelling van Winter en Milstein dat men voor de produktie van hoge affiniteits-antilichamen het beste gebruik kan maken van hypergemuteerde genen van een geïmmuniseerde muis, wordt door Griffiths ontkracht.

Winter C. & Milstein G. (1991) Nature 349, 293-299.
Griffiths G.A. et al. (1994) EMBO J 13, 3245-3260.

7   De verhoogde efficiëntie die gestroomlijnde computerfaciliteiten teweegbrengen in het arbeidsproces wordt deels teniet gedaan doordat deze verleiden tot het verminderen van andere essentiële werkzaamheden.

8   De waarneming dat congresgangers tijdens hun bijeenkomsten wel eens aan sex denken is alleen opmerkelijk wanneer de rest van de bevolking dat niet doet.

De Volkskrant, maandag 1 augustus 1994.

9   De kleurloze bezuinigingsoverwegingen van het kabinet om de studieduur van het hoger onderwijs te verminderen contrasteert sterk met de paarse signatuur.

10   Ondanks de sterke aandrang van de bedrijfsschap Horeca om café's rookvrij te maken, is het vinden van een rookvrij café net zo moeilijk als het vinden van een café zonder bier.

Stellingen behorende bij het proefschrift
  "Fluorescopic evaluation of protein-lipid relations in cellular signalling"

E.H.W. Pap.
Wageningen, 14 oktober 1994

Woord vooraf

Hoewel alleen mijn naam op de kaft van dit proefschrift pronkt, hebben vele collega's bijgedragen aan de totstandkoming van dit proefschrift. Hen die deze kar mede hebben getrokken wil ik hier graag bedanken. Het project is in 1988 geformuleerd en geïnitieerd door Ton Visser en Prof. K.W.A. Wirtz. Hun kritisch meedenken en morele steun waren voor mij tijdens het onderzoek van grote betekenis en hun correcties hebben mijn teksten bijzonder verhelderd. Ook Prof. C. Veeger heeft hiertoe bijgedragen. In het bijzonder wil ik Ton hiervoor bedanken. Ik heb veel geleerd van je spectroscopische kennis en je degelijke aanpak en ben er trots op in "jouw" werkgroep te hebben gewerkt. Ik denk met veel plezier terug aan de uren die ik samen met Arie in de kelder doorgebracht. Ik vind je een buitengewoon vakman, Arie, en waardeer je geduld met onze 'groene' monsters. Jillert wil ik bedanken voor de synthese van enkele fluorescente lipiden. Lab avon(d)turen met Jan Willem zijn bijzonder onvoorspelbaar en vruchtbaar en behoren gelukkig nog niet tot het verleden. Je plotselinge flirt met TNO heeft me de stuipen op het lijf gejaagd. Ik heb erg veel profijt gehad van de aanwezigheid van Philippe. Je passie voor onderzoek heeft mij bijzonder geïnspireerd. Je kritiek en bijdragen waren altijd zeer verfrissend. Ik hoop dat we ons samen nog eens in een ontzettend onverantwoord wetenschappelijk avontuur storten. Vele studenten hebben een belangrijke bijdrage gehad in het onderzoek: Jan Jaap, Joke, Marjan, Chantal, Pim, Petra en Martijn. Ik wil jullie bedanken voor de plezierige samenwerking en jullie grote inzet. I am very grateful to Pentti Somerharju for his hospitality and help in the synthesis of some very exotic fluorescent lipids in his friendly laboratory. I enjoyed my stay in Helsinki very much and feel unfortunate about the inability to phosphorylate the labelled PI's to workable amounts of PIP and PIP_2. The short collaboration with Andreas Hanicak was very enjoyable and fruitful. Andreas, thanks for your friendship. Een minder concrete bijdrage, maar desalniettemin essentieel was het meeleven van vele collega's. Ik heb altijd genoten van de nadrukkelijke aanwezigheid van mijn kamergenoten. Rik, je plotselinge ontdekking van de correlatie tussen het verdwijnen van jouw pennen en mijn aanwezigheid staat me nog helder bij. En wie had ooit kunnen denken dat wij nog eens één kamer zouden delen Dorus ? Je aansluiting bij Ton's family is erg verfrissend. De sprankelende momenten met collega's op lab-borrels, -feesten en in Loburgh, waarin we onze passie voor ons werk en meer nog voor wat daar helemaal niet mee te maken had vertolkten, zullen als dierbare herinneringen nog jarenlang bij mij blijven. Verder denk ik met veel plezier terug aan W632 in Utrecht, waar ik, vooral in de eerste jaren van het onderzoek, veel hulp en gastvrijheid heb ondervonden.

Abbreviations

|	
ADC	analogue to digital converter
Dansyl	dimethylamino-1-naphthalenesulfonyl
DCM	4-dicyanomethylene-2-methyl-6-(p-dimethyl-aminostyryl)-4H-pyran
DG	diacylglycerol
Dipyr	sn-$1,2$-(pyrenyldecanoyl)
$Dipyr_{10}$	di-('-pyrenedecanoyl)
$Dipyr_4$	di-('-pyrenebutyryl)
DMPC	dimyristoylphosphatidylcholine
DMSO	dimethylsulfoxyde
DOPC	dioleoylphosphatidylcholine
DPH	1,6-diphenyl-1,3,5-hexatriene
DPHcPC	2-[3-(diphenylhexatrienyl)-carboxyl]-3-palmitoyl-L-α–P C
DPHePC	2-[3-(diphenylhexatrienyl)-ethyl]-3-palmitoyl-L-α–P C
DPHpPC	2-[3-(diphenylhexatrienyl)-propanoyl]-3-palmitoyl-L-α–P C
DPPC	dipalmitoylphosphatidylcholine
DPPS	dipalmitoylphosphatidylserine
E/M	ratio of excimer to monomer fluorescence
EDTA	ethylenediamine-tetra-acetic acid
EGTA	ethylene glycol bis(β-aminoethyl ether)-N,N,N',N'-tetraacetic acid
FWHM	full width at half maximum
HEPES	N-(2-hydroxyethyl)piperaxine-N'-2-ethanesulfonic acid
MC	Milling Crowd
MEM	maximum entropy method
PC	phosphatidylcholine
PI	phosphatidylinositol
PIP	phosphatidylinositol-4-phosphate
PIP_2	phosphatidylinositol-4,5-biphosphate
PKC	protein kinase C
PLC	phospholipase C
PMA	phorbol myristate acetate
POPOP	1,4-bis[2-(5-phenyloxazolyl)]benzene
PPO	2,5-diphenyloxazole
PS	phosphatidylserine
PTF	p-terphenyl
RET	resonance energy transfer
r_{g3}	general rotational diffusion model
SSQ	sum of squares of residuals.
SUV	small unilamellar vesicles
TAC	time-to-amplitude converter
Thesit	polyoxyethylene-9-lauryl ether
TLC	thin-layer chromatography
TMA-DPH	1-[4-(trimethylamino)phenyl]-6-phenyl-1,3,5-hexatriene
Tris	tris(hydroxymethyl)-aminomethane

Contents

Chapter 1

Fluorescopic methods for detection of protein-lipid interaction

1.1. General Introduction

The interrelation between membrane proteins and lipids plays an essential role in the functioning of the cell membrane. Cellular signals are mediated by lipid messengers that modulate protein functions. In addition, many membrane-associated proteins only retain their functional, active conformation when they interact with lipids. Proteins bound to or within the lipid bilayer are also important as structural elements in membranes (Bertoli et al., 1987). A typical membrane consists of approximately 100 lipid molecules per integral protein molecule. These integral membrane proteins are responsible for intracellular transmembrane communication or for interactions within the membrane (Newton, 1993). Lipids interact in a dynamical fashion with amino acid residues at the protein surface (East et al., 1985; Paddy et al., 1981). Considering the protein to lipid molar ratio in the membrane and the large differences in protein and lipid molecular surfaces, a significant fraction of the total lipid interacts directly with protein residues, or is influenced indirectly via long range effects by proteins (Peters & Grant, 1984). In addition, to integral membrane proteins, many proteins associate peripherally with the membrane surface or penetrate partially into the bilayer, thereby interacting mainly with the lipid headgroups. In the latter case lipid molecules are hindered in their lateral mobility and the membrane structure is perturbed. Although protein-lipid interactions have been studied extensively with many complementary physical techniques, it is still difficult to understand how these interactions influence protein activity and the structural and dynamical properties of the membrane components. Among the techniques used, fluorescence spectroscopy is particularly advantageous, because it operates over distances comparable to molecular dimensions and on the time scale of Brownian diffusion of proteins and lipids.

The present chapter introduces various theoretical and experimental aspects of the application of fluorescence spectroscopy in the study of protein-lipid interaction. The report starts with an overview of the functional relevance and fundamental mechanisms of protein-lipid interaction. Then some fluorescopic tools are considered, illustrated with two types of investigations.
First, experiments are described that concern protein properties affected by the association with lipids (Figure 1A). In this case the physical observables are protein conformation and aggregation as well as its topology with respect to the plane of the membrane.
Second, experiments are summarised which characterise changes in the physical properties of lipids when they interact with proteins (Figure 1B). In this section attention is focused on motional properties of lipids, like reorientational and lateral diffusion and on organisational aspects. Finally an overview is given of interaction models which can be used for quantification of

interaction parameters like binding constants and binding stoichiometry (Figure 1c).
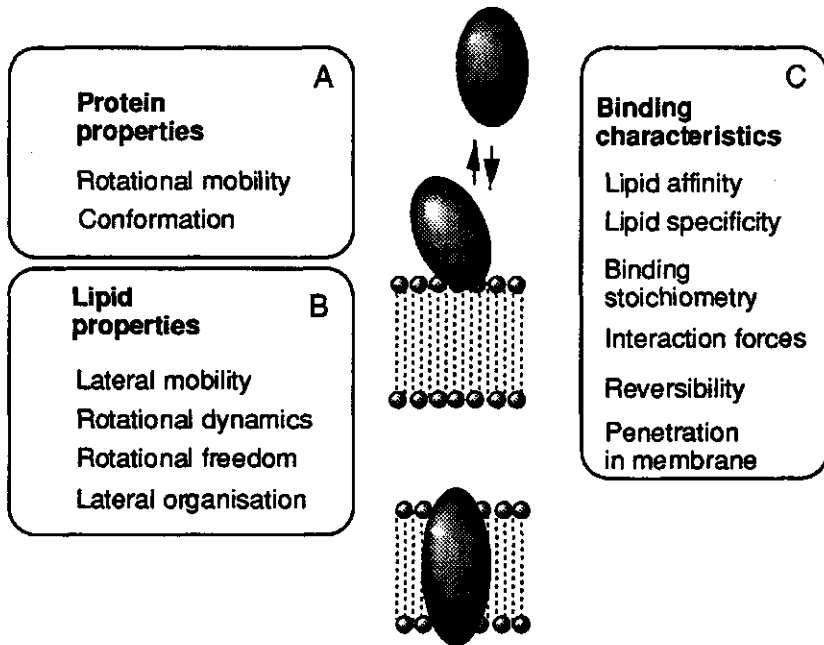
Figure 1. Schematic overview of some major goals in protein-lipid investigations.

1.1.1. Lipid regulation of protein function

Interaction with lipids can have a profound effect on the structure and function of proteins. Some of these effects arise from general physicochemical properties of the lipid environment (e.g. fluidity), while others are induced allosterically via specific binding to lipid cofactors. In this sense both the physical state and chemical composition of the lipid environment are essential for regulation of various integral membrane proteins and peripherally bound proteins.

1.1.1.1. Regulation by bulk membrane properties

Many proteins are sensitive to physico-chemical parameters of their local lipid environment. The membrane state depends on several factors like temperature, chemical composition, lateral pressure, ionic composition and pH of the aqueous medium. In most cases enzymatic activity of membrane-bound proteins drops dramatically when the membrane enters the gel phase (Sandermann, 1978). The bilayer properties modulate protein function by influencing its organisation (e.g. protein aggregation) or by stabilising specific functional or non-functional conformers of the proteins. On the other hand regulation can take place on the level of substrates, ligands or products. The membrane organisation and dynamics affect the diffusion and orientation of

substrates, products or ligands with respect to membrane receptors or enzymes (Bean et al., 1988; Sargent & Schwyzer, 1986, 1988).

Although the effects of these membrane properties on protein functioning are evident, it has still to be elucidated to which extent modulation of the physical properties of the membrane is actually employed in the regulation of protein function, since biological activity takes place under stable, moderate conditions of temperature and pressure. Controlled changes in the chemical composition of the membrane seems the simplest way to adjust these membrane properties. These adaptations of membrane properties will be slow, of long term, and aspecifc unless a mechanism exists that restricts the changes in membrane properties to definite local areas. Separate lipid domains can then be considered with different combinations of specific physical properties such as solid and fluid phases or with charged and uncharged lipids. Such pools with special properties and compositions have been suggested repeatedly in literature (Karnovsky et al., 1982; Levin et al., 1985; Wolf et al., 1988) and were demonstrated to occur in some biological membranes (Tocanne et al., 1989). However, evidence for their general appearance in cell membranes is difficult to establish. A special case in this non-allosteric regulation of protein function is the activation of protein kinase C (PKC). Several biochemical and biophysical studies showed that the activation of PKC is sensitive to acyl chain saturation in the membrane (Snoek et al., 1988; Bolen & Sando, 1992; Davis et al., 1985; Mori et al., 1982). In addition, many substances have been discovered which activate or inhibit PKC indirectly by altering the physical environment of the enzyme (Epand, 1993). Modulators can be classified as PKC-activators or inhibitors solely on the basis of their effects on the phase behaviour of model membranes (Epand, 1987; Epand & Lester, 1990). Hydrophobic substances which lower the bilayer-to-hexagonal phase transition temperature activate PKC while amphiphiles that raise the bilayer-to-hexagonal phase transition temperature, such as phosphatidylcholine or sphingomyeline, inhibit PKC. An important regulator of PKC that affects the bilayer structure is diacylglycerol (DG). This lipid compound induces major structural changes in the membrane at low concentrations by separating the headgroups of surrounding lipids whereas at sufficiently high concentrations hexagonal phases are induced (Cheng et al., 1991; Das & Rand, 1986; Das, 1984; Ohki et al., 1982). The motional freedom of DG in membranes is larger than that of phosphatidylcholine, and DG disturbs the lipid packing of dioleoyl phosphatidylcholine membranes (Chapter 4 of this thesis). It is thought that this type of perturbation plays a role in the activation mechanism of PKC (Epand & Lester, 1990). However, the fact that not all hexagonal phase promoters activate PKC (Epand et al., 1988) and that the sn-1, 3 isomer of DG promotes hexagonal phase but does not activate PKC (Boni & Rando, 1985) indicates that other interaction factors and allosteric effects play an additional, important role in the cofactor regulation of PKC activity.

1.1.1.2. Allosteric regulation of protein function by lipids

The regulation of enzyme activity by changing the concentrations of regulatory lipids is specific, relatively fast and of short-term, in contrast to the general, slowly changing overall physical properties of the membrane (see 1.1.1.1.). The transduction of extracellular signals into intracellular events and cellular proliferation are often mediated by lipids that specifically regulate protein functions. In this transmembrane signalling extra cellular molecules activate their receptors at the cell surface. In most cases activated receptors induce the production of messenger molecules in the cell (e.g. cAMP, calcium or lipid messengers) which modulate the activity of protein kinases (Cohen, 1982; Hanks et al., 1988). The turnover rate of the signal lipids is often very rapid. As a consequence their levels can be low in resting cells and increase rapidly and transiently in response to extracellular signals. Two types of lipid messengers play important roles in transmembrane signal transduction: glycerolipids and sphingolipids (Figure 2).
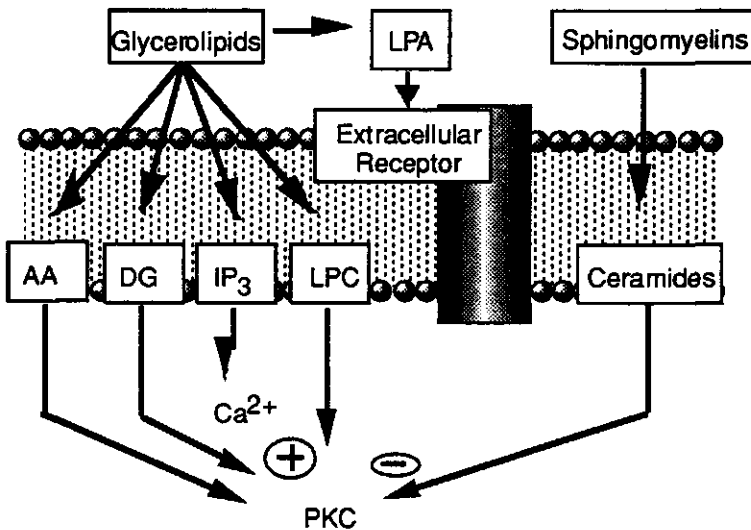
Figure 2. Scheme illustrating two major sources of lipid metabolites involved in transmembrane signalling: the glycerolipids and sphingomyelins. Arachidonic acid (AA), lysophosphatidylcholine (LPC), diacylglycerol (DG) and inositol 3-phosphate (IP$_3$) originate from phospholipase A$_2$ or phospholipase C catalysed hydrolysis of membrane glycerolipids. In addition, is lysophosphatidic acid (LPA) a very potent regulator of phospholipase C and of adenylylcyclase (Corven et al., 1989). Next to these glycerolipids metabolites are sphingoid bases potent regulators of protein kinases (Hannun et al., 1986) and oncogenes (see for a review Merrill et al., 1993). Also other intracellular targets than PKC are known for the lipid metabolites which are not presented in this figure.

One of the main targets of both glycerolipids and sphingomyelin derived second messengers is PKC. There are at least 12 PKC family members with different roles in cellular regulation (Dekker & Parker, 1994). These isozymes

can be divided into three distinct families, cPKC, nPKC and aPKC. The functional diversity of the PKC isozymes is partly indicated by different lipid cofactor requirements. cPKC and nPKC respond to DG and phorbol esters while aPKC does not. In addition, the PKC isozymes differ in response to calcium: nPKC and aPKC are calcium independent while cPKC require calcium for its activity. In the sphingomyelin pathway, growth factors induce the sphingomyelinase catalysed hydrolysis of sphingomyelin to ceramide. Ceramide then acts as a second messenger, by regulating the activity of protein kinases, and propagates the signal to nuclear activation. Several sphingolipid metabolites are known to down-regulate PKC (Hannun et al., 1986). In the glycerolipid pathway, receptor stimulation leads to the activation of phospholipases A_2 and C (Rhee et al., 1989).

Alternative routes → Inositol phosphates

ER

Ca^{2+}

PLA$_2$ PLCs   Inactive PKC Ca^{2+} Active PKC

PIP   DG Ca^{2+} DG

AA   AA
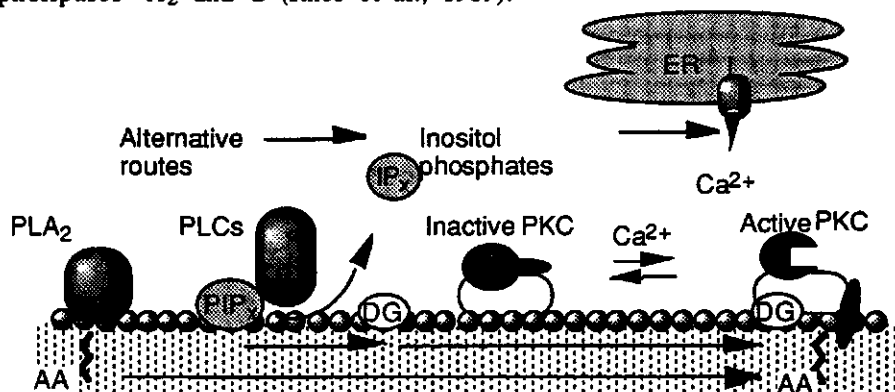
Figure 3 Scheme illustrating the intracellular regulation of PKC activity by the hydrolysis products of phosphoinositide lipids: DG and IP$_3$. Binding of IP$_3$ to receptors in the endoplasmatic reticulum (ER) releases calcium from this organelle thereby causing a transient fivefold rise of the calcium concentration in the cytosol (from $2*10^{-7}$ to 10^{-6} M). Interaction with calcium is essential for activation of PKC but its working mechanism and its requirement for the lipid interaction of PKC is unclear yet (see Chapter 5). PKC has a kinase domain (dashed) with a substrate binding site and a regulatory domain (open) with a pseudosubstrate region (solid) that contains positively charged amino acids. Binding of basic residues in the regulatory domain to anionic membranes, and binding of DG induces the exposure of the pseudosubstrate region and enables substrates to bind to the enzyme (Mosior & McLaughlin, 1991). Further details in the legend of Figure 2.

Phospholipase C then hydrolyses phosphatidylinositol (PI), phosphatidylinositol 4-phosphate (PIP) and phosphatidylinositol-4, 5-biphosphate (PIP$_2$) and in a later stage also other lipids (Pelech & Vance, 1989). This hydrolysis yields the intracellular messengers diacylglycerol (DG) and the phosphate headgroups of the various lipids. Inositol 3-phosphate (IP$_3$), headgroup of PIP$_2$, mobilises calcium from the endoplasmatic reticulum stores via a receptor mediated mechanism (Berridge, 1993). The interaction of PKC with acidic membranes, calcium and DG activates the protein by releasing a pseudosubstrate domain from the active site (House & Kemp, 1987; Makowske & Rosen, 1989; Mosior & McLaughlin, 1991; Orr et al., 1992) (Figure 3). Phospholipase A_2 catalysed hydrolysis of several phospholipids leads to the release of free fatty acids which synergistic enhance the activation of PKC by

diacylglycerol (Khan et al., 1992; Chen & Murakami, 1992). Evidence has been obtained that next to DG, PIP_2 (O'Brain et al., 1987; Lee & Bell, 1991; Chauhan & Brockerhoff, 1988; Huang & Huang, 1991) and other lipids and lipid-like compounds such as phorbol esters (Castagna et al., 1982) and lyso-phosphatidylcholine (Oishi et al., 1988) are able to activate PKC as well.

1.1.2. Forces and specificity in protein-lipid binding

Several interaction forces are involved in protein-lipid association depending on the protein or membrane system. The range of these forces varies largely. Coulomb interactions dominate at long distances and play a main role in peripheral binding of proteins to membranes. Most of the amino acid residues carrying a charge are located at the aqueous periphery of the protein molecule. Charged amino groups in the interior of the protein usually have formed ion pairs. In the case that the protein and lipid surfaces are oppositely charged, attractive electrostatic forces will result in peripheral binding of the protein to the membrane. In general, the equilibrium dissociation constants for peripheral binding of a protein to a membrane surface are relatively large resulting in short lifetimes of the protein-membrane complexes (Jain et al., 1987). Therefore, proteins adsorbed to a bilayer will exchange readily between populations of vesicles on a time scale of typically a few seconds (Jain et al., 1982; Chapter 2). In general van der Waals interactions tend to arrange water molecules to exposed hydrophobic groups. Therefore, dehydration and subsequent aggregation of non-polar components in an aqueous environment is favourable because it increases the disorder of water molecules. In aqueous solutions of proteins the various non-polar amino acid residues will tend to be buried in the interior of the molecule, thus shielded from water. These intramolecular hydrophobic interactions lead to a compact structure and to extra structural stability. Organisational defects in the membranes result in exposure of hydrophobic lipid elements to aqueous environment and favours the insertion of protein segments into the bilayer by increasing the ground state energy of a bilayer. Consequently, the lipid packing irregularities will decrease the apparent activation energy change associated with incorporation of proteins (Jain et al., 1987). For larger proteins the rate of incorporation is determined by conformational changes necessary for accommodation in the bilayer (Jain et al., 1987). Due to hydrophobic interactions the dissociation of an embedded or transmembrane protein from the lipid environment generally is extremely slow. Further stabilisation of protein-lipid complexes may arise from hydrogen bonding between protein and lipids. Reports on PKC activation by DG provide evidence for such bonding (Brockerhoff, 1986). Finally, effects of the protein binding on the lipid organisation like elimination of intermolecular lipid repulsion by charged groups on a protein contribute to the overall binding energy (Jain et al., 1987). In many cases the binding of proteins to membranes is influenced by metal ions like calcium, magnesium and zinc (see for a review on calcium-phospholipid binding proteins Klee (1988)). Various mechanism can play a role in this cation modulation of protein binding to membranes. Divalent cations are known to bind with considerable specificity to anionic phospholipids, thereby affecting the lipid organisation of the membrane (Bazzi & Nelsestuen, 1991; Brumfeld & Lester,

1990). Calcium or cadmium induced domains of nitrobenzoxadiazolyl labelled acidic phospholipids in vesicles and erythrocytes were visualised using fluorescence microscopy (Haverstick & Glaser, 1987). In these experiments, no effect on the lateral lipid organisation was observed when magnesium or zinc were used. Membrane patches enriched with negatively charged lipids may facilitate the electrostatic binding of proteins to membranes. Furthermore, divalent cations can have a dramatic effect on binding of proteins to membranes by affecting the electrostatic potential at the membrane surface (Trudell, 1989) and the hydrophobic interactions between phospholipids and membrane-bound proteins (Seelig, 1990) or by dehydrating protein or lipid surfaces. Other metal ions invoke the same effect only at much higher concentrations. Finally, the tertiary structure of several proteins is influenced by calcium or other divalent cations. For example, calcium induces considerable conformational changes in membrane bound PKC (Lester & Brumfeld, 1990).

In general, proteins exhibit preference for particular lipids by recognition of lipid structural elements. In many cases this preference originates from some general charge effects as was shown for the preference of the Ca^{2+}-ATPase for acidic phospholipids (Verbist et al., 1991). However some proteins possess sites complementary to the chemical composition or conformation of specific lipid headgroups or acyl chains. This receptor-ligand type of interaction often involves regulatory lipid components that are present at extremely low concentrations in the membrane. For example, the recognition of DG by PKC displays remarkable stereospecificity: only the 1, 2-*sn*-DG but not 2, 3-*sn*-D G can function as an effector (Rando & Young, 1984). PKC also possesses high specificity for PS. Alternation in the stereochemistry of the L-serine headgroup also results in reduction of the activation of PKC (Lee & Bell, 1989). Thus strict geometric and steric constraints regulate the productive binding of lipid headgroup to specific sites on PKC.

1.2. Fluorescence methods for protein-lipid association

1.2.1. Fluorescence relaxation

Illumination with light will bring fluorophores to excited singlet states. After ultrarapid relaxation to the lowest excited singlet, molecules decay to the ground state via several competing processes. First, there is spontaneous emission (fluorescence), which is a radiative process with rate constant k_f. Second, so-called radiationless decay processes deactivate the excited singlet, by loss of excitation energy to internal vibrational or rotational levels (of the ground state) or to surrounding solvent molecules. In special cases other intermolecular mechanisms contribute to the decay like the transfer of excitation energy to acceptor molecules by the Förster mechanism (Förster, 1948). The occurrence of these extra nonradiative processes accelerates the decay of the excited state. Therefore, fluorescence measurements yield information about nonradiative decay processes and hence about the local environment of fluorophores in protein-lipid systems. The time-dependent

depopulation of the excited state can be expressed as a first order rate process in which the fluorescence intensity f(t) decays in an exponential fashion

$$f(t) = f(0)e^{-\left(k_f + k_{nr}\right)t} \qquad (1)$$

Where k_f corresponds to the rate constant for fluorescence and k_{nr} to that for nonradiative transitions. The inverse of the total decay rate $\left(k_f + k_{nr}\right)^{-1}$ correspond to the lifetime of the excited state, τ. Fluorophores in biological systems often display a whole distribution of lifetimes because of the heterogeneity of their environment:

$$f(t) = \int_0^\infty \alpha(\tau)\, e^{-t/\tau}\, d\tau \qquad (2)$$

This distribution function can be represented by an exponential series of n separate terms which can be recovered by minimising the χ^2 statistic and maximising the Skilling-Jaynes entropy function (Jaynes, 1968). Alternatively, Lorentzian or Gaussian distribution functions with widths and centers determined by least-squares analysis can be used to model the unknown distribution function (Alcala et al., 1987a, 1987b; Lakowicz et al., 1987).

1.2.2. Intermolecular quenching

Fluorescence quenching refers to any process that results in a decreased fluorescence intensity of a fluorophore. Since quenching is a bimolecular process, it can be used to obtain intermolecular information like the degree of binding of a protein to specific lipids in the membranes. Two mechanisms of quenching exist. First a quencher molecule can form a nonfluorescent complex with the fluorophore already in the ground state.
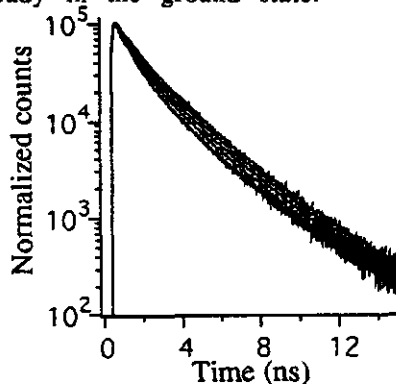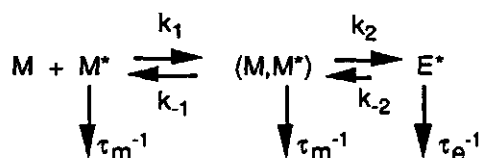

Figure 4 Progressive quenching of tryptophan fluorescence of lysozyme as a consequence of its association to different concentrations of pyrene loaded vesicles. In this system excited tryptophans in lysozyme partly transfer their excited state energy to pyrene moieties in the lipid bilayer via the Förster mechanism (Förster, 1948).

This process is called static quenching (Lakowicz, 1983). In case of dynamic quenching, the fluorescence is lost by frequent collisions between an excited fluorophore and the quencher molecule. Energy transfer from a donor to an acceptor can also be considered as a non-collisional type of dynamical quenching, in which the fluorescence lifetime of the excited donor is shortened (see Figure 4).

1.2.2.1. *Dynamic quenching*
Dynamic quenching is characterised by a shortening of the fluorescence lifetime and will consequently lead to a decrease in fluorescence quantum yield. This type of quenching occurs when heavy-atom or paramagnetic molecules collide with the excited fluorophores. A special case of dynamic 'quenching' is excimer formation in which an excited monomeric fluorophore (M*) interacts with a fluorophore in the ground state (M) to form a stable excited dimer (E*) (Förster, 1955). The excimer fluorescence is red-shifted with respect to the monomer fluorescence. In membranes, excimer formation is characterised by the rate constants τ_m^{-1} and τ_e^{-1} (in s^{-1}) for the decay of the excited monomer and excimer respectively and by two dynamic processes as illustrated in the following scheme (Vauhkonen et al., 1990):

$$M + M^* \underset{k_{-1}}{\overset{k_1}{\rightleftharpoons}} (M,M^*) \underset{k_{-2}}{\overset{k_2}{\rightleftharpoons}} E^*$$
$$\downarrow \tau_m^{-1} \qquad \downarrow \tau_m^{-1} \qquad \downarrow \tau_e^{-1}$$

First, there is neighbour formation (M + M* → (M, M*)) which is characterised by the rate constants k_1 and k_{-1}. These rate constants are related to the frequency of lipids exchanging positions in the membrane matrix (f) and to the number of lipid exchange events required before (M, M*) is formed. Secondly, the process of complexation of (M, M*) → E* which is governed by the rates of association k_2 and dissociation k_{-2}. Intramolecular excimer formation of two fluorophores attached to the same molecule ((M, M*) -> E*) is only determined by the second process. Consequently, registration of the excimer fluorescence of mono- and dipyrene labelled lipids reveals information about the lateral membrane organisation (Eklund et al., 1988, Chapter 8), lipid translational diffusion (Eisinger, 1986; Galla & Sackman, 1974; Sassaroli et al., 1990; Vanderkooi & Gallis, 1974; Vauhkonen et al., 1989) and acyl chain dynamics (Vauhkonen et al., 1990) in membranes (see also Chapters 5 and 8).

1.2.2.2. *Resonance energy transfer*
Another dynamic fluorescence quenching mechanism is resonance energy transfer (RET). This process involves long range transfer of excitation energy from the fluorophore (donor) to the quencher (acceptor) by a weak coupling of the transition moments (Förster, 1948; Stryer, 1978). The rate of this nonradiative process is highly dependent on the differences in donor and acceptor energy (spectral overlap), the separation and relative orientation of the donor and acceptor moieties (Förster, 1948). Therefore measurement of RET

can provide information about the geometry of the protein-lipid system like relative orientation or separation of donor and acceptor. The rate of energy transfer k_T (in ns^{-1}) can be expressed as (Förster, 1948):

$$k_T = 8.71 \times 10^{17} R^{-6} \kappa^2 n^{-4} k_r J \qquad (3)$$

where R is the intermolecular distance (in nm) between donor and acceptor, κ is the orientation factor (Steinberg, 1971; Dale et al., 1974) describing the relative orientation of donor and acceptor transition dipoles, n the refractive index of the intervening medium, k_r is the radiative rate of the donor (in ns^{-1}) and J is the overlap integral (in $M^{-1}cm^3$) given by:

$$J = \frac{\int_0^\infty \frac{F_d(\nu) \, \varepsilon_a(\nu)}{\nu^4} \, d\nu}{\int_0^\infty F_d(\nu) \, d\nu} \qquad (4)$$

$F_d(\nu)$ is the fluorescence intensity of the donor at frequency ν and ε_a is the extinction coefficient of the acceptor at ν. The rate of energy transfer can be determined from the reduction in donor fluorescence lifetime (leading to reduction in donor fluorescence quantum yield) or from the amount of sensitised fluorescence of the acceptor. Elimination of the acceptor by photobleaching should effectively remove energy transfer (Williams et al., 1990). In the analysis of RET data assumptions are often employed on the relative orientation and motional flexibility of the donor and acceptor dipoles. Recently some theoretical tools have been given for analysing RET without restrictive assumptions for the value of the orientation factor (van der Meer et al., 1992)

1.2.3. Fluorescence anisotropy

The mutual effects on protein and lipid motion is often experimentally approached with fluorescence anisotropy measurements. Illumination with polarised light will anisotropically excite fluorophores because light absorption exhibits a cosine-squared angular dependence between the direction of the electric field vector of light (e_i) and the absorption transition moment (μ). Similarly, emission of polarised light exhibits a cosine squared angular dependence between the detection polariser and the emission transition moment. The time dependent fluorescence intensity ($I(t)_{if}$) can be described by the following equation (Zannoni et al., 1983):

$$I(t)_{if} = k \left\langle (e_i.\mu)^2 (e_f.\varphi)^2 \right\rangle f(t) \qquad (5)$$

where $(e_i.\mu)^2 (e_f.\varphi)^2$ is the probability that a chromophore with absorption and emission dipole moments μ and φ, absorbs a photon with polarisation vector e_i

and emits a photon with polarisation vector e_f. $f(t)$ is the normalised decay function of the fluorescence and k a parameter to correct for instrumental factors and probe concentration. The polarisation of photons emitted directly after excitation with polarised light is determined by the angle between the excitation and emission transition dipole moments and yields the fundamental anisotropy of the system, $r(o)$. Each process that results in a more uniform distribution of φ will result in a decrease of the polarisation of the emitted light. By measuring the time-dependence of the parallel and perpendicular polarised emission components $I_{//}(t)$ and $I_\perp(t)$ relative to the polarisation direction of the exciting beam, one can recover the fluorescence anisotropy $r(t)$:

$$I_{//}(t) = P(t) * \left(\frac{2}{3} r(t) f(t) + \frac{1}{3} f(t) \right) \qquad (6)$$

$$I_\perp(t) = P(t) * \left(\frac{-1}{3} r(t) f(t) + \frac{1}{3} f(t) \right) \qquad (7)$$

where the multiplication sign indicates the convolution of the decay function with the instrument impulse response profile $P(t)$. Two processes are mainly responsible for depolarisation: probe rotation (Perrin, 1926) and energy transfer between identical chromophores with their transition moments oriented differently (Förster, 1948). Theoretical descriptions of the motional contribution to depolarisation are subdivided into two types. First there is isotropic rotation of, for instance, a probe in solution. In this type of rotation no orientational constraints are present and the anisotropy is given by a sum of n (=1-5) exponentials, where n depends on the shape of the probe molecule (Small & Isenberg, 1977; Weber, 1971). In most experimental cases, a single correlation time is measured which is the harmonic mean of the expected values (Dale et al., 1977). Second, there is anisotropic probe rotation when the fluorescent molecule can only move in a restricted manner. This is the case for a lipid acyl chain in a bilayer, in which the rotation of the probe is restricted by acyl chains of surrounding phospholipids. Time-resolved fluorescence anisotropy measurements can reveal structural and dynamical aspects of motionally restricted fluorophores. The anisotropy decay of membrane probes like diphenylhexatriene (DPH) has been successfully described with the rotational diffusion model (r_g3) in terms of a perpendicular diffusion coefficient $D_\perp$ and two order parameters $<P_2>$ and $<P_4>$ (Szabo, 1984; Van der Meer et al., 1984). The parameters $<P_2>$ and $<P_4>$ are related via an equilibrium orientation distribution function $f(\theta)$ of the DPH labels with respect to the membrane normal. When no assumptions are made about $f(\theta)$, $<P_2>$ and $<P_4>$ can be determined independently. The most unbiased orientation distribution function can then be constructed from the optimised $<P_2>$ and $<P_4>$ values by applying the maximum entropy formalism (Ameloot et al., 1984; Berne et al., 1968; Van Langen et al., 1987). This approach often yields bimodal distribution functions for linear membrane probes oriented parallel and perpendicular with respect to the normal of the membrane (Van Ginkel et al., 1989; Kooyman et al., 1983; Ameloot et al., 1984; Wang et al.,

1991) even when the probe is covalently attached to lipids (Chapter 3). This orientational heterogeneity is at odds with the known physico-chemical properties of lipid probes in membranes. The compound motion model, recently adapted for fluorescence anisotropy decay analysis of linear lipid probes, seems to be a more appropriate approach for analysis (Van der Sijs et al., 1994) but is unfortunately composed of 5 adjustable parameters. As a compromise the fluorescence anisotropy decays of membrane probes can be analysed with the r_{g3} model with the assumption that the labels are unimodal distributed parallel with respect to the phospholipid acyl chains (Chapter 4, Straume & Litman, 1987). Analysis of the anisotropy decay curves of probe-lipids then yields the dynamic component $D_\perp$ and a structural component describing the orientation distribution width of the DPH probes with respect to the membrane normal.

1.2.4. Fluorescent lipids and protein-lipid interactions

The observable properties of lipids labelled with a fluorophore can be used to draw conclusions about the dynamics and the structure of specific phospholipids in the membrane. Alternatively, the labelled lipids can act as energy acceptors of excited proteins in RET studies. Several hydrophobic fluorescent probes have been applied in protein-lipid association studies. Frequently used fluorescent groups include anthroyloxy-, dansyl-, parinaroyl-, nitrobenzoxadiazolyl-, DPH and pyrene-moieties. In order to make these probes resemble normal phospholipid molecules, they are covalently attached to host lipids, thereby replacing one or both natural acyl chain(s). The best characterised lipid probes in protein-lipid investigations are lipids labelled with DPH and pyrene.

The photo-physical properties of DPH-probes have been reviewed by Lentz (1989). This probe is cylindrically shaped with excitation and emission dipoles practically colinear with the long cylinder axis. Its fluorescence lifetime in membranes is on the proper time scale for registration of restricted rotational dynamics of the membrane. These properties make the probe very suitable for fluorescence anisotropy studies which may reveal acyl chain dynamics and motional constraints (see Chapters 3 & 4). In addition, DPH has been applied in lifetime measurements of protein-lipid systems. In these studies the sensitivity of the DPH lifetime is used to probe environmental heterogeneity in protein rich membranes (Fiorini et al., 1987; Williams et al., 1990).

Pyrene is a disk-like probe, that can be attached covalently to the terminal carbons of one or both acyl chains of lipids. The rotational motion of pyrene in bilayers is complex and can not be interpreted easily (Zannoni et al., 1983). In addition, the fluorescence lifetime of pyrene (>50 ns) is too long for accurate evaluation of the acyl chain motion (0.1-10 ns) in membranes. Therefore this probe is less useful for fluorescence anisotropy measurements. Pyrene-labelled lipids are, however, excellent probes to study dynamical and structural properties of membranes through their ability to form excimers (Förster, 1955). Pyrene lipids with one pyrene moiety report on lateral lipid organisation and dynamics while dipyrenyl lipids are more suitable for information on local

lipid chain dynamics as an empirical measure for membrane fluidity (see Chapters 5 and 8).

Together DPH- and pyrene-labelled lipids provide a complementary set of information about rotational and translational motion and lateral organisation of lipids chains in the membrane. In addition, both probes can function as acceptors of energy from UV excited intrinsic tryptophan residues in the proteins or, alternatively, as energy donor for proteins labelled with a suitable acceptor in protein-lipid binding studies.

1.3. Lipid systems for protein-lipid investigations

The ultimate challenge of protein-lipid investigations is to accurately assess their role in cellular processes in intact organism. The applicability of fluorescence microscopy in intact cells is now proceeding rapidly and will allow on-line detection of protein binding to membranes of individual cells or cellular organelles with molecular resolution (Gadella et al., submitted). In these in vivo investigations both lipid and protein molecules of interest should be equipped with a label and incorporated into intact (sub)cellular systems in order to discriminate them from the wide variety of other lipid and protein components present. This is often difficult to achieve. Model membrane systems are easier to manipulate than whole cells. Further advantages are that artificial membrane systems are well characterised and chemically less complicated than natural membranes. In general, three membrane-mimetic systems can be used, each with its own specific advantages and drawbacks. The simplest system is a micellar one. This approach for investigating protein-lipid interactions is well documented (Hannun et al., 1986) and particularly suited to determine the specificity and stoichiometry of the lipids introduced (see Chapter 6). The redistribution of fluorescent lipids among the micelles is fast (see Figure 5) allowing rapid, accurate manipulation of the system in lipid titration or competition experiments (see also Bazzi & Nelsestuen, 1987; Hannun et al., 1986). Furthermore, the high micellar concentration makes it possible to select conditions in which maximally one protein molecule binds per micelle which considerably simplifies binding models (see Chapter 6). Additional advantages of the use of micelles is that all lipids are exposed to the protein and that physico-chemical effects of the membrane on the interaction with the protein are limited. The fact, however, that many micellar detergent molecules are also used to extract membrane proteins from their lipid environment in protein purification procedures, implies that micellar systems certainly influence protein-lipid interaction forces. A second, useful model system for the study of protein-lipid interaction consists of monolayers of oriented phospholipids. Their composition and lipid packing density, as well as the nature of the subphase can easily be controlled. The study of protein-lipid interactions in monolayer systems at the air-water interface is often combined with fluorescence microscopy in which the effect of protein on the lateral organisation of the lipids can be monitored (Ahlers et al., 1990; Eklund et al., 1988; Reed et al., 1987). Alternatively, lipid monolayers can be transferred to solid supports coated with an alkylating agent. The third system consists of lipid vesicles that mimic the biological bilayer more closely than

the other model membranes. A disadvantage of using vesicles is that only probe lipids in the outer monolayer of the bilayer are accessible for externally added protein. The unpredictability and complexity of the vesicle structure accumulates uncertain factors which are difficult to control (e.g. surface curvature, phase).
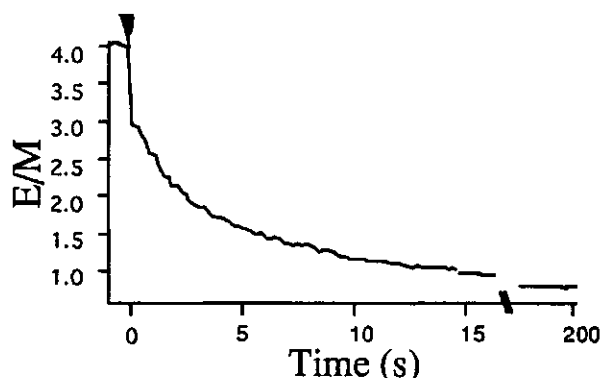
Figure 5 Spontaneous redistribution of 1-palmitoyl-2-pyrenedecanoyl phosphatidylserine in polyoxyethylene-9-lauryl ether micelles. Initially, two separate populations of micelles with equal volume are present, one of 100 μM polyoxyethylene-9-lauryl ether containing 10 mole % of *sn*-2-(pyrenedecanoyl) phosphatidylserine and the other of 100 μM polyoxyethylene-9-lauryl ether containing 10 mole % unlabelled phosphatidylserine. Both populations are mixed at time t=0 and the time dependence of pyrene excimer to monomer fluorescence intensity ratio is monitored. This ratio is a measure for the intermolecular collision frequency of the pyrene lipids and decreases within a few seconds to a final level, indicating a complete redistribution of the pyrene lipids over both micellar populations. This experiment was performed in 20 mM Tris-HCl pH 7.5, 120 mM NaCl at room temperature.

1.4. Fluorescopic probing of lipid modulated protein properties

1.4.1. Protein aggregation in membranes

Lipid-induced protein aggregation is an important regulation mechanism of the function of several proteins. Since RET is able to determine intermolecular distances with subnanometer resolution, it is suitable for observation of protein aggregation and organisation of proteins on membrane surfaces. In most of these types of investigations the efficiency of energy transfer is determined from pairs of labelled protein incorporated within vesicles. From the energy transfer efficiency the average protein-protein distance can be determined. If this distance is smaller than theoretically predicted for randomly distributed proteins in the lipid system, the proteins are aggregated. Addition of large amounts of unlabelled polypeptide should result in the formation of fewer donor/acceptor pairs and a corresponding decrease in RET. The self-association of the epidermal growth factor receptor (Carraway et al., 1989; Gadella et al., 1993) and cytolysin (Harris et al., 1991) on the membrane surface was demonstrated with this technique using a fluorescein-rhodamine donor-acceptor pair. Furthermore, RET was often applied to elucidate the

organisation of pore-forming peptides such as melittin (Hermetter & Lakowicz, 1986; John & Jähnig, 1991; Stankowski et al., 1991; Talbot et al., 1987; Vogel & Jähnig, 1986) and paradaxin (Rapaport & Shai, 1992) within membranes. In the case of paradaxin, not only the aggregation state, but also the orientation of the peptides with respect to the membrane could be determined by labelling the N-terminal amino acids specifically with donor probes (N-donor) and either the N- or C-terminal amino acids with acceptor probes (N- or C-acceptor). A correlation was found between self-aggregation of the different analogues within the membranes and their pore-forming abilities. Fluorescence energy transfer from N-donor labelled paradaxin to N-acceptor labelled paradaxin compared with that of N-donor and C-acceptor labelled paradaxin suggested that aggregates are formed in an ordered manner with preferentially a parallel orientation of monomers within the aggregate (Rapaport & Shai, 1991, 1992; Shai et al., 1991). Apart from these RET studies, fluorescence microscopy appeared to be a powerful tool for the detection of phospholipase A_2 domains induced after partial hydrolysis of the monolayer lipids (Ahlers et al., 1991; Grainger et al., 1989, 1990a, 1990b). Non-hydrolysable lipid substrates did not induce any protein aggregation, indicating that the formation of the phospholipase A_2 domains is dependent on the hydrolysis reaction.

1.4.2. Protein structure in membranes

The interaction with lipids is for many membrane-associated proteins essential to remain in their functional conformation. Most integral membrane proteins have α-helical transmembrane helices oriented parallel to the lipid acyl chains in the membrane but also other orientations of α-helices (Chung et al., 1992) and other peptide structures have been reported (Long et al., 1977). Since the excited state lifetime, the fluorescence intensity and the fluorescence spectral distribution of chromophores depend on the environment, registration of these fluorescence parameters allows the detection of lipid induced interconversions between substates of proteins. Along these lines evidence was provided that acid phospholipid vesicles produce conformational changes at the level of the tertiary structure of the antitumour protein α-sarcin. Fluorescence spectra of this protein were analysed into separate contributions of tyrosine and tryptophan residues. Upon binding to artificial membranes the quantum yields of both residues increase strongly. These changes were related to a decreased static quenching as a consequence of the conformational changes induced by these artificial membranes (Gasset et al., 1991). Time-resolved measurements of tryptophan fluorescence of the apocytochrome-c yielded detailed information about rearrangements of its structure induced by binding to membranes. Changes in the tryptophan fluorescence lifetime distribution of apocytochrome-c were observed upon its binding to membranes. Since the apocytochrome contains only one tryptophan residue, the authors could assign the various distributed lifetime peaks to different protein conformers. Stabilisation of protein conformers by the membrane could be observed using this approach (Vincent & Gallay, 1991) (see also Chapter 2). Besides to these examples in which only the intrinsic protein fluorescence is employed, RET can be used for conformational studies. Since

this technique allows recovery of the spatial distribution of donor molecules within a protein (like tryptophans) relative to acceptors in a lipid bilayer and is therefore sensitive for structural rearrangements within the peptide (Fleming et al., 1979; Koppel et al., 1979; Kleinfeld & Lukacovi, 1985; VanderKooi et al., 1993).

1.4.3. Protein topology with respect to the membrane

Two major approaches are employed to determine the orientation and longitudinal location of a protein in the membrane: RET and static quenching (East & Lee, 1982; Markello et al., 1985). Both techniques use quenching moieties (quencher atoms or energy acceptors) at different positions along the phospholipid acyl chains (East & Lee, 1982; Leto et al., 1980; Markello et al., 1985; Yeager & Feigenson, 1990). Determination of the quenching efficiency as a function of the position of the quenching groups on acyl chains, is used to reveal the depth of a labelled protein in the bilayer (McIntosh & Holloway, 1987). When static quenching of fluorescence is used this method is referred to as the parallax method (Chattopadhyay & London, 1987). Parallax studies of model ion channel peptides in phospholipid vesicles revealed information about their structure and orientation in membranes. Using nitroxide quenchers, the distance of tryptophan residues from the centre of the bilayer could be determined for peptides with tryptophans substituted at different positions. The results indicate that the helical axis of these peptides is oriented parallel to the surface of the membrane and located a few Ångstroms below the polar headgroup/hydrocarbon boundary (Chung et al., 1992). The same principle was used to determine the average membrane penetration depth of tryptophan residues of the nicotinic acetylcholine receptor (Chattopadhyay & McNamee, 1991). The orientation and penetration of cytochrome C to monolayers of phospholipids was determined with RET from dansylphosphatidylethanolamine in these membranes to the heme of the protein. The cytochrome was found to bind at an orientation such that its heme crevice is fully accessible to the aqueous space. Its penetration in the lipid layer was dependent on the ionic content of the subphase and the initial packing of the film. The perturbation induced in the lipid matrix by the binding appeared to be very localised (Teissie, 1981). Furthermore, quenching of intrinsic tryptophan fluorescence by both static and RET mechanism was used to investigate the association and subsequent penetration of PKC into membranes. For the static quenching experiments a combination of hydrophilic quencher and nitroxide labelled lipids was used. The hydrophilic quencher resulted in strong reduction of the intrinsic tryptophan fluorescence. In the RET experiments, anthroyloxy fatty acids functioned as acceptors of tryptophan excitation energy. Efficient quenching was observed with these depth probes, indicating that probably upon membrane binding, multiple tryptophan residues penetrate the membrane close to the carbon-16 position of the lipid chain (Brumfeld & Lester, 1990).

1.5. Fluorescopic probing of protein-modulated lipid properties

1.5.1. Lipid organisation

When a protein incorporates in the lipid bilayer, it affects several physical properties of the surrounding lipids (see for a review Lentz, 1988). Four major effects of proteins on the organisational properties of lipids can be distinguished:

1) Peripheral binding of proteins affects the packing density of phospholipids and the phase transition properties of the bilayers. This effect is generally observed with monolayer techniques that monitor the surface pressure of the lipid layers. Since the orientational freedom of fluorescent membrane probes is directly related to the packing density of the lipids in the membrane, measurement of the fluorescence anisotropy of for instance DPH-lipids (Baatz et al., 1990; Pink & MacDonald, 1986) or of the excimer formation of dipyrene lipids can be used as a tool to characterise this effect. For example, from a combined ESR and DPH-anisotropy study a reduction of the lipid packing was observed upon association of glycophorin to membranes. The number of lipid molecules that experience this reduced lateral pressure was dependent on the glycophorin conformation (Pink & MacDonald, 1986). Changes in the fluorescence intensity of nitrobenzoxadiazolylphosphatidylethanolamine were used to study the effects of melittin on the bilayer-to-H_{II} phase transition in vesicles of egg-PE. The results demonstrate that melittin acts as an inhibitor of the bilayer-to-H_{II} phase transition by stabilising the bilayer organisation (Nishiya & Hui, 1991). The effect of incorporated coat protein of the M13 bacteriophage on the phase behaviour of model membranes was characterised with anisotropy measurements of parinaroyl-labelled lipids (Kimelman et al., 1979; Wolber & Hudson, 1982). Upon incorporation of the protein into the membrane, the phase transition is lost as a consequence of smoothing the differences in acyl chain organisation at low and high temperatures in the vicinity of the protein (Kimelman et al., 1979; Wolber & Hudson, 1982).

2) Several proteins affect the lateral distribution of particular lipids. Various examples of quantitative studies of this effect have appeared in literature. Lateral phase separations induced by binding of prothrombin fragment 1 to charged lipid vesicles were observed with excimer formation of pyrene-labelled phospholipids in multilamellar membranes (Jones & Lentz, 1986). The results were interpreted in terms of a model in which prothrombin fragment 1 binds, probably via calcium bridges to several dioleoylphosphatidylglycerol molecules. More extensive clustering of acidic phospholipids is induced by PKC (Bazzi & Nelsestuen, 1991). Addition of PKC to phospholipid vesicles with nitrobenzoxadiazolyl-labelled acidic phospholipids resulted in extensive rapid and calcium dependent self quenching of the nitrobenzoxadiazolyl fluorescence. Only small fluorescence changes were observed in presence of large excess of unlabelled acidic lipids. Calcium was not able to induce the changes in fluorescence emission and was proposed to form bridges between the proteins and acidic phospholipids in the membrane rather than play a major role in the lateral lipid segregation itself (Bazzi & Nelsestuen, 1991).

3) Binding of lipids to irregular surfaces of membrane proteins influences the motional properties of their acyl chains. This perturbation of lipid chain ordening is known to persist over several lipid shells as was revealed by increased DPH steady state fluorescence anisotropies (Jähnig, 1979; Vogel et al., 1982; Lentz et al., 1983; Moore et al., 1978) and by parinaroyl labelled phospholipids (Kimelman et al., 1979; Wolber & Hudson, 1982). The effect of incorporated coat protein of the M13 bacteriophage on the chain ordening of parinaroyl labelled lipids in model membranes was characterised with anisotropy measurements (Wolber & Hudson, 1982). The protein orders the bilayer relative to the fluid-like liquid crystalline state as revealed by an increase in the limiting anisotropy in the presence of protein. The time-dependence of the parinaroyl-anisotropy is curved upward in the presence of the M13 coat protein. The protein induces an increase in the fluorescence lifetime relative to that of the probe in the fluid bilayer and increases the anisotropy for chains in the vicinity of the protein. As a consequence, at long times the observed anisotropy originates mainly from parinaric acid chains that interact with the M13 coat protein. The environmental heterogeneity induced by proteins in membranes was also probed by the fluorescence lifetime characteristics of DPH-labelled lipids. Both extrinsic and integral membrane proteins induce broad distributional widths of DPH-lipids while the major lifetime peak positions were hardly affected (Williams et al., 1990).

4) Integral membrane proteins contain trans-membrane portions which consist predominantly of hydrophobic amino acids. The dimensions of this transmembrane segment should match the thickness of the hydrophobic interior of the lipid-bilayer (determined by the hydrocarbon chain composition of phospholipids (Lewis & Enelman, 1983)). If this is not the case, nonpolar moieties will be exposed to the aqueous environment (Veld et al., 1991) or non-bilayer structures may be induced (Sanders et al., 1992).

1.5.2. Lipid lateral dynamics

Significant effects upon diffusion of lipid molecules in the plane of the membrane result from proteins that form simple physico-chemical barriers in the membrane (Jacobson, 1983; Vaz et al., 1984). When lipids function as metabolites in cellular signalling or as allosteric cofactors for proteins, their diffusive motion might be rate limiting and thus of great importance. Two experimental methods are widely employed to determine the translational fluidity of model membranes and cells, both of which employ fluorescent lipid probes.

Fluorescence recovery after photobleaching (Axelrod et al., 1976) measures the recovery of fluorescence in a region that has been bleached by means of a focused laser beam. This recovery is related directly to the diffusive motion of fluorescence membrane probes. The lateral mobility of nitrobenzoxadiazolyl-labelled phosphatidylethanolamine (PE) and cholesterol (Chol), was measured in liposomes, erythrocyte ghost membranes, and lipid extracts by using the fluorescence photo bleaching recovery technique. Both nitrobenzoxadiazolyl-PE and nitrobenzoxadiazolyl-Chol appeared to diffuse 4-fold faster in extracted

erythrocyte membranes than in ghost membranes suggesting a significant restriction of lipid lateral mobility by membrane protein (Golan et al., 1984).

A second method for obtaining the lipid lateral diffusion properties employs diffusion-limited quenching mechanism like excimer formation or static quenching. Using excimer formation techniques Eisinger and colleagues discovered that mainly long range diffusion of lipid is affected by proteins (Eisinger et al., 1986). The local diffusion coefficient of pyrene labelled lipids in the erythrocyte membrane appeared to be of the same order of magnitude as that of long range diffusion of probes in lipid membrane without protein. The long range diffusion of the pyrene lipids in the erythrocyte membrane, however, was considerable slower than in liposomes without protein (Eisinger et al., 1986) (see also Chapter 8).

1.6. Quantitation of binding isotherms

If the fluorescence approach distinguishes between the various components involved in protein-lipid binding, proper analysis may recover binding stoichiometry and specificity. Generally three types of protein-lipid equilibria exist; one is the binding of a protein to the membrane (Figure 6A). Here we define the "protein-site" on the membrane as the average number of lipid molecules affected by protein binding. This type of binding is responsible for the peripheral fixation of a protein at the membrane surface. Alternatively, we can consider an exchange between two different lipids at the same site on the protein (Figure 6B) or the interaction of a specific lipid with a given vacant lipid site on the protein (Figure 6C). Since each of these three binding equilibria are used in this thesis, a summary is given of the derivation of the binding equations.
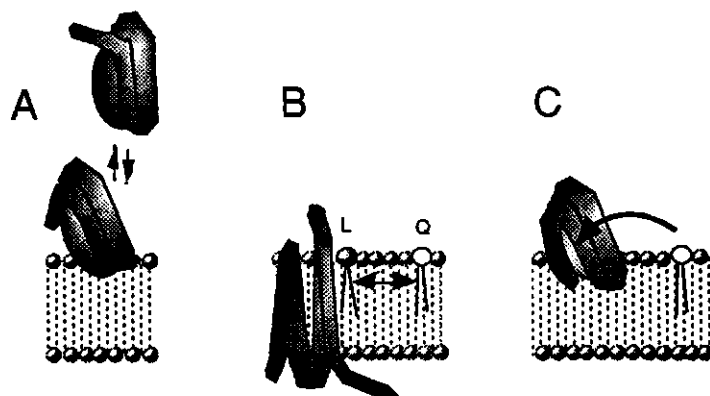
Figure 6 Schematic overview of three types of protein-lipid equilibria: **A** Binding of a protein to the membrane, **B** lipids exchanging at the protein surface and **C** lipids binding to specific sites that can not be occupied by other lipid species.

It should be noted that in the binding equilibria for proteins with multiple lipid sites identical binding properties are assumed for all sites. Introduction of individual binding parameters for each binding site would make the binding

models more realistic but would reduce the determinability of each parameter, especially from average observables such as quenching efficiency, to unacceptable levels.

1.6.1. *Binding of a protein to a membrane surface*

Free protein (P_f) is considered to be in equilibrium with interaction sites on the membrane. The fraction of proteins bound to the membrane (α) can then be modelled with a Langmuir adsorption isotherm, as a function of the microscopic association constant (K_a), the total concentration of protein (P_t), the total concentration of phospholipids (L_t) the maximum number of protein molecules that can bind to a vesicle (n) and the number of lipids per site (m).

$$\delta = \frac{[P_b]}{[L_t]/m} = \frac{n K_a [P_f]}{1 + K_a [P_f]} \tag{8}$$

Here δ is the fraction of occupied sites for the protein at the membrane surface. Since $P_b = \alpha P_t$ and $P_f = (1-\alpha)P_t$ (fractional concentrations) the following expression can be deduced for α (for $K_a \neq 1$)

$$\alpha = \frac{m + K_a(L_t n + P_t m) - K_a P_t m \sqrt{\frac{-4 L_t n}{P_t m} + \left(-1 - \frac{1}{K_a P_t} \frac{L_t n}{m P_t}\right)^2}}{2 K_a m P_t} \tag{9}$$

Eq. 9 can directly be applied to the dependencies of the protein fluorescence or fluorescence anisotropic properties in binding experiments where the protein or lipid concentration is varied. In practice, the quality of the data is such that a fit with eq. 9 yields multiple sets of solutions for parameters K_a, n and m. Therefore independent estimates for at least one of these parameters is required. For example, upper limits for n or m can be derived from the geometries of the protein/lipid system.

Protein association or activity often show sigmoidal dependencies on the mole fraction of a specific lipid. This kinetic cooperativity is mostly attributed to allosteric interactions between lipid binding sites (Bell, 1986) but can in most cases be explained by simple statistics. The probability that a lipid binds to a protein increases with the probability of finding the protein at the membrane surface, and thus with the number of lipids that already interact with the protein. Binding of the first lipids to a protein is thus less probable than binding of the last ones (Mosior & McLaughlin, 1992; Sandermann, 1982).

1.6.2. *Lipid binding to a protein with specific lipid sites*

When we assume reversible lipid binding to a single site at the protein molecule, the lipid binding to this site is simply governed by first order dissociation- (k^-) and second order association rate constants (k^+). For proper expression of the concentration of quencher lipid [Q] and protein [P] in (quasi) two-dimensional lipid aggregates some considerations are required. In a two-dimensional membrane, the concentration of a specific lipid or protein can be

expressed as "surface concentration" (mole/area). This yields binding equations with two-dimensional dissociation constants having units of mole $meter^{-2}$. Each protein molecule has w equivalent and independent lipid binding sites, which are either occupied with lipid Q or vacant. Vacant protein sites (B) are considered to be in equilibrium with specific quencher lipids (Q) in the membrane.

$$K = \frac{[Q]\,[B]}{[BQ]} \tag{10}$$

Considering mass balance relations, the fractional occupancy of a site (γ) with a quencher lipid can then be expressed as a function of the microscopic dissociation constant (k), the total surface concentration of protein (P_t), the quencher concentration in the membrane ($x\,L_t$) and the number of lipid sites per protein molecule (w). Solving the quadratic equation for the fractional occupancy of a site (γ) one obtains:

$$\gamma = \frac{1}{2\,m\,P_t}\left((m\,P_t + k + x\,L_t - \sqrt{(-4\,x\,L_t\,P_t\,m) + (-k - P_t\,m - x\,L_t)^2}\right) \tag{11}$$

Micelles are spherical microensembles consisting of only a few hundreds of molecules (Bastiaens et al., 1993; Hannun et al., 1985). Therefore, a two-dimensional geometry is not a proper approximation. It is more appropriate to replace the protein concentration by the number of protein molecules per micelle. The probability of finding q protein molecules at a micelle is binomially distributed. A simplification arises when the micellar concentration exceeds the protein concentration. Then the probability that more than one protein molecule binds per micelle is negligible yielding a protein "concentration" of either zero or one molecule per micelle. If we observe protein properties (e.g. the quenching of intrinsic tryptophan fluorescence), then cases consisting of micelles without protein molecules are not relevant, and thus P_t in eq. 11 becomes one molecule. When the rate of dissociation of the protein-lipid complex (typically $10^7\ s^{-1}$ (Jain et al., 1987; Devaux & Seigneuret 1985)) is larger than the rate of exchange of quencher lipids between different micelles (see Figure 6), the lipid molecules have to be considered as compartmentalised reactants. The concentration term $x.L_t$ in eq. 11 is then replaced by the number (i) of (quencher) lipid molecules per micelle. The probability (P_i) of finding i lipid molecules in a micelle of size S (S = surfactant number) at a labelling ratio (x) is binomially distributed

$$P_i = \frac{S!}{i!\,(S-i)!}\, x^i\,(1-x)^{S-i} \tag{12}$$

The unit of the association rate constant (k^+) becomes molecule s^{-1} and that of the first order dissociation rate constant remains s^{-1}.

1.6.3. *Lipid exchange at the protein surface*

Most protein-lipid binding processes in membranes can be treated as an equilibrium of two types of lipids L (normal lipid) and Q (quencher lipid), competing for sites on the protein within the bilayer. The relative binding constant K is equal to the ratio of the association constants of both individual lipids (k_Q and k_L) and is thus dimensionless:

$$K = \frac{k_Q}{k_L} = \frac{[L][BQ]}{[Q][BL]} \qquad (13)$$

Since K is a relative constant, it is independent of the actual concentration of quencher, lipid and protein. Only the protein-lipid molar ratio (ρ) is of importance in the derivation of γ. We assume that the individual binding sites are noninteracting and equivalent. Then the expression for the fractional occupancy of sites with lipid Q becomes:

$$\gamma = \frac{1}{2(K-1)w\rho}(1 - w\rho + Kw\rho - x(1-K) -$$

$$\sqrt{-4(-1+K)Kw\rho x) + (-1 + \rho w - Kw\rho + x - Kx)^2} \qquad (14)$$

Eq. 14 simplifies considerably if [BL] << [L] and [BQ] << [Q] (Yeager & Feigenson, 1990):

$$\gamma = \frac{Kx}{1 - x + Kx} \qquad (15)$$

1.6.4. *Relation of the lipid occupancy of a site on a protein to macroscopic properties*

Most investigations of protein-lipid interaction yield only macroscopic observables, like the overall quenching of tryptophan fluorescence by interacting lipid quenchers. When each site of the protein has equal lipid binding properties, the microscopic fractional site occupancy γ simply equals to the average number of sites occupied with the quencher lipid divided by the total number of lipid sites (occupancy state). This can be derived statistically by considering the description of occupancy states of each protein. The probability P_J for given occupancy state having J sites occupied out of a maximum of w sites, is given by a binomial distribution

$$P_J = \frac{w!}{J!(w-J)!}\gamma^J(1-\gamma)^{w-J} \qquad (16)$$

The average number of occupied sites per protein molecule is equal to

$$<J> = \sum_{J=0}^{M} JP_J \qquad (17)$$

Consequently, the fractional protein occupancy is:

$$\frac{<J>}{w} = \gamma \qquad\qquad (18)$$

In most protein-lipid binding experiments the dependence of an observable on the mole fraction of quencher lipid is examined. In these experiments the protein, lipid and quencher lipid concentrations are known. Application of eq. 17 to the macroscopic observations will yield multiple solutions for w, K, and S. Therefore, in the analysis of the binding experiments at least one of these parameters has to be obtained from independent sources.

7. Outline of this thesis

Cellular communication is partly mediated through the lipid modulation of protein activity, structure and dynamics. There are numerous uncertainties in understanding how proteins and lipids influence each others properties. The broad objective of this thesis is to evaluate the mutual modulation of protein and lipid organisation, structure and dynamics with complementary fluorescence approaches. Emphasis is given to protein and lipid components that play a keyrole in cellular communication: the inositol lipids PIP_2, PIP and PI, the lipid cofactor DG, PKC and the membrane ion channel Band 3. In most experiments, lipid binding is monitored by detection of energy transfer between the tryptophan residues in the proteins and the acceptor moieties attached to the lipids. Besides binding studies, several lipid properties influenced by protein interaction are documented. These lipid properties include the lateral dynamics and organisation of mono-pyrene lipids in the membrane, the intramolecular chain dynamics of dipyrene lipids and the rotational dynamics and motional constraints experienced by DPH labelled lipids. Conversely, protein structural and dynamical properties affected by lipids are evaluated as well. Before successful application of fluorescence methods to investigations of protein-lipid interaction, the fluorescence characteristics of proteins and lipid-probes must be understood in well defined systems. Therefore, two model studies were carried out. In Chapter 2, the association of lysozyme with acidic vesicles was considered. This Chapter focuses attention to protein conformation and dynamics when lysozyme interacts with acidic membranes. Apart from the general interest in protein-lipid interactions, this study demonstrates that a fractional analysis of time-resolved fluorescence and fluorescence anisotropy decay curves can provide accurate binding curves of protein molecules to lipid interfaces. The main advantage of the analysis is contained in its simplicity, conservation of time-resolved information and the omission of any detailed interpretation of the decays in terms of relaxation processes. Chapter 3 describes the fluorescence and motional properties of DPH covalently attached to lipid acyl chains of various length. It serves as an introduction to Chapter 4 which covers the effect of PKC interaction on the dynamics of DG labelled with DPH and phorbolester labelled with dansyl in micelles and vesicles. The angular distributions of these fluorescent labelled cofactors with respect to the radial axes of the micelles or vesicles are

compared with those of labelled PC. Complementary experiments were performed with pyrene analogues of lipid cofactors of PKC (Chapter 5). These pyrene labelled cofactors were employed to elucidate the calcium dependence, lipid specificity and interaction forces of the PKC-lipid interaction. The labelled lipids function in this study simultaneously as reporters of acyl chain dynamics and as acceptors of energy of the light-excited tryptophan residues in PKC. In Chapter 6 it is shown that the affinity of PKC for the phosphoinositides PIP_2 and PIP and for DG is high in contrast to several other lipids. Specific interaction with those three lipids was detected by monitoring energy transfer between tryptophan residues of PKC and the pyrene labelled lipids. In addition, evidence is provided that both pyr-PIP_2 and pyr-DG, effectively activates PKC. This observation may have large implications for the current models of the activation mechanism of PKC *in vivo*. The same pyrene labelled phosphoinositides were employed to elucidate the specificity of their interaction with human erythrocyte Band 3 protein in micelles. The efficiency of quenching of the tryptophan fluorescence differed largely for the various probes, decreasing from pyrPIP_2, pyrPIP, pyrPI and pyrPC indicating different affinity of Band 3 for these lipids. Information about the spatial distribution of the different lipids was obtained from a global analysis of the tryptophanyl fluorescence decays obtained in presence of the different pyrene lipids. In the analysis of these fluorescence decays, energy transfer was assumed to occur to pyrene lipids located either in the micellar shell solvating Band 3 or interacting with the hydrophobic regions of the protein. The average rate of energy transfer to each of these pyrene populations was obtained by employment of the Förster relation of energy transfer to distance probability functions of tryptophan - pyrene couples. The fraction of pyrene lipids located in the hydrophobic transhelice region of Band 3 was determined for each pyrene lipid independently, while the radius and height of the cylindrical Band 3 membrane domain and of the surrounding detergent shell were determined globally from simultaneous analysis of multiple quenched decays obtained with all four pyrene lipids. Complementary to Chapter 7, Chapter 8 focuses on the lateral organisation and dynamics of pyrene labelled inositide lipids PIP_2, PIP and PI in the absence and presence of erythrocyte Band 3. In this Chapter an attempt is made to describe the effect of Band 3 on the inter- and intramolecular pyrene collision frequency in terms of a simple two domain model. Finally a summarising discussion of the previous chapters is given (Chapter 9).

1.8. References

Ahlers, M., Hoffmann, M., Ringsdorf, H., Rourke, A.M. & Rump, E. (1991) *Makromol. Chem. Macromol. Symp.* 46, 307-311.

Alcala, J.R., Gratton, E. & Prendergast, F.G. (1987a) *Biophys. J.* 51, 925-936.

Alcala, J.R., Gratton, E. & Prendergast, F.G. (1987b) *Biophys. J.* 51, 587-596.

Ameloot, M., Hendrickx, H., Herreman, W., Pottel, H., van Cauwelaert, F. & van der Meer, W. (1984) *Biophys. J.* 46, 525-539.

Axelrod, D., Koppel, D.E., Schlessinger, J., Elson, E. & Webb, W.W. (1976) *Biophys. J.* 16, 1055-1069.

Baatz, J.E., Eiledge, B. & Whitsett, J.A. (1990) *Biochemistry* 29, 6714-6720.

Bastiaens, P.I.H., DeBeus, A., Lacker, M. & Somerharju, P., Eisinger, J. (1990) *Biophys. J.* 58, 665-675.

Bastiaens, P.I.H., Pap, E.H.W., Borst, J.W., Van Hoek, A., Kulinski, T., Rigler, R. & Visser, A.J.W.G. (1993) *Biophys. Chem.* 48, 183-191.

Bazzi, M.D. & Nelsestuen G.L. (1987) *Biochemistry* 26, 115-122.

Bazzi, M.D. & Nelsestuen G.L. (1991) *Biochemistry* 30, 7961-7969.

Bean, J., Sargent, D. & Schwyzer, R. (1988) *J. Receptor Res.* 8, 375-389.

Bell, R.M. (1986) *Cell* 45, 631-632.

Berne, P.J., Pechukas, P. & Harp, G.D. (1968) *J. Chem. Phys.* 49, 3125-3129.

Berridge, M.J. (1993) *Nature* 361, 315-325.

Bertoli, E., Chapman, D., Cambria, A. & Scapagnini, U. (1987) *Biomembrane and Receptor Mechanisms* 7, 97-111.

Bolen, E.J. & Sando, J.J. (1992) *Biochemistry* 31, 5945-5951.

Bom, V.J.J. & Bertina, R.M. (1990) *Biochem. J.* 265, 327-336.

Boni, L.T & Rando R. (1985) *J. Biol. Chem.* 260, 10819-10825.

Brockerhoff, H. (1986) *FEBS Lett.*, 201, 1-4.

Brumfeld, V. & Lester, D.S. (1990) *Arch. Biochem. Biophys.* 227, 318-323.

Carraway, K.L., Koland, J.G. & Cerione, R.A. (1989) *J. Biol. Chem.* 264, 8699-8707.

Castagna, M., Takai, Y., Kaibuchi, K., Sano, K., Kikkawa, U. & Nishizuka, Y. (1982) *J. Biol. Chem.* 257, 7847-7851.

Chattopadhyay, A. & London, E. (1987) *Biochemistry* 26, 39-45.

Chattopadhyay, A. & McNamee, M. (1991) *Biochemistry* 30, 7159-7164.

Chauhan, V.P.S., & Brockerhoff H. (1988) *Biochem. Biophys. Res. Commun.* 155, 18-23.

Chen, S.G. & Murakami, K. (1992) *Biochem. J.* 28, 33-39

Cheng, K.H., Chen, S.Y., Butko, P., van der Meer, W.B. & Somerharju, P. (1991) *Biophys. Chem.* 39, 137-144.

Chung, L.A., Lear, J.D. & Degrado, W.F. (1992) *Biochemistry* 31, 6608-6616.

Cohen, P. (1982) *Nature* 296, 613-619.

Corven, E.J., Groenink, A., Jalink, K., Eicholtz, T. & Moolenaar, W.H. (1989) *Cell* 59, 45-54.

Dale, R.E., Chen, L.A. & Brand, L. (1977) *J. Biol. Chem.* 252, 7500-7510.

Dale, R.E. & Eisinger, J. (1974) *Biopolymers* 13, 1573-1605.

Dale, R.E., Eisinger, J. & Blumberg, W.E. (1979) *Biophys. J.* 26, 161-194.

Das, S. & Rand, R.P. (1986) *Biochemistry* 25, 2882-2889.

Das, S.&.Rand, R.P. (1984) *Biochem. Biophys. Res. Comm.*, 124, 491-496.

Davis, R.J., Ganong, B. R., Bell, R. M. & Czech, M. P. (1985) *J. Biol. Chem.*, 260, 1562-1566.

Devaux, P.F. & Seigneuret, M. (1985) *Biochim. Biophys. Acta* 822, 63-125.

Dolder, M., Walz, T., Hefti, A. & Engel, A. (1993) *J. Mol. Biol.* 231, 119-132.

East, J.M. & Lee, A.G. (1982) *Biochemistry* 21, 4144-4151.

East, J.M., Melville, D. & Lee, A.G. (1985) *Biochemistry* 24, 2615-2623.

Eisinger, J., Flores, J. & Petersen, W.P. (1986) *Biophys. J.* 49, 987-1001.

Eklund, K., Vuorinen, J., Mikkola, J., Virtanen, J. & Kinnunen, P. (1988) *Biochemistry* 27, 3433-3437.

Epand, R.M. (1987) *Chem. Biol. Interactions*, 63, 239-247.

Epand, R.M., Epand, R. F. & Lancaster, C. R. D. (1988) *Biochim. Biophys. Acta* 945, 161-166.

Epand, R.M. in: *Protein kinase C. Current Concepts and Future Perspectives.* Eds. New York: Ellis Horwood, (1993) 135-156

Epand, R.M. & Lester, D.S. (1990) *Trends Pharm. Sci.* 11, 317-320.

Fiorini, R.M, Valentino, M., Wang, S., Glaser, M. & Gratton, E. (1987) *Biochemistry* 26, 3864-3870.

Fleming, P.J., Koppel, D.E., Lan, A.L.Y. & Strittmatter, P. (1979) *Biochemistry* 18, 5458-5464

Förster, T. (1948) *Ann. Physik.* 2, 55-75.

Förster, T. (1955) z. Elektrochem. 59, 976-980.

Fung, B.K.-K. & Stryer, L. (1978) *Biochemistry* 17, 5241-5248.

Gadella T.W.J. Arndt -Jovin D.J. & Jovin, T.M. (1994), Submitted to *Journal of fluorescence.*

Gadella T.W.J. & Jovin, T.M. (1994), Manuscript in preparation.

Galla, H.J. & al., e. (1979) *J. Membrane Biol.* 48, 215-219.

Galla, H.J. & Sackman, E. (1974) *Biochim. Biophys. Acta* 339, 103-115.

Gasset, M., Onaderra, M., Goormaghtigh, E. & Gavilanes, J. (1991) *Biochim. Biophys. Acta* 1080, 51-58.

Golan, D., Alecio, M., Veatch, W. & Rando, R. (1984) *Biochemistry*, 23, 332-339.

Grainger, D., Reichert, A., Ringsdorf, H. & Salesse, C. (1989) *FEBS Lett.* 252, 73-82.

Grainger, D., Reichert, A., Ringsdorf, H. & Salesse, C. (1990b) *Biochim. Biophys. Acta* 1023, 365-379.

Grainger, D., Reichert, A., Ringsdorf, H., Salesse, C., Davies, D. & Lloyd, J. (1990a) *Biochim. Biophys. Acta* 1022, 146-154.

Hanicak, A., Pap, E., van Hoek, A. & Visser, A.J.W.G. (1994) Manuscript in preparation.

Hanks, S.K., Quinn, A. M. & Hunter, T. (1988) *Science* 241, 45-52.

Hannun, Y.A. Loomis, C.R., Merrill, A.H., & Bell, R.M. (1986) *J. Biol. Chem.* 261, 12604-12609.

Hannun, Y.A., Loomis, C. R. & Bell, R. M. (1985) *J. Biol. Chem.* 260, 10039-10043.

Harris, R.W., Sims, P.J. & Tweten, R.K. (1991) *J.Biol. Chem.* 266, 6936-6941.

Haverstick, D.M. & Glaser, M. (1987) *Proc. Natl. Acad. Sci.* 84, 4475-4479.

Hermetter, A. & Lakowicz, J.R. (1986) *J. Biol. Chem.* 261, 16704-16713.

House, C. & Kemp, B.E. (1987) *Science* 238, 1726-1728.

Huang F.L. & Huang K.P. (1991) *J. Biol. Chem.* 266, 8727-8733.

Jacobson, K. (1983) *Cell Mobility* 3, 367-373.

Jähnig, F. (1979) *Proc. Natl. Acad. Sci.* 76, 6361-6365.

Jähnig, F., Vogel, H. & Best, L. (1982) *Biochemistry* 21, 6790-6798.

Jain, M.K., Egmond, M.R., Verheij, H.M., Apriz-Castro, R.J., Dijkman, R. and De Haas, G.H. (1982) *Biochim. Biophys. Acta* 688, 341-348.

Jain, M.K. & Zakim, D. (1987) *Biochim. Biophys. Acta* 906, 33-68.

Jaynes, E.T. (1968) *Trans. Biomed.* 4, 227-234.

John, E. & Jähnig, F. (1991) *Biophys. J.* 60, 319-328.

Jones, M. & Lentz, B. (1986) *Biochemistry* 25, 567-574.

Karnovsky, M.J., Kleinfeld, A.M., Hoover, R.L. & Klausner, R.D. (1982) *J.Cell. Biol.* 94, 1-6.

Khan, W.A., Blobe, G.C. & Hannun, Y.A. (1992) *J. Biol. Chem.* 267, 3605-3612.

Kimelman, D., Tecoma, E.S., Wolber, P.K., Hudson, B., Wickner, W.T. & Simoni, R.D. (1979) *Biochemistry* 18, 5874-5882.

Klee, C.B. (1988) *Biochemistry* 27, 6645-6653.

Kleinfeld, A.M. & Lukacovic, M.L. (1985) *Biochemistry* 24, 1883-1890.

Koda, Y., Wada, A., Yanagihara, Y., Uezono, Y. & Izumi, F. (1989) *Neuroscience* 29, 495-502.

Koppel, D.E., Flemming, P.J. & Strittmatter, P. (1979) *Biochemistry* 18, 5450-5457.

Lakowicz, J.R. *Principles of Fluorescence Spectroscopy.* New York: Plenum Press, 1983.

Lakowicz, J.R., Johnson, M.L., Wiczk, A.B. & Steiner, R.F. (1987) *Chem. Phys. Lett.* 138, 587-593.

Lee, M.H. & Bell, R.M. (1989) *J. Biol. Chem.* 264, 14797-14805.

Lee, M.H. & Bell R.M. (1991) *Biochemistry* 30, 1041-1049.

Lentz, B. in: "Organisation of membrane lipid by intrinsic membrane proteins." Lipid domains and the relationship to membrane function. Aloia R.C., Curtain, C.C. & Gordin L. Eds. New York: 1988, 141-162.

Lentz, B. (1989) *Chem. Phys. Lipids* 50, 171-178.

Lentz, B., Clubb, K., Barrow, D. & Meissner, G. (1983) *Proc. Natl. Acad. Sci.* 80, 2917-2921.

Lester, D.S. & Brumfeld V., *Int J. Biol. Macromol.*, 12, 251-256.

Leto, T.L., Roseman, M.A. & Holloway, P.W. (1980) *Biochemistry* 19, 1911-1916.

Levin, I.W., Thompson, T.E., Barenholz, Y. & Porter, N.A. (1985) *Biochemistry* 24, 6282-6286.

Lewis, B.A. & Enelman, D.M. (1983) *J. Mol. Biol.* 166, 211-217.

Long, M.M., Urry, D.W. & Stoeckenius, W. (1977) *Biochem. Biophys. Res. Commun.* 75, 725-731.

Makowske, M. & Rosen, O.M. (1989) *J. Biol. Chem.* 264, 16155-16159.

Markello, T., Zlotnick, A., Everett, J., Tennyson, J. & Holloway, P.W. (1985) *Biochemistry* 24, 2895-2901.

McIntosh, T.J. & Holloway, P.W. (1987) *Biochemistry* 26, 1783-1788.

Merrill, A.H., Hannun, Y.A. & Bell, R.M. (1993) In: *Advances in Lipid Research: Sphingolipids and their Metabolites* (Bell, RM., Hannun, Y.A. & Merrill A.H. eds.) Academic Press, San Diego, 25, 1-24

Moore, B., Lentz, B. & Meissner, G. (1978) *Biochemistry* 17, 5248-5255.

Mori, T., Takai, Y., Yu, B., Takahashi, J., Nishizuka, Y. & Fujikura, T. (1982) *J. Biochem.* 91, 427-431.

Mosior, M. & McLaughlin, S. (1991) *Biophys. J.* 60, 149-159.

Mosior, M. & McLaughlin, S. (1992) *Biochim. Biophys. Acta* 1105, 185-187.

Newton, A.C. (1993) *Annu. Rev. Biophys. Biomol. Struct.* 22, 1-25.

Nishiya, T. & Hui, L. (1991) *J. Biochem.* 110, 732-736.

Nishizuka, Y. (1992) *Science* 258, 607-614.

Ohki, K.O., Sekiya, T., Yamauchi, T. & Nozawa, Y. (1982) *Biochim. Biophys. Acta* 693, 341-350.

Oishi, K., Raynor, R.L., Charp, P.A. & Kuo, J.F. (1988) *J. Biol. Chem.* 263, 6865-6971.

Ono, Y., Fujii, T., Igarashi, K., Kuno, T., Tanaka, C. Kikkawa, U. & Nishizuka, Y. (1989) *Proc. Natl. Acad. Sci.* 86, 4868-4871.

Orr, J.W., Keranen, L.M. & Newton, A.C. (1992) *J. Biol. Chem.* 267, 15263-15266.

Owen, C.S. (1975) *J. Chem. Phys.* 62, 3204-3207.

Paddy, M.R., Dahlquist, F.W., Davis, J.H. & Bloom, M. (1981) *Biochemistry* 20, 3152-3162.

Pelech, S.L. & Vance, D.E. (1989) *Trends Biochem. Sci.* 14, 28-30.

Peters, M. & Grant, C. (1984) *Biochim. Biophys. Acta* 775, 273-282.

Pink, D. & MacDonald, A. (1986) *Biochim. Biophys. Acta* 863, 243-252.

Quest, A.F.G., Bloomenthal, J., Bardes, E.S.G. & Bell, R.M. (1992) *J. Biol. Chem.* 267, 10193-10197.

Rando, R.R. & Young, N. (1984) *Biochem. Biophys. Res. Commun.* 122, 818-823.

Rapaport, D. & Shai, Y. (1991) *J. Biol. Chem.* 266, 23769-23775.

Rapaport, D. & Shai, Y. (1992) *J. Biol. Chem.* 267, 6502-6509.

Rhee, S.G., Suh, P.G., Ryh, S.H. & Lee S.Y. (1989) *Science* 244, 546-550

Sandermann, H. (1978) *Biochim. Biophys. Acta* 515, 209-217.

Sandermann, H. (1982) *Eur. J. Biochem.* 127, 123-128.

Sanders, J.C., Poile, T.W., Wolfs, C.J.A.M. & Hemminga, M.A. (1992) *Biochim. Biophys. Acta* 1110, 218-224.

Sargent, D.F., Bean, J.W. & Schwyzer, R. (1988) *Biophys. Chem.* 31, 183-93.

Sargent, D.F. & Schwyzer, R. (1986) *Proc. Natl. Acad. Sci* 83, 5774-5778.

Sassaroli, M., Vaukonen, M., Perry, D. & Eisinger, J. (1990) *Biophys. J.* 57, 281-290.

Kooyman R.P.H., Vos M.H., and Levine Y.K. (1983) *Chem Phys.* 81, 461-472.

Seelig, J. (1990) *Cell Biol.* 14, 353-360.

Shai, Y.F., Caratasch, C., Shih, Y.L., Edwards, C. & Lazarovici, P. (1991) *J. Biol. Chem.* 266, 22346-22354.

Small, E.W. & Isenberg, I. (1977) *Biopolymers* 16, 1907-1928.

Snoek, G. T., Feijen, A., Halem, W. J., Rotterdam, W. V. & De Laat, S. W. (1988) *Biochem. J.* 255, 629-637.

Stankowski, S., Pawlak, M., Kaisheva, E., Robert, C. & Schwarz, G. (1991) *Biochim. Biophys. Acta* 1069, 77-86.

Steinberg, 1.Z. (1971) *Annu. Rev. Biochem.* 40, 83-114.

Straume, M. & Litman, B. (1987) *Biochemistry* 26, 5113-5120.

Stryer, L. (1978) *Annu. Rev. Biochem.* 47, 819-846.

Szabo A. (1984) *J. Chem. Phys.* 81, 150-167.

Talbot, J.C., Faucon, J.F. & Dufourq, J. (1987) *Eur. Biophys. J.* 15, 147-157.

Teissie J. (1981) *Biochemistry* 20, 1554-1560

Tocanne, J.F., Dupou-Cezanne, L., Lopez, A. & Tournier, J.F. (1989) *FEBS Lett.* 257, 10-16.

Van der Meer, W., Pottel, H., Herreman, W., Ameloot, M., Hendrickx, H. & Schröder, H. (1984) *Biophys. J.* 46, 515-523.

Van der Meer, B., Raymer, M.A., Wagoner, S.L., Hackney, R.L., Beechem, J.M. & Gratton, E. (1992) in: *SPIE Time Resolved Laser Spectroscopy* in *Biochemistry III* 1640, 220-229.

Van der Sijs, D.A., Van Faasen, E.E. & Levine, Y.K. (1994) *Chem. Phys. Letters* 216, 559-565.

Van Langen, H., Levine, Y.K., Ameloot, M. & Pottel, H. (1987) *Chem. Phys. Lett.* 140, 394-400.

Van Ginkel G., van Langen H., Levine Y.K. (1989) *Biochimie* 71 23-32.

Vanderkooi, J.M. & Gallis, J.B. (1974) *Biochemistry* 13, 4000-4007.

Vanderkooi, J.M., Kaposi, A. & Fidy, J. (1993) *Trends Biochem. Sci.* 18.

Vauhkonen, M., Sassaroli, M., Somerharju, P. & Eisinger, J. (1989) *Eur. J. Biochem.* 186, 465-471.

Vauhkonen, M., Sassaroli, M., Somerharju, P. & Eisinger, J. (1990) *Biophys. J.* 57, 291-300.

Vaz, W.L.C., Goodsaid-Zalduondo, F. & Jacobson, K. (1984) *FEBS Lett.* 174, 199-207.

Veld, G., Driessen, A., Denkamp, J. & Konings, W. (1991) *Biochim. Biophys. Acta* 1065, 203-212.

Verbist, J., Gadella, T.W.J., Raeymaekers, L., Wuytack, F., Wirtz, K.W.A. & Casteels, R. (1991) *Biochim. Biophys. Acta* 1063, 1-6.

Vincent, M. & Gallay, J. (1991) *Eur. Biophys. J.* 20, 183-191.

Vogel, H. & Jähnig, F. (1986) *Biophys. J.* 50, 573-582.

Weber, G. (1971) J. Chem. Phys. 55, 2399-2407.

Wang S., Beechem J.M., Gratton E. and Glaser M. (1991) *Biochemistry* 30, 5565-5572.

Williams, W.B., Scotto, A.W. & Stubbs, C.D. (1990) *Biochemisty* 29, 3248-3255.

Wolber, P.K. & Hudson, B. (1982) *Biophys. J.* 37, 253-262.

Wolf, D.E., Libscomb, A.C. & Maynard, V.M. (1988) *Biochemistry* 27, 860-865.

Yeager, M.D. & Feigenson, G.W. (1990) *Biochemistry* 29, 4380-4392.

Zannoni, C., Arcioni, A. & Cavatorta, P. (1983) *Chem. Phys. Lipids* 32, 179-250.

Reed, R., Mattai, A., Shipley, J., Graham G. (1987) *Biochemistry* 26, 824-832.

Chapter 2

A novel method for quantitative studies of protein membrane interactions: lysozyme adsorption to phospholipid vesicles

Abstract

Experiments directed to the interaction of lysozyme with liposomes consisting of phosphatidylcholine (PC) and phosphatidylserine (PS) have been conducted using a double approach, monitoring both protein and lipid fluorescence and fluorescence anisotropy of the protein. The binding of lysozyme to the unilamellar vesicles was quantified using a novel method of analysis in which the fractional contribution at moderate binding conditions is determined from either the total fluorescence or anisotropy decay curves of tryptophan decay profiles corresponding to limiting binding conditions. In the energy transfer experiments PC and PS molecules labelled with two pyrene moieties served as energy acceptors of the excited tryptophans in lysozyme. The binding exhibited a strong dependence on the mole fraction of negatively charged PS in neutral PC membranes and on the ionic strength. Changes in the tryptophan fluorescence decay characteristics were found to be connected with long correlation times indicating conformational rearrangements induced by binding of the protein to these lipid membranes. The dynamics of membrane bound protein appeared to be dependent on the physical state of the membrane. Independent from protein fluorescence studies, formation of a protein-membrane complex can also be observed from the lipid properties of the system. The interaction of lysozyme with di-pyrenyl-labelled phosphatidylserine in anionic PS/PC membranes resulted in a substantial decrease of the intramolecular excimer formation, while the excimer formation of dipyrenyl-labelled phosphatidylcholine in neutral PC membranes barely changed in the presence of lysozyme.

8.1 Introduction

The interaction of proteins with lipids is relevant for a wide range of biological and biotechnological processes. For example, various peripheral proteins are activated upon binding to membranes. To elucidate the principles that govern protein adsorption to lipid interfaces and conformational stability upon absorption, it is necessary to examine simple, well-defined systems and to have methods available for quantification of the absorbed amounts. Since lysozyme is a stable, well-characterised protein with known 3-dimensional structure having six tryptophanyl residues (Imoto et al., 1972), it can easily serve as a model protein in these interaction studies. In this paper we report on the rotational dynamics of lysozyme molecules interacting with phospholipid vesicles derived from the anisotropy decays of tryptophan fluorescence of the protein. The dependence of this interaction on the ionic strength and on the membrane surface charge was investigated. A simple method of analysis of time-resolved fluorescence data is applied to these protein-lipid systems. Reversible association of lysozyme to the membrane was

also studied by monitoring resonance energy transfer from excited tryptophans in lysozyme to pyrene labelled phosphatidylserine (PS) and phosphatidylcholine (PC). Both techniques have proven to be very sensitive for following protein association at membrane surfaces (Pap et al., 1993; Bastiaens et al., 1993; Omata & Friedman, 1991; Vincent & Gallay, 1991; Houbre et al., 1990). However, precise quantitation of the absorbed amount of protein is often a problem in such studies. In fluorescence lifetime distribution analysis, no unique lifetime class of tryptophan residues arises from interactions of lysozyme with the membrane vesicles, which makes it not very suitable for direct quantitation of protein adsorbed to lipid vesicles. In principle, the average tryptophan fluorescence lifetime can be obtained from the fluorescence decay and related to the efficiency of energy transfer to lipid acceptors (Dale et al., 1979). This parameter can then be used to quantify the interaction between protein and quencher lipids (Pap et al., 1993; Bastiaens et al., 1993). A disadvantage of this approach is that the time-resolved information is averaged out. An alternative method is global analysis, in which decay parameters characteristic for the bound or free form are globally linked in a set of experiments (Beechem et al., 1991). This has proved to be a powerful method of analysis, but an interpretation of the fluorescence and anisotropy decays using a specific model is needed, and only a limited number of relaxation parameters can be employed for the analysis. The complexity of a system containing multiple intrinsic tryptophan residues does not allow for a detailed photophysical interpretation of the decay. In this paper an alternative method is proposed to obtain the fraction of bound protein from time-resolved fluorescence and anisotropy decays provided that the decay curves corresponding to free protein and of a sample where the majority of the protein molecules is bound are known. Next to this quantitative analysis of lysozyme-lipid interaction, distribution analysis of the tryptophan fluorescence and fluorescence anisotropy recovered changes in the conformation and dynamics of lysozyme accompanied with its binding to membranes.

2.2 Experimental procedures

Materials

Hen egg white lysozyme was purchased from Boehringer (Mannheim). Bovine brain phosphatidylserine (PS), 1, 2-dipalmitoyl-L-phosphatidylserine, 1, 2-dimyristoyl-L-phosphatidylcholine and 1, 2-dipalmitoyl-L-phosphatidylcholine were obtained from Sigma (St. Louis, MO). Di-('-pyrenedecanoyl)-PC (dipyr$_{10}$PC) and di-('-pyrenebutyryl)-PC (dipyr$_4$PC) were synthesised by methods described previously (Patel et al., 1979). Transphosphatidylation of labelled phosphatidylcholine by phospholipase D yielded di-pyrene PS (Comfurius et al., 1990). Purification of the lipids was performed with high performance liquid chromatography on a silicic acid column (240 x 10 mm, LiChroprep Si 60, Merck, Germany). Elution was performed with an increasing methanol gradient (0-40%) in chloroform. All buffers were made with nanopure water. All other chemicals were of analytical grade. Unless otherwise noted, experiments were performed using 20 mM Tris HCl buffer, pH 7.5, 20 μM EGTA at 20 °C.

Vesicle Preparation

Small unilamellar vesicles were prepared by sonication using the method of Barenholz et al. (1977). The total phospholipid content was determined by phosphate analysis according to the method of Rousser et al., (1970). The pyrene concentration was determined by measuring the optical density at 342 nm in ethanol/DMSO (75:25 v/v) (ε=39700 $M^{-1}cm^{-1}$).

Fluorescence methods

Pyrene monomer and excimer fluorescence intensities were recorded on a DMX-1000 spectrofluorometer (SLM Aminco, Urbana, IL). The measurements were corrected for the background emission and the spectral instrument variations. Both excitation and emission monochromator bandwidths were set at 4 nm. Monomer and excimer emissions were detected at 377 nm and 480 nm, respectively. In the excimeric experiments the excitation wavelength was 347 nm, while in the energy transfer experiments dual wavelength excitation was used (290 and 335 nm).

Time-resolved fluorescence measurements were carried out with a time-correlated single photon counting setup as described elsewhere (Pap et al., 1993). The excitation wavelength was 295 nm. Fluorescence was selected using a 3 mm WG 335 cut-off filter (Schott, Mainz), an interference filter at 348.8 nm (Schott, bandwidth 4.8 nm FWHM) and a sheet type polariser (Polaroid type HNP'B). All measurements consisted of a number of sequences of registration of 10 s parallel and 10 s perpendicular polarised emission. After each sample the background of samples in the absence of lysozyme was measured, at one fifth of the time of sample acquisition. p-Terphenyl (Eastman Kodak Co.) dissolved in ethanol served as reference compound (τ =1.06 ns (Vos et al., 1987)) to yield the dynamic instrumental response function of the set-up (van Hoek et al., 1985). The sample temperature was 20 °C. The data were collected in a multichannel analyser (Nuclear Data model ND66); 1024 channels were used per experimental decay with a time spacing of 30 ps per channel. After transfer the data were analysed on a Silicon Graphics Personal Iris computer model 4D-35 using the maximum entropy method (Maximum Entropy Data Consultants Ltd., Cambridge, UK) of analysis yielding fluorescence-lifetime and correlation-time distributions of the enzyme (Livesey & Brochon, 1987; Brochon et al., 1992; Vincent & Gallay, 1991). Two-dimensional methods were used which investigate cross-correlations between τ and ϕ (Brochon et al., 1992).

2.3   Computational   Methods

Fractional analysis of decay curves

The goal of analysis using the fractional approach is simply to obtain an accurate value of the fraction of limiting states in a multicomponent sample. We assume that a multicomponent system (e.g. bound and free protein) is a mixture of these limiting states only. In the remainder of this section we will explore the details of this approach.

The case of energy transfer from tryptophan residues to lipid acceptors

The energy transfer fluorescence experiments yielded two limiting fluorescence decays: a strongly quenched one, $F(t)_s$, where the majority of the protein molecules is associated to pyrene containing vesicles and a non-quenched decay $F(t)_0$ of the protein in buffer. Provided that only two forms of the protein exist (bound and free), decays measured at moderate binding conditions, $F(t)_x$, can be described as a combination of both limiting decays $F(t)_0$ and $F(t)_s$. Elimination of differences in the instrumental response (experiments were conducted at different days) was achieved by convolution of the linear combination of the ideal (response to δ pulse) fluorescence $f(t)_0$ and $f(t)_s$ with the impulse response profile of the intermediate decay, $P(t)_x$. The actual decays $f(t)_0$ and $f(t)_s$ were obtained from transformation of MEM obtained lifetime distributions of the corresponding experimental decays from the lifetime domain into the time domain:

$$f(t)_{0,s} = \int_0^\infty a(\tau)\, e^{-t/\tau}\, d\tau \qquad (1)$$

where $\alpha(\tau)$ is the contribution of lifetime τ in the decay. The experimental decay at moderate binding conditions can then be described as a combination of two convolution products:

$$F(t)_x = (1-\beta)\, N_0\, P(t)_x * f(t)_0 + \beta\, N_s\, P(t)_x * f(t)_s \qquad (2)$$

where β and $(1-\beta)$ represent the fractional contributions of the limiting decays to $F(t)_x$ and N_O, N_s normalisation factors which eliminate differences in initial total fluorescence intensity in the various experiments $(f_{n(t=0)}/f_{x(t=0)})$.

The case of fluorescence anisotropy in which the protein bound to the membrane is more immobilised than free in solution

Similarly, in the time-resolved fluorescence anisotropy titration experiments the characteristic decays at limiting binding conditions can be used to describe the anisotropy decay at moderate binding conditions (R_x). The relationship between the calculated intermediate anisotropy decay and the polarised components $(f_{/\!/n}, f_{\perp n})$ of the limiting decays is given by:

$$r(t)_x = \frac{(1-\beta)\, D(t)_0 + \beta\, D(t)_s}{f(t)_x} \qquad (3)$$

where $D(t)_0$ and $D(t)_s$ correspond to $f(t)_{/\!/0}\text{-}f(t)_{\perp 0}$ and $f(t)_{/\!/s}\text{-}f(t)_{\perp s}$ respectively. $r(t)_x$ is obtained from the experimental polarised components:

$$F(t)_{/\!/} = P(t)_x * \left(\frac{2}{3} r(t)_x f(t)_x + \frac{1}{3} f(t)_x \right) \qquad (4)$$

$$F(t)_\perp = P(t)_x * \left(\frac{-1}{3} r(t)_x f(t)_x + \frac{1}{3} f(t)_x \right) \qquad (5)$$

Relationship of β and the fraction of bound protein

Until now the fractional contribution was determined assuming that only two forms are present in the two-component mixtures samples. To assign the fractional contribution β to the actual fraction of bound protein in the sample (α) we have to consider the following: In a mixed sample, the fluorescence and fluorescence anisotropy properties of non-interacting lysozyme will contribute to respectively $F(t)_0$ and $D(t)_0$. Lysozyme molecules associated with membranes contribute to the decays $F(t)_m$ or to $D(t)_m$ which are approached by $F(t)_s$ and $D(t)_s$, but in principle unknown. Similarly to earlier explanations $F(t)_s$ can be expressed with a linear combination of x $F(t)_0$ and (1-x) $F(t)_m$. Substituting this expression for $F(t)_s$ into eq. 2 or 3 yields a relation of β to the actual fraction of bound protein in the sample α:

$$\beta = \frac{(\alpha - 1)}{(x - 1)} \qquad (6)$$

β directly reflects the fraction of bound lysozyme (α) if $F(t)_s$ corresponds to $F(t)_m$ (x = 0). If $F(t)_s$ does not correspond to $F(t)_m$ (x > 0), some type of model dependent step will need to be performed to obtain a value for x which describes the association of the protein to the lipid interface.

Binding model

Free protein (P_f) is considered to be in equilibrium with interaction sites on the membrane. The binding sites on the membrane surface must be interpreted as the average number of phospholipid molecules affected by the protein. The fraction of bound proteins (α) can then be modelled with a Langmuir adsorption isotherm, as a function of the association constant (K_a), the total concentration of protein (P_t), the total concentration of phospholipids (L_t) the maximal number of protein molecules that can bind to a vesicle (n) and the number of lipids per site (m).

$$v = \frac{[P_b]}{[L_t] / m} = \frac{n K_a [P_f]}{1 + K_a [P_f]} \qquad (7)$$

Here v is the fraction of occupied sites for the protein at the membrane surface. Since $P_b = \alpha P_t$ and $P_f = (1-\alpha) P_t$ (fractional concentrations) the following expression is obtained for α:

$$\alpha = \frac{m + K_a (L_t n + P_t m) - K_a P_t m \sqrt{\dfrac{-4 L_t n}{P_t m} + \left(-1 - \dfrac{1}{K_a P_t} \dfrac{L_t n}{m P_t}\right)^2}}{2 K_a m P_t} \qquad (8)$$

This function can be applied to the β values obtained with the fractional analysis.

2.4 Results and Discussion

### 2.4.1. Conformational alterations accompany membrane binding

Although lysozyme contains six tryptophanyl residues, it has been estimated that more than 80% of its fluorescence comes from two residues (Trp-62 and/or Trp-108) (Imoto et al., 1971). Figure 1A shows the result of a two-dimensional maximum entropy analysis of tryptophan fluorescence of lysozyme in aqueous buffer solution describing the associative behaviour between the fluorescence lifetime components and the rotational correlation times. The results are given in the form of contour plots which have a relatively simple pattern. The fluorescence lifetime distribution of tryptophan in lysozyme, is described by two discrete lifetime peaks. A main contour ($\tau = 1.7$ ns, $\phi = 4.4$ ns) in the image accounts for 92 % of the emission. The relatively short correlation time (for a protein with molecular mass of 14900 Da) might partly originate from a faster apparent depolarisation due to homo-energy transfer between tryptophan residues within the protein molecule. In the presence of DPPC vesicles, the total tryptophan fluorescence image is almost similar. An additional minor contour (the contour levels are log-scaled) appears at long correlation times indicating a small second population of membrane bound lysozyme molecules with different motional properties (Figure 1B). In the presence of anionic membranes consisting of DPPC and DPPS (3:1) however, the contour peak of free enzyme is fully replaced by two other peaks with fluorescence lifetime barycenters of 0.29 and 1.58 ns associated with very long correlation times (Figure 1C). Here all the lysozyme molecules are immobilised by the lipid membranes. Interactions of lysozyme with vesicles do not only lead to changes in the protein dynamics, but also change the tryptophan fluorescence lifetime distribution (see also Vincent & Gallay, 1991; Brochon et al., 1992). Since a faster decay of tryptophan fluorescence is characteristic for a 'quenched' conformation of the protein we conclude that stabilisation of structural conformers of lysozyme by the membrane leads to the appearance of shorter lifetime distribution components associated with long correlation time components. The lipid binding may affect hydrogen bonding, hydrophobic or electrostatic interactions within the protein and, consequently, may lead to conformational rearrangements that make the tryptophan residues more accessible to water or lead to . These observations are in agreement with the lipid induced enhancement of helical secondary structure of lysozyme observed by Lippert and coworkers (Lippert et al., 1980).
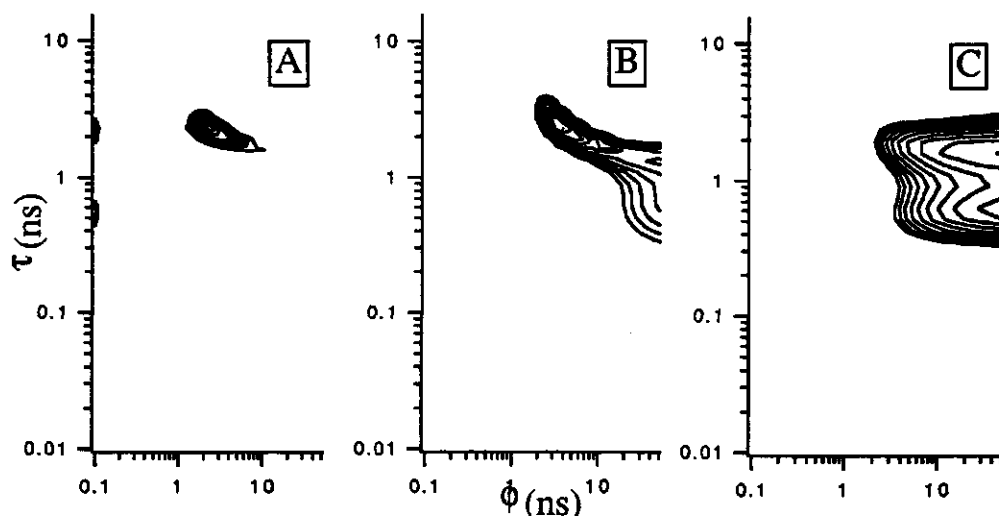
Figure 1 MEM recovered contour plots (τ, ϕ) of polarised tryptophan fluorescence of lysozyme in buffer (A), in the presence of vesicles of 60 µM DOPC (B), and in presence of 60 µM DOPC/brainPS (70:30) (C). An initial anisotropy of 0.23, obtained from the one-dimensional anisotropy analysis, was fixed in the two-dimensional analysis

2.4.2. Reversibility of binding

In order to investigate reversibility of binding a competition experiment was performed in which pyrene loaded vesicles interacting with lysozyme molecules were replaced by unloaded vesicles. In this experiment the monomeric pyrene steady state emission was monitored at 377 nm. The ratio was determined of monomer fluorescence when exciting at the pyrene excitation minimum at 290 nm and at the pyrene excitation maximum at 330 nm. At the first exciting wavelength, mainly the pyrene moieties within the Förster radius of lysozyme are excited via resonance energy transfer from primary excited tryptophans. The excitation at 330 nm excites pyrene directly and this signal is used as an internal control to correct for secondary effects like changes in the excimer/monomer intensity ratio. In figure 2 the monomer fluorescence ratio is plotted for DOPC/brainPS/dipyr$_{10}$PS (3:1:1) and DOPC/dipyr$_{10}$PC (4:1) as a function of the lysozyme concentration. In case of the anionic membranes, the monomer ratio increases with the lysozyme concentration, indicating an increase of sensitised pyrene excitation via lysozyme, and thus illustrating membrane binding of the protein. Saturation of this effect is achieved. When a 10-fold excess of anionic vesicles without pyrene lipids is added, the ratio reduces to almost its original value of 0.21. This indicates that the binding of lysozyme to charged membranes is essentially reversible. In case of the neutral PC membranes no systematic effect is observed upon addition of lysozyme indicating the absence of binding to the membrane.
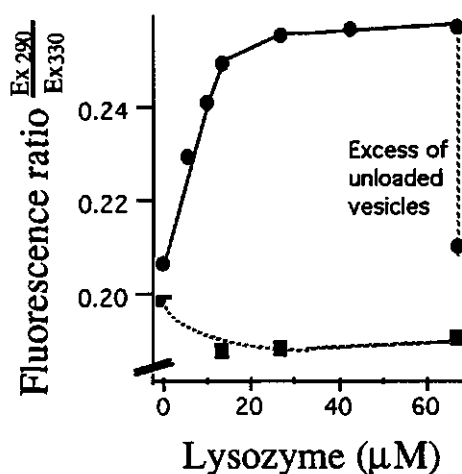
Figure 2 The dependence of monomer fluorescence ratio at two excitation wavelengths (290 nm/330 nm) of dipyrene lipids on the lysozyme concentration. The vesicles consisted of DOPC/brain-PS/dipyr$_{10}$PS (3:1:1) (●) and DOPC/dipyr$_{10}$PC (4:1) (■). The total lipid concentration was kept constant to a concentration of 10 μM during the protein titration. After addition of an excess of DOPC/brain-PS without pyrene lipid (final concentration 100 μM) the ratio of monomeric pyrene fluorescence reverses to its initial value, indicating that the binding is reversible.

The reversibility of binding is in not accordance with previous studies using artificial solid surfaces (Schmidt et al., 1990; Horsey et al., 1991). In case of hydrophobic surfaces, however, the interaction is governed by other forces. The strong interaction with hydrophobic interfaces partly unfolds the protein irreversibly (Schmidt et al., 1990; Horsey et al., 1991). Even larger denaturation effects were observed with lysozyme irreversibly interacting with charged silica as adsorption surface (Horsey et al., 1991). This is not surprising, since in lipid membranes the charged headgroups are mobile and they can adapt their position with respect to opposite charges at the protein surface. The charges at the silica surface, however, are strongly localised and might be responsible for spreading the lysozyme molecule out on the surface (Horsey et al., 1991). This could lead to more extended conformational adaptations causing irreversibility of binding.

2.4.3. The effect of the state of the membrane on bound lysozyme dynamics
The influence of lipid phase of the membrane on fluorescence and dynamical behaviour of lysozyme was investigated by measuring the fluorescence and anisotropy decays in the presence of model membrane systems of DPPC (gel state, neutral), DPPC/DPPS (70:30) (gel state, negatively charged) or DOPC/brain-PS (70:30) (fluid, negatively charged). Correlation time distributions, obtained from MEM analysis of the anisotropy decays of lysozyme in the presence of these vesicles having different states of the membrane are presented in figure 3.
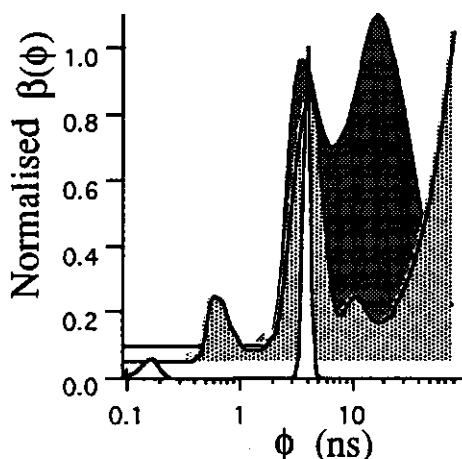
Figure 3 MEM recovered correlation time spectra from fluorescence anisotropy decay of lysozyme in the presence of DPPC vesicles (☐), vesicles of DPPC/DPPS (70:30) (▨) and vesicles of DOPC/brain-PS (70:30) (▧). The used lysozyme and lipid concentrations were 1.5 µM and 60 µM respectively.

In presence of the electrically neutral DPPC vesicles, the decay of anisotropy is mainly described with a single correlation time distribution characteristic of that of enzyme in aqueous solution. In the presence of charged membranes next to this peak an additional peak appears, which originates from lysozyme bound to the membranes. The fluorescence of the lysozyme-vesicle complex depolarised more slowly when lysozyme interacted with membranes in the gel state (DPPC/DPPS (3:1)) than with membranes in the fluid state (DOPC/brain-PS (3:1)). The effective rotational correlation time of lysozyme bound to DPPC/DPPS vesicles is increased to an infinitely long correlation time as compared to a value of approximately 30 ns for lysozyme bound to DOPC/brain-PS vesicles. The absence of such very long rotational correlation time indicates that the rotational motion of lysozyme associated to DOPC/brain-PS membranes is essentially isotropic, while the finite anisotropy at long times (r_∞) in case of DPPC/DPPS vesicles indicates that the protein rotates anisotropically with respect to the surface of the gel-phase bilayer. The physical state of the membrane thus significantly affects the dynamical behaviour of peripherally associated lysozyme. This effect can be due to differences in headgroup packing in the different lipid phases or alternatively to differences in hydrophobic interaction between lysozyme and lipid acyl chains.

2.4.4. Dependence of lysozyme-membrane association on mixed lipid concentration

In order to evaluate the binding of lysozyme to acidic membranes the polarised decays of lysozyme were monitored in the presence of various amounts of vesicles composed of DPPC/DPPS/dipyr$_4$PC (67.5:27.5:5). In the presence of these pyrene loaded vesicles, the tryptophan fluorescence is quenched (Figure 4A, lower panel) and reduction of the barycenter value for

each lifetime class is observed (data not shown). The titration data were analysed in two steps in order to obtain a value for the binding constant (K_a) of lysozyme for the mixed lipid membranes. In the first step the dependence of the fractional contribution β on the concentration of mixed lipid, was obtained by applying the fractional approach of fluorescence analysis (see eq. 2) to all these fluorescence decays.
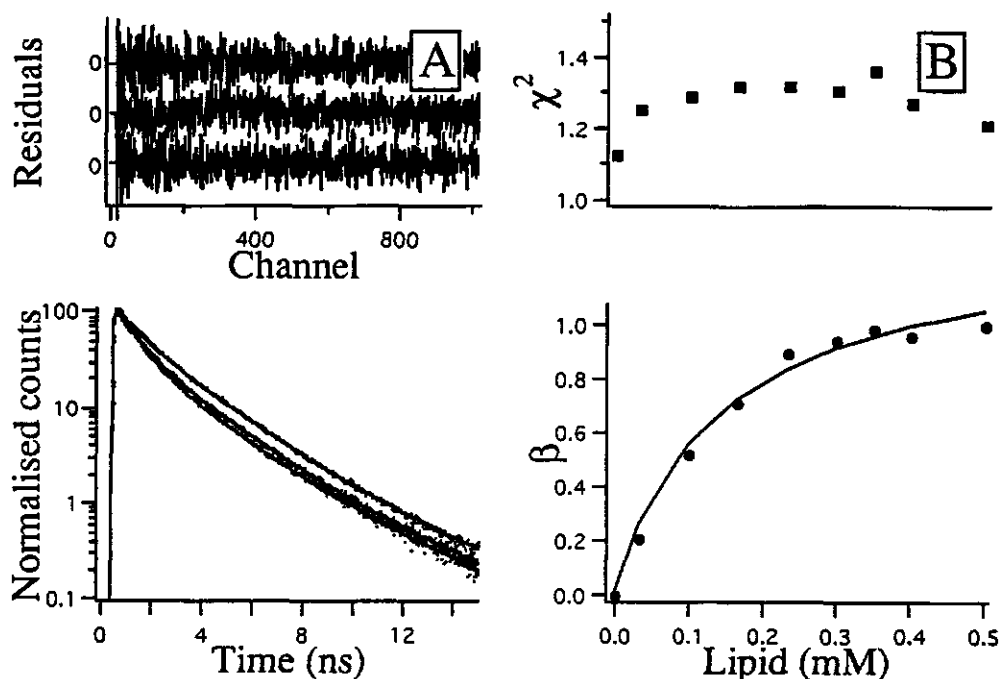
Figure 4A The lower panel shows the fluorescence decay profiles (dots) of lysozyme in the absence (non-quenched) and in the presence (quenched) of different amounts of mixed lipid vesicles composed of DPPC/DPPS/dipyr$_4$PC (67.5:27.5:5). The (solid) curves are the best fits to the experimental data obtained by fractional analysis. The intermediate decay was analysed with a linear combination of the limiting decays yielding an optimised value for β of 0.71. The weighted residuals of the analyses to the corresponding curves are given in the upper panel. **B**. The dependence of the fractional contribution (β) on the mixed lipid concentration is plotted in the lower panel and the fit quality (reduced χ^2) to the experimental fluorescence decay data corresponding to each β value is presented in the upper panel. In this lipid titration experiment, a lysozyme concentration of 1.5 μM was used. A simple one-step binding model was applied to the dependence of β on the mixed lipid concentration (solid line). See text for further details.

In this analysis the fluorescence decay of lysozyme in buffer represented a non-quenched decay $F(t)_o$, while its decay in a sample with 0.5 mM of mixed lipid was assumed to approximate the decay of lysozyme molecules bound to the vesicle membranes. The lower panel of figure 4A shows both limiting fluores-cence decays with their fitted curves and an example of an intermediately

quenched fluorescence decay in the presence of 0.17 mM of the mixed lipid. The upper panel shows weighted residuals of the corresponding analyses.

The fractional contribution β obtained from the analysis of titration experiments with this approach and corresponding reduced χ^2 values are presented in Figure 4B. The average value of the reduced χ^2 obtained from all analyses corresponds to 1.27, which is a acceptable fit quality, especially when we take into account the χ^2 values of 1.13 and 1.21 obtained with the advanced distribution analysis (with MEM) of the limiting decay curves ($F(t)_o$ and $F(t)_s$). Since β is proportional with the fraction of lysozyme bound to the membranes, these experiments clearly show the gradual increase of bound lysozyme molecules with increasing amounts of mixed lipid present in the sample.

In the second step the dependence of β on the lipid concentration was modelled by applying a simple one-step binding model (described in the computational method section) yielding an optimised value for the fractional contribution x (of $F(t)_o$ in $F(t)_s$) and a value for the binding constant K_a. In this analysis we assumed that $n = 350$ protein molecules can bind to a vesicle surface and $m = 14$ (These values are based on a protein and vesicle radius of 1.7 (Blake et al., 1965) and 150 nm, respectively, and a lipid area of 0.7 nm^2 (Demel et al., 1967)). The analysis yielded a value of 0.25 for x and 34 mol^{-1} mixed lipid for K_a. From the preceding results we have seen that membrane binding is accompanied with structural changes in the protein. Therefore the one step binding process assumed in this analysis is a first approximation and the optimised values for X and K_a should be considered as rough estimates.

2.4.5. Dependence of the membrane association of lysozyme on membrane surface charge and ionic strength as determined from fractional analysis of the fluorescence anisotropy

The dependence of lysozyme binding on membrane surface charge was studied by monitoring the polarised tryptophan fluorescence decays at various mole fractions of DPPS in mixed DPPC/DPPS vesicles. The polarised decays were analysed with the fractional approach of anisotropy analysis (see eq. 3). The decays of lysozyme in the presence of pure DPPC vesicles and DPPC/DPPS (70:30 molar ratio) vesicles were taken to represent the decay of non-bound lysozyme and of membrane-bound lysozyme, respectively. The lower panel of figure 5A shows a typical decay of polarised fluorescence components ($I_{//}$ and $I_{\perp}$) lysozyme in presence of DPPC/DPPS vesicles at moderate binding conditions. The solid curve represents the fit obtained with the fractional analysis to the experimental points. The weighted residuals of the corresponding fit are presented in the upper panel. The results of fractional analysis as a function of the mol% PS and the χ^2 values of the fits are presented in figure 5B. Increasing the molar fraction of PS in the mixed neutral/anionic membranes causes a gradual enhancement of bilayer affinity of lysozyme. In order to demonstrate that the specificity of lysozyme for PS is ionic in nature, the polarised fluorescence decays of lysozyme in the presence of 60 µM DPPC/DPPS (70:30) vesicles were determined as a function of ionic strength by adding 0 to 500 mM NaCl to the sample.
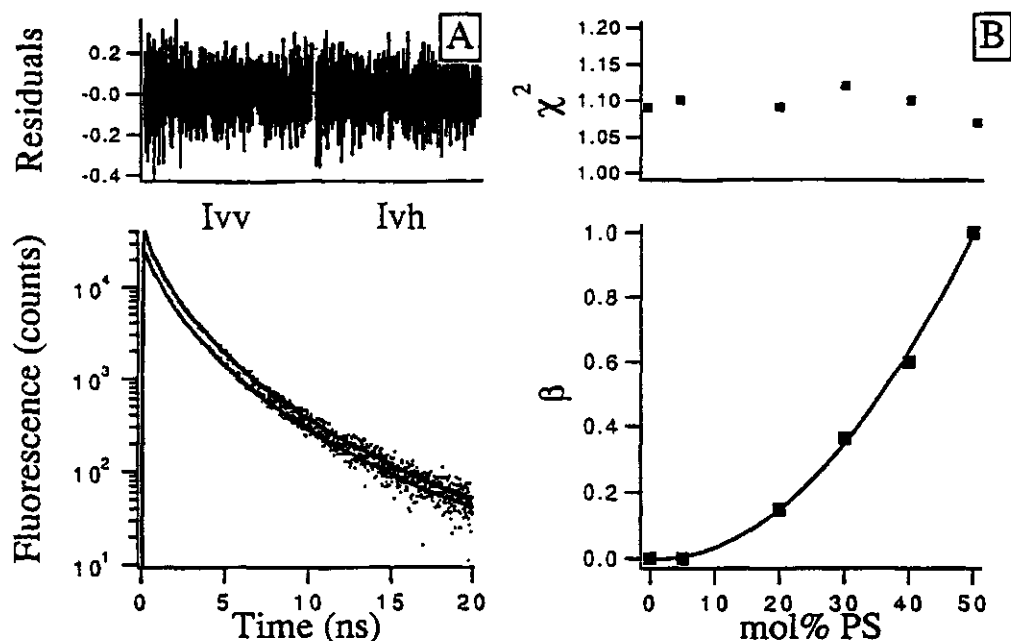
Figure 5 Dependence of fraction bound lysozyme on the mole fraction of DPPS in DPPC vesicles. The data points are obtained from fractional analysis of the fluorescence and anisotropy data sets. In this experiment the total lipid and lysozyme concentrations were 60 μM and 1.5 μM, respectively.

Fractional analysis of these anisotropy data yielded β as a function of NaCl concentration (figure 6). In this analysis a sample with 500 mM NaCl represented non-associated protein while one without NaCl a sample of mainly associated lysozyme. It is apparent from figure 6 that the amount of binding of lysozyme to DPPC/DPPS vesicles decreases with increasing ionic strength of the buffer. The convincing dependence of association on the ionic strength clearly supports the conclusion that electrostatic interactions play a dominant role in the association of lysozyme with phospholipid bilayers.
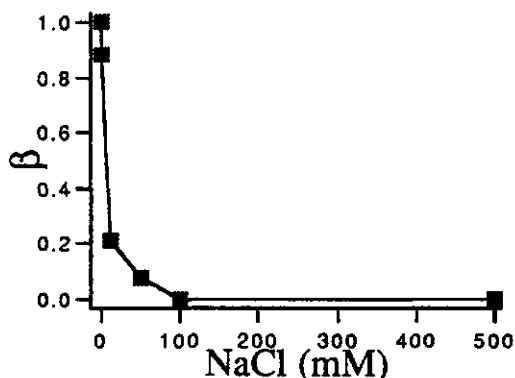
Figure 6 Effect of ionic strength variation on the fraction bound lysozyme. Vesicles (60 μM of DPPC/DPPS (70/30)) and lysozyme (1.4 μM) were incubated at various ionic strength (NaCl concentrations from 0 to 500 mM). The data were obtained from fractional analyses of the anisotropy decays from the various samples.

Perturbation of the membrane bilayer

To investigate the effects of lysozyme association on the physical properties of the lipid environment, the excimer-monomer fluorescence intensity ratio (E/M) of dipyr$_{10}$PC and dipyr$_{10}$PS was monitored as a function of lysozyme concentration in DOPC and DOPC:brainPS (3:1) vesicles, respectively. Formation of an intramolecular excimer of two pyrene moieties that are attached to the same lipid molecule refers to a collisional encounter between an excited and a non-excited pyrene moiety (Galla & Sackman, 1974), and the frequency of such events is governed by the rotational dynamics of the pyrene chains, the motional freedom superimposed by the local lipid environment and the geometry of the parent molecule (Cheng et al., 1991).
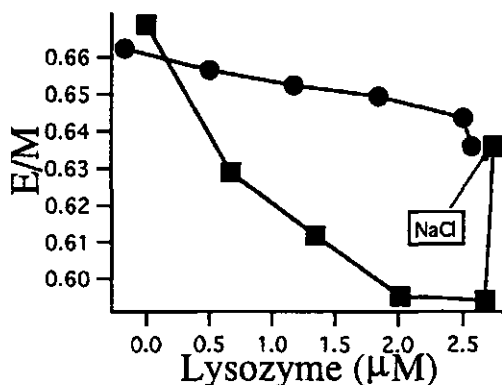
Figure 7 The dependence of the excimer-monomer fluorescence intensity ratio (E/M) of dipyr$_{10}$PS and dipyr$_{10}$PC on the concentration of lysozyme. The concentration total lipid was kept constant (10 μM). Points ● show the effect on neutral PC/dipyr$_{10}$PC (100:1) vesicles and points ■ that of DOPC/brainPS/ dipyr$_{10}$PS (75:25:1) membranes. In the latter case, reversibility of this acyl chain effect is demonstrated by addition of an excess of NaCl to a final concentration of 100 mM.

Binding of lysozyme leads specifically to a reduction of excimer formation of dipyr$_{10}$PS, and not of dipyr$_{10}$PC, confirming the specificity for acidic lipids in the interaction. The results of this experiment are presented in figure 7. Addition of NaCl to a final concentration of 100 mM abolishes the association process and the E/M ratio of dipyr$_{10}$PS recovers to almost its value in absence of protein. This observation can be interpreted as a decrease in the intramolecular collisional dynamics of the two pyrene fluorophores in PS or by a change in the cylindrical packing geometry of the lipid induced by the protein. The binding of a protein at the membrane surface may affect acyl chain motion in the hydrophobic core of the membrane due to condensing or disrupting effects on the head-group packing. These effects may alter the lipid chain motion by modifying the free volume accessible to each lipid molecule. In addition, the protein might penetrate the membrane, thereby reducing the collision frequency of the acylchains directly by forming a protein-lipid boundary. Penetration studies of lysozyme however show that at neutral pH the protein hardly enters the membrane bilayer (Arnold et al., 1992).

2.5 Conclusions

The major purpose of the present study is to demonstrate that a fractional analysis of fluorescence decay curves can provide accurate binding curves of proteins to lipid interfaces. The results of the analyses enable the investigation of macromolecular adsorption in a very detailed manner. The fractional analysis has several advantages: 1) A physical interpretation of the observed fluorescence or anisotropy decays in terms of decay parameters is omitted. 2) The maximum amount of information is conserved since the whole decay is used, and not some "average" parameter like the average fluorescence lifetime. 3) The number of adjustable parameters is minimal. 4) Both total fluorescence (sum of polarised decays) and anisotropy (difference of polarised decays) should yield independently identical fractions of the limiting decays. We think that this way of analysis will be applicable not only for the investigation of macromolecular adsorption, but for any multiple component system.

Another result arisen from this work is the characterisation of conformational and dynamical aspects of lysozyme adsorption to lipid membranes. The experimental findings are schematically summarised in figure 8. Lysozyme exhibits a very weak non-specific binding to bilayers of pure PC and a strong binding to PC containing negatively charged PS. In the latter case the protein can be detached by increasing the ionic strength indicating that the selectivity for PS is mainly of electrostatic nature. The rotational dynamics of lysozyme molecules are significantly faster when the protein is adsorbed to fluid membranes rather than to membranes in the gel state. Interaction with the charged membrane surface leads to a change in protein conformation. From the membrane point of view the E/M results indicate that the adsorption of lysozyme changes the structural and/or dynamical properties of the membrane. Accompanied effects of peripheral protein binding on lipid motion or organisation were observed by others (See Jain & Zakim, 1987; Marsh, 1991). In general, the overall result of this surface interaction is an increase of lipid packing density, which reduces the extent of lipid chain motion as recorded by the intramolecular excimer formation. It can, however, not be excluded that

lysozyme, like some other proteins, interacts more directly with the lipid chains, additional to the generalised condensing or disrupting effects on head-group packing. Partial penetration of lysozyme into PS bilayers at low pH was observed by others (Arnold et al., 1992)
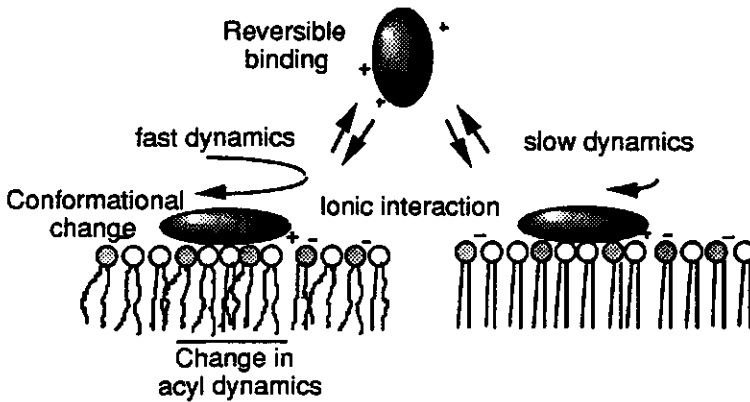
Figure 8 Schematic representation of the interaction of lysozyme with negatively charged phospholipid vesicles below (left) and above (right) the phase transition.

2.7 References

Arnold, K., Hoekstra, D., Ohki, S. (1992) *Biochim. Biophys. Acta* 1124, 88-94.

Barenholz, Y., Gibbes, D., Litman, B.J., Goll, J., Thompson, T.E., Carlson, F.D. (1977) *Biochemistry* 16, 2806-2810.

Bastiaens, P.I.H, Pap, E.H.W., Borst, J.W., van Hoek, A., Kulinski, T., Rigler, R.Visser, A.J.W.G. (1993) *Biophys. Chem.* 48, 183-191.

Bastiaens, P.I.H., van Hoek, A., Wolkers, W.F., Brochon, J.C., Visser, A.J.W.G. (1992) *Biochemistry* 31, 7050-7060.

Beechem, J.M, Gratton, E., Ameloot, M., Knutson, J.R. Brand, L. in: *Topics in Fluorescence Spectroscopy*; Lakowicz, J.R., Ed.; Plenum Press: New York. (1991) 241-305.

Blake, C.C.F., Koenig, D.F., Mair, G.A., North, A.T.C., Philipids, D.C., Sarma, V.R. (1965) *Nature* 206, 757-761.

Brochon, J.C., Mérola, F., Livesey, A.K., in: *Synchrotron Radiation and Dynamic Phenomena* (1992) 435-452.

Cheng, K.H., Chen, S.Y., Butko, P., v.d. Meer, W.B., Somerharju, P. (1991) *Biophys. Chem.* 39, 137-144.

Comfurius, P., Bevers, E.M., Zwaal, R.F.A. (1990) *J. Lipid Res.* 31, 1719-1721.

Dale, R.E., Eisinger, J. Blumberg, W.E. (1979) Biophys. J. 26, 161-194.

Demel, R.A., Van Deenen, L.L.M., Pethica, B.A. (1967) Biochim. Biophys. Acta. 135, 11-19.

Galla, H.J., Luisetti, J. (1980) *Biochim. Biophys. Acta* 596, 108-116.

Galla, H.J., Sackman, E. (1974) *Biochim. Biophys. Acta*, 339, 103-115.

Görrissen, J.H., Marsh, D., Rietveld, A., De Kruijff, B. (1986) *Biochemistry* 25 2904-2910.

Hoek, A. Visser, A.W.J.G (1985) *Anal. Instrum.* 14 359-378.

Horsey, D., Herron, J., Hlady, V., Andrade, J.D. (1991) *Langmuir* 7, 218-222.

Horsey, D., Herron, J., Hlady, V., Andrade, J.D. In: *ACS Symp. Ser.* (1987) 290.

Houbre, D., Kuhry, JG., Duportail, G. (1988) *Biophys. Chem.* 30, 245-255.

Imoto, T., Forster, L.S., Rupley, J.A, Tanaka, F. (1971) *Proc. Natl. Acad. Sci.*, 69, 1151-1155.

Imoto, T., Johnson, L.N. North, A.C.T., Phillips, D.C. & Rupley, J.A. (1972) in *The enzymes* (Boyer, P. Ed.) 3 rd edn., vol 7, 665-868, Academic Press, New York.

Jain, M.K. and Zakim, D. (1987) *Biochim. Biophys. Acta* 906, 33-68.

Lester, D.S., Orr, N., Brumfeld, V. (1990) *Biochim. Biophys. Acta* 1054, 297-303.

Lippert, J.L., Lindsay, R.M. and Schultx, R. (1980) *Biochim. Biophys. Acta* 599, 32-41.

Livesey, A.K. Brochon, J.C. (1987) *Biophys. J.* 52, 693-706.

Marsh, D. (1991) *FEBS Lett.* 268, 371-375.

Omata, Y., Friedman, FK. (1991) *Biochem Pharmacol* 42, 97-101.

Pap E.H.W., Bastiaens P.I.H., Borst J.W., van den Berg P.A.W., van Hoek A., Snoek G.T., Wirtz K.W.A. and Visser A.J.W.G. (1993) *Biochemistry* 32, 13310-13317.

Patel, K.M., Morrisett, J.D.Sparrow, J.T. (1979) *J. Lipid. Res.* 20, 674-677.

Rousser, G., Fleischer, S. A., Yamamoto, A. (1970) *Lipids* 5, 494-496.

Sankaram, M.B., Brophy, P.J., Marsh, D. (1989) *Biochemistry* 28, 9685-9691.

Schmidt, C.F., Zimmermann, R.M.Gaub, H.E. (1990) *Biophys. J.* 57, 577-588.

Vincent, M., Gallay, J. (1991) *Eur. Biophys. J.* 20, 183-191.

Vos, K., van Hoek, A.Visser, A.J.W.G (1987) *Eur. J. Biochem.* 165, 55-63.

Chapter 3

Fluorescence dynamics of diphenyl-1, 3, 5-hexatriene-labelled phospholipids in bilayer membranes

Abstract

A comparative study of the dynamical fluorescence properties of three phosphatidylcholines having a diphenyl-1, 3, 5-hexatriene (DPH) group attached at different depths from the headgroup incorporated into membrane vesicles has been carried out. The probes were covalently attached to the *sn-2* position of the glycerol part of the phosphatidylcholine via either carboxyl, ethyl or propanoyl links. The vesicles were composed of either dimyristoylphosphatidylcholine or dipalmitoylphosphatidylcholine. The experimental time-resolved polarised fluorescence data of the probes were analysed by two different methods: maximum entropy and global analysis. Distributed fluorescence lifetimes and correlation times of the DPH derivatives were obtained with the maximum entropy method. All DPH derivatives exhibited a bimodal distribution of fluorescence lifetimes with a dependence of the lifetime peak positions on the lipid phase, confirming previous data in the literature. The anisotropic rotational dynamics of the DPH-moieties in the membranes could be described by several distributed correlation times. In the fluid phase of the membrane the residual anisotropy of free DPH became very small in contrast with those of the other probes, indicating that restriction of probe rotation is mainly imposed by the molecular geometry of the lipid probes. A two-dimensional analysis using the maximum entropy method demonstrated that both rotational correlation times were associated with the same set of fluorescence lifetimes. Global analysis of the data sets according to the general rotational diffusion model yielded weighted orientational distributions. Unexpectedly, a component of the DPH moiety oriented parallel to the membrane surface was obtained in the orientational distributions of the DPH lipids (as was reported earlier for DPH and TMA-DPH), which seems at variance with the geometric constraints imposed by the headgroups.

3.1 Introduction

Fluorescence spectroscopy of lipid probe molecules provides us with a valuable tool for studying structure and dynamics of membrane bilayers with the advantage of having a minimal disturbing effect on the membrane. Many time-resolved fluorescence studies (summarised in Lentz (1989)) on the physical properties of the cylindrically shaped probe diphenyl-1, 3, 5-hexatriene (DPH) and its charged analogue TMA-DPH have been reported yielding detailed information on the physical state of the phospholipid bilayers. Several studies distinguished two distinct DPH populations, distributed parallel and perpendicular with respect to the normal of the membrane (Ginkel et al., 1989; Deinum et al., 1988; Kooyman et al., 1983; Vos et al., 1983; Ameloot et al., 1984; Best et al., 1987; Wang et al., 1987; van

Langen, 1987). A better defined orientational distribution would be desirable. To achieve this goal we have used three distinct DPH-labelled phosphatidylcholines with the DPH moieties incorporated at different depths at the *sn-2* position (Figure 1). These DPH lipids are expected to have a more defined orientational distribution and, in addition, they do not significantly perturb the bilayer packing.

We have undertaken a comparative time-resolved fluorescence study of these DPH lipids, and DPH and TMA-DPH. Two methods of analysis of time-resolved data have been employed. The first non a-priori method consists of a mathematical description in distribution of relaxation times (both for total fluorescence and for fluorescence anisotropy) using the maximum entropy method (MEM) (Gentin et al., 1990; Livesey & Brochon, 1987; Mérola et al., 1989; Brochon et al., 1992). The physical parameters which can be extracted from this mathematical description of the anisotropy decay are the initial anisotropy (r_0) and the perpendicular rotational diffusion coefficient ($D_\perp$) of this cylindrically symmetrical molecule. Secondly, the polarised time-resolved fluorescence data were subjected to a global analysis with the (a-priori) general diffusion model (r_{g3}) to yield the target parameters $D_\perp$ and the second-rank and fourth-rank order parameters ($<P_2>$ and $<P_4>$) (van der Meer et al., 1984; Szabo, 1984). The measurements were performed as a function of temperature by using macroscopically isotropic, small unilamellar vesicles (SUVs) of dimyristoylphosphatidylcholine (DMPC) and dipalmitoylphosphatidylcholine (DPPC) with lamellar phase transition temperatures (T_m) of 24°C and 42°C, respectively (Houslay & Stanley, 1982).

3.2 Experimental procedures

Materials

DMPC and DPPC were purchased from Sigma (St. Louis, MO, USA) and used without further purification. The fluorescent probes DPH, TMA-DPH, DPHpPC and DPH-carboxylic acid were obtained from Molecular Probes (Eugene, OR, USA). DPH-acetic acid was purchased from Lambda (Graz, Austria). The lipid probes DPHePC and DPHcPC were synthesised as described below. The probes were dissolved in absolute ethanol and stored under nitrogen in the dark at -20°C.

Methods

Synthesis of 2-[3-(diphenylhexatrienyl)-ethyl-3-palmitoyl-L-α–phosphatidyl-choline and of 2-[3-(diphenylhexatrienyl)-carboxyl-3-palmitoyl-L-α–phosphatidylcholine

DPHePC and DPHcPC were synthesised essentially as described for *sn-2-*(pyrenyldecanoyl)-PC by Somerharju and Wirtz (Somerharju & Wirtz, 1982). Because of the low solubility of the DPH probes in chloroform, pyridine was used as solvent during the esterification. The DPH-labelled lipids were purified on a silicic acid column, using a methanol gradient in chloroform as eluent.

The final yield of the fluorescent phospholipids, based on phosphorous content was about 5%.
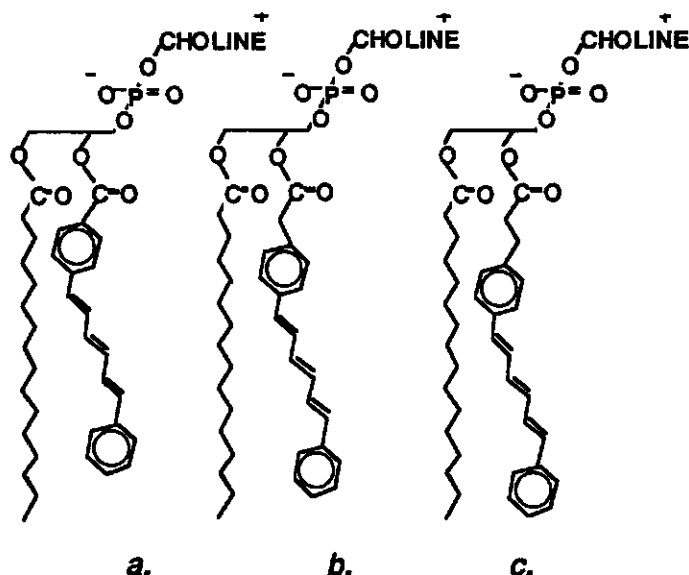
Figure 1 Chemical structures of the used DPH-labelled phosphatidylcholines. a) DPHcPC, b) DPHePC, c) DPHpPC.

Vesicle Preparation

SUV's were prepared by injecting 10 µl of a lipid solution (20 mM lipid in ethanol) through a Hamilton syringe into 1 mL of a magnetically stirred buffer solution (0.1 M NaCl, 10 mM Tris, pH 8.0) at a temperature 15 degrees higher than the transition temperature of the used phosphatidylcholine species. This procedure produces SUV's having an average diameter of the vesicles at this lipid concentration of 30 nm (Kremer et al., 1977). The probe:lipid ratio was 1:500 on molar basis. The total phospholipid content was determined by phosphate analysis according to the method of Rousser et al., (1970).

Fluorescence methods

Time-resolved fluorescent measurements were carried out using the time-correlated single photon counting technique (O'Connor & Philips, 1984). For excitation with light of 345 nm a frequency-doubled synchronously pumped dye laser (DCM) was used (van Hoek et al., 1987). An electro-optic modulator set-up was used to decrease the excitation pulse rate from 76 MHz to 596 kHz. The emission light was collected with a single photon counting detection system. A combination of a Schott KV399 cut-off filter and Schott 441.7 nm interference filter was used to select the emission wavelength. POPOP (Eastman Kodak Rochester, NY, USA) dissolved in ethanol was used as a reference compound to yield the dynamic instrumental response function of the set-up. In the analysis of the polarised fluorescence data, the single exponential reference fluorescence decay time was fixed to a value of 1.35 ns (Vos et al.,

1987). All measurements consisted of a number of sequences of registration of 10 s parallel and 10 s perpendicular polarised emission. The temperature of the samples in a thermostated cuvet holder was regulated using a temperature controller (Oxford model ITC4). After measuring the fluorescence of a sample the background emission of samples without DPH probes was measured, at one fifth of the time of sample acquisition, and then used for background subtraction. The background emission was always below 1.5% of the total fluorescence of DPH-labelled samples. The data were collected in a multichannel analyser and after transfer, analysed on a Silicon Graphics Personal Iris (model 4D35) computer using the commercially available second generation global analysis package (Globals Unlimited[TM], Urbana, IL, USA) and MEM (Maximum Entropy Data Consultants Ltd., Cambridge, UK).

Maximum entropy method

MEM analyses polarised fluorescence data without restrictions on number, shape and position of relaxation time distributions. Since this method of analysis is fully described in references (Gentin et al., 1990; Livesey & Brochon, 1987; Mérola et al., 1989; Brochon et al., 1992) we will only briefly describe the principle of the maximum entropy method in relation to our application. The recovery of the distribution of exponentials describing the decay of the fluorescence which is convolved by the shape of the excitation flash, is accomplished by minimising the χ^2 statistic and maximising the Skilling-Jaynes entropy function (Jaynes, 1968).

The expression for the parallel and perpendicular intensity components after deconvolving the instrumental response function is given in eqs. 1 and 2. The total fluorescence decay is obtained by summing the parallel ($i_{//}$) and twice the perpendicular ($i_\perp$) components

$$i_{//}(t) = \frac{1}{3} \int_0^\infty \int_0^\infty \int_{-0.2}^{0.4} \gamma(\tau,\phi,r_0)\, e^{-t/\tau} d\tau d\phi dr_0 + \frac{2}{3} \int_0^\infty \int_0^\infty \int_{-0.2}^{0.4} r_0 \cdot \gamma(\tau,\phi,r_0)\, e^{-t/\tau} e^{-t/\phi} d\tau d\phi dr_0 \quad (1)$$

$$i_\perp(t) = \frac{1}{3} \int_0^\infty \int_0^\infty \int_{-0.2}^{0.4} \gamma(\tau,\phi,r_0)\, e^{-t/\tau} d\tau d\phi dr_0 - \frac{1}{3} \int_0^\infty \int_0^\infty \int_{-0.2}^{0.4} r_0 \cdot \gamma(\tau,\phi,r_0)\, e^{-t/\tau} e^{-t/\phi} d\tau d\phi dr_0 \quad (2)$$

where $\gamma(\tau, \phi, r_0)$ represents the number of fluorophores with lifetime τ, rotational correlation time ϕ and initial anisotropy r_0 (Brochon et al., 1992). One also is able to recover the distribution pattern of the fluorescence anisotropy given by r(t):

$$r(t) = \frac{i_{//}(t) - i_\perp(t)}{i_{//}(t) + 2i_\perp(t)} \qquad (3)$$

In case that there is a correlation between τ and ϕ (associative modelling), the complete three-dimensional image given by $\gamma(\tau, \phi, r_0)$ can be resolved from time-resolved polarised fluorescence experiments. In the two-dimensional MEM

analysis, assuming a constant r_0, the cross-correlations between lifetimes and rotational correlation times are disclosed (Gentin et al., 1990; Livesey & Brochon, 1987; Mérola et al., 1989; Brochon et al., 1992).

If one assumes *a priori* that there is no correlation between τ and ϕ, (non-associative modelling) the images $\alpha(\tau)$ and $\beta(\phi)$ are independent, and eqs. 1 and 2 can be simplified to:

$$i_{//}(t) = \frac{1}{3}\int_0^\infty \alpha(\tau)e^{-t/\tau}d\tau \int_0^\infty \{1+2\beta(\phi)e^{-t/\phi}\}d\phi \qquad (4)$$

$$i_\perp(t) = \frac{1}{3}\int_0^\infty \alpha(\tau)e^{-t/\tau}d\tau \int_0^\infty \{1-\beta(\phi)e^{-t/\phi}\}d\phi \qquad (5)$$

The integrated amplitude $\beta(\phi)$ corresponds to the fundamental anisotropy r_0. When using this separation the time dependence of the anisotropy can be described with the integral:

$$r(t) = \int_0^\infty \beta(\phi)e^{-t/\phi}d\phi \qquad (6)$$

In the anisotropy analysis with MEM, this integral is approximated by a sum of n exponentials (n = 40 in our analyses) yielding the spectrum of amplitudes β against correlation times ϕ. The rotational diffusion coefficient $D_\perp$ is defined as (van der Meer et al., 1984):

$$D_\perp = \frac{1}{6r_0}\lim_{t\to 0}\frac{\partial r}{\partial t} \qquad (7)$$

where $\partial r/\partial t$ at time zero is calculated from the correlation time spectra according to eq. 8:

$$\lim_{t\to 0}\frac{\partial r}{\partial t} = \sum_{i=1}^n \frac{\beta_i}{\phi_i} \qquad (8)$$

where the summation is carried out over the whole range (n) of β_i values divided by the corresponding correlation times (ϕ_i). In this calculation $D_\perp$ was obtained by assuming an average initial anisotropy of the DPH probes of 0.36.

Global analysis

We also analysed our experimental data with the rotational diffusion model (r_{g3}) in which the motion of the probe is described as diffusion in an anisotropic environment (van der Meer et al., 1984; Szabo, 1984). The parameters of this model are the second rank and fourth rank order parameters, $<P_2>$ and $<P_4>$, the diffusion coefficient $D_\perp$ and the initial

anisotropy r_0. Multiple experiments of each DPH probe were simultaneously analysed by linking the initial anisotropy over all temperatures. All fits were subjected to a rigorous error analysis based on an exhaustive search along each parameter axis as to find a minimum χ^2. The error of the fitting parameters was determined according to a F-statistic criterion at the 67 % confidence level (Beechem et al., 1991). Weighted orientational distribution functions were reconstructed from the resolved $<P_2>$ and $<P_4>$ pairs using relationships established by others (Ameloot et al., 1984; van Langen et al., 1987; Berne et al., 1968).

3.3 Results

3.3.1 Analysis of fluorescence lifetime distributions

As a typical example the experimental total fluorescence decay of DPHpPC in DPPC vesicles at 45°C is presented in Figure 2. In all experiments the weighted residuals and autocorrelation functions of the residuals were randomly scattered around zero as illustrated in Figure 2.
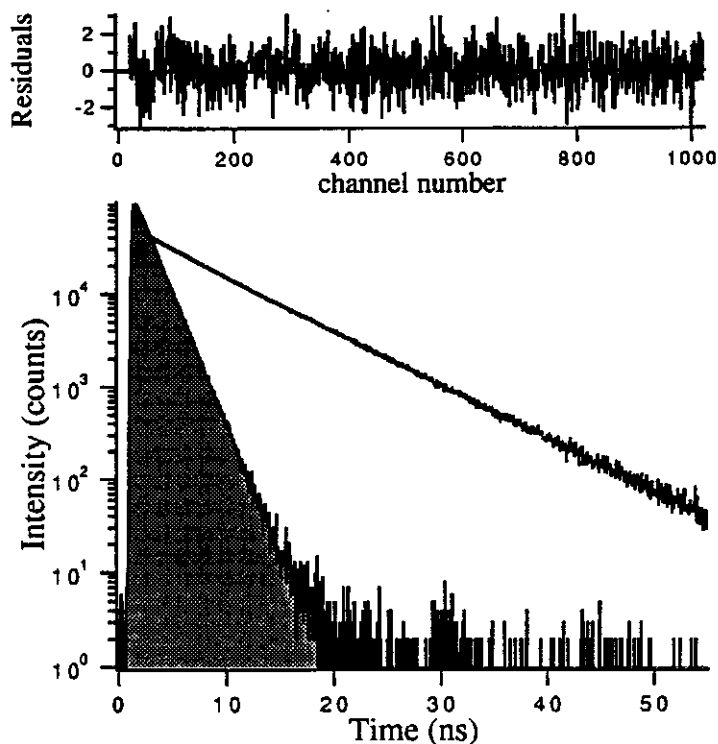
Figure 2 Experimental total fluorescence decay of DPHpPC in DPPC vesicles at 45°C. Also shown is the response of the POPOP reference compound (shaded). The plots of residuals and autocorrelation of the residuals in the upper panel arise from the fit in a lifetime distribution. These plots are typical for the quality of the fits of all other analyses.
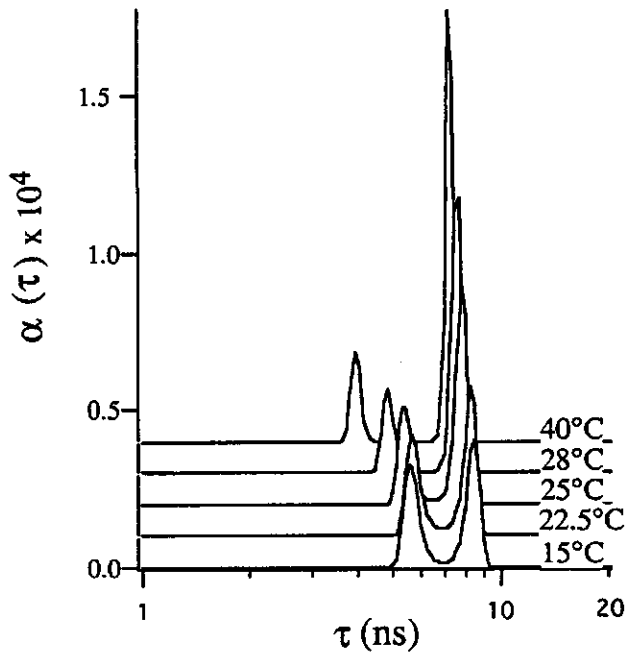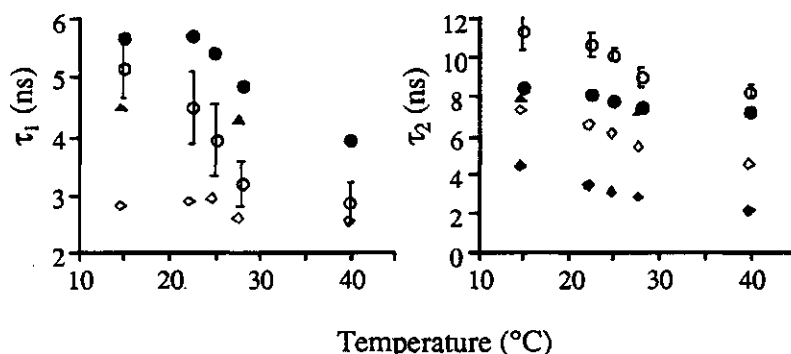
Figure 3 Temperature dependence of the fluorescence lifetime distribution of DPHpPC in DMPC vesicles. The plots at different temperatures have different offsets which implicates that the ordinate values apply only to the data at 15°C.

The results of a distribution analysis of the fluorescence decay of DPHpPC in DMPC vesicles at several temperatures are shown in Figure 3. The barycenters of the peaks in the lifetime distribution of the DPH derivatives at several temperatures are presented in Figure 4. The values of these barycenters agree with published values (Deinum et al., 1988; van der Meer et al., 1984; Parente & Lentz, 1985; Fiorini et al., 1987; Chen et al., 1977; Mateo et al., 1991). All the DPH derivatives show a bimodal distribution, although this is less clear for DPHcPC. The shorter component (denoted τ_1) as well as the longer component (denoted τ_2) are dependent on temperature and physical state of the vesicle (Figure 3). Because of the low accuracy of τ_1 in the lifetime distribution of DPHcPC, these barycenters have been omitted in Figure 4. The separation between the peak values of τ_1 and τ_2 decreases from DPH > DPHpPC $\approx$ DPHePC > DPHcPC $\approx$ TMA-DPH. The lifetime distributions of the DPH derivatives in DPPC-vesicles are below and above the phase transition temperature (T_m) essentially the same as in DMPC-vesicles. When we compare the lifetime distributions of the different DPH derivatives the following conclusions can be drawn:
i) The widths of the distributions of TMA-DPH and DPHcPC are broader than those of DPH and DPHpPC which might be due to the fact that DPH in the first two probes resides in a region with a large polarity gradient (Fiorini et al., 1987).
ii) The lifetime spectrum of DPHePC is similar to that of DPHpPC, indicating that the dielectric constant near the headgroups is not detectably different

within a distance of one C-C bond ($\approx$ 1.8 Å). Differences in barycenters of both probes are within the error margins.

iii) The lifetime distribution pattern of DPHcPC is shifted to shorter time as compared to that of the other lipid probes. This shift in distribution is probably related to the sensitivity of the fluorescence lifetime of the DPH moiety to substitutions directly in the phenyl group of DPH (Alford & Palmer, 1982). All DPH probes exhibit a shortening of the lifetimes with increasing temperature as shown in Figs. 3 and 4 which is consistent with increased water penetration into bilayers. The relative temperature dependence of the average fluorescence lifetime of the probes located close to the headgroup region of the bilayer (TMA-DPH and DPHcPC) is slightly more marked than that of the other probes (see also (Straume & Litman, 1987)). The width of the distribution decreases at higher temperature, which might be a consequence of an increasing rate of exchange between states of slightly different lifetimes within one distribution (Fiorini et al., 1987). During the phase transition the barycenters of both distributed lifetime components of all DPH derivatives shift to shorter times, indicating the sensitivity of the lifetime values to the phase of the lipid bilayer (see also (Fiorini et al., 1987; Barrow & Lentz, 1985; Klausner et al., 1980; Parasassi et al., 1984)).


Temperature (°C)

Figure 4 Temperature dependence of the barycenters of the bimodal fluorescence lifetime distribution of different DPH probes in DPPC bilayers. A: the shorter fluorescence lifetime τ_1. B: the longer fluorescence lifetime τ_2. O: DPH, ●: DPHpPC, ◇: TMA-DPH, ◆: DPHcPC, ▲: DPHePC. In each plot one representative data set is presented with error bars.

3.3.2 Distribution of correlation times from fluorescence anisotropy decay

An example of the experimental fluorescence anisotropy decay of DPHpPC in DPPC at 45°C is presented in Figure 5. We have analysed the polarised fluorescence decay data in terms of a distribution of correlation times and a limiting anisotropy at infinite time (r_∞). For all analyses the weighted residuals are randomly scattered around zero (see relevant plots).
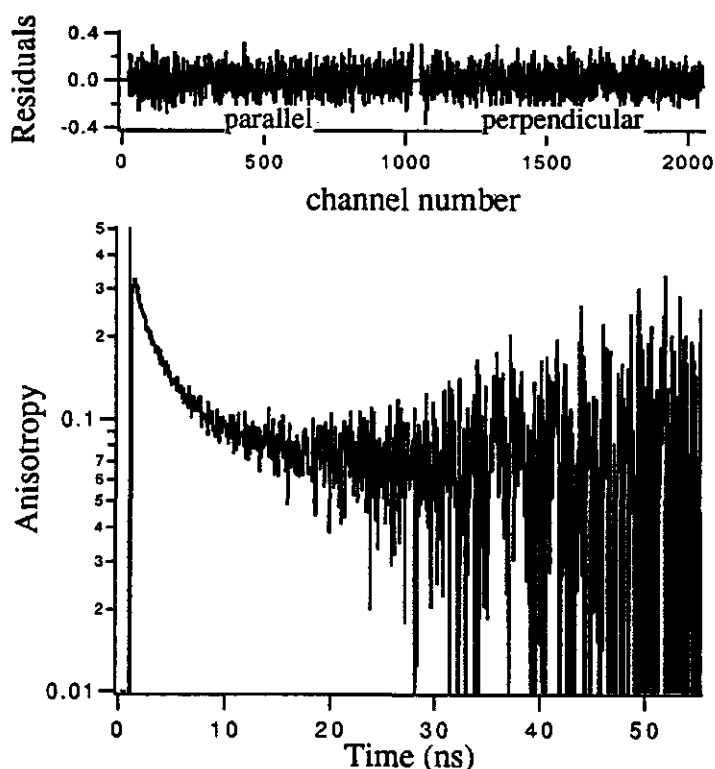
Figure 5 Experimental, reconstructed fluorescence anisotropy decay of DPHpPC in DMPC vesicles at 28°C. A plot of residuals in the upper panel arise from the fit in a correlation time distribution. These plots are typical for the quality of the fit of all other analyses.

The correlation time spectra of DPHpPC in DMPC as function of temperature are given in Figure 6. The time-resolved fluorescence anisotropy of the DPH probes at lower temperatures can be described by a unimodal distribution and at higher temperatures by a distribution with at least two components, which can satisfactorily be explained by anisotropic rotation of the DPH-moieties using the rotational diffusion model (van der Meer et al., 1984; Szabo, 1984). This result agrees with that of discrete exponential analysis (Best et al., 1987; Fiorini et al., 1987; Deinum et al., 1985; Davenport et al., 1986). In the inset of Figure 6 the temperature dependence of the limiting anisotropy r_∞ is given. The contribution of the limiting anisotropy accounts for more than 80% of the initial anisotropy in the gel state of the membrane bilayer. At $T > T_m$, the anisotropy of free DPH tends to relax to a value of r_∞ close to zero, while r_∞ of the other DPH derivatives has still a finite value (Figure 7A). This behaviour has been explained by assuming a hindered rotation of DPH in lipid bilayers in which the angular barriers are formed by a potential cage consisting of the fatty acid chains in an all-trans configuration, making an angle with the normal of the bilayer (Deinum et al., 1988; Davenport et al., 1986). When

exceeding T_m rotational isomerizations of the fatty acid chains take place causing a drastic increase in rotational freedom in the liquid-crystalline phase.
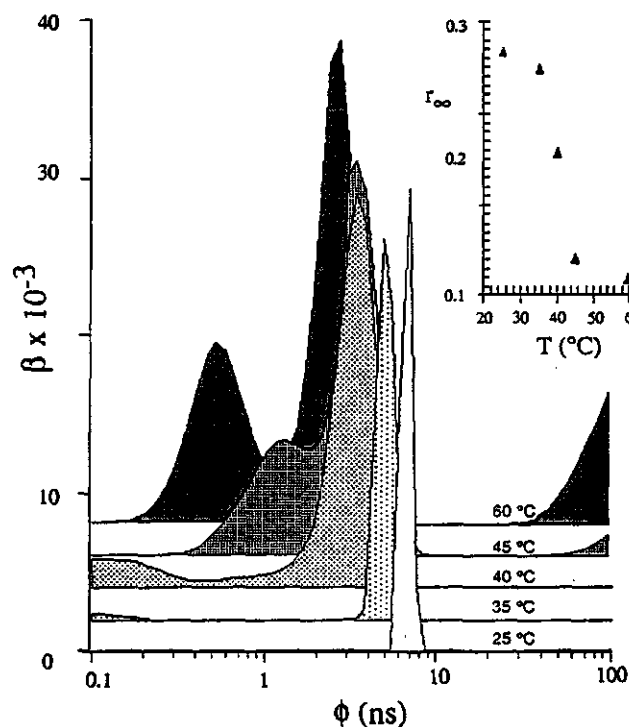
Figure 6 Temperature dependence of the correlation-time distribution of DPHpPC in DPPC vesicles as obtained with a non-associative MEM-analysis. The distributions have different offset values, which implicates that the ordinate values apply only to the data at 25°C. The temperature dependence of the anisotropy at limiting time (r_∞) is presented in the inset.

Because the pattern of r_∞ at $T < T_m$ is essentially the same for all probes used, it seems that the limiting anisotropy in the gel phase is only determined by the environment around the fluorescent lipid, and not by intramolecular geometrical restrictions. At higher temperatures the differences between the limiting anisotropies of DPH lipids and free DPH become considerable. Apparently, geometrical constraints or differences in location in the bilayer become relatively more important in determining the limiting anisotropy in fluid membranes. The r_∞ of DPHcPC and TMA-DPH is at $T \gtrsim T_m$ significantly larger than that of DPHePC and DPHpPC. In Figure 7B, C the barycenters of the main distributed correlation time and the integrated amplitude are given as function of temperature (barycenters of the shorter distributed correlation time could not be determined accurately). The barycenters move to shorter time scale at higher temperatures, which can be explained by faster restricted DPH movements. The barycenters of the main distributed correlation times of the DPH derivatives in DMPC and DPPC vesicles at equal temperatures are

essentially the same, while the r_{∞} differs largely at temperatures between 20°C and 45°C, which is an obvious consequence of the differences in phase of the two membrane bilayers. The perpendicular diffusion coefficients ($D_{\perp}$) of the DPH probes in DMPC vesicles, calculated with eqs. 7 and 8, are presented in Table 1. In this approach $D_{\perp}$ is considered to be an average diffusion coefficient of all chromophores in the membrane. The $D_{\perp}$ values of DPH and TMA-DPH agree rather well with those found by others (Ameloot et al., 1984; Best et al., 1987; Wang, 1987).
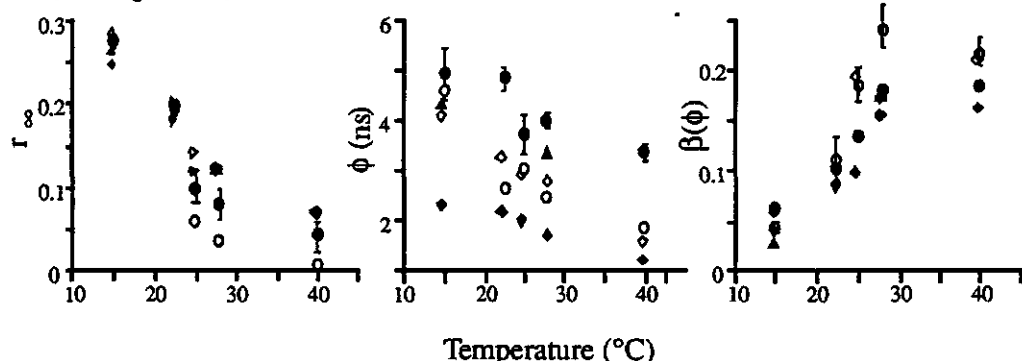
Figure 7 Temperature dependence of r_{∞} (A) and the barycenter (B) and contribution (C) of the main peak in the correlation-time distribution of different DPH probes in DMPC bilayers. O: DPH, ●: DPHpPC, ◇: TMA-DPH, ◆: DPHcPC, ▲: DPHePC. In each plot one representative data set is presented with error bars.

The results in Table 1 show that the $D_{\perp}$ values are considerably smaller for the DPH lipids than for DPH; $D_{\perp}$ increases in the following order: DPHcPC = TMA-DPH < DPHePC < DPHpPC < DPH. An increase in temperature accelerated the depolarising motions of the probes in each of the vesicle systems examined. An abrupt change in rate of diffusion was observed during the phase transition for the probes DPH and DPHpPC. For the other probes the changes were more gradual. $D_{\perp}$ values of DPH, obtained with MEM (Table 1) agree with values earlier reported using discrete exponential analysis (Wang, 1987).

T °C	DPHpPC	DPHePC	DPHcPC	DPH	TMA-DPH
15	0.002	0.004	0.006	0.023	0.006
22.5	0.016		0.026	0.018	0.027
25	0.071		0.049	0.152	0.048
28	0.097	0.082	0.061	0.163	0.068
40	0.118		0.132	0.198	0.138

Table 1 Temperature dependence of the perpendicular rotational diffusion coefficient (ns^{-1}) of the DPH probes in DMPC vesicles. $D_{\perp}$ was calculated from the correlation time distributions (obtained from MEM) using eqs. 7 and 8. The error bars result from repeated experiments.

3.3.3 Two-dimensional maximum entropy analysis

All experimental results were further analysed with a two-dimensional maximum entropy analysis in which the associative behaviour between the

fluorescence lifetimes and the rotational correlation times was investigated. As a typical example the results of the analysis of DPHpPC in DMPC at 40°C is presented in Figure 8. The pattern clearly displays the two lifetime components centred at their true positions along the τ-axis ($\tau_1 = 3.7$ and $\tau_2 = 7.6$ ns). Along the ϕ-axis we can see the two separated correlation-time peaks associated with τ_1 and τ_2, next to the limiting anisotropy at $\phi = \infty$. Three conclusions from these two-dimensional analyses can be drawn:

i) The two correlation-time peaks share the same fluorescence lifetimes. The association of the resolved correlation-time peaks with both lifetimes is ambiguous due to iso-kappa interference (Gentin et al., 1990; Brochon et al., 1992). The four peaks A, B, C and D in Figure 8 belong to two different iso-kappa curves and three combinations A+D, B+C or A+B+C+D accurately fit the data, only the relative proportion of these peaks being changed. Additional information is needed to resolve this ambiguity.

ii) The main lifetime τ_2, associated with the correlation-time peaks A and B, is in most experiments slightly (≤ 1 ns) shorter than the fluorescence lifetime associated with r_∞ (see Figure 8). Simulations (results not shown) in which both correlation-time peaks and r_∞ were associated with the main lifetime peak τ_2, indicated that this difference in lifetimes could be satisfactorily explained by the fact that at long times the observed anisotropy is dominated by the species with the longest lifetime (Ruggiero & Hudson, 1989).

iii) None of the analyses demonstrated an association of the limiting anisotropy term with the shorter lifetime τ_1.
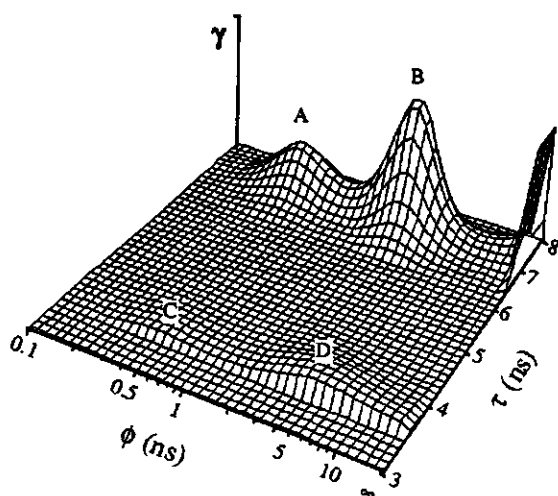

Figure 8 A three-dimensional plot (τ, ϕ, γ) for DPHpPC in DMPC vesicles at 40°C. The ϕ-axis extends between 0.1 and 20 ns. Infinite time scale ($\phi \rightarrow \infty$) is indicated at the last point of this axis.

3.3.4 Weighted orientational distribution from global analysis of fluorescence anisotropy decay

In addition, to the mathematical approach, the experimental fluorescence anisotropy decays were globally analysed using the r_{g3} model (see Methods section). To obtain optimal fits, the order parameters $<P_2>$, $<P_4>$ and the diffusion constant $D_\perp$ were associated with two discrete lifetimes. These fluorescence lifetimes were obtained from a separate analysis of the total fluorescence decay. The lifetime values obtained approached those of the barycenters from the lifetime distributions (see section 3.1). The initial anisotropy for each probe was linked over experiments at all temperatures. The results of the global analysis are presented in Table 2. The ambiguity of the solution for $<P_4>$ was investigated for DPHpPC in DMPC at 40°C. Although two minima in the dependence of the χ^2 on the value of $<P_4>$ were obtained (data not shown), the χ^2 minimum at $<P_4> = 0.4$ ($\chi^2 = 1.06$) is lower than the minimum at $<P_4> = -0.2$ ($\chi^2 = 1.43$). As expected, both $<P_2>$ and $<P_4>$ of all derivatives decrease with temperature. At temperatures below T_m, the $<P_2>$ and $<P_4>$ values of the different DPH compounds are almost equal, while at temperatures above T_m differences in $<P_2>$ and $<P_4>$ values become pronounced. It is hard to explain the differences between the estimates for the diffusion coefficient $D_\perp$ obtained by MEM (Table 1) and the r_{g3} model (Table 2). One possibility might be that the value of the initial anisotropy, which is determined differently in both programs, has a strong effect on the diffusion coefficient values. The value of the initial anisotropy is determined in the MEM analysis for each experiment individually, while in the r_{g3} analysis it is determined globally from several experiments. The real nature of the difference remains to be investigated systematically. Plots of the weighted orientational distribution of probe molecules against the angle of the emission dipole moment θ with the membrane normal could be constructed from the $<P_2>$ and $<P_4>$ values (Ameloot et al., 1984; van Langen et al., 1987; Berne et al., 1968). These plots contain information about the angular displacement which is determined by both sterical and geometrical constraints. An example of such a plot for the three DPH lipids is given in Figure 9. The weighted orientational distributions for the DPH derivatives indicate that the reorientational freedom is restricted both in the hydrophobic core and at the bilayer-water interface. The width of the weighted distribution of DPHpPC and DPHePC is smaller than that of DPHcPC (see Figure 9), DPH and TMA-DPH (data not shown) indicating that DPH attached the former two lipids has a narrower angular distribution around the membrane normal.
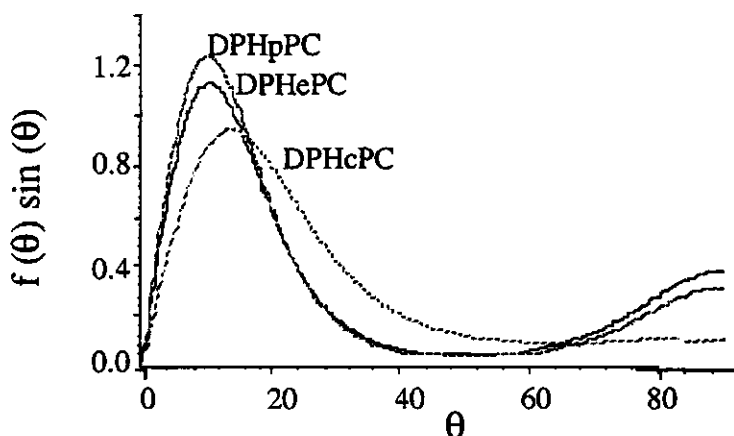
The weighted orientational distributions of the DPH derivatives show a considerable sensitivity to temperature (data not shown). The effect of increasing temperature on the weighted distribution patterns leads us to distinguish three effects:

i) The distribution shows broadening.

ii) A shift of the most populated angle in the distribution from shorter values to longer ones.

Both effects indicate a decrease of acyl chain ordering.

iii) A shift of the orientation in favour of alignment of the DPH fluorophore perpendicular to the acyl side chains. This shift was also observed by other

workers for DPH (Ginkel et al., 1989; Deinum et al., 1988; Kooyman et al., 1983; Vos et al., 1983; Ameloot et al., 1984; Best et al., 1987; Wang et al., 1987) and TMA-DPH (Best et al., 1987; van Langen et al., 1987).

Figure 9 The weighted orientational distribution $f(\theta)\sin(\theta)$ for DPHpPC, DPHePC and DPHcPC in DPPC vesicles at 45°C. The area under the curve represents the probability of finding the probe at a certain angle.

At 60°C in DPPC, the hydrophobic core is even so fluid that DPH rotates almost isotropically, while the other DPH derivatives still have an appreciable distribution minimum between $\theta=30°$ and $\theta=70°$, and hence consists of a heterogeneous probe population of anisotropically rotating probes. As shown in Figure 9 a significant population of DPHpPC and DPHePC molecules is oriented parallel to the plane of the DMPC bilayer at 28°C. This bimodal distribution is less clear and broader for DPHcPC. This remarkable result is due to a relatively high contribution of $<P_4>$ (Table 2). Unexpectedly, the weighted orientational distributions of both TMA-DPH and DPHcPC are broader and shifted to longer angles than those of DPHePC and DPHpPC. The relatively high position of DPH in the hydrocarbon region of the former probes might affect the heterogeneity in orientation angles. Because the rotational freedom experienced by the DPH portion of the lipids is an effect of both lipid environmental and intramolecular motional restrictions, one would predict that the DPH moiety of DPHcPC and TMA-DPH is more hindered than DPHpPC. It is unclear which two factors determine the differences in the weighted orientational distributions.

No significant differences could be detected in the weighted distribution functions of the DPH derivatives in DMPC compared with those in DPPC at equal temperature and lipid phase.

Probe	T (°C)	$\langle P_2 \rangle$	$\langle P_4 \rangle$	$D_\perp$ (ns^{-1})	global r_0	global χ^2
DPH	15	0.89 (0.87-0.9)	0.79 (0.72-0.83)	0.06 (0.04-0.09)		
	22.5	0.72 (0.71-0.74)	0.64 (0.62-0.72)	0.12 (0.08-0.18)		
	25	0.44 (0.41-0.46)	0.47 (0.42-0.56)	0.23 (0.16-0.38)	0.350	1.09
	28	0.34 (0.32-0.35)	0.41 (0.39-0.46)	0.28 (0.19-0.40)		
	40	0.17 (0.13-0.18)	0.11 (0.07-0.16)	0.43 (0.36-0.49)		
TMA-DPH	15	0.89 (0.88-0.90)	0.80 (0.74-0.82)	0.03 (0.02-0.08)		
	22.5	0.75 (0.73-0.77)	0.62 (0.59-0.70)	0.11 (0.09-0.16)		
	25	0.65 0.62-0.68	0.52 (0.50-0.62)	0.15 (0.13-0.31)	0.355	1.24
	28	0.61 (0.56-0.66)	0.46 (0.41-0.51)	0.20 (0.16-0.28)		
	40	0.49 (0.45-0.55)	0.18 (0.13-0.24)	0.30 (0.28-0.38)		
DPHpPC	15	0.86 (0.68-0.91)	0.77 (0.74-0.84)	0.03 (0.02-0.08)		
	22.5	0.76 (0.66-0.8)	0.66 (0.62-0.77)	0.06 (0.05-0.1)		
	25	0.68 (0.64-0.71)	0.63 (0.61-0.68)	0.10 (0.07-0.15)	0.361	1.09
	28	0.63 (0.56-0.64)	0.56 (0.51-0.63)	0.11 (0.08-0.21)		
	40	0.53 (0.49-0.55)	0.43 (0.38-0.52)	0.15 (0.13-0.30)		
DPHePC	15	0.84 (0.81-0.89)	0.77 (0.74-0.83)	0.03 (0.02-0.08)	0.356	1.23
	28	0.57 (0.51-0.6)	0.53 (0.49-0.58)	0.21 (0.14-0.37)		
DPHcPC	15	0.86 (0.68-0.92)	0.73 (0.72-0.82)	0.07 (0.05-0.10)		
	22.5	0.77 (0.69-0.80)	0.59 (0.53-0.66)	0.12 (0.09-0.24)		
	25	0.71 (0.63-0.74)	0.50 (0.47-0.59)	0.17 (0.10-0.36)	0.355	1.29
	28	0.64 (0.61-0.66)	0.40 (0.35-0.48)	0.28 (0.23-0.45)		
	40	0.45 (0.43-0.53)	0.13 (0.96-0.19)	0.49 (0.42-0.67)		

Table 2 Results of global analysis of the data sets of the DPH probes in DMPC vesicles at various temperatures using the r_{g3} model. The numbers within the parentheses correspond to the errors as determined from a rigorous error analysis at a 67 % confidence level. In the analysis the initial anisotropy of each lipid probe was globally linked.

3.4. **Discussion**

3.4.1 Distribution width

In general the width of a distribution depends on the number of slightly different environmental substates of probe molecules in the membrane and on the rate of exchange between those states. Since all time-resolved fluorescence experiments were carried out using the same total integrated intensity, we can compare the widths of the distributions of different samples. The width of the lifetime distribution depends on temperature and lipid bilayer phase (see also (Fiorini et al., 1987)). In Figure 10 the rotational diffusion coefficient $D_\perp$, which is a measure for the (perpendicular) rotational exchange rate, is plotted against the relative width of τ_2 for DPHpPC and free DPH in DPPC at several temperatures. Although the uncertainty in the points is large, it is evident that the dependencies of the distribution width on $D_\perp$ is different for both DPH molecules. In case of DPHpPC the plot is shifted to lower values. From this it can be concluded that DPH is more heterogeneously distributed in the lipid bilayer than DPHpPC.
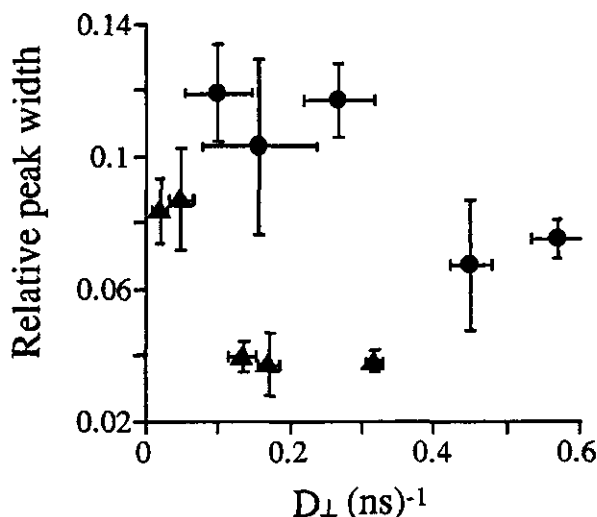
Figure 10 The rotational diffusion coefficient $(D_\perp)$ versus the relative peak half width $(\Delta\tau/\tau)$ of the longer lifetime component (τ_2) of DPH (●) and DPHpPC (▲) in DPPC vesicles at various temperatures. Presented are averages with standard errors of values (obtained by MEM) of duplicate experiments.

3.4.2 Lifetime and correlation time distributions

The fluorescence decay of the DPH probes in lipid bilayers is described by a bimodal distribution. In chloroform we observed also a bimodal lifetime distribution for DPH and DPHpPC, although the contribution of τ_1 to the fluorescence relaxation is only 6-12 percent (results not shown). Several explanations for the physical origin of the shorter lifetime component have been summarised by Lentz (1989). A new viewpoint has recently been given by Brand and coworkers (Toptygin et al., 1992). A double exponential character of

the fluorescence decay is expected on the basis of an orientational dependence of the radiative decay rate in optically anisotropic systems. Because we observed also a bimodal lifetime distribution of DPH in isotropic systems (unpublished observations) this phenomenon can not be the only mechanism causing the complex fluorescence relaxation. The ratio of the integrated amplitude, $\alpha(\tau_1)/\alpha(\tau_2)$, varied upon changing the state of the membrane. If two different probe environments would be responsible for the bimodal fluorescence relaxation, both populations would exist at each temperature, in fluid and gel-phase of either DMPC and DPPC membranes.

The two-dimensional MEM analyses of all data sets showed that r_∞ is not associated with the shorter lifetime component τ_1, indicating that the anisotropic behaviour of chromophores associated with τ_2 is different from the behaviour of those responsible for τ_1. Non-associative fluorescence anisotropy data analysis as applied in the one-dimensional MEM-analysis or r_{g3} global analysis, is therefore a first order approximation. Excitation and emission wavelength-dependence of the ratio $\alpha(\tau_1)/\alpha(\tau_2)$ might provide information on the possibility of photoproducts or on the presence of two energetically close excited states (Rullière & Declémy, 1987) as the origin of the shorter lifetime component.

At higher temperatures the anisotropy decay of the DPH derivatives is mathematically described by at least two distributed components of rotational correlation times, next to a limiting anisotropy term. This behaviour is expected in the r_{g3}-model (three exponentials and a constant term) in which the preexponential factors are dependent on the actual values of $<P_2>$ and $<P_4>$ and the relaxation times on $<P_2>$, $<P_4>$ and $D_\perp$.

3.4.3 Weighted orientational distribution of the DPH lipids

According to the results of the fits to the rotational diffusion model, all DPH derivatives have a significant population of probe molecules oriented perpendicular with respect to the normal of the membrane.

This result is in contradiction with the current physical model of intrinsically oriented DPH lipids in which it is assumed that the DPH moiety is located in the hydrocarbon region oriented parallel to the acyl chains of the bilayer. Although the uncertainty in the value of $<P_4>$ is large (Table 2), attempts to force the $<P_4>$ values down to values necessary for a unimodal orientational distribution gave according to the F-statistic criterion (see Methods section), an unacceptable rise in χ^2 values. Either the r_{g3} model or the physical description of motional restriction of intrinsically oriented probes should be further investigated. The parameters used in the r_{g3} model reflect average properties (rotational dynamics and angular barriers) experienced by all probe molecules. With this assumption a bimodally oriented population of probe molecules is found (Figure 9). The limitation of the r_{g3} approach can be envisaged by considering that both populations probably consist of probe molecules with different order and diffusion properties. Since the fluorescence lifetimes are hardly dependent on the lipid environment, one is not able to separate both populations on the basis of fluorescence lifetimes. On the other hand it has been shown with molecular dynamics simulations (Egberts & Berendsen, 1988) that the overall structure of the membrane shows considerable disorder. If

there is a population with the DPH-moiety oriented parallel to the membrane plane, these fluorophores are probably not located very high in the hydrocarbon zone, because one would expect a shortening of the average fluorescence lifetime of these chromophores (Fiorini et al., 1987) which is not observed.

3.4.4 DPH lipids

Comparing the fluorescence and anisotropy relaxations of the different DPH-labelled lipids we can conclude that the substitution of the carbonyl group directly to the phenyl ring of DPH (DPHcPC) strongly influences the photophysical properties like observed with TMA-DPH. All distributions are broader than those of DPHePC or DPHpPC, indicating a less defined, heterogeneous environment. On the other hand, the total fluorescence properties and anisotropic behaviour of DPHePC and DPHpPC are very similar. From a comparison of the fluorescence lifetime distributions and weighted orientational distributions of DPHpPC and DPHePC with those of DPH, we can conclude that the DPH lipids exhibit more defined emission properties (sharper lifetime peaks), slower rotational diffusion and narrower angular distributions around the membrane normal.

3.5 References

Alford P.C. & Palmer T.F. (1982) *Chem. Phys. Lett.* 86, 248-253.

Ameloot M., Hendrickx H., Herreman W., Pottel H., van Cauwelaert F., & van der Meer W. (1984) *Biophys. J.* 46, 525-539.

Barrow D.A. & Lentz B.R. (1985) *Biophys. J.* 48, 221-234.

Beechem J.M., Gratton E., Ameloot M., Knutson J.R. & Brand L. (1991) in "Topics in Fluorescence Spectroscopy" (J.R. Lakowicz, Ed.) Vol 2, p 241-305, Plenum Press, New York.

Berne P.J., Pechukas P. & Harp G.D. (1968) *J. Chem. Phys.* 49, 3125-3129.

Best L., John E. & Jähnig F. (1987) *Eur. Biophys. J.* 15, 87-102.

Brochon J.C., Mérola F. & Livesey A.K. (1992) in "Synchrotron Radiation and Dynamic Phenomena" (American Institute of Physics, Ed.) 435-452 New York.

Chen L.A., Dale R.E., Roth S. & Brand L. (1977) *J. Biol. Chem.* 252, 2163-2169.

Dale R.E., Chen L.A. & Brand L. (1977) *J. Biol. Chem.* 252, 7500-7510.

Davenport L., Knutson J.R. & Brand L. (1986) *Biochemistry* 25, 1811-1816.

Deinum G., van Langen H., van Ginkel G., Levine Y.K. (1988) *Biochemistry* 27, 852-860.

Dekker L.V. & Parker, P.J. (1994) *Trends Biochem.Sci.* 19, 73-77

Egberts E. & Berendsen H.J.C. (1988) *J. Chem. Phys.* 89, 3718-3732.

Fiorini R., Valentino M., Wang S., Glaser M., Gratton E. (1987) *Biochemistry* 26, 3864-3870.

Gentin M., Vincent M., Brochon J.C., Livesey A.K., Cittanova N., & Gallay J. (1990) *Biochemistry* 29, 10405-10412.

Houslay M.D. & Stanley K.K. (1982) in: "Dynamics of Biological Membranes" (Ed.) p 54. John Wiley & Sons, Ltd., New York.

Jaynes E.T. (1968) *Trans. Biomed.* 4, 227.

Klausner R.D., Kleinfeld A.M., Hoover R.L & Karnovsky M.J. (1980) *J. Biol. Chem.* 255, 1286-1295.

Kooyman R.P.H., Vos M.H. & Levine Y.K. (1983) *Chem Phys.* 81, 461-472.

Kremer J.M.H., vd Esker M.W.J., Pathmamanoharan C. & Wiersema P.H. (1977) *Biochemistry* 16, 3932-3935.

Lentz, B.R. (1989) *Chem. Phys. Lipids* 50, 171-190.

Livesey A.K. & Brochon J.C. (1987) *Biophys. J.* 52, 693-706.

Mateo C.R., Lillo M.P., Gonzalez-Rodriguez & Acuña A.U., *Eur. Biophys. J.* (1991) 20, 41-52.

Mérola F., Rigler R., Holmgren A. & Brochon J.C. (1989) *Biochemistry* 28, 3383-3398.

O'Connor D.V. & Philips D. (1984) Time-correlated single photon counting, Academic Press, London.

Parasassi T., Conti F., Glaser M. & Gratton E. (1984) *J. Biol. Chem.* 259, 14011-14017.

Parente R.A. & Lentz B.R. (1985) *Biochemistry* 24, 6178-6185.

Rousser G., Fleischer S. & Yamamoto A. (1970) *Lipids* 5, 494-496.

Ruggiero A. & Hudson B. (1989) *Biophys. J.* 55, 1125-1135.

Rullière C. & Declémy A. (1987) *Chem. Phys. Lett.* 135, 3, 213-218.

Somerharju P.J. & Wirtz K.W.A. (1982), *Chem. Phys. Lipids* 30, 81-91.

Straume M. & Litman B.J. (1987) *Biochemistry* 26, 5113-5120.

Szabo A. (1984) *J. Chem. Phys.* 81, 150-167.

Toptygin D., Svobodova J., Konopasek I. andBrand L. (1992) *J. Chem. Phys.* 96, 7919-7930.

Van der Meer W., Pottel H., Herreman W., Ameloot M., Hendrickx H. & Schröder H. (1984) *Biophys. J.* 46, 515-523.

Van Ginkel G., van Langen H., Levine Y.K. (1989) *Biochimie* 71, 23-32.

Van Hoek A., Vos K. & Visser A.J.W.G. (1987) *J. Quantum Electron.* *QE*-23, 1812-1820.

Van Langen H., Levine Y.K., Ameloot M. & Pottel H. (1987) *Chem. Phys. Lett.* 140, 394-400.

Vos K., van Hoek A. & Visser A.J.W.G. (1987) *Eur. J. Biochem.* 165, 55-63.

Vos M.H., Kooyman R.P.H., Levine Y.K. (1983) *Biochem. Biophys. Res. Comm.* 116, 462-468.

Wang S., Beechem J.M., Gratton E. & Glaser M. (1991) *Biochemistry* 30, 5565-5572.

Chapter 4

Reorientational properties of fluorescent analogues of the protein kinase C cofactors diacylglycerol and phorbol ester in vesicles and mixed micelles

Abstract

The reorientational properties of the fluorescently labelled protein kinase C (PKC) cofactors diacylglycerol (DG) and phorbol ester (PMA) in vesicles and mixed micelles have been investigated using time-resolved polarised fluorescence. The sn-2 acyl chain of DG was replaced by diphenylhexatriene-(DPH) propionic acid, while a dansyl labelled analogue of phorbol ester was used. The polarised fluorescence properties of DPH-DG and the control choline lipid DPH-PC were compared in bilayer vesicles. The extent of ordering of DPH-DG in vesicles turned out to be slightly different from those of DPH-PC. Addition of PKC to vesicles containing 30 mole % brain PS considerably slowed down the DPH-DG anisotropy decay. This was not observed when DPH-DG was replaced by DPH-PC, indicating that this effect of PKC on the DPH-DG anisotropy decay originates from specific interaction with PKC. In order to investigate the calcium and PS dependence of PKC-cofactor interaction, the DPH-lipids were dispersed in micelles composed of the non-ionic surfactant polyoxyethylene-9-laurylether mixed with 10 mole % of the essential phosphatidylserine (PS). Analysis of the fluorescence anisotropy decays of these DPH-lipids in micelles allowed estimation of their lateral diffusion, orientation distribution and reorientational dynamics within the micelles. Addition of PKC resulted in a significantly slower decay of the fluorescence anisotropy of both DPH-lipids even in the absence of calcium. This reduced depolarisation appeared to originate mainly from slower overall rotation of the micelle and reduced lateral diffusion of the DPH-lipids in the micelles, indicating a calcium independent complexation of PKC with the PS containing micelles. Addition of calcium resulted in a further reduction of the decay of anisotropy of DPH-DG caused by slower overall rotation of the micelle, reduced lateral diffusion and reorientational freedom of DPH-DG. This effect was not seen when DPH-DG was replaced by DPH-PC or when PS was replaced by PC indicating that the immobilisation is cofactor-specific and that negatively charged lipids are required for association of PKC to the micellar system. Similar specific interactions with PKC resulted in a slower decay of dansylated PMA when calcium and PS were present. Addition of a four-fold excess of unlabelled PMA yielded the same anisotropy decay of dansyl-PMA as the one obtained in the absence of PKC indicating a reciprocal relationship of labelled and unlabelled PMA with respect to PKC binding.

4.1. Introduction

The compounds diacylglycerol (DG) and phorbol esters have large regulatory effects on several cellular processes. The mechanism by which these molecules operate has been the focus of intensive study and has resulted in an

increasingly detailed picture of cellular signalling. In many cases both compounds induce similar biological responses (Kikkawa & Nishizuka, 1986) which can be attributed to either activation or down regulation of PKC at the membrane level (Ashendel, 1985; Bazzi & Nelsestuen, 1988a, 1989a; Brockerhoff, 1986; Nishizuka, 1984). In addition, DG is involved in the activation of other regulatory enzymes, several phospholipases (Dawson, 1983; Dawson et al., 1984; Zidovetzki & Lester, 1992) and transmembrane proteins (Arnold & Newton, 1992) and multiple target proteins have been found for phorbol esters (Ahmed et al., 1993). Among the three PKC subfamilies, cPKC and nPKC respond to DG and phorbol esters while αPKC does not. Phorbol esters and DG bind similarly with one to one stoichiometry to PKC (Brockerhoff, 1986; Castagna et al., 1982b; Chauhan et al., 1989; Ganong & Loomis, 1986; Gschwendt, 1991; Hannun et al., 1985) and compete for binding to the kinase (Castagna et al., 1982a; Chauhan et al., 1989), although the existence of two phorbol ester binding domains has also been suggested (Burns, 1991). Interaction with anionic lipids and calcium (for cPKC) is essential for the activation of PKC by phorbol esters or DG (Bazzi & Nelsestuen, 1989b; Chapter 5, 6). The precise working mechanism of calcium and its requirement for the lipid interaction of cPKC however remains to be elucidated (Chapter 5, Zidoveski & Lester, 1992). Generally, it is assumed that the substrate binding pocket of inactive PKC is blocked by a so-called pseudosubstrate. Conformation changes after activation with anionic lipids, DG and calcium lead to the dissociation of the pseudosubstrate from the catalytic domain and consequently enables substrates to bind to the enzyme (Mosior & McLaughlin, 1991).

Biochemical studies suggest that activation of PKC by DG requires a specific stereochemical configuration of DG which indicates that the cofactors interact with specific structural elements of PKC. In addition, it was observed that only DG molecules with unsaturated acylchains activate PKC effectively. It is unclear whether structural properties of these unsaturated chains or specific perturbations of the lipid bilayer structure induced by the unsaturated chain of DG result in the maximal stimulation of PKC (see also Zidoveski & Lester, 1992). In some cases membrane perturbation alone can induce partial PKC activation as observed by Lester and co-workers (Lester et al., 1990). It has even been suggested that the activation of PKC by DG mainly is a consequence of DG-induced changes in the physical properties of the membrane (Epand et al., 1992). Many research groups observed that DG separates lipid headgroups in the membrane at low concentrations, whereas high concentrations of DG induce the formation of non-bilayer phases (Cheng et al., 1991; Das & Rand, 1986; Ohki et al., 1982, Epand & Bottega, 1988). The relevance of non-bilayer structures in the regulation of PKC is questionable, bearing in mind that the amount of DG is low in natural membranes. For example, the DG in a rat kidney cell can rise from 0.6 mole % (normal) to 1.4 mole % (transformed) (Preiss et al., 1986). Although these studies provide valuable information about the potency of DG to modulate the membrane properties most of these studies were performed with unnatural high concentrations of DG or lipid compositions that already form quasi-stable bilayers by themselves.

In this study the motional freedom and dynamics of DPH-labelled DG and dansyl-labelled phorbol ester are compared with those of DPH-labelled PC. The

fact that the direct environment of DG is probed by its labelled acyl chain and is quantified in terms of chain dynamics and local order, adds to the previous DG studies where merely average bulk properties of the membrane were observed. In addition, the effect of PKC on the motional freedom and dynamics of probe lipids was determined from their fluorescence anisotropy decays in mixed micelles and vesicles. Vesicles are relatively large lipid systems which mimic physico-chemical properties of the biological bilayer more closely than micelles. Typically, micelles have a diameter in the nanometer range. Complexation with proteins will affect the overall rotation of the micelles and, consequently, the fluorescence anisotropy decay of lipid probes within these lipid systems. Therefore, fluorescence anisotropy forms a suitable tool to monitor association of PKC to the micellar surface. More specific interactions between the protein and cofactor will not only influence the micellar overall motion, but also the cofactor motions within the micelle. Consequently, specific interactions can be probed by measuring the fluorescence anisotropy decay of the cofactor probes in the micelle.

4.2. Experimental Procedures

Materials
Bovine brain L-α-phosphatidylserine (PS), dioleoyl-PC (DOPC), diacylglycerol (DG), thesit (polyoxyethylene-9-lauryl ether), EGTA, phospholipase C from *Bacillus cereus*, phenylmethanesulfonyl fluoride, sephacryl S200, polylysine-agarose were supplied by Sigma Chemical Co (St. Louis, MO, USA). Phenyl-sepharose CL-4B and DEAE-sepharose FF S200 were from Pharmacia (Uppsala, Sweden). All other phospholipids used were synthesised as described in the methods section. Dansyl phorbol ester and *sn-2*-(diphenylhexatriene)-PC were obtained from Molecular Probes (Eugene, OR, USA). Unless otherwise noted, experiments were performed at 277 K.

Purification of PKC
Protein kinase C was purified from the cytosolic extract of homogenised Wistar rat brains similar to the procedure described by Huang et al., (1986) and consecutively by DEAE, phenyl-sepharose, sephacryl S200 and polylysine agarose chromatography. The final preparation (with isozyme composition as described elsewhere (Huang and Huang, 1986; Sekiguchi, 1987)) was essentially pure as demonstrated by silver staining of a polyacrylamide gel, and was stored at -80°C in buffer (20 mM Tris pH 7.9, 0.5 mM EGTA, 0.5 mM EDTA, 1 mM BME) with 25% glycerol (Merck, Darmstadt, Germany, fluorescence microscopy grade).

Synthesis of DPH-labelled diacylglycerol
sn-2-(Diphenylhexatriene)-DG was synthesised by a phospholipase C catalysed hydrolysis of the diglyceride-phosphate linkage in DPH-PC as described by (Myher and Kuksis, 1984). An incubation time of 15 minutes was sufficient for 100 % conversion to DPH-DG. Therefore, further purification was not needed and acyl chain isomerisation of DPH-DG could be omitted. All experiments were performed with freshly synthesised DPH-DG.

Micelle preparation

Mixed lipid micelles were prepared by drying the required amounts of lipids under a stream of nitrogen in a glass tube followed by solubilisation in buffer (1 mM Thesit, 20 mM Tris/HCl 120 mM NaCl and 20 μM EGTA (pH 7.4)) by vortexing and brief bath sonication. In the binding studies the thesit concentration was 100 μM and the PS concentration was 10 μM (10 mole %). The DPH-lipid concentration was 0.1 μM. The phospholipid content was determined by phosphate analysis (Rousser et al., 1970). The DPH-lipid concentration was estimated by measuring the light absorption at 355 nm in chloroform (ε = 60100 M^{-1}cm^{-1} (Lentz, 1988)).

Vesicle preparation

Small unilamellar vesicles were prepared by injecting 2 μL of lipid dissolved in ethanol/DMSO through a Hamilton syringe into 200 μL of a magnetically stirred buffer solution (20 mM Tris/HCl 120 mM NaCl and 20 μM EGTA (pH 7.4)) (Kremer et al., 1977). The ratio of labelled lipid to unlabelled lipid was 1:150 on a molar basis. When the interaction of the DPH-lipids with PKC was measured, the lipid solution in ethanol was injected into buffer solution containing the protein, EGTA or calcium. With this procedure, DPH-lipid molecules located at the inner and outer membrane leaflet of the vesicles are accessible for PKC.

Time-resolved fluorescence and fluorescence anisotropy measurements

The polarised fluorescence decays were measured by use of a time correlated single photon counting setup as described elsewhere (Pap et al., 1993). The excitation wavelength was 340 nm. The fluorescence emission of the probes was selected using a KV 399 cut-off filter (Schott, Mainz, Germany) and an interference filter at 441.7 nm (Schott, bandwidth 10.9 nm FWHM) for the DPH lipids and a KV 500 cut-off filter (Schott) for dansyl labelled phorbol ester. After each sample the background of samples in the absence of DPH-lipids was measured for correction of the sample polarised decays. 2, 5-Diphenyloxazole (Eastman Kodak Co.) dissolved in ethanol served as reference compound (τ = 1.6 ns (Berlman, 1971)) to yield the dynamical instrumental response function of the set-up (van Hoek et al., 1987). The samples were thermostated at 277 K.

Data Analysis

By measuring the time-dependent parallel and perpendicular polarised emission components $I(t)_{\parallel}$ and $I(t)_{\perp}$ relative to the polarisation direction of the exciting beam one can recover the fluorescence anisotropy $r(t)$:

$$I(t)_{\parallel} = P(t) * \left(\frac{2}{3} r(t) f(t) + \frac{1}{3} f(t) \right) \qquad (1)$$

$$I(t)_{\perp} = P(t) * \left(\frac{-1}{3} r(t) f(t) + \frac{1}{3} f(t) \right) \qquad (2)$$

The multiplication sign indicates the convolution of the decay function with the instrument impulse response profile P(t). f(t) is the intrinsic fluorescence decay function and r(t) the anisotropy decay function which is described by the following time correlation function (Berne, & Pecora, 1976):

$$r(t) = \frac{2}{5} \langle P_2 \left[\mu_a(0)\mu_e(t) \right] \rangle \tag{3}$$

where the factor 2/5 accounts for the maximum theoretical anisotropy as a result of photoselection, $P_2[\mu_a(0)\mu_e(t)]$ is the second-order Legendre polynomial, $\mu_a(0)$ is the direction of the absorption transition moment in the molecular frame at zero time and $\mu_e(t)$ is the direction of the emission transition moment at time t. The brackets <.> denote an ensemble average. Each process that results in a more uniform distribution of μ_e will give a decrease of the anisotropy of the emitted light. Therefore the molecular order and rotational dynamics of probe molecules in lipid systems can be determined from the relaxation of the anisotropy (Szabo, 1984; Van der Meer et al., 1984). When lipid probes are dispersed in micelles, three independent motional processes may contribute to the observed anisotropy decay: (1) internal rotation of the lipids within the micelles, (2) lateral diffusion of the lipid probes within the micelle and (3) overall rotation of the micelle. In larger lipid systems like vesicles only rotational motion of the lipid probes within the bilayers contribute to the anisotropy decay. The rotational diffusion model (r_g3) describes the depolarisation induced by rotational motion of probes like DPH in terms of a perpendicular diffusion coefficient $D_\perp$ and the two order parameters <P_2> and <P_4> (Szabo, 1984; Van der Meer et al., 1984). The parameters <P_2> and <P_4> are related via an equilibrium orientation distribution function f(θ) of the DPH labels with respect to the membrane normal:

$$< P_2 > = \frac{1}{N} \int_0^\pi f(\theta) \, P_2 \, (cos \, \theta) \, sin \, \theta \, d\theta \tag{4}$$

$$< P_4 > = \frac{1}{N} \int_0^\pi f(\theta) \, P_4 \, (cos \, \theta) \, sin \, \theta \, d\theta \tag{5}$$

$$N = \int_0^\pi f(\theta) \, sin \, \theta \, d\theta \tag{6}$$

When no assumptions are made about the orientation distribution, <P_2> and <P_4> are determined independently. By applying the maximum entropy formalism, the most unbiased orientation distribution function can be constructed from optimised <P_2> and <P_4> values (Ameloot et al., 1984; Berne et al., 1968). This approach, however, often yields bimodal orientation

distribution functions for DPH, even when the labels are covalently attached to lipids (see Chapter 2). Such an orientational heterogeneity is not consistent with the known physico-chemical properties of DPH-lipids and membrane system. Apparently, in this approach a lowering of $<P_2>$ is interpreted to arise from an increase in the perpendicular oriented population of probes. The compound motion model, recently adapted for fluorescence anisotropy decay analysis of DPH-like probes, seems to be a more appropriate approach for analysis (Van der Sijs et al., 1994), but contains 5 adjustable parameters which restricts its application to macroscopically oriented lipid systems. Therefore, we analysed the anisotropy decay originating from rotation of DPH-lipids in micelles and vesicles according to the r_{g3} model with the intuitive assumption that the orientation of the DPH-labels is Gaussian distributed parallel with respect to the direction of the phospholipid acyl chains with distribution width θ_g (see also Straume & Litman (1987)):

$$f(\theta) = e^{-\left(\theta/\theta_g\right)^2} + e^{-\left((\pi-\theta)/\theta_g\right)^2} \tag{7}$$

Upon binding of PKC to vesicles, two populations of DPH-lipids might arise with different orientation distributions. One fraction $(1-\beta)$ of free DPH-DG molecules will remain in the bulk membrane with an orientation distribution width (θ_{gf}) similar to the situation without addition of protein. A second fraction β of the DPH-DG molecules will interact with PKC with unknown orientation distribution (θ_{gb}).

$$f(\theta) = \beta\left[e^{-\left(\theta/\theta_{gb}\right)^2} + e^{-\left((\pi-\theta)/\theta_{gb}\right)^2}\right] + (1-\beta)\left[e^{-\left(\theta/\theta_{gf}\right)^2} + e^{-\left((\pi-\theta)/\theta_{gf}\right)^2}\right] \tag{8}$$

Global analysis of multiple DPH anisotropy decays measured at various concentrations of PKC with the bimodal distribution of DPH-probes (eq 8) will then recover the fraction of DPH-DG molecules interacting with PKC (β), and the angular distribution of the bound cofactor molecules (θ_{gb}).

In micelles, the anisotropy decay curves of the DPH-lipids in micelles were analysed by a product of three correlation functions corresponding to the overall motion of the micelle with rotational correlation time ϕ_r, the probe lateral motion expressed by translational correlation time ϕ_T and the probe internal motion described by $D_\perp$ and θ_g in the r_{g3} model:

$$r(t) = e^{-t/\phi_r} \, e^{-t/\phi_T} \, C(r_0, D_\perp, \theta_g, t) \tag{9}$$

The correlation time ϕ_T is related to the lipid lateral diffusion D_L by:

$$\phi_T = \frac{r_m^2}{4\,D_L} \tag{10}$$

where r_m corresponds to the radius of the micelle. In these analyses ϕ_r was determined independently from translational diffusion of micelles (coefficient D_m in $m^2 s^{-1}$) measured with fluorescence correlation spectroscopy (Bastiaens et al., submitted). In the present calculations the rotation of micelles are assumed to be isotropic. While this assumption may not be realistic for micelles complexed with PKC, it is unlikely to introduce a serious error. The correlation time ϕ_r is then related to D_m by:

$$\phi_r \approx \frac{6.25 \ 10^{-4} \ k^2 \ n_2 \ T^2}{n_1^3 \ D_m^3} \qquad (11)$$

where k, T, n_1 and n_2 correspond respectively to the Boltzmann constant, temperature and viscosity of the sample measured with correlation spectroscopy and the sample measured with time correlated single photon counting (n_1 = 17.4 and n_2 = 11.1 mPa s). The parameters ϕ_T, $D_\perp$ and θ_g were determined for each experiment independently while the initial anisotropy, r_0, was adjusted globally from multiple experiments. When the DPH-lipids were dispersed in vesicles, ϕ_r and ϕ_T were fixed to large values in the ms range.

4.3. Results

4.3.1. Orientation distribution of DPH analogues of DG and PC in DOPC vesicles
In Figure 1 the experimental anisotropy decays of DPH-DG and DPH-PC in DOPC vesicles are presented. The smooth curves through the data points represent the optimised fits according to the r_{g3} model with the assumption that the orientation distribution of the DPH-lipids is Gaussian shaped. It can be seen that the motional constraints of DPH-DG and DPH-PC in these fluid state membranes differ slightly. In the lower panel of Figure 1 the weighted residuals of the fit to the parallel and perpendicular fluorescence decay curves of both DPH lipids are given. As can be concluded from the random scattering of the residuals the model adequately fits the decay curves of both DPH-lipids at longer times. At shorter times however, the model is not able to perfectly match the experimental data, which results in underestimation of the initial anisotropy r_0. Therefore this approach is compromising the advantage of a minimal number of adjustable parameters ($D_\perp$, θ_g) and an intuitively correct probe orientation with a sub-optimal fit to the experimental data.

No significant differences in the fluorescence decay characteristics were observed for the different DPH-lipids (data not shown), which is not surprising bearing in mind that the DPH moiety is linked identically to both lipids. In Table 1 the recovered θ_g and $D_\perp$ values, and corresponding $<P_2>$ and $<P_4>$ values (calculated from θ_g according to eqns. 4 and 5) are presented. Since both DPH-PC and DPH-DG closely mimic their natural lipids, the probe order parameters will reflect the overall molecular ordering experienced by their natural analogues in the membrane. From the experimental plots and the recovered parameters listed in Table 1 it can be concluded that when DPH is attached to DG its fluorescence anisotropy decays to lower values than when attached to PC. The differences are however small. This observation indicates a

lower degree of ordering of the neighbouring lipid chains experienced by DPH-DG. The lack of the phosphocholine headgroup in the DG host lipid apparently induces a packing failure of a close fit to the neighbouring lipid chains which results in slightly more angular freedom.
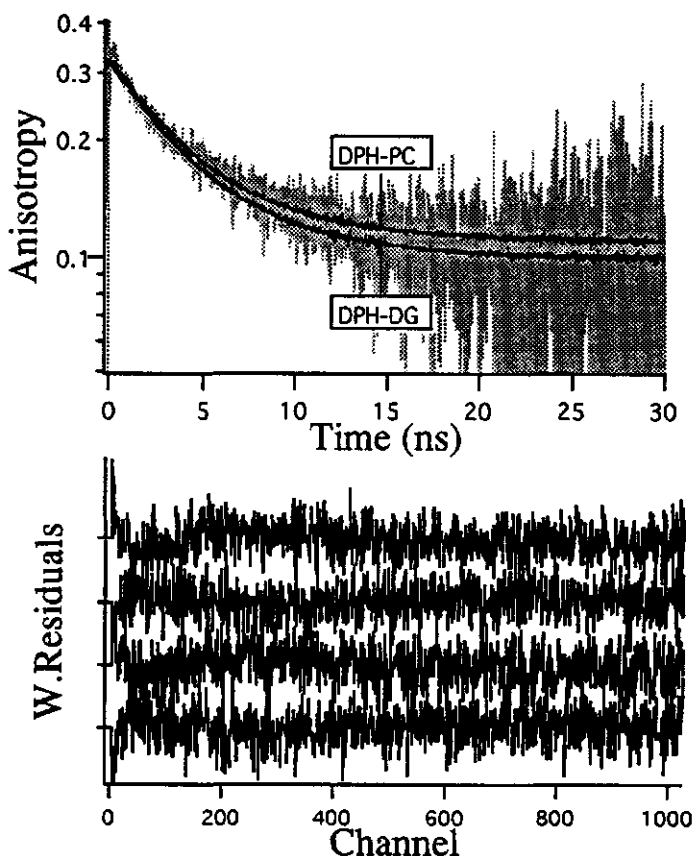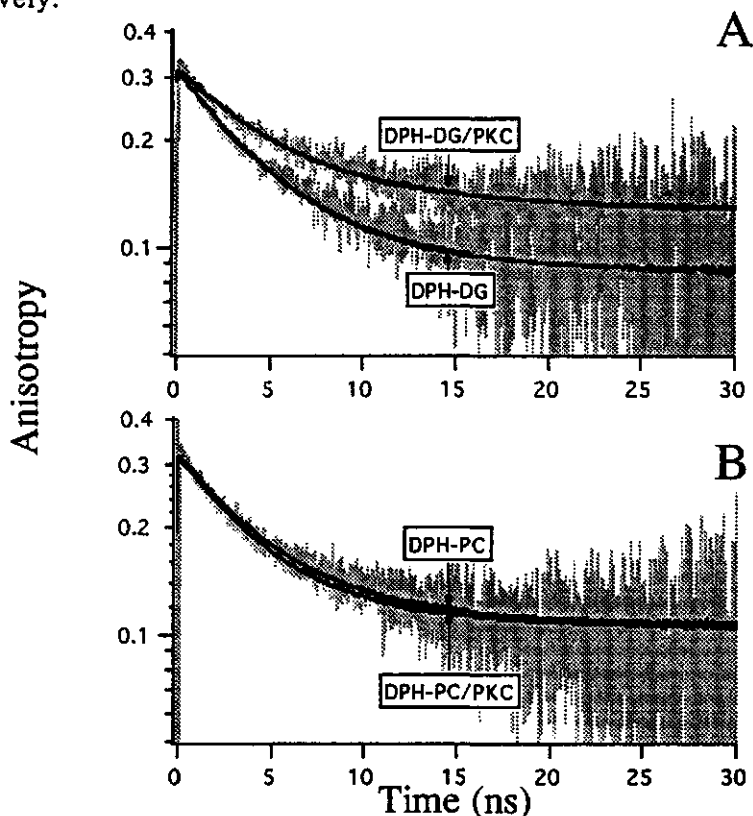

Figure 1. Experimental and fitted anisotropy decays of DPH-DG and DPH-PC in DOPC vesicles. The smooth curve corresponds to the optimal fit with the r_{g3} model assuming a Gaussian orientation distribution. In the lower panel the weighted residuals of the fit to the perpendicular and parallel decay curves of DPH-PC (upper two curves) and DPH-DG (lower two curves) are presented.

Probe	System	θ_g	$<P_2>$	$<P_4>$	$D_\perp$ (μs^{-1})	χ^2
DPH-DG	DOPC	0.63 (0.62-0.65)	0.56	0.15	28 (26-32)	1.21
DPH-PC	DOPC	0.59 (0.57-0.61)	0.60	0.18	27 (25-32)	1.23

Table 1. Optimised θ_g and $D_\perp$ values from analysis of the data sets of DPH lipid probes in DOPC vesicles using the r_{g3} model. The initial anisotropy was linked over all experiments and amounts to 0.323. The numbers between parentheses correspond to the errors as determined from a rigorous error analysis at a 67 % confidence level. The $<P_2>$ and $<P_4>$ values were calculated from θ_g using eqns. 4 and 5.

4.3.2. Interaction between PKC and DPH-DG in a vesicular lipid system

In order to investigate the effect of interaction with PKC on the rotational properties of DG and PC in DOPC/PS vesicles, the polarised decays of both DPH-lipids were measured in the presence of various concentrations of PKC. To facilitate PKC binding to DPH-lipids located at the inner and outer leaflets of the membrane, the vesicles were prepared by injecting small aliquots of the mixed lipids in ethanol into buffer solutions with or without PKC. The experimental fluorescence anisotropy decays of DPH-DG and DPH-PC in the absence and presence of 0.4 μM PKC are given in Figures 2A and 2B, respectively.

Figure 2. Experimental anisotropy decays of DPH-DG (A) and DPH-PC (B) in vesicles of DOPC/PS (80:20) in the presence and absence of PKC (0.4 μM). In the blank experiments without PKC, the dialysis buffer of PKC was added to the vesicles. The smooth curve corresponds to the optimal fit with the $r_{g}3$ model assuming a Gaussian orientation distribution.

The fluorescence anisotropy of DPH-DG decays to higher residual values when PKC is present than when it is absent, indicating additional motional restriction of the labelled cofactor when it interacts with PKC. Such an effect is not observed in the fluorescence anisotropy decay of DPH-PC and thus it seems to be specific for DPH-DG. The difference in the anisotropy decays in the presence and absence of PKC indicates a distinct difference between the

motional properties in the protein boundary and lipid bilayer regions. Since the only difference between the labelled DG and PC is the lack of the phosphocholine headgroup (note that DPH-DG was synthesised from DPH-PC) this result indicates that specific chemical features of the DPH-DG headgroup provides the interaction with PKC. Alternatively, specific physico-chemical features of the DPH-DG lipid environment may be recognised by PKC. Analysis of the anisotropy decays with the r_{g3} model with the assumption of a unimodal probe orientation (eq. 7) yielded optimised values for θ_g and $D_\perp$ (Table 2).

Probe	System	θ_g (rad)	$<P_2>$	$<P_4>$	$D_\perp$ (μs^{-1})	χ^2
DPH-DG	PS/PC/Ca^{2+}	0.65 (0.64-0.68)	0.53	0.12	27 (25-29)	1.19
	PS/PC/Ca^{2+}/PKC	0.54 (0.52-0.57)	0.65	0.24	20 (19-22)	1.26
DPH-PC	PS/PC/Ca^{2+}	0.60 (0.59-0.61)	0.59	0.17	25 (24-27)	1.19
	PS/PC/Ca^{2+}/PKC	0.60 (0.59-0.61)	0.59	0.17	27 (25-29)	1.17

Table 2. Optimised θ_g and $D_\perp$ values from analysis of the data sets of DPH lipid probes in DOPC/PS (8:2) vesicles using the r_{g3} model. The initial anisotropy was linked over multiple experiments and amounts to 0.323. In the experiments 0.5 mM calcium and 0.4 μM PKC were used. The total lipid concentration was 15 μM. See for further details the legend of Table 1.

It is obvious from these θ_g values that in presence of PKC, the DPH moiety attached to DG is oriented with smaller angles to the membrane normal than in absence of PKC. In addition, the rotational dynamics of DPH-DG is slightly reduced by PKC. It is important to note that the optimised θ_g value obtained in presence of PKC reflects the average motional freedom of DPH-DG molecules which are interacting with PKC and of those which are free in the bulk membrane. To derive an indication of the orientation distribution of the DPH-DG probes bound to PKC separate from those in the bulk lipid, the anisotropy decay curves of DPH-DG at various concentrations of PKC were analysed globally with a weighted sum of two Gaussian distributions (eq. 8). In this analysis, the Gaussian width of non-interacting DPH-DG molecules (θ_{gf}) was fixed to 0.65 as obtained without PKC (Table 2). In the analysis of ten fluorescence anisotropy decays obtained at different PKC concentration, the angular distribution of the bound cofactor molecules (θ_{gb}) and $D_\perp$ were adjusted globally, while the fraction of DPH-DG molecules interacting with PKC (β) was recovered individually for each experiment. The analysis yielded an optimised value of 0.41 for θ_{gb}. As can be expected from a multiparameter fit, the uncertainty in θ_{gb} is relatively large (0.26-0.54). Therefore this analysis should be considered as an approximate one. The weighted orientation distributions of the probes with respect to the membrane normal (which represent the probability of finding the probe at a certain angle) were constructed from the optimised θ_{gf} and θ_{gb} values (Figure 3A). The fractional contribution β of DPH-DG with Gaussian width θ_{gb} as a function of the PKC concentration is plotted in Figure 3B. It can thus be concluded that the DG acyl chains are restricted in their motion upon specific interaction with PKC.
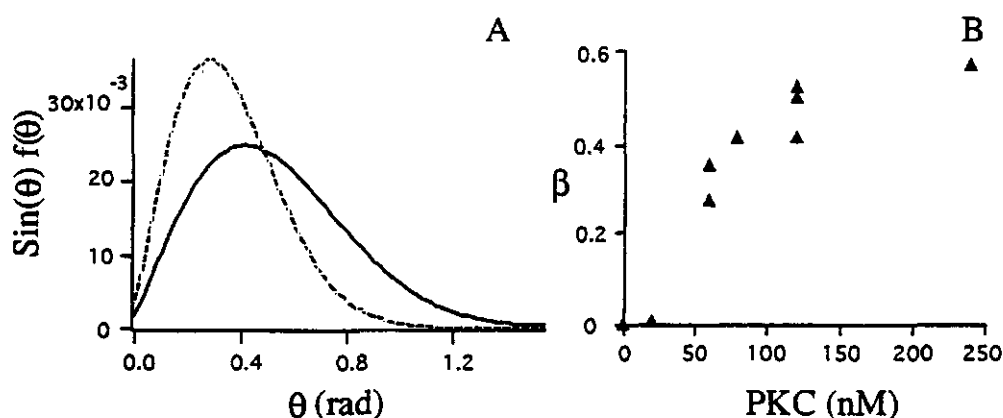
Figure 3. (A) Orientation distributions of probe molecules with Gaussian width of 0.65 (—) and 0.41 (---). These values correspond to the optimised values of free and PKC-bound DPH-DG, respectively (B) The fractional contribution (β) of bound DPH-DG with Gaussian width θ_{gb} as a function of PKC concentration. The orientation distribution of DPH-DG was assumed to be composed of two Gaussian distributions of free and bound DPH-DG as described in the Experimental Procedures. In this analysis the motional freedom of the free DPH-DG lipids θ_{gf} was fixed to the value obtained in the absence of PKC. The inset shows the probe orientational distribution functions for free and bound DPH-DG. The total lipid concentration was 15 μM.

4.3.4. Interaction between PKC and DPH-DG in a mixed micellar lipid system

In order to investigate the role of PS and calcium in the PKC-DG interaction, the anisotropy decays of DPH-DG and DPH-PC dispersed in micelles were determined at various binding conditions. Since PKC and thesit micelles have approximately similar sizes, the interaction of PKC to micellar lipids is expected to influence multiple independent motions; the isotropic rotation (ϕ_r) of the relatively small micelles and the translational diffusion (ϕ_T) and rotational motion of the probes (θ_g, $D_\perp$) around the radial vector of the micelle. Evaluation of each individual motional component at various PKC-lipid binding conditions will yield information which is difficult to obtain with vesicles. In Figure 4A the fluorescence anisotropy decays of DPH-DG in thesit micelles containing 10 mole % PS are presented. The fastest decay corresponds to DPH-DG in the absence of PKC. From visual comparison of this decay with the one obtained in vesicles (Figure 1) one can conclude that additional slow rotational motions are registered by DPH-lipids in micelles which result in a continuous decay of the anisotropy, even at longer times. These slow depolarisation processes originate from micellar rotation and lateral motion of lipids within the micelle. The rotational correlation time of micelles in absence PKC was calculated from translational diffusion coefficients obtained from

fluorescence correlation spectroscopy (Bastiaens et al., submitted) and amounts to 37 ns for free micelles (Table 3). Under approximation of spherical micelles this correlation time corresponds to a Stokes radius of 3.1 nm. No significant differences are observed between the experimental decays of DPH-DG and DPH-PC in absence of PKC (Figure 4B). This is not surprising, since the micellar rotation and lipid translational motion are mainly determined by the properties of the micelle itself and thus insensitive to DPH-lipid species. Global analysis of the anisotropy decay curves of DPH-DG and DPH-PC, in which r_0 was linked and ϕ_T and θ_g were determined from the individual decays of the DPH-lipids, yielded optimised values of 81 ns for ϕ_T and ≈ 0.45 radians for θ_g (Table 3). The errors of ϕ_T and θ_g at the 67 % confidence level, determined with an error analysis indicate that the differences between the θ_g values of both DPH-lipids are within the error of the experiment. The translational diffusion coefficient is related to ϕ_T (eq. 10) and amounts to 6.5×10^{-11} m^{2}s^{-1} which is larger than values obtained for lipids in bilayer membrane with pyrene excimer experiments ($\approx 10^{-11}$ m^{2}s^{-1} (Vauhkonen et al., 1989; Chapter 8).
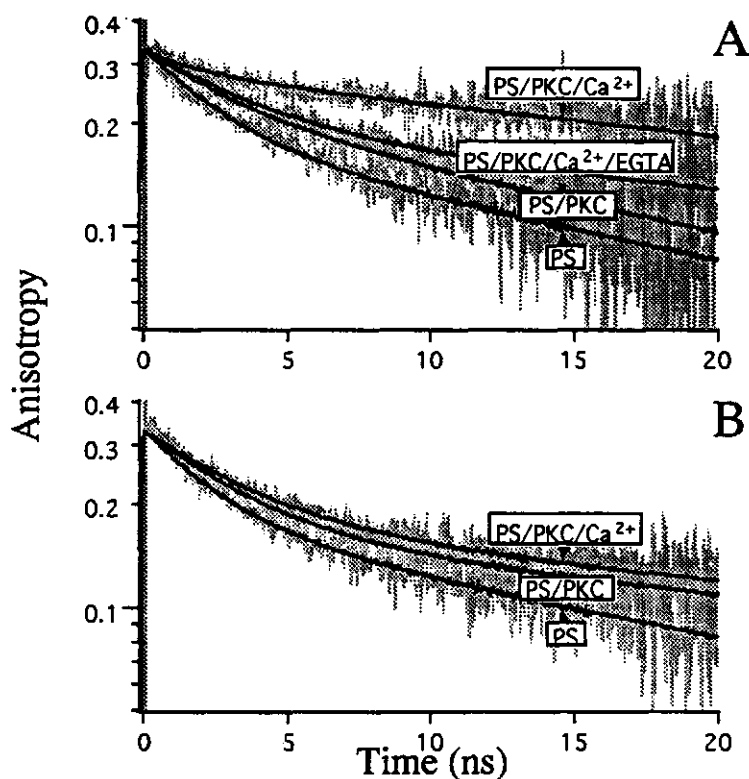
Figure 4. Experimental anisotropy decays of DPH-DG (A) and DPH-PC (B) in thesit micelles containing 10 mole % PS at various binding conditions (see text).

Addition of PKC leads to a slower decay of the anisotropy of both DPH-DG (Figure 4A) and DPH-PC (Figure 4B) even in the absence of calcium (50 µM EGTA). This observation indicates a calcium independent interaction of PKC with the micelles. In these experiments, with a thesit concentration of 100 µM, micelles are composed of approximately 300 detergent molecules (Bastiaens et al., 1993). Thus on the average one out of three micelles contains a DPH-lipid molecule, and at a PKC concentration of 0.4 µM, the protein is present in approximately 1.5 fold excess over the micelles. No effect of PKC on the DPH-DG anisotropy decay is observed when 10 mole % PS is replaced by 10 mole % PC in thesit micelles (data not shown) confirming that PS is a prerequisite for the interaction of PKC with a membrane surface (Bazzi & Nelsestuen, 1987; Rodriguesz-Paris et al., 1989). Conversely, mixed micelles containing 5 mol % PS are fully capable to bind PKC in the presence of calcium. Probably calcium is needed for the interaction of PKC with PS. Binding of PKC to PS molecules precedes the interaction with pyrene lipid cofactors which then leads to activation of PKC.

From correlation spectroscopy, we obtained a value of ϕ_r = 63 ns for the micellar rotation under these experimental conditions (Bastiaens et al., submitted). Analysis of the experimental fluorescence anisotropy decays (eq. 9) yielded optimised values for ϕ_T and θ_g. As is shown in Table 3, in absence of calcium, PKC mainly influences the overall rotation of the micelle and the translational diffusion of the lipids within the micelle. No significant differences were obtained between DPH-PC and DPH-DG indicating that in this stage of PKC-association to PS, hardly any specificity is obtained for DPH-DG. Addition of calcium leads to a further slowing down of the anisotropy of both DPH-PC and DPH-DG. In this case, however, large differences are obtained between the anisotropy decays of DPH-DG and DPH-PC, indicating that calcium enhances binding of PKC to PS containing membranes.

Probe	System	ϕ_r (ns)	ϕ_T (ns)	θ_g (rad)	$\langle P_2 \rangle$	$\langle P_4 \rangle$	$D_\perp$ (µs^{-1})	χ^2
DPH-DG	PS	37	84 (58-340)	0.46 (0.43-0.52)	0.73	0.35	29 (26-33)	1.13
	PS/PKC	63	112 (85-400)	0.43 (0.41-0.47)	0.76	0.40	28 (26-32)	1.21
	PS/PKC/Ca^{2+}	98	103 (80-400)	0.22 (0.20-0.31)	0.93	0.78	12 (10-18)	1.19
DPH-PC	PS	37	88 (60-320)	0.46 (0.44-0.52)	0.73	0.35	29 (27-32)	1.14
	PS/PKC	63	120 (73-∞)	0.46 (0.43-0.51)	0.73	0.35	24 (22-29)	1.18
	PS/PKC/Ca^{2+}	98	126 (75-∞)	0.43 (0.41-0.48)	0.75	0.38	21 (19-24)	1.21

Table 3. Optimised ϕ_T, θ_g and $D_\perp$ values from analysis of the data sets of DPH lipid probes in thesit micelles. The initial anisotropy was linked over multiple experiments and amounts to 0.325. The ϕ_r values were calculated from the translational diffusion coefficients of micelles independently measured by fluorescence correlation spectroscopy (Bastiaens et al., 1994). See for further details the legend of Table 1.

In presence of PKC and calcium a correlation time of 98 ns was derived for the rotation of the micelles from its translational diffusion (Bastiaens et al., submitted). Analysis of the anisotropy decays (eq. 9) yielded optimal values for ϕ_T, θ_g and $D_\perp$ (Table 3). Apparently, in the presence of calcium PKC interacts with higher affinity to the PS containing micelles which results in a further reduction of the overall rotational motion of the micelles. No

significant effects were observed of calcium on the translational diffusion (note that for a probe with a fluorescence lifetime of 10 ns a correlation time longer than 100 ns seems to be already infinitely long). Next to this general complex formation between PKC and micelles, a strong reduction of the θ_g and $D_\perp$ values of DPH-DG is observed when calcium is added, indicating that the rotational freedom and dynamics of DPH-DG interacting with PKC is very limited. When DPH-PC is used instead of DPH-DG, these lipid motional parameters are hardly influenced indicating that only in the presence of calcium specificity is obtained for DPH-DG. This calcium modulation of lipid specificity can be explained by statistical and/or allosteric mechanisms.

The statistical explanation is based on similar mechanism as was proposed to explain the sigmoidal dependencies of PKC binding and activity on the PS mole fraction in membranes (Mosior & McLaughlin, 1992; Sandermann, 1982; Newton, 1993). The probability of DG binding to PKC increases with the probability of finding PKC at the micellar surface. In absence of calcium PKC is only loosely bound to the micelles, dynamically exchanging between buffer and micellar surface. Under these binding conditions, the time that the protein is retained at the micellar surface is too short for interaction with DG. When calcium is added, the protein becomes more firmly bound to the micellar surface (as can be concluded both from fluorescence correlation spectroscopy and time-resolved fluorescence anisotropy) resulting in a higher probability of interaction with DG.

The second alternative option is that in absence of calcium PKC is already bound to the micellar surface but for unknown reasons it is not able to interact with DPH-DG. Calcium does not only change the binding characteristics of PKC to PS but also affects the protein in such a way that direct interaction with DPH-DG is possible. In this context one might hypothesise that inactive PKC is not able to bind DG. Binding of calcium to PKC allosterically affects the protein conformation thereby facilitating binding of DPH-DG. The interaction of DG with PKC stabilises the active form of PKC. Distinguishing between these two mechanisms has to be done in further investigations.

4.3.5. Interaction of PKC with dansyl labelled phorbol ester in vesicles and micelles

In order to investigate the effect of PKC on the reorientational properties of phorbol esters, we performed similar experiments with dansyl labelled PMA as described above for DPH labelled lipids. In the absence of PS no effects of PKC on the anisotropy decay of dansyl labelled PMA could be detected indicating that like in the case of DG, PS is a prerequisite for the interaction of PKC with phorbol ester. In the presence of PS and calcium large effects were observed on the anisotropy decay of this labelled compound when PKC was added. The decay curves of dansyl-PMA in micelles containing 10 mole % PS in the presence and absence of PKC are given in Figure 5. Specific trends of PKC on the motional properties of the labelled PMA were detected, analogous to those of DPH-DG. Addition of a four-fold excess of unlabelled PMA yielded the same anisotropy decay of dansyl-PMA as the one obtained in absence of PKC indicating a reciprocal relationship of labelled and unlabelled PMA with respect to PKC binding.
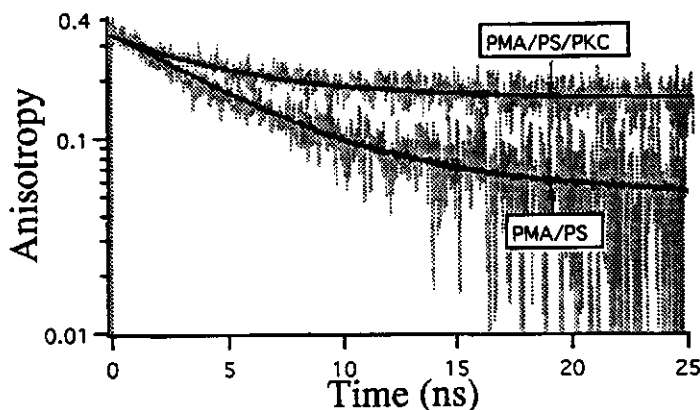
Figure 5. Anisotropy decays of dansyl-PMA in mixed micelles in the presence and absence of PKC. The micelles were composed of thesit, 10 mole % PS. The smooth curve through the data points represents an optimised fit with a model consisting of a sum of three exponentials.

4.4. Discussion

Motional properties of fluorescent cofactors of protein kinase C have been characterised in vesicles and micelles by monitoring the decay rate of the fluorescence anisotropy. Applied to micelles, this technique enables registration of the binding of PKC to PS containing micelles. In addition, specific interaction of PKC can be observed from anisotropy decay patterns of labelled cofactors in vesicles and micelles. In this sense both membrane-mimetic systems reveal complementary information about the general binding to membrane and subsequent interaction with cofactors. The rotational freedom of DPH-DG in DOPC vesicles is slightly larger than that of DPH-PC while the rotational dynamics of both probes are approximately similar. The lack of the phosphocholine headgroup of DPH-DG apparently influences the organisation of its lipid neighbours in such a way that additional motional freedom is obtained. The probable failure of DPH-DG to be tightly accommodated in the lattice of surrounding lipid chains would allow more extended chain motions than for DPH-PC which is arranged in a complementary manner to DOPC lipids. Organisational defects in the membranes induced by DG may result in exposure of hydrophobic lipid elements to the aqueous environment which increases the ground state energy of a bilayer. Consequently the lipid packing irregularities will decrease the apparent activation energy change associated with incorporation of proteins like PKC (Jain et al., 1987). The incorporation of PKC may precede or even be strictly required for direct (stereospecific) interactions with DG that further stabilise the active PKC.

The fact that in presence of EGTA, the rotation and translational diffusion of PS containing micelles slows down considerably upon addition of PKC shows that this protein is able to interact with PS containing membranes in the absence of calcium (see also Chapter 5; Brumfeld & Lester, 1990; Bazzi &

Nelsestuen, 1988b). Addition of calcium enhances the interaction of PKC with PS containing membranes and results in binding of PKC to DG. Apparently, the binding of PKC to PS containing membranes is stabilised by calcium. Several other studies have provided evidence that calcium is essential for association of PKC with phospholipid membranes (Bazzi, 1988a, 1989a, 1990, Bell, 1986) and significant conformational rearrangements of PKC have been observed upon it interaction with calcium and upon the binding of PKC to membranes (Lester & Brumfeld, 1990). Both in micelles and vesicles the presence of PKC and calcium leads to a reduction of the motional freedom of DPH-DG, whereas its rotational dynamics is barely affected. We can therefore conclude that the motion of the DG chains at the protein surface is restricted. The fact that the fluorescence properties of DPH-DG barely change when it interacts with the protein indicates that the dielectric constant of the DPH environment is invariant upon interaction. Therefore, movement of DPH-DG from the hydrophobic membrane core to a more hydrophilic environment accompanied with binding to PKC is not likely. It is more probable that DPH-DG interacts in a dynamical fashion with the protein surface within the hydrophobic membrane or even is trapped in grooves in the polypeptide. Whether the calcium dependence of DG binding to PKC is a direct consequence of the enhanced binding of PKC to PS membranes or a results from allosteric effects induced by calcium that result in exposure of a shielded lipid cofactor site for DG is unclear. Insertion of PKC into membranes has been observed by several research groups (Brumfeld & Lester 1990, Bazzi & Nelsestuen, 1988a). It is tempting to explain the calcium dependence of binding to PS and DG in terms of a calcium induced shift from loosely peripheral bound PKC to inserted PKC. The hydrophobic interaction forces between the inserted PKC segments and lipid acyl chains will add to the electrostatic interactions between the protein and PS headgroups and may induce structural rearrangements that enable binding of DG to PKC. On its turn, the binding of DG may stabilise the inserted active form of PKC and will thus lower the calcium requirement for the activation of PKC as was observed by several groups (Kishimoto et al., 1980).

References

Ahmed, S., Kozma, R., Lee, J., Monfires, C., Harden, N. & Lim, L. (1991) *Biochem. J.* 280, 233-241.

Ahmed, S., Lee, J., Kozma, R., Best, A., Monfries, C. & Lim, L. (1993) *J. Biol. Chem.* 268, 10709-10712.

Ameloot, M., Hendrickx, H., Herreman, W., Pottel, H., van Cauwelaert, F. & van der Meer, W. (1984) *Biophys. J.* 46, 525-539.

Arnold, R.S. & Newton, A.C. (1992) *Biophys. J.* 61, A89.

Ashendel, C.L. (1985) *Biochim. Biophys. Acta* 822, 219-242.

Bastiaens, P.I.H, Pap, E.H.W., Borst, J.W., van Hoek, A., Kulinski, T., Rigler, R.Visser, A.J.W.G. (1993) *Biophys. Chem.* 48, 183-191.

Bastiaens, P.I.H., Pap, E.H.W., van Hoek, A., Rigler, R. & Visser, A.J.W.G. (1994) *Journal of Fluorescence submitted.*

Bazzi, M.D. & Nelsestuen, G.L. (1987) *Biochemistry* 26, 115-122.

Bazzi, M.D. & Nelsestuen, G.L. (1988a) *Biochemistry* 27, 7598-7593.

Bazzi, M.D. & Nelsestuen, G.L. (1988b) *Biochemistry* 27, 6776-6783.

Bazzi, M.D. & Nelsestuen, G.L. (1989a) *Biochemistry* 28, 3577-3585.

Bazzi, M.D. & Nelsestuen, G.L. (1989b) *Biochemistry* 28, 9317-9323.

Beechem, J.M & Gratton, E., Proc. SPIE., (1988) 909, 70-81.

Berlman, I.B. in "Handbook of fluorescence spectra of aromatic molecules" 2nd ed. Academic Press, New York and London, 1971.

Berne, B.J. Pecora, R. (1976) Dynamic Light Scattering; Wiley: New York.

Berne, P.J., Pechukas, P. & Harp, G.D. (1968) *J. Chem. Phys.* 49, 3125-3129.

Brockerhoff, H. (1986) *FEBS Lett* 201, 1-4.

Burns, D. J. & Bell, R. M. (1991) *J. Biol. Chem.* 266, 18330-18338.

Brumfeld, V., & Lester, D.S. (1990) *Arch. Biochem. Biophys.* 277, 318-323.

Castagna, M., Takai, Y., Kaibuchi, K., Sano, K., Kikkawa, U. & Nishizuka, Y. (1982) *J. Biol. Chem.* 257, 7847-7851.

Chauhan, A., Chauhan, V.P.S., Deshmukh, D.S. & Brockerhoff, H. (1989) *Biochemistry* 28, 4952-4956.

Cheng, K.H., Chen, S.Y., Butko, P., Van der Meer, W.B. & Somerharju, P. (1991) *Biophys. Chem.* 39, 137-144.

Das, S. & Rand, R.P. (1986) *Biochemistry* 25, 2882-2889.

Dawson, R.M.C, Irvine, R.F., Bray, J., Quinn P.J. (1984) *Biochem. Biophys. Res. Commun.* 117, 196-201.

Dekker LV. & Parker P.J. (1994) *Trends Biochem. Sci.* 19, 73-77.

Epand, R.M. & Bottega, R. (1988) *Biochim. Biophys. Acta* 944, 144-154.

Epand, R.M. Stafford, A.R. & Lester, D.S. (1992) *Eur. J. Biochem.* 208, 327-332.

Epand, R.M. & Lester, D.S. (990) *Trends Pharm. Sci.* 11, 317-320.

Epand, R.M. Stafford, A.R., Cheetham, J.J, Bottega, R., Ball, E.H. (1988) *Biosci. Rep.* 8, 49-54.

Eppand R.M. (1985) *Biochemistry* 24, 7092-7095.

Ganong, B. & Loomis, C., Hannun, Y. & Bell, R. M. (1986) *Proc. Natl. Acad. Sci. USA*, 83, 1184-1188.

Gschwendt, M., Kittstein, W. & Marks, F. (1991) *Trends Biochem. Sci.* 16, 167-169.

Hannun, Y.A., Loomis, C.R. & Bell, R.M. (1985) *J. Biol. Chem.* 260, 10039-10043.

Huang, K.P. & Huang, F.L. (1986) *J. Biol. Chem.* 261, 14781-14787.

Hubbard, S.R., Bishop, W.R., Kirschmeier, P., George, S.J., Cramer, S.P. & Hendrickson, W.A. (1991) *Science* 254, 1776-1779.

Kishimoto, A., Takai, Y., Mori, T., Kikkawa, U & Nishizuka, Y. (1980) *J. Biol. Chem.* 255, 2273-2276.

Kikkawa & Nishizuka (1986) *Annu. Rev. Cell. Biol.* 2, 149-152.

Kremer, J.M.H., vd Esker, M.W.J., Pathmamanoharan, C. & Wiersema, P.H. (1977) *Biochemistry* 16, 3932-3935.

Lentz, B.R. in: Spectroscopic membrane probes. Ed. Loew, L.M. CRC Pres, 1988. 1: 28-42.

Lester, D.S., Orr, N. & Brumfeld, V. (1990) *Biochim. Biophys. Acta.* 1054, 297-303.

Lester, D.S & Brumfeld, V. (1990) *Int. J. Biol. Chem.* 12, 251-256.

Myher, J.J. & Kuksis (1984) *J. Biochem. Cell Biol.* 62, 352-356.

Newton, A.C. (1993) *Annu. Rev. Biophys. Biomol. Struct.* 22, 1-25.

Nishizuka, Y. (1984) *Nature* 308, 693-697.

Nishizuka, Y., (1984) *Science* 225, 1365-1370.

Ohki, K.O., Sekiya, T., Yamauchi, T. & Nozawa, Y. (1982) *Biochim. Biophys. Acta* 693, 341-350.

Ono, Y., Fujii, T., Igarashi, K., Kuno, T., Tanaka, C. Kikkawa, U. & Nishizuka, Y. (1989) *Proc. Natl. Acad. Sci. USA,* 86, 4868-4871.

Pap, E.H.W., Bastiaens, P.I.H., Borst, J.W., Berg, van den P.A.W., van Hoek, A., Snoek, G.T., Wirtz, K.W.A. & Visser, A.J.W.G. (1993) *Biochemistry* 32, 13310-13317.

Pap, E.H.W., ter Horst, J.J., van Hoek, A. & Visser, A.J.W.G., (1994) *Biophys. Chem.* 48, 337-351.

Preiss, J., Loomis, C.R., Bishop, W.R., Stein, R., Niedel, J.E. & Bell, R.M. (1986) *J. Biol. Chem.* 261, 8597-8600.

Rodriguesz-Paris, J.M., Shoji, M., Yeola, S., Liotta, D., Vogler, W.R. & Kuo, J.F. (1989) *Biochem. Biophys. Res. Commun.* 159, 495-500.

Rousser, G., Fleischer, S. & Yamamoto A. (1970) *Lipids* 5, 494-496.

Sekiguchi, K., Tsukuda, M., Ogita, K., Kikkawa, U. & Nishizuka, Y. (1987) *Biochem. Biophys. Res. Commun.,* 145, 797-802.

Straume, M. & Litman, B.J. (1987) *Biochemistry* 26, 5113-5120.

Szabo, A. (1984) J. *Chem. Phys.* 81, 150-167.

Van der Meer, W.H.P.W.H., Ameloot, M., Hendrickx, H. & Schröder, H. (1984) *Biophys. J.* 46, 515-523.

Van der Sijs, D.A., Van Faasen, E.E. & Levine, Y.K. (1994) *Phys. Chem. Letters* 216, 559-565.

van Hoek, A., Vos, K. & Visser, A.J.W.G. (1987) *IEEE J. Quantum Electron. QE-* 23, 1812-1820.

Vauhkonen, M., Sassaroli, M., Somerharju, P. & Eisinger, J. (1989) *Eur. J. Biochem.* 186, 465-471.

Zidovetzki, R. & Lester, D.S. (1992) *Biochim. Biophys. Acta* 1134, 261-272.

Chapter 5

Parallel probing of lipid and protein properties results in a refined description of the interaction of protein kinase-C and lipid cofactors

Abstract

The interaction of protein kinase C (PKC) with lipids was probed by a dual approach. Pyrene labelled lipid analogues of diacylglycerol (DG), phosphatidylserine (PS), phosphatidylinositol (PI), phosphatidylinositol-4-phosphate (PIP) and phosphatidylcholine (PC) were used both as acceptors of tryptophan excitation energy of PKC and as membrane probes for intra- and intermolecular lipid chain collisions by measuring the excimer-to-monomer fluorescence intensity ratio (EM). The lipids DG, PS, PC, PI and PIP equipped with either one or two pyrene decanoyl chains were dispersed in polyoxyethylene-9-laurylether micelles or in dioleoyl-PC vesicles containing 10 mole % PS. In both lipid systems interaction of PKC with monopyrenyl PS (pyrPS) in the absence of calcium resulted in a relatively slow increase in monomer fluorescence at the expense of excimer fluorescence (decreasing EM ratio), indicating a reduction of the intermolecular collision frequency of the pyrene labelled PS molecules. This effect on the lipid dynamics was accompanied by quenching of the tryptophan fluorescence of PKC. When pyrPS was absent in the membrane-mimetic systems no significant response was registered on the tryptophan fluorescence. Furthermore, the EM ratio was not influenced by adding buffer solution, indicating that both techniques simultaneously monitor calcium independent interaction of PKC with PS containing membranes. Addition of calcium resulted in a rapid further decrease of the EM ratio of (mono) pyrPS and in additional quenching of the tryptophan fluorescence, as a consequence of a calcium dependent shift of the binding equilibrium towards the membrane bound form of PKC and/or of a partial insertion of PKC into the membranes. Addition of EGTA reversed the tryptophan fluorescence quenching and the EM ratio to approximately their values before addition of calcium. When 4 mole % of pyrPS was replaced by 0.5 mole % of dipyrenyl labelled DG (dipyrDG) a decrease of the intramolecular excimer formation rate and of the tryptophan fluorescence could only be detected in the presence of calcium and PS indicating that calcium is needed for the interaction of PKC with DG. Addition of phorbol ester (PMA) recovered the EM value of dipyrDG to its value in the absence of PKC. Strong binding was also observed with dipyrenyl labelled PIP (dipyrPIP), but not with the other dipyrenyl labelled lipids: PI, PS or PC. In addition, the EM values of dipyrPIP were not affected by PMA, indicating that PMA and dipyrPIP can bind simultaneously to PKC.

5.1. Introduction

Protein kinase C (PKC) is a serine/threonine specific kinase involved in cellular signalling (Nishizuka, 1989). Interaction with specific lipids is essential in the activation of this regulatory kinase (Bazzi & Nelsestuen, 1988, 1989; Brockerhoff, 1986; Newton, 1993; Nishizuka, 1984; Zidovetzki & Lester, 1992). The components required for activation of the various PKC-isozyme families (nPKC, cPKC and αPKC) have now been established by extensive biochemical, biophysical and genetic analysis. Essential factors are anionic lipids (Huang et al., 1988; Sekiguchi et al., 1988), in particular L-phosphatidylserine (PS) (Burns et al., 1990; Lee et al., 1989, Orr et al., 1992a, 1992b) and (for cPKCs) calcium. In addition, cPKC and nPKC families require for maximal activation lipid-like cofactors like sn-1, 2 diacylglycerol (DG) or phorbol esters (PMA) (Castagna et al., 1982; Hannun et al., 1985; Kaibuchi et al., 1981; Takai et al., 1979). Binding to these cofactors is highly (stereo-)specific (Bazzi & Nelsestuen, 1989; Boni, 1985; Brockerhoff, 1986; Rando & Young, 1984). Specific structural elements of PMA were shown to interact with cysteine-rich sequences of PKC (Burns & Bell, 1991) and a one-to-one stoichiometry for the binding of both DG and PMA to PKC has been reported (Brockerhoff, 1986; Ganong & Loomis, 1986; Gschwendt et al., 1991; Hannun et al., 1985). Although the components for PKC activation have been identified now, very little is known about the mutual dependencies of the interaction of PKC with these factors. Especially the role of calcium in the PKC-lipid interaction and/or in the activation of cPKC is unclear. Most initial investigations of the lipid modulation of PKC activity were performed with PKC preparations from rat brain which is mainly composed of the calcium dependent isozymes (Huang & Huang, 1986; Sekiguchi et al., 1987). Calcium has long been considered to be the cofactor that regulates association of this PKC with anionic lipids (Bazzi & Nelsestuen, 1987; Bell, 1986). Bell and coworkers have proposed a model for PKC-Ca^{2+}-PS-DG complexation. In this model calcium stabilises the binding of PKC to PS containing membranes (see also Bazzi & Nelsestuen, 1988, 1989; Brockerhoff, 1986; Nishizuka, 1984). The interaction of the PKC-Ca^{2+}-PS complex with DG induces a release of a pseudo-substrate domain from the active site, thereby allowing access of substrates (House & Kemp, 1987; Makowske & Rosen, 1989; Mosior & McLaughlin, 1991; Orr et al., 1992c). This calcium-dependent lipid interaction is essentially reversible (Bazzi & Nelsestuen, 1987, 1988; Souvignet et al., 1991; Lester et al., 1990) and insufficient for activation of PKC (Bazzi & Nelsestuen, 1987). Furthermore, it was shown that after initial association, PKC penetrates the membrane which is accompanied by some additional conformational changes which led to partial calcium independence of the binding (Bazzi & Nelsestuen, 1987, 1990, 1991; Brumfeld & Lester, 1990; Lester et al., 1990). Cofactors like DG and PMA might stabilise this inserted active PKC. According to this concept calcium modulates the lipid binding of PKC by inducing conformational changes in the protein. Alternatively, calcium may bind more aspecifically to PKC or the membrane, thereby affecting the electrostatic potential at the membrane surface (by neutralisation of repulsive electrostatic interaction forces between PKC and the membrane) (Trudell et al., 1989) and/or the lipid organisation in the bilayer (Bazzi & Nelsestuen, 1991a;

Brumfeld & Lester, 1990). Furthermore, calcium is known to affect hydrophobic interactions (Seelig, 1990) and hydration between phospholipids and membrane-bound protein forces. These more aspecifc effects of calcium can have dramatic effects on binding of PKC to membranes, although they do not appear to be of major importance in the association of PKC with lipids (Bazzi & Nelsestuen, 1991a; Brumfeld and Lester, 1990).

In contradiction with earlier observations, Lester and coworkers demonstrated that both association and subsequent penetration of PKC into membranes is independent of divalent cations, but very sensitive to pH (Lester et al., 1990). Using circular dichroism, large and specific conformational changes were observed upon binding to phosphatidylserine vesicles in the absence of calcium (Shah et al., 1992; Lester et al., 1990). Based on these observations it was speculated that the inactive form of PKC may be loosely associated to the membrane. At odds with the concept of calcium modulation of lipid binding, these authors considered phospholipids as modulators for the binding of calcium to PKC (Brumfeld & Lester, 1990; Lester et al., 1990). The enzyme is first associated with the lipids and then binds calcium which is needed for activity. Cofactors like DG shift the calcium dependence of PKC activity to lower concentrations of calcium (Epand et al., 1992; Nishizuka, 1986).

In the present report the binding of PKC to PS and DG is re-evaluated by simultaneous observation of quenching of PKC tryptophan fluorescence by resonance energy transfer (RET) and of lipid dynamic properties at various conditions. In these studies pyrene-labelled analogues of DG, PS, PC PI and PIP dispersed in vesicles or mixed micelles served not only as acceptors of tryptophan excitation energy but also as reporters of lipid acyl chain dynamics by measuring the ratio of excimer-to-monomer fluorescence intensities (EM). Formation of a protein-lipid complex resulted in an increased quenching of tryptophan fluorescence and in a reduced EM ratio of the pyrene lipids. A major advantage of this approach is the simultaneous employment of two independent methods for registration of the same events from both lipid and protein viewpoints. In addition, the approach allowed on-line and specific detection of interaction between PKC, and, the various lipids, and combined with the high sensitivity, enabled the use of low concentrations of protein and lipid probes.

5.2. Experimental Procedures

5.2.1. Materials

Bovine brain L-α-phosphatidylserine (PS), dioleoyl-PC, diacylglycerol (DG), thesit (polyoxyethylene-9-lauryl ether), EGTA, phospholipase D from *Streptomyces species*, phospholipase C from *Bacillus cereus* were supplied by Sigma Chemical Co (St. Louis, MO).

Purification of PKC

Protein kinase C was purified from the cytosolic extract of homogenised Wistar rat brains similar to the procedure described by Huang and Huang (1986) and consecutively by DEAE, phenyl-sepharose, sephacryl S200 and

polylysine agarose chromatography. The final PKC preparation (with isozyme composition as described elsewhere (Huang & Huang, 1986; Sekiguchi et al., 1987) was essentially pure as demonstrated by silver staining of a polyacrylamide gel, and was stored at -70°C in buffer (20 mM Tris pH 7.9, 0.5 mM EGTA, 0.5 mM EDTA, 1 mM β-mercaptoethanol) with 25% glycerol (Merck, Darmstadt, Germany, fluorescence microscopy grade).

Synthesis of dipyrenyl-labelled phospholipids

Di('-pyrenedecanoyl)-PC (dipyrPC) was synthesised by methods described previously (Patel et al., 1979). Di('-pyrenedecanoyl)-DG was synthesised by a phospholipase C catalysed hydrolysis of the diglyceride-phosphate linkage in dipyrPC essentially as described by Myher and Kuksis (1984). Transphosphatidylation of dipyrPC by phospholipase D yielded di('-pyrenedecanoyl)-PS (Comfurius et al., 1990). The synthesised lipids, were purified with high performance liquid chromatography on a silicic acid column (240 x 10 mm, LiChroprep Si 60, Merck, Germany). Elution was performed with an increasing methanol gradient in chloroform. Di('-pyrenedecanoyl)-PI and di('-pyrenedecanoyl)-PIP were a kind gift of Drs. W.F. Nieuwenhuizen (University of Utrecht).

Preparation of micelles

Mixed lipid micelles were prepared by drying the required amounts of lipids under a stream of nitrogen in a glass tube followed by solubilisation in buffer (1 mM Thesit, 20 mM Tris/HCl (pH 7.5) 120 mM NaCl and 50 μM EGTA) by vortexing and brief bath sonication. In the binding studies the thesit concentration was 100 μM and the PS concentration was 10 μM (10 mole %). The fluorescent lipid concentration was 0.5 μM for the dipyrenyl labelled lipids and 4 μM for the monopyrenyl lipids. The phospholipid content was determined by phosphate analysis according to the method of Rousser et al., (1970). The pyrene concentration was estimated by measuring the absorbance at 342 nm in ethanol/DMSO (75:25 v/v) ($\varepsilon = 39700$ $M^{-1}cm^{-1}$). In the fluorescence experiments the PKC concentration was 400 nM.

Preparation of vesicles

Small unilamellar vesicles were prepared by injecting 5 μL of lipid dissolved in ethanol/DMSO through a Hamilton syringe into 0.5 mL of a magnetically stirred buffer solution (20 mM Tris/HCl 120 mM NaCl and 50 μM EGTA, pH 7.5) at room temperature (Kremer et al., 1977). For further details, see the previous section describing the preparation of micelles.

5.2.2. Methods

Resonance energy transfer

The tryptophan fluorescence of PKC is quenched by pyrene lipids according to the resonance energy transfer (RET) mechanism. This process involves transfer of excitation energy from the tryptophan residues to the pyrene moieties by a weak coupling of the transition moments involved (Förster, 1948; Stryer, 1978). The rate of this nonradiative process is highly dependent on the

separation of the donor and acceptor molecules (Förster, 1948). Since the critical Förster distance for a pyrene-tryptophan couple is approximately 2.7 nm, we assume that the majority of the tryptophan quenching originates from pyrene lipids that directly interact with PKC (Förster, 1948).

Theory of pyrene excimer formation

Next to their resonance energy acceptor ability the pyrene-labelled lipids are excellent probes to study the organisation and dynamics of lipid components in membranes through their ability to form excimers (a complex between a pyrene molecule in the excited state with a pyrene molecule in the ground state (Förster & Kasper, 1955). The excimer fluorescence is at higher wavelengths than the monomer. The ratio of excimer to monomer emission of pyrenyl probes is a measure for the collision frequency of the pyrene moieties and can be related to parameters describing membrane dynamics and organisation (Galla & Sackman, 1974; Sassaroli et al., 1990; Vanderkooi & Gallis, 1974). In this study two kinds of pyrene lipids are employed to investigate PKC-lipid interaction: lipids with one pyrene decanoyl moiety at the sn-2 position of the lipid (monopyrene) and lipids with two pyrene decanoyl moieties (dipyrene) at the terminal of both acyl chains. The collision of monopyrene lipids is an intermolecular event and reports on the lateral lipid organisation and dynamics, while intramolecular excimer formation of dipyrenyl lipids is directly related to the local motional freedom and dynamics of lipid acyl chains in the membrane.

Fluorescence methods

Pyrene and tryptophan fluorescence intensities were monitored successively on a DMX-1000 steady state spectrofluorometer (SLM Aminco, Urbana, IL) with computer-driven excitation and emission monochromators. One measurement cycle consisted of registration of tryptophan fluorescence and of pyrene monomer and excimer fluorescence intensities. The tryptophan residues were excited at 285 nm and their fluorescence was detected at 340 nm. Subsequently, the excitation wavelength was advanced to 347 nm to monitor the pyrene monomer and excimer emission by setting the emission monochromator at 377 nm and 487 nm, respectively. The experiments were performed at 40 cycles per minute. The measurements were corrected for background emission and spectral instrument characteristics. Excitation and emission bandwidths were set at 4 nm. The measurements were performed at room temperature (20° C).

5.3. Results

5.3.1 The role of calcium in the binding of PKC to PS containing membranes

In order to evaluate the role of calcium in the interaction of PKC to PS, the excimer formation of pyrPS or pyrPC and their ability to quench tryptophanyl fluorescence of PKC was examined in thesit/PS micelles and DOPC/PS vesicles. Both lipid systems yielded comparable calcium independent and calcium dependent effects on the tryptophan fluorescence and pyrene excimer formation. Figure 1 shows the dependence of the tryptophan fluorescence

(Figure 1A) and of the EM ratio (Figure 1B) of 4 mole % of pyrPS (solid line) or pyrPC (dashed line) in thesit micelles. In an earlier study it was found that one thesit mixed micelle consists of approximately 330 surfactant molecules (Bastiaens et al., 1993). Thus each mixed micelle contains on the average 13 pyrene lipids. In the absence of PKC the EM values of pyrPS and pyrPC scatter around a value of 0.6 as a consequence of collision between the different pyrene lipids. Addition of PKC (at t = 50 s) to a final concentration of 400 nM yields a tryptophan fluorescence signal which is for convenience normalised to unity (the background fluorescence at the tryptophan emission wavelength in the absence of PKC is less than 2 %). At this PKC concentration approximately equal molar ratios of PKC and micellar aggregates are present.
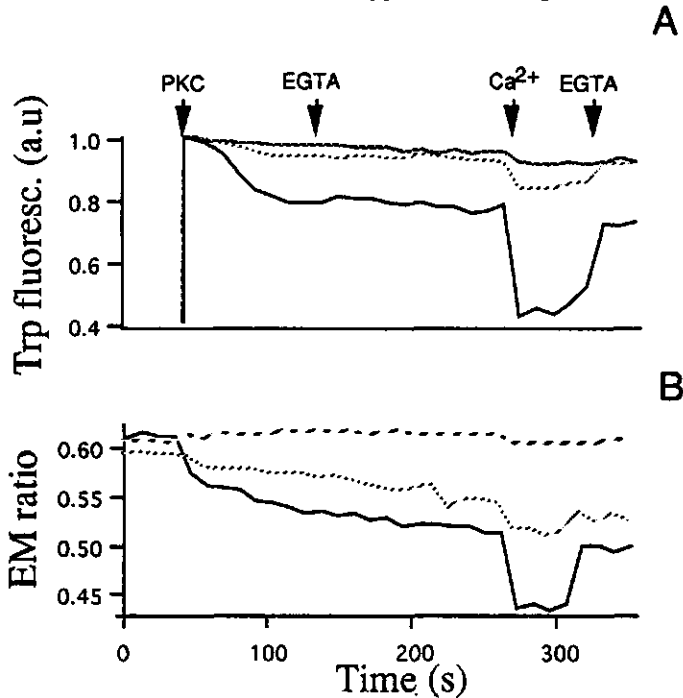
Figure 1. A. Probing of PKC binding to thesit micelles containing 10 mole % brain PS, 4 mole % pyrPS (—) or pyrPC (··) from the tryptophan fluorescence quenching of PKC. The PKC fluorescence signal in presence of PS containing micelles without pyrene lipids is included as a control experiment (—). B. Parallel to the registration of the PKC tryptophan fluorescence quenching the pyrene EM ratio of pyrPS (—) or pyrPC (··) was monitored. As a control experiment, the EM values of pyrPS in micelles were measured in buffer only (- -). The experiments were performed in 20 mM Tris buffer (pH 7.5, 120 mM NaCl, 5 µg/ml leupeptine and (initially) 50 µM EGTA)at 293 K.

In the absence of calcium (50 µM EGTA) the tryptophan fluorescence decays slowly to a level of 80 % of the original intensity when pyrPS is present in the micelles (Figure 1A). This effect is not observed if unlabelled micelles are present (dashed line in Figure 1A). Addition of extra EGTA to a final concentration of 200 µM (or even higher) does not affect the tryptophan

emission. Upon PKC addition the EM ratio of pyrPS decays from 0.61 to an almost steady level of 0.51 (Figure 1B). This effect is not observed if buffer is added (dashed line in Figure 1B) instead of PKC. It can thus be concluded that the decrease in intermolecular collision frequency of the pyrPS molecules is a consequence of the interaction of PKC with the micelles. When pyrPC is used instead of pyrPS in the thesit/PS micelles, a similar but less strong reduction of the EM value is observed (dotted line in Figure 1B). The calcium independent interaction with PKC apparently reduces the motional freedom of pyrPS by direct interaction with these lipids. The fact that binding of PKC to unlabelled PS in micelles containing pyrPC does not leave the intermolecular collisions of this pyrene lipid unaffected, indicates that noninteracting PC molecules in the micelle also trace the binding of PKC. Furthermore, the binding of PKC to pyrPS containing micelles results in quenching of tryptophan fluorescence. Since the average distance between tryptophan donors of PKC in solution and pyrPS in micelles is too large for effective energy transfer, the quenching of tryptophan fluorescence independently confirms a calcium independent interaction of PKC with pyrPS as was concluded from the EM experiments. PyrPC is also able to quench the tryptophan fluorescence of PKC, but weaker than pyrPS indicating that pyrPC is not interacting with PKC but is rather randomly distributed in the micelle. A rapid, further reduction of both tryptophan fluorescence and of the EM ratio is observed when calcium (0.4 mM) is added (See Figure 1). This observation suggests a calcium dependent reduction of the lipid dynamics and a more efficient quenching of tryptophan residues in PKC. Upon addition of an excess of EGTA (5 mM), the calcium induced reduction of both the EM ratio and tryptophan fluorescence is largely recovered to their values observed before addition of calcium. The calcium dependent reduction and EGTA induced recovery of both tryptophan fluorescence and EM values can be repeated several times per experiment, indicating that the action of EGTA is based primarily on the removal of calcium and that detergentlike effects of EGTA (Wallach, 1974) play a minor role. The calcium dependence of the quenching and excimer characteristics can be explained by a calcium dependent shift of the equilibrium of free and bound PKC to the bound form. Alternatively, it can be envisaged that addition of calcium does not affect the relative amount of PKC bound to micelles, but induces a (partial) insertion of PKC into the hydrophobic core of the micelle. This insertion leads to a closer average distance between the tryptophan donors in PKC and the pyrene acceptors in the micelle and thus to more efficient quenching and to simultaneous changes in the lipid dynamics.

5.3.2. Effect of NaCl on calcium independent binding of PKC to PS
In general several interaction forces are involved in protein-lipid association depending on the membrane or protein system. The range of these forces varies largely. Electrostatic forces dominate the interactions at relatively long distances and, generally, play a major role in peripheral binding of proteins to membranes. In this case both the protein and lipid surfaces carry oppositely charged groups. Hydrophobic peptide domains interacting with the phospholipid acyl chains may contribute to the interaction as well. Since low ionic strength enhances the electrostatic interactions between charged

molecules and reduces the hydrophobic ones, evaluation of the tryptophan fluorescence of PKC and excimer formation of pyrPS in calcium free buffer at various concentrations of NaCl will yield information about the forces involved in the interaction between PKC and PS. As is shown in Figure 2, the absence of NaCl leads to a stronger decrease of the EM ratio of pyrPS and tryptophan fluorescence than in the presence of 120 mM NaCl (see also Figure 1). The overall effect of a low ionic strength leads apparently to an enhancement of the total interaction between PKC and the micellar surface. This observation indicates that in absence of NaCl electrostatic interaction forces play a dominant role in the calcium independent association.
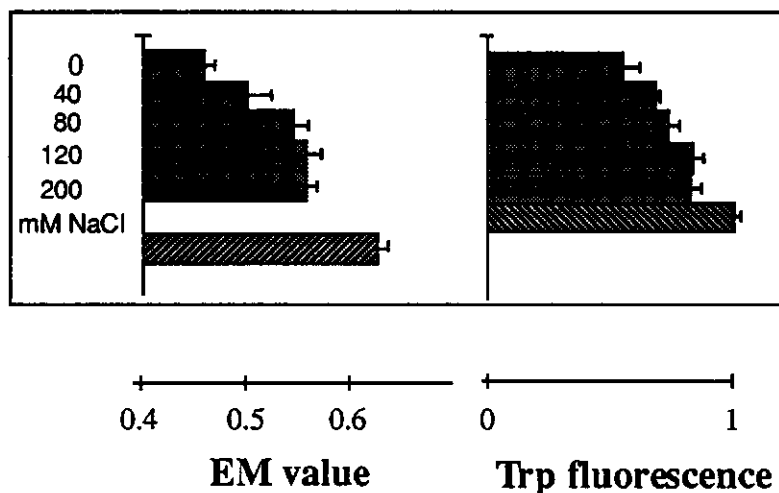
Figure 2. Dependence of the EM values of pyrPS and of the tryptophan fluorescence of PKC on the NaCl concentration in the buffer solution. In the left panel the EM values are presented determined in presence of PKC at various concentrations of NaCl (■). During the experiments the PKC concentration was kept constant at 0.4 µM. The lowest bar in the left panel represents the EM ratio of pyrPS in absence of PKC (▨). In the right panel the parallel monitored tryptophan fluorescence intensities of PKC are presented (■), normalised to the fluorescence intensity obtained with unlabelled micelles (▨). See legend to Figure 1 for more experimental details.

Stepwise titration of NaCl up to a concentration of 120 mM gradually changes both the EM value and tryptophan fluorescence to their values obtained initially in the presence of 120 mM NaCl. The lowest bar in the left panel represents the EM ratio of pyrPS in absence of PKC. This value was essentially the same at the various NaCl concentrations, indicating that the increase of the EM ratio and of tryptophan fluorescence originates from reduction of the overall interaction forces between PKC and the micelles by NaCl. Further increase in the NaCl concentration (> 120 mM) does not lead, however, to a further increase of both signals. Apparently, hydrophobic interaction forces are able to keep at least a part of the PKC population associated to the micellar surface at an ionic strength that approaches the physiological one, confirming

the fluorescence studies of Brumfeld and Lester (1990), Banno et al., (1992) and Bazzi and Nelsestuen (1988).

5.3.3. Calcium and PS-dependence of DG-binding to PKC

In the experiments described in the previous sections, the association of PKC with PS containing membranes was evaluated using a relatively high concentration of pyrene labelled PS. Large effects are only observed when PKC interacts directly with the pyrene labelled lipid. Since it has been reported that the cofactor DG interacts stoichiometrically with PKC (1:1) (Brockerhoff, 1986; Ganong & Loomis, 1986; Gschwendt et al., 1991; Hannun et al., 1985), evaluation of its binding to PKC and the role of calcium in this interaction, has to be approached slightly differently from the investigation of PKC-PS interaction. At a molar fraction of DG in the membranes comparable to that used with PS, only a minority of the DG molecules will interact with PKC and, consequently, the interaction will barely influence the EM value. At lower molar fractions, the intermolecular excimer formation of pyrene labelled DG will be very low even in the absence of PKC and thus will not allow the detection of binding. Therefore, dipyrenyl labelled DG (dipyrDG) was used instead of a monopyrene analogue to characterise the interaction of PKC with this lipid messenger. The intramolecular excimer formation of these doubly labelled lipids enables detection of interaction with PKC at low mole fractions of labelled DG (0.5 mole %). DipyrDG dispersed in mixed micelles containing 10 mole % PS yielded a value of the EM ratio of approximately 0.54. Further dilution of dipyrDG in the micelles by addition of an excess of thesit detergent hardly reduced the EM values indicating that excimer formation mainly originates from intramolecular collisions between the two pyrenes on the same lipid. Analogous to the pyrPS experiments, the measurements were performed sequentially in the absence of calcium, in the presence of calcium, in the presence of PKC and then with saturating amounts of EGTA. The values of the EM ratio measured under various conditions are presented in the left panel of Figure 3. The tryptophan fluorescence monitored in parallel to these pyrene EM measurements is displayed (normalised) in the right panel of Figure 3. Initially, in the absence of calcium (50 μM EGTA) the values of the EM ratio scatter around a value of 0.54. Addition of calcium has no significant effect on the EM values. Subsequent addition of PKC results in a 40% reduction of the EM values of dipyrDG when 10 mole % of unlabelled PS is present in the micelles, and leads to tryptophan fluorescence quenching (Figure 3A). Addition of extra PKC did not give a further reduction of the EM value (data not shown), indicating that PKC is already present at a saturating concentration. The effect of PKC on the EM value of dipyrDG can be largely, but not completely, reversed by removal of calcium with EGTA as is shown in the last column of Figure 3A. At the same time, addition of EGTA leads to a significant increase in tryptophan fluorescence indicating a removal of tryptophan quenching by resonance energy transfer from tryptophan in PKC to dipyrDG.
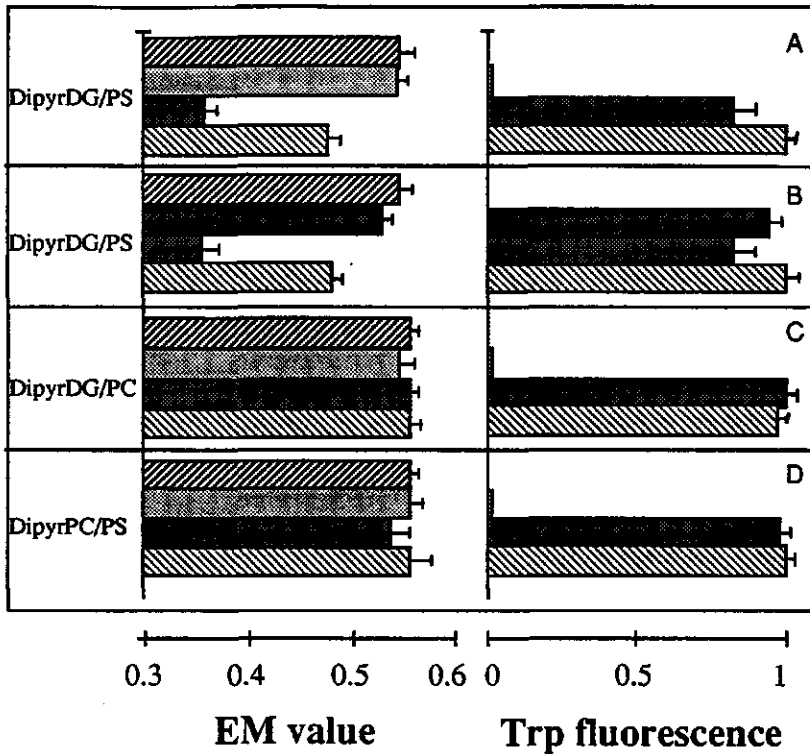
Figure 3. A, C, D. EM values (left panels) of dipyrDG and dipyrPC and of the parallel-monitored tryptophan fluorescence intensities of PKC (right panels) measured in absence of PKC and calcium (▨) and then after sequential addition of calcium (0.4 mM, ▨), PKC (0.4 μM, ■) and EGTA (5 mM, ◩). In B PKC was added (■) before the addition of calcium (■). The dipyrene lipids were dispersed in thesit micelles containing 10 mole % PS or PC. See legend to Figure 1 for more experimental details.

The tryptophan fluorescence quenching by dipyrDG is relatively small as compared to that obtained with pyrPS since the concentration of dipyrDG in the micelles is eight times lower than in pyrPS experiments. When this experiment is repeated with addition of buffer instead of PKC, no effect on the excimer formation is observed (data not shown). Like the pyrPS experiment in the previous section, the interaction of PKC with dipyrDG changes the motional properties of the lipid chains and results in quenching of the tryptophan fluorescence. The reduction of excimer formation of dipyrDG is independent of the sequence of addition of the various compounds as is shown in the experiment described in Figure 3B. When PKC is added in the absence of calcium, the excimer formation is only slightly reduced, indicating that dipyrDG hardly traces the PKC which interacts in a calcium independent fashion with PS lipids. Addition of calcium to this sample with PKC then leads to a further reduction of the excimer formation to similar values as obtained in the experiment described in Figure 3A. Furthermore, if unlabelled PS (10

mole %) in these micelles is replaced by PC (10 mole %) no effect is observed even when both PKC and calcium are present in both excimer formation and tryptophan fluorescence experiments (Figure 3C). Similarly, experiments with dipyrPC instead of dipyrDG also did not give a change, even when 0.5 mole % of unlabelled DG is present in the micelles (Figure 3D). It is thus clear that the excimer formation of dipyrDG, but not that of dipyrPC, is only affected when the three components calcium, PS and PKC are simultaneously present, independent of the sequence of addition. This effect can only be explained by a physical interaction between PKC and dipyrDG which is not established if calcium or PS are lacking. This conclusion is confirmed by the quenching of tryptophan fluorescence which accompanies the effect on excimer formation. All experiments presented in Figure 3 were also performed in vesicles instead of in micelles. The EM values obtained in these membraen bilayers were fully comparable with those obtained in micelles, but the standard errors of the EM values are larger, which is probably due to a lower reproducibility of the vesicle preparation. Two sets of sequential experiments with dipyrDG and dipyrPC in DOPC/PS vesicles (8:2) are presented in Figure 4.
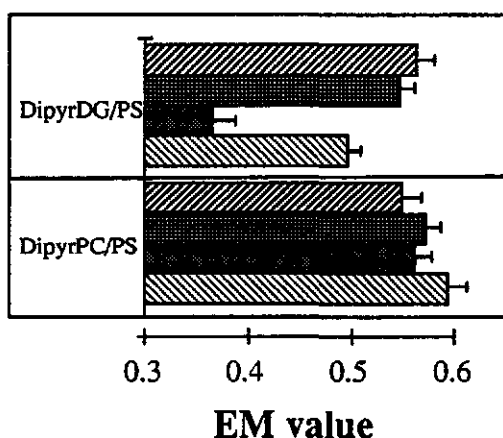
EM value

Figure 4. EM values of dipyrDG and dipyrPC dispersed in DOPC/PS (8:2) vesicles in absence of PKC and calcium (▨) and then after sequential addition of PKC (0.4 µM, ▥), calcium (0.4 mM, ▦) and EGTA (5 mM, ▨). The total lipid concentration was 20 µM and the probe:lipid ratio was 1:50.

Both explanations proposed for the calcium dependence of PKC-PS binding (Figure 1) may fit to the calcium modulation of DG binding observed in Figures 3 and 4. When calcium simply enhances the binding of PKC to PS lipids, the probability of finding a PKC molecule at the micellar surface is larger when calcium is present than when it is not. Consequently, the probability of interaction of PKC with dipyrDG is enhanced. Alternatively, calcium may facilitate the binding of dipyrDG to PKC more directly by changing the protein conformation in such a way that its binding to dipyrDG is altered.

5.3.4. Effect of PKC-membrane interaction on the excimer formation of pyrene labelled phosphoinositides and phosphatidylserine

In order to investigate the specificity of PKC for other dipyrene lipids, the EM values of dipyrene labelled phosphoinositides PI (dipyrPI) and PIP (dipyrPIP) and of PS (dipyrPS) were measured in micelles analogous to the dipyrDG experiments described in the previous section. The EM values of these experiments are given in Figure 5. In case of dipyrPIP, relatively large effects of PKC were observed on the EM value (Figure 5A). The reduction of this EM value is comparable with that found for dipyrDG. Apparently, dipyrPIP interacts with PKC to similar extent as dipyrDG. In absence of unlabelled PS, no interaction is observed indicating that PS is a prerequisite for the interaction of PKC with dipyrPIP (Figure 5B) (see also Pap et al., 1993).
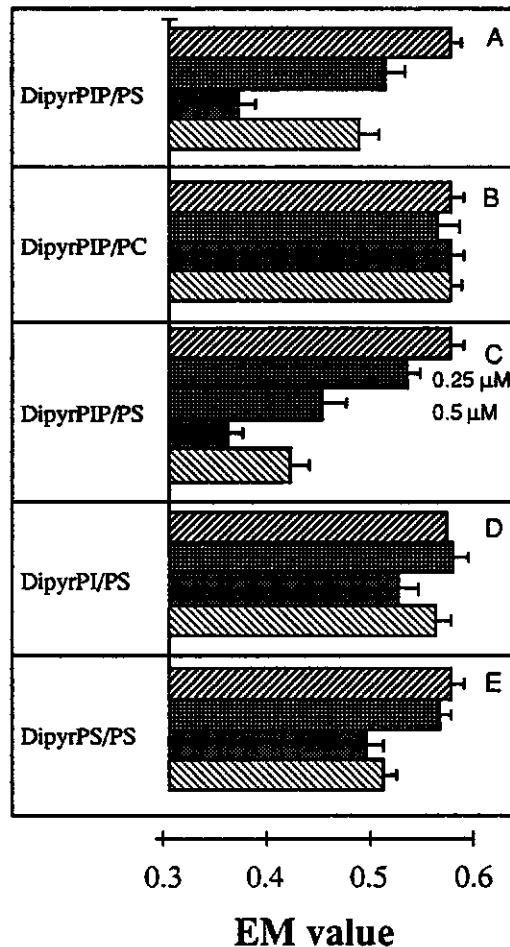
Figure 5. EM values of dipyrenyl phosphoinositides and dipyrPS dispersed in thesit micelles containing 10 mole % PS or PC. The values were obtained in absence of PKC and calcium (▨), then after sequential addition of PKC (0.4 μM, ▥), calcium (0.4 mM, ▦) and EGTA (5 mM, ▧).

Stepwise addition of PKC in absence of calcium leads to a concentration dependent reduction of the EM value of dipyrPIP (Figure 5C) which is not observed when PKC is replaced by buffer. If then calcium is added, the EM value reduces to a similar one as obtained in the experiment described in Figure 5A. The effect of PKC on the EM value in absence of calcium indicates that PKC is able to change the intramolecular collision frequency of dipyrPIP even without this cation. If the same experiment is performed with a dipyrene analogue of the natural precursor of PIP, dipyrPI, only small effects are observed (Figure 5D). When PKC, PS and calcium are present, only a 7% reduction of the EM value is observed as compared with the 35 % reduction observed when dipyrPIP is used. The simplest explanation is that the affinity of PKC for labelled PI is lower than that for PIP. This is remarkable if one bears in mind that the only difference between PI and PIP is a (charged) phosphate group on the 4-position of the inositol head group which is apparently responsible for the binding of dipyrPIP. The results obtained with dipyrPS as labelled lipid showed similar effects as were obtained with dipyrPI (Figure 5D). Although it has been established in the experiments described in the previous sections, that PS is required for the interaction of PKC with dipyrDG and dipyrPIP, the effects are relatively small. This is probably because dipyrPS, like dipyrPI, has to compete with the 10-fold excess of unlabelled PS in the micelles for interaction sites on the protein surface.

5.3.5. Competition experiments with unlabelled DG and phorbol ester

In order to investigate the ability of unlabelled DG to reverse the EM value of dipyrDG in micelles by replacing this labelled analogue at the protein surface of PKC a competition experiment was performed. The mole fraction of unlabelled DG in the mixed micelles was varied while keeping that of dipyrDG constant to 0.5 mole %.
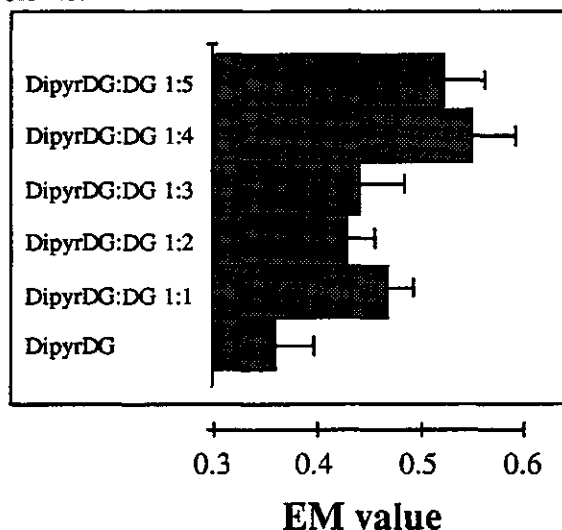

EM value

Figure 6. EM values of dipyrDG dispersed in thesit micelles containing 10 mole % PS and various mole fractions of unlabelled DG. The values were obtained in presence of PKC (0.4 μM) and calcium (0.4 mM).

The EM values obtained in the presence of PKC and calcium are presented in Figure 6. Unlabelled DG is capable to compete with dipyrDG, but especially at higher concentrations of DG, the EM values are highly scattered, and irreproducible, indicating that secondary effects like instability of lipid aggregates at high concentrations of DG may play a role in these experiments (note that DG is a bilayer-to-hexagonal phase promoter). The actual reason for this has to be investigated further systematically.

It has previously been reported that DG and PMA have a common binding site (Castagna et al., 1982; Chauhan et al., 1989). When unlabelled phorbol ester (PMA) is added to a micellar solution containing PKC and dipyrDG, the reduced EM value is instantaneously restored to the original value measured in the absence of PKC (Figure 7A).
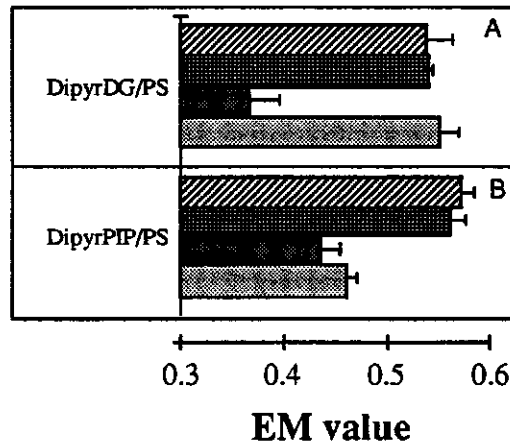

Figure 7. EM values of dipyrDG and dipyrPIP dispersed in thesit micelles containing 10 mole % PS. The values were obtained in absence of PKC and calcium (▨), then after sequential addition of PKC (0.4 µM, ▦), calcium (0.4 mM, ▦) and PMA (0.5 µM, ▦).

Apparently, PMA binds to PKC and is able to completely reverse the effect of PKC on dipyrDG. This can be explained by assuming that PMA and dipyrDG are not able to bind simultaneously to the same PKC molecule. This inverse binding relationship might originate from a shared binding site of DG and PMA or allosteric effects like, for instance, a PMA stabilised PKC conformation which is not able to interact with dipyrDG. Since in similar binding experiments dipyrPIP and dipyrDG were almost equally affected by PKC, it is of interest to see if PMA is able to replace dipyrPIP. A similar replacement would provide some evidence for a shared binding site of dipyrDG and dipyrPIP. However, no significant recovery of the EM values upon addition of PMA is observed (Figure 7B). This indicates that the binding of PMA to PKC does not induce a dissociation of dipyrPIP from the PKC surface, and both molecules are able to bind simultaneously to PKC.

5.4. Discussion

In the present chapter the binding of PKC to PS and DG is re-evaluated by simultaneous monitoring of quenching of PKC tryptophan fluorescence by resonance energy transfer (RET) to pyrene lipids and of excimer-to-monomer fluorescence intensity ratio (EM) of the pyrene lipids. The simultaneous registration methods of PKC-lipid interaction reduces experimental uncertainties and evaluates the binding event from both lipid and protein viewpoints. In addition, fast and sensitive detection and the use of close analogues of natural lipid cofactors allows rapid on-line observation of specific PKC-lipid interactions.

Several mechanism may contribute to the reduction of intermolecular excimer formation of pyrPS and pyrPC observed in presence of PKC (Figure 1). It can be envisaged that the interaction with PKC with the vesicular or micellar membranes will affect the lateral organisation of the pyrene lipids. Bazzi and Nelsestuen (1991a) observed that PKC induced lateral segregation of nitrobenzoxadiazolyl labelled phosphatidic acid in membranes. Formation of such lipid domains enriched with anionic lipids would lead, however, to an increase of intermolecular excimer formation of pyrPS. Since we observe rather a decrease of excimer formation in both micelles and vesicles when PKC is added, other mechanisms will dominate the effects of lipid domain formation: (1) pyrene lipids adjacent to inserted protein elements are surrounded by a reduced number of lipid neighbours and therefore have a reduced probability to form an excimer (see also Chapter 8). Since a pyrene moiety is separated 10 carbon atoms from the lipid head group region, segments of PKC have to insert considerably into the membrane hydrophobic region before a pyrene moiety is partly shielded from its chain neighbours. In addition, the lateral diffusion (2) of the pyrene lipids within the micelle and rotational diffusion (3) of the pyrene moieties in the vicinity of the PKC surface may be reduced considerably. If these diffusion rates become smaller than the average fluorescence decay rate of an excited pyrene (0.02 ns^{-1}, Chapter 8), the probability of excimer formation of a pyrene lipid at the protein surface even approaches zero. By comparing the results of the intermolecular excimer formation of pyrPS and pyrPC with those obtained with dipyrDG one can draw conclusions about the motional properties that are influenced by the binding of PKC to the membranes. The only processes which govern the intramolecular excimer formation of the dipyrene lipids are the rotational diffusion and freedom of the pyrene acyl chains. Since calcium independent association can be probed in intermolecular excimer forming experiments (Figure 1) but not (or hardly) in the intramolecular excimer forming experiments (Figure 3), it can be concluded that the calcium independent association of PKC mainly affects the lipid-lipid lateral organisation and lipid lateral diffusion within the micelles, but not the acyl chain rotational order and dynamics. Peripheral binding of PKC to the membrane surface could, for instance, decrease the lipid lateral diffusion of the monopyrene lipids. The pyrene lipids that directly interact with the protein (like pyrPS) will be laterally immobilized during the pyrene emission lifetime. Pyrene lipids that do not interact directly with PKC (like

pyrPC) will still be hindered in their lateral motions by the interaction of surrounding lipids with PKC.

When calcium is added a strong reduction of the excimer formation of pyrPS and of dipyrDG is observed in vesicles and micelles. Apparently, in absence of calcium loose accommodation of the pyrene lipids in the lattice of surrounding lipid and nonionic detergent molecules allows more extended and/or faster chain motions than in presence of calcium. The calcium dependence of the quenching and excimer characteristics can be explained by two alternative mechanism. The first explanation is that in the absence of calcium only part of the PKC population loosely interacts with the micellar surface. Addition of calcium shifts the equilibrium of free and bound PKC to the bound form. This enhanced binding will simply intensify the fluorescence quenching and reduction of the excimer formation of pyrPS which were already induced by the weaker binding in absence of calcium. In absence of calcium, PKC is bound loosely to the micelles, dynamically exchanging between buffer and micellar surface. Under these binding conditions, the time that the protein is retained at the micellar surface is too short for interaction with DG. When calcium is added, the protein becomes more firmly bound to the micellar surface. As a consequence of increased probability of finding the protein at the membrane surface, the probability of the of PKC with dipyrDG is enlarged. Alternatively, it can be envisaged that in absence of calcium the majority of PKC molecules interacts peripherally with the anionic micelles. This surface bound PKC is not able to interact with dipyrDG. Addition of calcium does not affect the relative amount of PKC bound to micelles but affects the protein in such a way that its binding to dipyrDG and PS are dramatically changed. In this context one might hypothesise that only the calcium bound form of PKC is able to bind dipyrDG. Calcium may induce an insertion of PKC segments into the hydrophobic region of the micelles. This insertion leads to a closer tryptophan-pyrene distance and thus to more efficient quenching. Accompanied changes in the lipid organisation and dynamics induced by protein insertion will lead to an additional reduction of excimer formation of pyrPS and pyrPC. Furthermore, direct interaction between PKC and dipyrDG leads to a large reduction of the acyl chain dynamics of dipyrDG. Unfortunately, based on the experiments described in this chapter, no conclusive distinction can be made between the two different concepts of PKC-membrane interaction. In presence of calcium, PKC reduces the excimer formation of dipyrPIP and dipyrDG considerably, while for the dipyrene analogues of PC, PS and PI only small effects were observed. In addition, both dipyrPIP and dipyrDG do not interact with PKC in absence of unlabelled PS (see also Pap et al., 1993). The fact that in competition experiments PMA displaces dipyrDG, but not dipyrPIP, from PKC indicates, however, that the PIP analogue does not bind at the cofactor site of PKC. Its binding to PKC is more analogous to PS since both dipyrPIP and pyrPS interacts with PKC in absence of calcium. The fact that the PKC induced reduction of dipyrPIP excimer formation clearly exceeds that of dipyrPS suggests that PKC has a higher affinity for PIP than for PS (Pap et al., 1993). The failure of binding to dipyrPIP in absence of (unlabelled PS) may thus simply be due to insufficient anionic lipid density in the micelles.

5.5. References

Banno, Y., Nakashima, T., Kumada, T., Ebisawa, K., Nonomura, Y. & Nozawa, Y. (1992) *J. Biol. Chem.* 267, 6488-6494.

Bastiaens, P.I.H., Pap, E.H.W., Borst, J.W., Hoek, A., Kulinski, T., Rigler, R. & Visser, A.J.W.G. (1993) *Biophys. Chem.* 48, 183-191.

Bazzi, M.D. & Nelsestuen, G.L. (1987) *Biochemistry* 26, 115-122.

Bazzi, M.D. & Nelsestuen, G.L. (1988) *Biochemistry* 27, 7589-7593.

Bazzi, M.D. & Nelsestuen, G.L. (1989) *Biochemistry* 28, 3577-3585.

Bazzi, M.D. & Nelsestuen, G.L. (1990) *Biochemistry* 29, 7624-7630.

Bazzi, M.D. & Nelsestuen, G.L. (1991a) *Biochemistry* 30, 7961-7969.

Bazzi, M.D. & Nelsestuen, G.L. (1991b) *Biochemistry* 30, 971-979.

Bell, R.M. (1986) *Cell,* 45, 631-632.

Boni, L.T & Rando, R. (1985) *J. Biol. Chem.* 260, 10819-10825.

Brockerhoff, H. (1986) *FEBS Lett.* 201, 1-4.

Brumfeld, V. & Lester, D.S. (1990) *Arch. Biochem. Biophys.* 227, 318-323.

Burns, D. & Bell, R. (1991) *J. Biol. Chem.* 266, 18330-18338.

Burns, D.J., Bloomenthal, J., Lee, M.H. & Bell, R.M. (1990) *J. Biol. Chem.,* 265, 12044-12051.

Castagna, M., Takai, Y., Kaibuchi, K., Sano, K., Kikkawa, U. & Nishizuka, Y. (1982) *Biol. Chem.* 257, 7847-7851.

Chauhan, A., Chauhan, V.P.S., Deshmukh, D.S. & Brockerhoff, H. (1989) *Biochemistry* 28, 4952-4956.

Comfurius, P., Bevers, E.M. & Zwaal, F.A. (1990) *J. Lipid Res.* 31, 1719-1721.

Epand, R.M., Stafford, A. R. & Lester, D. S. (1992) *Eur. J. Biochem.* 208, 327-332.

Förster, T. (1948) *Ann. Physik.* 2, 55-75.

Förster, T. & Kasper, K. (1955) *Z. fur Elektrochem.* 59, 976-980.

Galla, H.J. & Sackman, E. (1974) *Biochim. Biophys. Acta* 339, 103-115.

Ganong, B. & Loomis, C., Hannun, Y. & Bell, R. M. (1986) *Proc. Natl. Acad. Sci. USA* 83, 1184-1188.

Gschwendt, M., Kittstein, W. & Marks, F. (1991) *Trends Biochem. Sci.* 16, 167-169.

Hannun, Y.A., Loomis, C. R. & Bell, R. M. (1985) *J. Biol. Chem.* 260, 10039-10043.

House, C. & Kemp, B.E. (1987) *Science* 238, 1726-1728.

Huang, K.P. & Huang, F.L., Nakabayashi, H. & Yoshida, Y. (1988) *J. Biol. Chem.* 263, 14839-14845.

Huang, K.P. & Huang, F.L. (1986) *J. Biol. Chem.* 261, 14781-14787.

Kaibuchi, K., Takai, Y. & Nishizuka, Y. (1981) *J. Biol. Chem.,* 256, 7146-7149.

Kremer, J.M.H., van de Esker, M.W.J., Pathmamanoharan, C. & Wiersema, P.H. (1977) *Biochemistry* 16, 3932-3935.

Lee, M.Y. & Bell, R.M. (1989) *J. Biol. Chem.* 264, 14797-14805.

Lester, D., Doll, L., Brumfeld, V. & Miller, I. (1990) *Biochim. Biophys. Acta* 1039 33-41.

Makowske, M. & Rosen, O.M. (1989) *J. Biol. Chem.* 264, 16155-16159.

Mosior, M. & Mclaughlin, S. (1991) *Biophys. J.* 60, 149-159.

Myher, J.J. & Kuksis (1984) *J. Biochem. Cell Biol* 62, 352-356.

Newton, A.C. (1993) *Annu. Rev. Biophys. Biomol. Struct.* 22, 1-25.

Nishizuka, Y. (1984) *Nature,* 308, 693-697.

Nishizuka, Y. (1986) *Science,* 233, 305-312.

Nishizuka, Y. (1989) *JAMA,* 262, 1826-1833.

Orr, J.W., & Newton, A.C. (1992a) *Biochemistry* 31, 4661-4667.

Orr, J.W., & Newton, A.C. (1992b) *Biochemistry* 31, 4667-4673.

Orr, J.W. Keranen, L.M. & Newton, A.C. (1992c) *J. Biol. Chem.,* 267, 15263-15266.

Pap, E.H.W., Bastiaens, P.I.H., Borst, J.W., van den Berg, P.A.W., van Hoek, A., Snoek, G.T., Wirtz, K.W.A. & Visser, A.J.W.G. (1993) *Biochemistry* 32, 13310-13317.

Patel, K.M., Morrisett, J.D. & Sparrow, J.T. (1979) *J. Lipid Res.* 20, 674-677.

Rando, R.R. & Young, N. (1984) *Biochem. Biophys. Res. Commun.* 122, 818-823.

Sassaroli, M., Vaukonen, M., Perry, D. & Eisinger, J. (1990) *Biophys. J.* 57, 281-290.

Seelig, J. (1990) *Cell Biol. Int. Rep.* 14, 353-360.

Sekiguchi, K., Tsukuda, M., Ase, K., Kikkawa, U. & Nishizuka, Y. (1988) *J. Biochem.* 103, 759-765.

Shah, J. & Shipley, G.G. (1992) *Biochim. Biophys. Acta* 1119, 19-26.

Souvignet, C., Pelosin, J.-M., Daniel, S., Chambaz, E. M., Ransac, S. & Verger, R. (1991) *J. Biol. Chem.,* 266, 40-44.

Stryer, L. (1978) *Annu. Rev. Biochem.* 47, 819-846.

Takai, Y., Kishimoto, A., Kikkawa, U., Mori, T. & Nishizuka, Y. (1979) *Biochem. Biophys. Res. Commun.,* 91, 1218-1224.

Trudell, J.R., Costa, A. K. & Csemansky, C. A. (1989) *Biochem. Biophys. Res. Commun.* 162, 45-50.

Vanderkooi, J.M. & Gallis, J.B. (1974) *Biochemistry* 13, 4000-4007.

Wallach, D. F. H. & Zingler, R. J. (1974) in: "Evolving Strategies and Tactics in Membrane Research. Springer-Verlag, Berlin, 74-78.

Zidovetzki, R. & Lester, D.S. (1992) *Biochim. Biophys. Acta* 1134, 261-272.

Chapter 6

Quantitation of the interaction of protein kinase C with diacylglycerol and phosphoinositides by time-resolved detection of resonance energy transfer

Abstract

Quantitative studies of the binding of protein kinase C (PKC) to lipid cofactors were performed by monitoring resonance energy transfer with time-resolved fluorescence techniques. For that purpose, diacylglycerol (DG), phosphatidylinositol-4, 5-biphosphate (PIP_2), phosphatidylinositol-4-phosphate (PIP), phosphatidylinositol (PI), phosphatidylcholine (PC), and phosphatidylserine (PS) were labelled with a pyrenyl decanoyl moiety at the sn-2 position of the lipid glycerol. These labelled lipids proved excellent energy acceptors of light excited tryptophan residues in PKC. The quenching efficiency of the tryptophan fluorescence was determined as function of lipid probe concentration in mixed micelles consisting of polyoxyethylene-9-lauryl ether, PS, and various mole fractions of probe lipid. The experimental conditions and method of data analysis allowed the estimation of binding constants of single or multiple pyrene lipids to PKC. The affinity of PKC for inositide lipids increases in the order PI < PIP < PIP_2. The affinity of PKC for PIP and PIP_2 is higher than that for DG. Determination of PKC activity in the presence of labelled lipids and PS, showed that only PIP_2 and DG activate PKC. Double-labelling experiments suggest that PIP_2 and DG are not able to bind simultaneously to PKC, indicating a reciprocal binding relationship of both cofactors. The results support the notion that besides DG, PIP_2 can be a primary activator of PKC.

6.1. Introduction

Protein kinase C (PKC) has emerged as a crucial factor in transmembrane signal transduction influencing a great number of cellular processes including secretion, cell growth, and differentiation (Nishizuka, 1986; Kikkawa & Nishizuka, 1986). The interaction of PKC with specific lipids plays an essential role in the regulation of its activity. In vitro the enzyme is activated by PS in the presence of calcium and DG. Activation is accompanied by binding of PKC to the membrane. This binding is controlled by strong electrostatic forces and weak hydrophobic interactions (Brumfeld & Lester, 1990). Although binding to the membrane occurs with any negatively charged phospholipid (König et al., 1985; Bazzi & Nelsestuen, 1987) PS seems to be the most effective in the binding reaction (Hannun et al., 1985; Ganong et al., 1986). In contrast to the binding reaction, the lipid requirement for the activation of PKC is highly specific being met by DG and the tumour-promoting phorbol esters (Bazzi & Nelsestuen, 1988a, 1989; Brockerhoff, 1986). Recently, evidence has been obtained that besides these lipid cofactors PIP_2 is also able to activate PKC efficiently (O'Brain et al., 1987; Lee & Bell, 1991; Chauhan & Brockerhoff, 1988; Huang & Huang, 1991). At low PS concentrations the affinity of PKC for PIP_2 is higher than for

DG while the maximal PKC activation is lower with PIP_2 than with DG (Lee & Bell, 1991; Chauhan & Brockerhoff, 1988; Huang & Huang, 1991). Different affinities toward PIP_2 were reported for the three major $Ca^{2+}/PS/DG$-dependent PKC species (Huang & Huang, 1991). In addition, it was found that both DG and PIP_2 inhibited the binding of phorbol-12, 13-dibutyrate to PKC, which is indicative for a common binding site for PIP_2 and DG (Chauhan et al., 1989). In contrast others observed that PIP_2 interacts at a site different from that of phorbol ester and concluded that the mechanism by which PIP_2 activates PKC is different from that of DG (Lee & Bell, 1991; Huang & Huang, 1991). The fact that PIP_2 may act as an activator of PKC as well has far reaching consequences for the regulation of PKC activity. In order to verify these observations additional experiments are required to directly measure the binding of DG and PIP_2 to PKC, thereby allowing the determination of the binding constant of either lipid cofactor to PKC and providing the answer to the question whether PIP_2 and DG bind to either one or two sites on the kinase. To achieve this goal specific pyrene-labelled analogues of PIP_2 and DG were synthesised for use in studies in which the interaction with PKC was determined on line from time-resolved fluorescence detection of resonance energy transfer (RET). A major advantage of this technique is the direct and specific detection of interaction between PKC and the labelled cofactors in combination with high sensitivity and large dynamical range which allow the use of low concentrations of protein and lipid probes in the binding experiments. Verification of competition of pyrDG and unlabelled DG for binding to PKC was performed in a parallel study, the results of which suggested that both molecules bind for the same site (Bastiaens et al., 1993). The pyrene-labelled lipids were presented to PKC as part of a micellar system. This approach for investigating PKC-lipid interactions is well characterised (Hannun et al., 1985) and particularly suitable to determine the specificity and stoichiometry of the lipid requirement. The high concentration of micelles used validates the assumption that maximally one PKC molecule binds per micelle. Additional advantages of the use of micelles are that all (pyrene) lipids are exposed to the protein and that any effects that the physical state of a bilayer membrane may have on the interaction with the protein, are eliminated.

6.2. Experimental procedures

Materials
  Bovine brain L-α-phosphatidylserine (PS), dioleoyl-PC, diacylglycerol (DG), thesit [poly(oxyethylene)-9-lauryl ether], EGTA, HEPES, histone type IIIS, neomycin sulphate, phospholipase D from *Streptomyces species*, phospholipase C from *Bacillus cereus*, phenylmethanesulfonyl fluoride, Sephacryl S200, poly(lysine)-agarose, histone H1 from calf thymus, and trypsin from bovine pancreas (L-1-(tosylamino)-2-phenylethylchloromethylketone treated, 1.22 x 10^4 BAEE units mg^{-1}) were supplied by Sigma Chemical Co (St. Louis MO). Phenyl-sepharose CL 4B and DEAE-sepharose FF S200 were from Pharmacia (Uppsala, Sweden) and [γ-^{32}P]ATP (3000 Ci $mmol^{-1}$) was from Amersham (U.K.). The scintillation counting cocktail was from Packard (Meriden). All other phospholipids used were synthesised as described in the methods

section. All solvents were distilled before use. All other chemicals were of reagent grade. Unless otherwise noted, experiments were performed using 20 mM Tris, pH 7.5, 50 mM KCl and 20 μM EGTA at 20° C.

Purification of PKC
Protein kinase C was purified from cytosolic extract of homogenised Wistar rat brains similar to the procedure described by Huang et al., (1986) and consecutively by DEAE, phenyl-sepharose, sephacryl S200 and polylysine agarose chromatography. The final preparation [with isozyme composition as described elsewhere (Huang et al., 1986; Sekiguchi et al., 1988)] was essentially pure as demonstrated by silver staining of a polyacrylamide gel, and was stored at -70°C in buffer (20 mM Tris pH 7.9, 0.5 mM EGTA, 0.5 mM EDTA, 1 mM BME) with 25% glycerol (Merck, Darmstadt, Germany, fluorescence microscopy grade).

Assay of PKC activity
The dependence of the calcium and phospholipid-dependent PKC activity was assayed at a temperature of 20° C, essentially as described by Snoek et al., (1988) using mixed micelles of 300 μM thesit, 5 mol % PS, and 0.01 to 4 mol % pyrene labelled lipid.

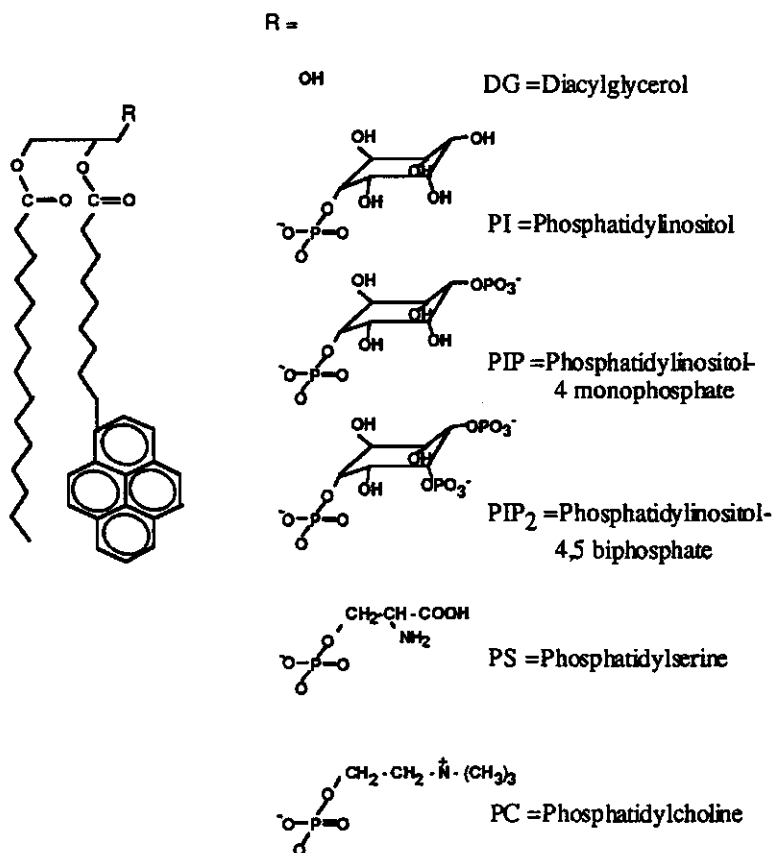*Synthesis of pyrene-labelled phosphoinositides*
sn-2-(Pyrenyldecanoyl)-PI (pyrPI) was synthesised from yeast PI according to Somerharju et al., (1982, 1985). Pyrene-labelled analogues of phosphatidylinositol-4-phosphate (pyrPIP) and phosphatidylinositol-4, 5-phosphate (pyrPIP$_2$) were synthesised from pyrPI using partially purified PI and PIP kinase preparations as described by Gadella et al., (1990). The products were identified as pyrPIP and pyrPIP$_2$ on TLC and from their elution behaviour on immobilised neomycin columns. For structures of the compounds see Figure 1.

Synthesis of pyrene-labelled phosphatidylcholine, phosphatidylserine, and diacylglycerol
sn-2-(Pyrenyldecanoyl)-PC (pyrPC) was synthesised from egg-PC as described by Somerharju et al., (1982). Pyrene-labelled PS (pyrPS) was obtained enzymatically from pyrPC by transphosphatidylation catalysed by phospholipase D (Comfurius et al., 1990). PyrDG was synthesised by a phospholipase C catalysed hydrolysis of the diglyceride-phosphate linkage in pyrPC essentially as described by Myher and Kuksis (1984). Purification of the lipids was performed with high performance liquid chromatography on a silicic acid column (240 x 10 mm, LiChroprep Si 60, Merck, Germany). Elution was performed with an increasing methanol gradient in chloroform (0 40%). Structures of the compounds used are given in Figure 1.

Micelle Preparation
Mixed lipid micelles were prepared by drying the required amounts of lipids under a stream of nitrogen in a glass tube followed by solubilisation in buffer [1 mM Thesit, 20 mM Tris/HCl (pH 7.4) 50 mM KCl and 20 μM EGTA] by

R =

OH

DG =Diacylglycerol

PI =Phosphatidylinositol

PIP =Phosphatidylinositol-
4 monophosphate

PIP$_2$ =Phosphatidylinositol-
4,5 biphosphate

PS =Phosphatidylserine

PC =Phosphatidylcholine

Figure 1. Chemical structures of the pyrene-labelled phospholipids.

vortexing and brief bath sonication. In the binding studies the thesit concentration was 100 μM and the PS concentration was 5 μM (5 mol %). The fluorescent lipid concentration ranged from 0.01 to 4 μM (0.01 - 4 mol %). The phospholipid content was determined by phosphate analysis according to the method of Rousser et al., (1970). The pyrene concentration was estimated by measuring the absorption at 342 nm in ethanol/DMSO (75:25 v/v) (ε =39700 $M^{-1}cm^{-1}$). In the fluorescence experiments the PKC concentration was 80 nM.

Instrumental

Time-resolved fluorescence measurements were carried out using a time-correlated single photon counting set-up as described earlier (Bastiaens et al., 1992). A mode-locked cw YLF laser (Coherent model Antares 76-YLF, Palo Alto, CA), that was equipped with an LBO frequency doubler to obtain output at 527-nm wavelength was used for the synchronously pumping of a cavity-dumped Rhodamine 6G dye laser (Coherent model 701-2 CD). The light output of the dye laser was frequency doubled using a BBO crystal (3x4x7 mm^3, Gsänger, Planegg, Germany). A variable waveplate (New Focus model 5540,

Mountain View, CA) was used to rotate the polarisation of the vertically polarised output light of the dye laser to horizontally polarised light to have again vertically polarised (UV) light available for excitation after the type I frequency doubling in the BBO crystal. The repetition rate of excitation pulses was 951 kHz, the excitation wavelength 295 nm, the duration about 4 ps FWHM and the pulse energy in the tens of pJ range. Fluorescence was selected using a 3 mm WG 335 cut-off filter (Schott, Mainz, Germany), an interference filter at 348.8 nm (Schott, bandwidth 4.8 nm FWHM) and a sheet type polariser (Polaroid type HNP'B, Cambridge, MA) that could be rotated under computer control to parallel and perpendicular with respect to the direction of excitation polarisation. Singlephoton responses from the microchannel-plate photomultiplier (Hamamatsu, model 1645U, Hamamatsu, Japan) were amplified by a wide band amplifier (Hewlett Packard model 8447F, Palo Alto, CA), analysed in one channel of a quad constant fraction discriminator (Tennelec modified model TC 454, Oak Ridge, Tennessee) and then used as a start signal for the time-to-amplitude converter (TAC, Tennelec model TC 864). The stop signal for the TAC was generated using another channel of the TC 454, driven by the pulses from a fast PIN photodiode (Hewlett Packard model 5082 4203 at 45 V reverse bias) that was excited with red light left from the frequency doubling set-up (van Hoek & Visser, 1990). The output signal of the TAC was analysed by an analogue-to-digital converter (Nuclear Data model ND 582, a 1.5 μs fixed death time ADC, Schaumburg, IL), and the output signal of the ADC was gathered in a multichannel analyser (Nuclear Data model ND66); 1024 channels were used per experimental decay with a time spacing of 30 ps per channel. Measurements consisted of a number of sequences of measuring during 10-s parallel and 10-s perpendicular polarised emission. After measuring the fluorescence of a sample the background emission of PKC-free samples was measured, at one-fifth of the time of sample acquisition, and then used for background subtraction. PTF (BDH, Poole, U.K.) dissolved in ethanol, 1.06 ns single exponential decay time (Vos et al., 1987) served as a reference compound to yield the dynamic instrumental response function of the set-up (van Hoek & Visser, 1985). The sample temperature was 20 °C.

Computational methods
The inverse Laplace transform of the fluorescence decay [I(t)] of the enzyme [the spectrum of contributions $\alpha(\tau)$ to the lifetimes (τ)] was obtained with the commercially available maximum entropy method (Maximum Entropy Data Consultants Ltd., Cambridge, U.K.):

$$I(t) = \int_0^\infty \alpha(\tau)e^{-t/\tau}d\tau \qquad (1)$$

The principle of this method is fully described in previous publications (Gentin et al., 1990; Livesey et al., 1987; Brochon et al., 1992; Bastiaens et al., 1992).
Since PKC contains multiple tryptophan residues (eight for PKC from bovine brain (Parker et al., 1986)), the fluorescence decay is complex, and no unique

lifetime class arises in the lifetime distribution of PKC without or with quenching by RET. Upon quenching by RET, however, several lifetime peaks are shifted to shorter time, which makes it difficult to determine the fraction of lipid sites occupied with pyrene lipids from analysis of the lifetime spectra. Therefore the average fluorescence lifetime $<\tau>$ was used as an observable to monitor the occupancy of a PKC molecule with pyrene lipids. The average lifetime was calculated from the lifetime spectra according to

$$<\tau> = \frac{\sum_{i=1}^{s} \alpha_i \tau_i}{\sum_{i=1}^{s} \alpha_i} \qquad (2)$$

where the summation is carried out over the whole range (s) of τ_i values of an $\alpha(\tau)$ spectrum. The fluorescence quenching of tryptophan residues of PKC by pyrene lipids is described as follows. Vacant lipid sites at the protein surface and pyrene lipids in the micelle are in binding equilibrium. The fluorescence lifetimes are assumed to be short relative to the mean residence time of a pyrene lipid in a lipid 'site' on the protein and it is assumed that only pyrene lipid molecules that interact with PKC contribute to the tryptophan quenching. This is a reasonable assumption, since the characteristic critical Förster distance for a pyrene-tryptophan couple was calculated to be 2.7 nm as compared with the dimensions of a spherical PKC molecule with a hydrodynamic diameter of $=$ 6 nm, and of a micelle with a diameter of $=$ 7 nm (both dimensions are based on measured rotational correlation times, data not shown). The average distance between pyrene lipids randomly distributed within the micelle and the protein is thus too large for efficient energy transfer. Furthermore, it is assumed that binding of pyrene lipid to a 'site' on the protein contributes additively to the total fluorescence quenching rate, resulting in a shortening of the average fluorescence lifetime. A binding equation can be deduced in which γ is defined as the fraction of sites occupied by a pyrene lipid. Since the concentration of PKC is an order of magnitude lower than the concentration of micelles, the probability that more than one PKC molecule binds to one micelle can be neglected, resulting in a binding equation independent of the PKC concentration. Similarly, the probability that more than one pyrene lipid is present in a micelle can be neglected at low concentrations of pyrene lipid. When we assume reversible lipid binding to a single site at the PKC molecule, the lipid binding to this site is simply governed by first-order dissociation (k^-) and association rate constants (k^+) and the equilibrium constant K for the binding becomes

$$K = \frac{k^-}{k^+} = \frac{(1-\gamma)(1-\gamma)}{\gamma} \qquad (3)$$

When each PKC molecule has m equivalent and independent lipid binding sites, and n pyrene lipids are allowed in the micelle, the units of the association rate constant becomes second order and the dissociation rate

constant remains first order. The average number of free sites per micelle occupied with a PKC molecule can then be expressed as $m(1-\gamma)$, and the average number of free lipid molecules per micelle equals to $(n-m\gamma)$ where $(n \geq m\gamma)$. The equilibrium constant K becomes:

$$K = \frac{(1-\gamma)\ (n-m\gamma)}{\gamma} \tag{4}$$

Solving the quadratic equation for $\gamma(n, m)$ one obtains

$$\gamma(n,m) = \frac{1}{2}\left[(1 + \frac{K}{m} + \frac{n}{m}) - \sqrt{(\frac{-4\,n}{m}) + (-1 - \frac{K}{m} - \frac{n}{m})^2} \right] \tag{5}$$

When the rate of dissociation of the complex is larger than the rate of exchange of pyrene lipids between micelles, the lipid molecules have to be considered as compartmentalised reactants, in which the probability (P_n) of finding n lipid cofactor molecules in a micelle of size S (surfactant number) at a labelling ratio (χ_T) is binomially distributed:

$$P_n = \frac{S!}{n!\ (S-n)!}\ \chi_T{}^n\ (1-\chi_T)^{S-n} \tag{6}$$

The total fraction of occupied lipid sites at a given labelling ratio and number of lipid sites per PKC molecule is then given by:

$$\gamma_{tot} = \sum_{n=1}^{S} P_n\ \gamma(n,m) \tag{7}$$

Since the microscopic fractional occupancy of lipid sites directly corresponds to the macroscopic fractional occupancy of PKC we can directly apply this model to the dependence of the average lifetime on the mole fraction of pyrene-labelled lipids to determine the equilibrium constant K for $m = 1$ to 6:

$$<\tau> = <\tau_o> - X\ \gamma_{tot} \tag{8}$$

where fitting parameter $<\tau_o>$ corresponds to the average lifetime of the non-quenched PKC and X to the decrease in average lifetime when PKC is maximally quenched.

6.3. Results

6.3.1. Tryptophanyl fluorescence decay and distribution of lifetimes

Figure 2 shows the experimental fluorescence decay and the analysis in a distribution of lifetimes of PKC in the presence and absence of pyrPIP$_2$ in thesit-PS mixed micelles. In all experiments the residuals of the fits were randomly scattered around zero indicating an optimal fit (results not shown). As

expected, the fluorescence decay of tryptophan in this enzyme is complex (note that the vertical scale in Figure 2 is logarithmic), probably because there are multiple classes of emitting tryptophan residues in the protein.
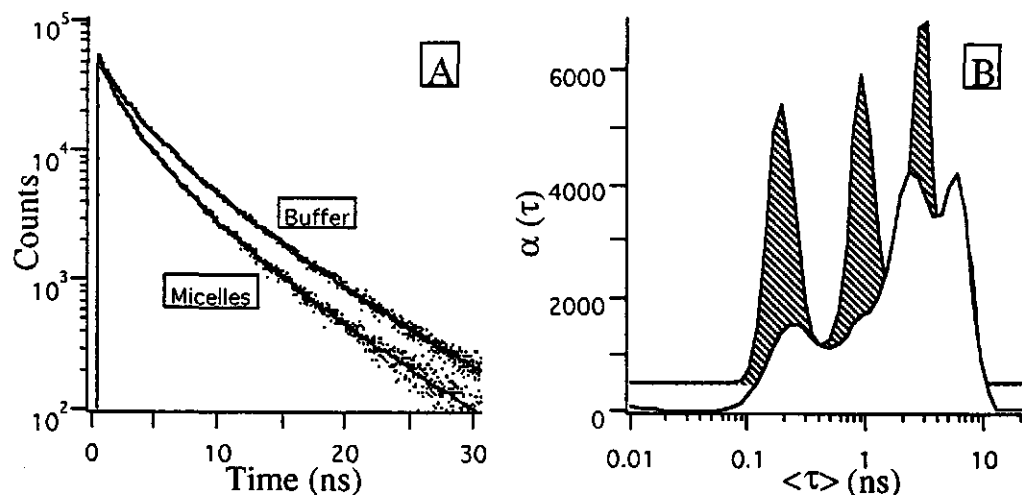
Figure 2 A. Experimental and fitted decays of tryptophan fluorescence of PKC in buffer (80 nM) and in the presence of 100 µM thesit micelles containing 5 mol % PS and 4 mol % pyrPIP$_2$. **B.** The MEM-recovered lifetime distributions of tryptophan fluorescence of PKC in buffer ▣ and in the presence of the above mentioned mixed micelles ▅. The measurements were performed in 20 mM Tris buffer (pH 7.5, 50 mM KCl and 1 mM CaCl$_2$) at 293 K.

In all analyses at least three peaks appeared in the lifetime distribution which may originate from three subclasses of tryptophan emitters. Addition of 4 mol % pyrPIP$_2$ to mixed micelles containing 5 mol % PS caused quenching of tryptophan fluorescence as manifested by a more rapid fluorescence decay. A substantial reduction of the barycenter values for each lifetime class is observed, indicating that each subclass of emitters is within the range of critical energy transfer distance of the pyrene moiety of PIP$_2$.
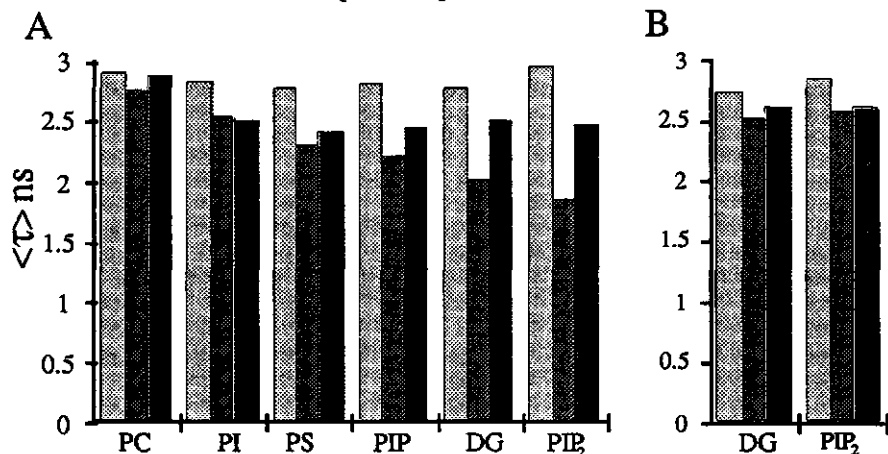
The average lifetime of tryptophan fluorescence in the enzyme was found to be independent on the concentration of mixed micelles above 100 µM thesit with 5 mol % PS and 1 mol % pyrDG (Figure 3), revealing that saturation of binding is approached at this lipid concentration. The presence of 5 mol % brain PS in the micelles apparently provides sufficient binding capacity for PKC. This was confirmed in an identical system using fluorescence correlation spectroscopy (Bastiaens et al., 1993). Thus we further assume that PKC is associated with the micelles if calcium and 5 mol % PS are present, independent of the pyrene-lipid concentration.
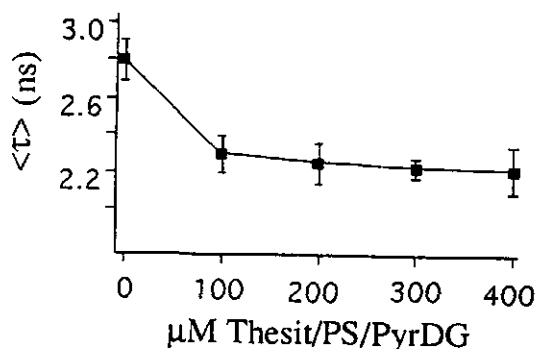
Figure 3. Average fluorescence lifetime ($<\tau>$) of PKC as a function of the concentration thesit with 5 mol % PS and 1 mol % pyrDG. The experiment was performed in 20 mM Tris buffer (pH 7.5, 50 mM KCl and 1 mM CaCl$_2$) at 293 K.

6.3.2. Calcium and PS-dependence of PIP$_2$- and DG-binding to PKC

In order to examine the relationship between calcium requirement and pyrene lipid binding the average lifetime of tryptophan fluorescence in PKC was measured sequentially in the absence of calcium, in the presence of calcium and then in the presence of saturating amounts of EGTA. In the absence of calcium (20 µM EGTA) no effect of pyrene lipids is observed (Figure 4A). The average lifetimes of tryptophan fluorescence, obtained in the presence of the various pyrene lipids, display values scattered around the one obtained with micelles not loaded with probe lipid.

Figure 4. Comparative effects of various pyrene-labelled phospholipids in micelles on the average fluorescence lifetime of tryptophan residues in PKC. PKC was incubated with 100 µM mixed micelles containing 1 mol % pyrene lipid in the presence of 5 mol % PS (A). and in presence of 5 mol % DOPC (B). The measurements were performed by adding successively 10 µM EGTA (▨), 0.5 mM calcium (▦) and 10 mM EGTA (■).

Addition of calcium caused only a slight decrease of the average lifetime of tryptophan fluorescence when micelles with 2 mol % of pyrPC or pyrPI were present. In case of micelles containing 2 mol % of pyrene-labelled PS, PIP, DG and PIP$_2$ a substantial reduction of the fluorescence lifetime is observed upon addition of calcium. The effect of calcium on the quenching of tryptophan fluorescence by the pyrene lipids decreases in the order PIP$_2$ > DG > PIP > PS. As is shown in the last column of Figure 4A, this effect can be largely reversed by removal of calcium with EGTA. The effect of calcium on the activation of PKC by the above-mentioned lipids revealed qualitatively a similar result (see below). On removal of calcium by EGTA, the average lifetime increases to almost 90% of the value obtained before addition of calcium, demonstrating major reversibility of PKC-lipid cofactor binding as was also found by other groups (Bazzi & Nelsestuen, 1987, 1991). In addition, the binding of pyrDG and pyrPIP$_2$ was investigated in the absence of 5 mol % brain PS. As can be seen in Figure 4B, PS is an absolute prerequisite for the interaction of the protein with its lipid cofactors DG and PIP$_2$. The simplest explanation of these results is that for activation by pyrDG and pyrPIP$_2$, direct interaction of these cofactors with PKC is required. This interaction is not established in the absence of either PS or calcium [see also Bazzi & Nelsestuen, (1987) and Rodriguesz-Paris et al., (1989)]. Conversely, mixed micelles containing 5 mol % PS are fully capable to bind PKC in the presence of calcium. Probably calcium is needed for the interaction of PKC with PS. Binding of PKC to PS molecules precedes the interaction with pyrene lipid cofactors which then leads to activation of PKC.

6.3.3. Fluorescence quenching by the various pyrene lipids

The dependence of tryptophan fluorescence quenching of PKC on the mole fraction of pyrene-lipids was examined in a range of 0 - 4 mol %. The data were analysed in terms of lifetime distributions and the average fluorescence lifetime $<\tau>$ was calculated using eq. 2. In Figure 5 the average lifetime is plotted as a function of the pyrene lipid mole fraction for the various lipid analogues. A steep decrease in the plot of the average lifetime against the mole fraction of pyrene lipid indicates a high affinity between PKC and the lipid, while the average lifetime at saturating levels of pyrene lipids is governed by the eventual binding configuration and stoichiometry. The quenching characteristics of pyrPIP, pyrPIP$_2$ and pyrDG are different from those of pyrPI and pyrPS in two aspects. First, within the mole fraction range saturation of the quenching effect is approached for pyrPIP, pyrPIP$_2$ and pyrDG in strong contrast with the almost linear dependence of the average lifetime on the mole fraction of pyrene-labelled PI and PS. This difference implies that the affinity of PKC for pyrPI and pyrPS is considerably lower than for pyrPIP, pyrPIP$_2$ and pyrDG. Second, the average lifetimes obtained at higher concentrations of pyrPIP$_2$ and pyrDG are substantially shorter as compared to the other lipids. The lifetime value at saturating amounts of pyrPIP seems to be intermediate to those of pyrPI and pyrPIP$_2$. The quenching of PKC fluorescence by pyrPIP, pyrPIP$_2$, and pyrDG was suitable for the determination of the binding constant because quenching approached saturation with these lipids within the experimental mole fraction range. From the dependence of the average lifetime on the mole fraction of pyrene lipid in the micelles, the binding constants were

determined for 1-6 lipid binding sites (m) per PKC molecule, according to the model as described under Experimental Procedures (eq. 10). In this analysis it was assumed that a micelle consists of 300 molecules ($S = 300$), based on fluorescence correlation spectroscopic studies with an identical micellar system (Bastiaens et al., (1993)). The results of the fit are listed in Table 1.
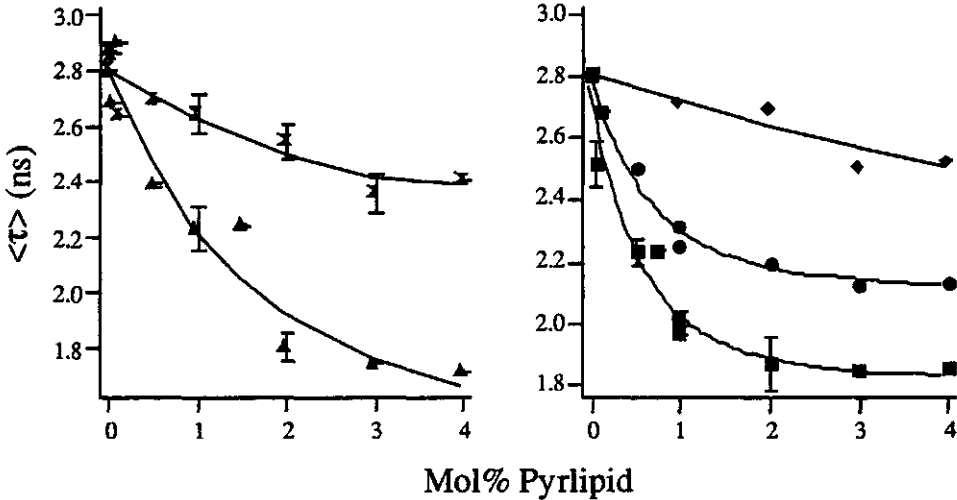
Figure 5. Dependence of the average fluorescence lifetime of tryptophan residues in PKC on the mole fraction of pyrene-labelled PIP$_2$ (■), PIP (●), PI (◆), PS (✗) and DG (▲) in 100 μM mixed micelles containing 5 mol % PS. The measurements were performed in 20 mM Tris buffer (pH 7.5, 50 mM KCl and 1 mM CaCl$_2$) at 293 K.

The quality of the analysis of the average lifetime dependence on the mole fraction of pyrene labelled PIP and PIP$_2$ decreases considerably when more than 3 binding sites were assumed per PKC molecule. From the standard error of the average lifetime values and the number of degrees of freedom the significant increase of χ^2 from its minimum value can be determined at a confidence interval of 0.67 according to a so-called fstat test (Beechem et al., 1991). With this approach χ^2 limits of $6.8*10^{-3}$, $2.2*10^{-3}$ and $1.9*10^{-2}$ were obtained for pyrPIP$_2$, pyrPIP and pyrDG respectively.

	PIP$_2$		PIP		DG	
m	K	SSQ	K	SSQ	K	SSQ
1	0.431	0.0053	0.676	0.0016	3.2	0.0146
2	0.119	0.0053	0.264	0.0013	2.58	0.0145
3	2×10^{4}	0.0059	0.003	0.0013	1.84	0.0144
4	6×10^{4}	0.0090	6×10^{4}	0.0037	1.01	0.0143
5	8×10^{-5}	0.0139	8×10^{-5}	0.0086	0.43	0.0141
6	2×10^{-5}	0.0197	4×10^{-5}	0.0142	0.052	0.0141

Table 1. Values of the equilibrium constant K for the binding of single (m=1) or multiple (m = 2-6) pyrene-labelled PIP$_2$, PIP and DG molecules to PKC and the quality of the fit (SSQ), obtained from the analysis of the average fluorescence lifetime dependence on the mole fraction of these pyrene lipids.

It can thus be concluded that the pyrPIP and pyrPIP$_2$ data only allow adequate fits if three or less binding sites per PKC molecules are assumed. Since the lifetime dependency on the mole fraction of pyrDG is less pronounced than for the former two lipids, the number of DG sites has no clear effect on the quality of the fit. Apparently, the quality of the data does not allow determination of the absolute number of DG binding sites. For each value of m, however, the equilibrium constant of PKC for pyrPIP and pyrPIP$_2$ is considerably lower than that for pyrDG, indicating a higher affinity for either phosphoinositide than for DG.

6.3.4. Activation of PKC by pyrene-labelled lipids

The dependency of PKC activation on pyrene-labelled lipids in the presence of 0.5 mM calcium and 5 mol % brain PS was measured in the range of 0 - 4 mol %, in parallel with the fluorimetric binding studies. Without calcium and 5 mol % PS no significant PKC activity was found. The activity profiles with either effector, pyrDG or pyrPIP$_2$ in the presence of 5 mol % PS were found to be quite different.
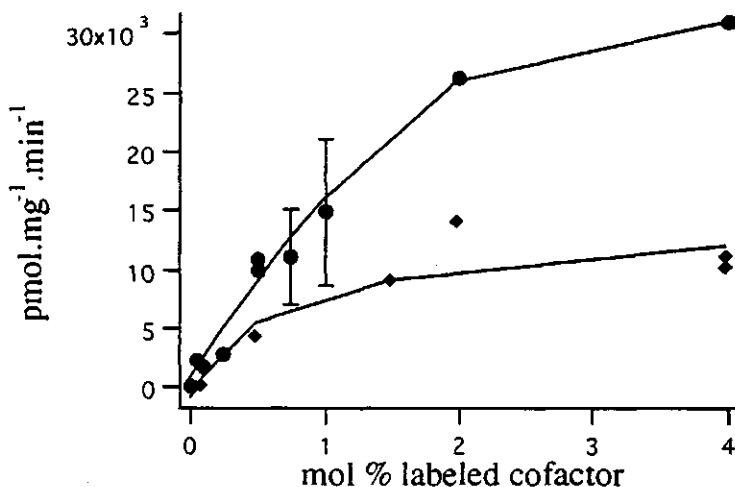
Figure 6. PIP$_2$-(●) or DG- (◆) stimulated PKC activity in the presence of labelled cofactors. The activity is expressed in nmol of phosphate incorporated into histone IIS per minute per mg of PKC.

The maximal activity attained with pyrPIP$_2$ is higher than that achieved by pyrDG (Figure 6). None of the other pyrene labelled phospholipids supported activation even up to 4 mol %. Therefore the activation of PKC displays, in agreement with the binding studies, high specificity for pyrDG and pyrPIP$_2$. In addition, these results refute the possibility of pyrene itself being the activating factor in the fluorescent lipids. The activity of the enzyme is roughly proportional to the fraction of PKC bound to pyrPIP$_2$ and pyrDG (Figure 6).

6.3.5. Double-labelling experiments

In order to investigate the relationship between DG- and PIP$_2$-binding to PKC, double-labelling experiments were performed by monitoring the tryptophan fluorescence decays in the presence of various molar ratios of pyrDG and pyrPIP$_2$ while keeping the total concentration of pyrene cofactor constant. In this approach it is assumed that each pyrene lipid that binds to PKC quenches the protein fluorescence additively. This approach was preferred over competition experiments using nonlabelled lipid cofactors since possible effects of the pyrene moiety on the binding to PKC are then omitted. If both cofactors interact independently with PKC at separated sites, a more efficient quenching is expected at equal molar ratios than when one of the cofactors is solely present. However, when the lipid cofactors interfere in each other's binding, e.g. when they share the same binding 'site', no effect is expected from a change in the molar ratios of the two pyrene cofactors.
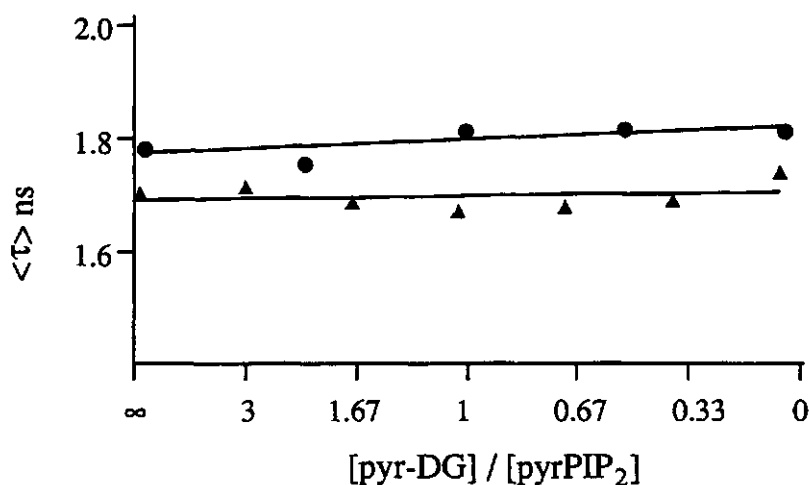
Figure 7. Double-binding experiment with pyrPIP$_2$ and pyrDG. Binding of lipid cofactors to PKC was measured in thesit mixed micelles containing PS at 5 mol % at various molar ratios of pyrDG to pyrPIP$_2$ while keeping the total concentration of pyrene-labelled cofactor constant at 3.5 (●) and 5 (▲) μM.

In these double-labelling experiments, the total amount of lipid cofactors must be high in order to eliminate micelles containing only one of the cofactors. Figure 7 shows the tryptophan average fluorescence lifetime as a function of the molar ratio of pyrDG and pyrPIP$_2$ at 3.5 and 5 mol % total pyrene lipid cofactor. The tryptophan average lifetimes are scattered around a value of 1.8 and 1.7 ns respectively. The dependency of the lifetime values on the molar ratios is found to be linear, rather than 'parabolic', indicating that the binding of either cofactor inhibits the binding of the other one.

6.4. Discussion

The binding of DG, PIP_2 and various other lipids to PKC was investigated by measuring the quenching of tryptophan fluorescence in PKC as a result of radiationless energy transfer to pyrene-labelled analogues of the natural lipids in mixed micelles. The results of the lipid titration experiments were quantified in terms of number of lipid binding sites per PKC molecule and binding constants for the lipid cofactors. In addition, the effect of the presence of both labelled cofactors at various relative concentrations on the average lifetime of PKC was studied in double-labelling experiments. Our results show that the affinity of PKC for lipids decreases in the order PIP_2 > PIP > DG > PI, PS, PC. The affinity of PKC for DG is relatively low (binding constant is 3.2 molecules, $m=1$) as compared to its affinity to PIP and PIP_2. In a parallel study however, using 10 mol% PS in the mixed micelles, a binding constant of 0.15 molecules ($m=1$) for the interaction of PKC with pyrDG is reported (Bastiaens et al., 1993), indicating that binding of PKC to DG is highly dependent on the mole fraction PS in the micelles [see also Lee and Bell (1991)]. When multiple sites are encompassed in our model, identical binding characteristics are assumed. This is justified by the hyperbolic dependence of the binding isotherms without inflection points. The exact number of lipid sites could not be determined from the pyrDG data, but in the case of $pyrPIP_2$ and pyrPIP this number is probably less than three, confirming the results of Huang & Huang (1991). Other workers reported that the lipid cofactor DG binds to PKC in a one to one stoichiometry (Brockerhoff et al., 1986; Gschwendt et al., 1991; Hannun et al., 1985; Ganong et al., 1986). Of all the lipid analogues examined, only PIP_2 and DG were able to activate PKC. Although the affinity of PKC for PIP is high, no activation of PKC is induced by the interaction with this lipid, indicating that strong binding is insufficient for activation and that special features of DG and PIP_2 lead to PKC activity during the interaction. This is supported by the observation that the tryptophan fluorescence of PKC in the presence of saturating amounts of pyrPIP is considerably less quenched than in the presence of saturating amounts of $pyrPIP_2$ or pyrDG indicating a different binding configuration or stoichiometry. Since the analysis of the tryptophan average lifetime dependence on the mole fraction of PIP does not allow more than three PIP sites per PKC molecule, in agreement with PIP_2, both inositol lipids might share the same binding site(s) on PKC. The binding of PIP_2 to these site(s) might, like DG, stabilise an active PKC conformation, in which the tryptophan residues are transferring energy more efficiently to pyrene. The high affinity binding of its precursor PIP to these sites, however, is not competent to stabilise this active and more "quenchable" protein conformation. These stabilising features may arise from favourable geometrical structures as reported for DG (Kerr et al., 1987; Ono et al., 1989), or from electrostatic interactions (in case of PIP_2) satisfying particular binding conditions. The effect of conformational changes of PKC induced by cofactor molecules on the equilibrium constant of binding has to be systematically investigated further. In case that binding of the cofactors is not reversible, the model cannot be applied.

Besides the structural requirements of the lipid cofactors, it is reported that PKC can be activated by membrane bilayer perturbations induced by DG [summarised by Zidovetzki and Lester, (1992)]. In this respect it is worth noting that there is evidence that both PIP_2 and DG are both capable to form non-bilayer lipid phases (Hendrickson, 1969; Das et al., 1986; De Boeck & Zidovetzki, 1989). Similar physicochemical disturbances of the bilayer by both cofactors could increase the accessibility of hydrocarbon regions of the membrane for PKC, thereby intensifying hydrophobic interactions, possibly accompanied by conformational changes. However, since in this study the lipid cofactors were incorporated in less ordered mixed micelles, where specific structural membrane arrangements or lipid phases are absent, the particular molecular features of DG and PIP_2 seem to be absolutely required and sufficient for PKC activation.

Contradictory conclusions were reported concerning the shared or separate site of PIP_2 and DG on PKC. These reports are based on observations that PIP_2 does (Chauhan et al., 1989) or does not (Lee & Bell, 1991; Huang & Huang, 1991) inhibit phorbol-12, 13-dibutyrate binding. Although the reason for these different experimental results is unknown, the double-labelling experiments in this paper provides a direct approach to show the mutual dependence of the binding of both cofactors to PKC. Since no additive fluorescence quenching was found when both labelled cofactors were present at equal molar ratios, as compared with the quenching in the presence of one of the labelled cofactors, simultaneous binding of both cofactors to PKC does not seem to be probable. In the shared binding site model, competition in binding is in agreement with the double-labelling results. The occupation of a site by one of the cofactors simply prevents the binding of the other cofactor. However, the separate site model is not rigorously rejected by these results. If there are separate sites for DG and PIP_2, the binding of one of these lipids to the protein could stabilise the active PKC conformation which is not able to bind the other cofactor lipid. In addition, allosteric effects or steric effects of the cofactors at closely spaced sites may prevent the binding of the other lipid cofactor.

Our results strongly support the notion that PIP_2 has a dual role in the activation mechanisms of PKC (Lee & Bell, 1991; Chauhan et al., 1989). First, PIP_2 can function as a precursor for DG in the phospholipase C catalysed hydrolysis. In this role PIP_2 itself is inert and only its hydrolysis is the switch for the PKC activation. In a later stage of the activation also other lipids can function as a precursor for DG (Nishizuka, 1992). Second, PIP_2 itself is a high affinity ligand and effective activator of PKC in the presence of calcium. This implies that PKC can be activated independently from the inositide breakdown route when calcium is provided via alternative routes (like calcium channels in the plasma membrane). Reports of oscillatory cytosolic calcium waves, independently of stimulated inositol 1, 4, 5-trisphosphate formation (Rooney et al., 1991), are consistent with this second model of activation. In the DG-dependent activation, the time response of PKC activity depends mainly on the presence of DG (Bazzi & Nelsestuen, 1988a; Nishizuka, 1986, 1992), while in the PIP_2-dependent activation, regulation of PKC activity is probably controlled by the temporal availability of calcium in the cytosol. Regulation of the kinase activation via the availability of PIP_2 by PIP-kinase and PLC, responsible for the

synthesis and degradation of PIP_2, is not very likely, since the degradation of PIP_2 leads automatically to the generation of DG, which is at least an equally competent activator of the kinase. This would thus only be useful if the activation of PKC by PIP_2 and DG would lead to an active kinase with distinct characteristics, like substrate specificity. Physiological significance of the activation of PKC by PIP_2, however, will require additional cellular studies focused on PKC activation independent from the inositol breakdown route.

6.5. References

Bastiaens, P.I.H., Hoek, A. van, Benen, J.A.E., Brochon, J.C., Visser, A.J.W.G. (1992) *Biophys. J.* 63, 839-853.

Bastiaens, P.I.H, Pap, E.H.W., Borst, J.W., van Hoek, A., Kulinski, T., Rigler, R.Visser, A.J.W.G. (1993) *Biophys. Chem.* 48 183-191.

Bazzi, M.D. & Nelsestuen, G.L. (1987) *Biochemistry* 26, 115-122.

Bazzi, M.D. & Nelsestuen, G.L. (1988a) *Biochemistry.* 27, 7598-7593.

Bazzi, M.D. & Nelsestuen, G.L. (1988b) *Biochem. Biophys. Res Commun.* 152, 336-343.

Bazzi, M.D. & Nelsestuen, G.L. (1989) *Biochemistry.* 28, 3577-3585.

Bazzi, M.D. & Nelsestuen, G.L. (1991) *Biochemistry* 30, 971-976.

Beechem, J.M., Gratton, E. Ameloot, M., Knutson, J.R. & Brand, L. (1991) in Topics in Fluorescence spectroscopy (Lakowicz, J.R. Eds).

Brochon, J.C., Mérola, F. & Livesey, A.K. (1992) in "Synchrotron Radiation and Dynamic Phenomena" (American Institute of Physics, Ed.) p 435, New York.

Brockerhoff, H. (1986) *FEBS Lett.* 201, 1-4.

Brumfeld, V. & Lester, D.S. (1990) *Arch. Biochem. Biophys.* 227, 318-323.

Chauhan, A., Chauhan V.P.S., Deshmukh D.S. & Brockerhoff H. (1989) *Biochemistry* 28, 4952-4956.

Chauhan, V.P.S. & Brockerhoff H. (1988) *Biochem. Biophys. Res. Commun.* 155, 18-23.

Comfurius, P., Bevers E.M. & Zwaal F.A. (1990) *J. Lipid Res.* 31, 1719-1721.

Das, S. & Rand, R.P. (1986) *Biochemistry* 25, 2882-2889.

De Boeck, H. & Zidovetzki, R. (1989) *Biochemistry* 28, 7439-7449.

Gadella, T.W.J., Moritz, A., Westerman, J. & Wirtz, K.W.A. (1990) *Biochemistry* 29, 3389-3395.

Ganong, B.R., Loomis, C.R., Hannun, Y.A. & Bell, R.M. (1986) *Proc. Natl. Acad. Sci. U.S.A* 83, 1184-1188.

Gentin, M., Vincent, M., Brochon, J.C., Livesey, A.K., Cittanova, N., Gallay, J. (1990) *Biochemistry* 29, 10405-10412.

Hannun, YA., Loomis C.R. & Bell R.M. (1985) *J. Biol. Chem.* 260, 10039-10043.

Hendrickson, H.E. (1969) *Ann. New York Acad. Sci.* 165, 668-676.

Huang, K.P., Nakabayashi, H. & Huang, F.L. (1986) *Proc. Natl. Acad. Sci. U.S.A.* 83, 8535-8539.

Huang F.L. and Huang K.P. (1991) *J. Biol. Chem.* 266, 8727-8733.

Hubbard, S.R., Bishop, W.R., Kirschmeier, P., George, S.J., Cramer, S.P., Hendrickson, W.A. (1991) *Science* 254, 1776-1779.

Kerr, D.E., Kissinger, L.F., Gentry, L.E., Purchio, A.F. & Shoyab, M. (1987) *Biochem. Biophys. Res. Commun.* 148, 776-782.

Kikkawa, U. & Nishizuka, Y. (1986) *Annu. Rev. Cell Biol.* 2, 149-152.

König, B., Dinitto, P.A. & Blumberg, P.M. (1985) *J. Cell Biochem.* 27, 165-175.

Lee, M.H. & Bell R.M. (1991) *Biochemistry* 30, 1041-1049.

Livesey, A.K. & Brochon, J.C. (1987), *Biophys. J* 52, 693-706.

Myher, J.J. and Kuksis (1984), *J. Biochem. Cell Biol.* 62, 352-356.

Nishizuka, Y. (1986) *Science* 233, 305-312.

Nishizuka, Y. (1992) *Science* 258, 607-614.

O'Brain, C.A., Arthur, W.L. & Weinstein, I.B. (1987) *FEBS Lett.* 214, 339-342.

Ono, Y., Fujii, T., Igarashi, K., Kuno, T., Tanaka, C., Kikkawa, U., Nishizuka, Y. (1989) *Proc. Natl. Acad. Sci. U.S.A.* 86, 4868-4871.

Parker, P.J., Coussens, L., Totty, N., Rhee, L., Young, S., Chen, E., Stabel, S., Waterfield, M.D., Ullrich, A. (1986) *Science* 233, 853-859.

Rodriguesz-Paris, J.M., Shoji, M., Yeola, S., Liotta, D., Vogler, W.R. & Kuo, J.F. (1989) *Biochem. Biophys. Res. Commun.* 159, 495-500.

Rooney, T.A., Renard, D.C., Sass, E.J. & Thomas, A.P. (1991) *J. Biol. Chem.* 266, 12272-12282.

Rousser, G., Fleischer, S. & Yamamoto A. (1970) *Lipids 5*, 494-496.

Sekiguchi, K., Tsukuda, M., Ase, K., Kikkawa, U. & Nishizuka, Y. (1988) *J. Biochem.* 103, 759-765.

Snoek, G.T., Feijen, A., Hage, W.J., Rotterdam, W. & de Laat, S.W. (1988) *Biochem. J* 255, 629-637.

Somerharju P.J. & Wirtz K.W.A. (1982), *Chem. Phys. Lipids* 30, 81-91.

Somerharju, P. J., Virtanen, J. A., Eklund, K. K., Viano, P., & Kinnunen, P. K. J. (1985) *Biochemistry* 24, 2773-2781.

Vos, K., Van Hoek, A. & Visser, A.J.W.G. (1987) *Eur. J. of Biochem.* 165, 55-63.

Van Hoek, A. & Visser, A.J.W.G. (1990) *Appl. Optics* 29, 2661-2663.

Van Hoek, A. & Visser, A.J.W.G. (1985) *Anal. Instrum.* 14, 359-378.

Zidovetzki, R. & Lester, D.S. (1992) *Biochim. Biophys. Acta* 1134, 261-272.

Chapter 7

Band 3 - phosphoinositide interactions revealed by fluorescence spectroscopy

Abstract

The interaction of various phosphoinositides with human erythrocyte Band 3 protein was monitored by steady-state and time-resolved detection of resonance energy transfer. For this purpose, phosphatidylinositol-4,5-biphosphate (PIP$_2$), phosphatidylinositol-4-phosphate (PIP), phosphatidylinositol (PI) and phosphatidylcholine (PC) labelled with a pyrenyl-decanoyl moiety at the sn-2 position were used as acceptors for energy transfer from excited tryptophan residues in Band 3. The quenching efficiency of the tryptophan fluorescence was determined in steady state fluorescence experiments as a function of pyrene lipid concentration in mixed micelles consisting of polyoxyethylene-9-laurylether and various mole fractions of pyrene lipid. The efficiency of quenching of the tryptophan fluorescence decreased pyrPIP$_2$, pyrPIP, pyrPI to pyrPC, respectively, indicating different affinities of Band 3 for these lipids. In order to obtain more specific information about the spatial distribution of the different lipids the tryptophanyl fluorescence decays were registrated in the presence of various concentrations of pyrene lipids. In the analysis of these fluorescence decays, energy transfer was assumed to occur to pyrene lipids located either in the micellar shell solvating Band 3 or interacting with the hydrophobic regions of the protein. The average rate of energy transfer to each of these pyrene populations was obtained by applying of the Förster relation of energy transfer to distance probability functions of tryptophan - pyrene couples. These functions describe the probability of finding a pyrene acceptor at a certain distance of a tryptophan donor and were derived from simulations that calculated the distance between randomly positioned tryptophan donors in a cylindrical protein volume and pyrene acceptors randomly positioned within the protein volume (transhelical regions) or in a surrounding micellar cylinder (detergent shell). The fraction of pyrene lipids located in the hydrophobic transhelice region of Band 3 was determined for each pyrene lipid independently, while the radius of the surrounding detergent shell was determined globally from simultaneous analysis of multiple quenched decays obtained with all four pyrene lipids.

7.1. Introduction

Band 3 is a multifunctional intrinsic membrane glycoprotein abundantly present in membranes of erythrocytes. The membrane domain of Band 3 is thought to span the membrane with up to 14 transmembrane segments (Dolder et al., 1993) which are entirely α-helical in conformation (Oikawa et al., 1985). Its primary function in vivo is the exchange of anions such as Cl$^-$ and HCO$_3^-$ across the erythrocyte membrane. This transport is important for the removal of CO$_2$ from the cell interior (Passow, 1986; Jennings, 1989). Other functions of Band 3 are water transport (Yoon et al., 1984; Chasan et al. 1984)

and mediation of structural stability of the erythrocyte by linking its cytoskeleton and plasmamembrane (Low, 1986; Shen et al, 1986). Furthermore, Band 3 is associated with cytoplasmic proteins like haemoglobin (Shaklai et al., 1977) and various intracellular enzymes (Strapazon & Steck, 1977; Higashi et al., 1979; Kliman & Steck, 1980). Band 3 only retains its functional conformation when it interacts with lipids or other membrane constituents. The optimal chemical composition and physical state of the lipid environment of Band 3 remains to be established, however. Evidence for association of phosphoinositide lipids with Band 3 has been obtained from copurification studies (Hanicak et al., 1994). Furthermore, Hagelberg and Allan (1990) reported microvesicle release from echynocytic human erythrocytes resulting in segregation of Band 3 and glycophorin into microvesicles. Both observations indicate preferential interactions between Band 3 and phosphoinositides. These phosphoinositides are known to interact with several membrane proteins. For example, the EGF receptor, erythrocyte Band 4.1 and Ca^{2+}-ATPase are preferentially surrounded (Den Hartigh et al., 1993; Gascard et al., 1993; Hagelberg & Allan, 1990; Verbist et al., 1991) and considerably affected (Den Hartigh et al., 1993; Missiaen et al., 1989) by phosphoinositides. In addition, it has been shown that PIP_2 can function as lipid activator of protein kinase C in the presence of phosphatidylserine (PS) (Brockerhoff, 1986; Lee & Bell, 1991; Pap et al., 1993).

In the present study the interaction of Band 3 with pyrene labelled phosphoinositides was characterised by steady state and time-resolved detection of energy transfer from excited tryptophan residues of Band 3 to pyrene labelled lipids. To this goal, purified Band 3 protein was reconstituted in micelles containing pyrene labelled phosphatidylcholine (PC), phos-phatidylinositol (PI), phosphatidylinositol-4-phosphate (PIP) or phosphatidyl-inositol-4,5-biphosphate (PIP_2). Analysis of the tryptophan fluorescence decays recovered rough indices for the spatial distribution of the pyrene lipids with respect to the protein. For these experiments directed to the recovery of the lipid specificity of Band 3, micelles appeared particular advantageous since they are easy to manipulate and allow accurate lipid titration (Hannun et al., 1985). In addition, the biochemical and biophysical properties of Band 3 in detergent solutions have been characterised extensively and various studies have shown that Band 3 maintains its native structure in detergents (Reithmeier et al., 1989) or when it is reconstituted in liposomes (Passow & Bamberg, 1993).

7.2. Experimental Procedures

7.2.1. Materials

sn-2-(Pyrenyldecanoyl)-PC (pyrPC) was synthesised from egg yolk PC (Sigma) as described by Somerharju et al., (1985). sn-2-(Pyrenyldecanoyl)-PI (pyrPI) was synthesised from yeast PI as described by Somerharju & Wirtz (1982) and Somerharju et al., (1985). Purification of pyrPC and pyrPI to homogeneity was performed with HPLC on a silicic acid column. Elution was performed with an increasing methanol gradient in chloroform (0-40%). sn-2-(Pyrenyldecanoyl)-PIP (pyrPIP) and sn-2-(Pyrenyldecanoyl)-PIP_2 (pyrPIP$_2$) were synthesised

enzymatically from sn-2-(Pyrenyldecanoyl)-PI (pyrPI) using partially purified PI and PIP-kinase preparations from bovine brain as described by Gadella et al., (1990). Unless otherwise stated, experiments were performed using buffer containing 0.5 mM EDTA, 10 mM Tris HCl, 50 mM NaCl and 0.01% (w/w) polyoxyethylene-9-laurylether (thesit, Sigma) at pH 7.5.

7.2.2. Methods

Isolation of Band 3 protein and loading of micelles with pyrene lipids

Band 3 protein was isolated from haemoglobin-free human erythrocyte ghosts obtained from fresh erythrocyte concentrate (Blutspendezentrale Hessen, Frankfurt/Main), according to the method of Dodge et al., (1963), modified by Schubert et al., (1972). The isolation of Band 3 protein was carried out by adapting a method described by Yu and Steck (1975) and Pappert and Schubert (1983) for spectroscopical investigations. A pre-extraction of membranes in 1% (w/w) Brij 58, where almost all glycophorins and proteolytical activity are removed is followed by solubilization of Band 3 with 1% (w/w) thesit. After centrifugation the supernatant contains mainly Band 3 protein and membrane lipids. Further purification and lipid removal is obtained by ion exchange chromatography (DEAE-cellulose) resulting in lipid-free protein (monitored by the Bartlett assay (1959). To prevent protein aggregation, desalting is achieved by gel-filtration (Sephadex G-25, with buffer containing 0.1% thesit). Final protein concentration was set to 150 nM, final thesit concentration to 200 μM. SDS-PAGE (using the Laemmli system (1990)) revealed a protein purity > 95%. Micelles were loaded with pyrene-lipids by adding small aliquots (max. 5% of sample volume) of lipid stock solution in ethanol/DMSO 75:25 (v/v). The pyrene-lipid concentration in the stock solution was measured by absorption spectroscopy (ε=39700 M^{-1}cm^{-1} in ethanol/DMSO at 345 nm). This was followed by incubation overnight at 4°C prior to fluorescence measurements.

Steady-state fluorescence measurements

Tryptophan emission intensities were monitored on a DMX-1000 spectrofluorometer (SLM Aminco, Urbana, IL). The measurements were corrected for the background emission and the spectral output of monochromator-photomultiplier combination. The excitation wavelength was 295 nm and the tryptophan emission was recorded at 335 nm. The cuvette holder was thermostated at 4°C and the chamber filled with dry nitrogen to avoid condensation.

Time-resolved fluorescence measurements

Time-resolved fluorescence measurements were performed on a time-correlated single photon counting setup as described elsewhere (Pap et al., 1993). The repetition rate of excitation pulses was 951 kHz, the wavelength 295 nm, the duration about 4 ps FWHM and the pulse energy in the tens of pJ range. Fluorescence was selected using a 3 mm WG 335 cut-off filter (Schott, Mainz), an interference filter at 348.8 nm (Schott, Bandwidth 4.8 nm FWHM) and a sheet type polariser (Polaroid type HNP'B) that could be rotated under

computer control parallel and perpendicular with respect to the direction of excitation polarisation. All measurements consisted of a number of registration sequences of 10 s parallel and 10 s perpendicular polarised emission. After each sample the background in the absence of Band 3 was measured, at one fifth of the time of sample acquisition. Para-terphenyl (Eastman Kodak Rochester, NY) dissolved in ethanol served as reference compound ($<\tau>=1.06$ ns (Vos et al., 1987)) to yield the dynamic instrumental response function of the set-up (Van Hoek & Visser, 1985). The sample was thermostated at 4°C using a cold gas flow from a liquid nitrogen container and an Oxford Instruments model ITC4 temperature controller.

Global determination of the fraction associated pyrene lipid and approximation of the pyrene-tryptophan distance distributions

In general the decay of fluorescence f(t) of excited chromophores is governed by the rate constant for fluorescence (k_f) and for nonradiative transitions (k_{nr}).

$$f(t) = f(0)e^{-\left(k_f + k_{nr}\right)t} \tag{1}$$

The lifetime of the excited state, $\tau = \left(k_f + k_{nr}\right)^{-1}$, is usually measured from the decay of fluorescence. Because of environmental heterogeneity, fluorescence of tryptophan residues in proteins often decays with a whole distribution of lifetimes.

$$f(t) = \int_0^\infty \alpha(\tau)\, e^{-t/\tau}\, d\tau \tag{2}$$

This distribution function can be represented by an exponential series of n separate terms and can be recovered by the Maximum Entropy Method (Livesey & Brochon, 1987; Brochon et al., 1992). Resonance energy transfer (RET) to acceptor molecules results in a faster decay of the excited state of the donor (Förster, 1948; Stryer, 1978). The general description that relates the rate of energy transfer (k_t) of a donor-acceptor pair to their relative orientation Ω and separation r is (Förster, 1948):

$$k_t(\Omega,r) = \left(\frac{R_0}{r}\right)^6 \tau^{-1} \tag{3}$$

where R_0 corresponds to the characteristic Förster distance for a donor-acceptor pair at which the efficiency of RET is 0.5. This parameter depends on the difference in donor and acceptor energy (spectral overlap) and on the orientation factor κ^2 which is related to the relative orientation of the donor and acceptor transition dipoles (Ω) and on the refractive index (= 1.4 for proteins) (Steinberg, 1971; Dale & Eisinger, 1974). The orientation factor κ^2 corresponds to 2/3 if the tryptophan and pyrene moieties rotate isotropically and rapidly relative to their fluorescent lifetimes. Although this assumption is

not a realistic one, it is unlikely to introduce serious errors in the analysis. From the spectral overlap of a pyrene-tryptophan couple one can calculate that R_o corresponds to approximately 2.7 nm (assuming $\kappa^2 = 2/3$). By measuring the fluorescence decays of donors at various densities of acceptor, distributions of k_t can be obtained which are related to the spatial distribution of acceptor probes with respect to donor moieties. Several examples of these RET studies of proteins-lipid systems are given in literature (Bastiaens et al., 1990; Fung & Stryer, 1978).

When micelles are used to elucidate the lipid specificity of membrane proteins one has to consider pyrene lipids exchanging between three populations. These populations of pyrene lipids will differently contribute to the quenching of the tryptophan fluorescence when their lipid exchange is slow compared to the tryptophan fluorescence. The first population is composed of pyrene lipids that interact with peptide helices of Band 3 (Figure 1). These bound pyrene lipids are located close to or within the Band 3 protein and are therefore effective quenchers of the tryptophan fluorescence. The second population is composed of non-interacting pyrene lipids in the surrounding micellar shell of Band 3 (Figure 1). The third population is composed of pyrene lipids in micelles that do not contain Band 3 and consequently do not contribute to the quenching of the tryptophan fluorescence. Preferred interactions between Band 3 and acceptor lipids will lead to different spatial distributions of the pyrene lipids within the micelles containing Band 3 and will result in an enrichment of pyrene lipids in micelles containing Band 3 at the expense of those without Band 3. Generally, the probability (P_i) of finding i probe lipids in a certain lipid population is binomially distributed:

$$P_i = \frac{S!}{i! \ (S-i)!} \ x^i \ (1-x)^{S-i} \qquad\qquad (4)$$

where S corresponds to the maximal number of probe lipids that can be accommodated within the lipid probe population and x to the fractional occupancy of the population (the average number of probe molecules present divided by S). The maximum number of pyrene lipids that can interact with Band 3 (S_{B3}) is, in principle, unknown. It will be shown that the results of the analysis are invariant for a broad range of S_{B3} values. The number of pyrene lipids that can be accommodated within the micelle surrounding Band 3 can be derived from the micellar geometry and the area occupied per lipid (≈ 70 nm^2 (Demel et al., 1967)). From simple mass balance relations one can derive that the fractional occupancy of the pyrene lipid population associated with the Band 3 protein (x_b) and within the micellar shell surrounding Band 3 (x_f) correspond to:

$$x_b = \beta \ \frac{[P]}{[B_3] \ S_{B3}} \qquad \text{and} \qquad x_f = (1-\beta) \ \frac{[P]}{[T] - [B_3] \ S_{B3}} \qquad (5)$$

where [P], [B$_3$] and [T] correspond to the total concentration of pyrene, Band 3 and thesit, respectively. β corresponds to the fraction of pyrene molecules bound to Band 3. The rates of energy transfer will depend on the probability of

finding an acceptor at distance r from a tryptophan and thus on β and the geometry of the Band 3-micelle system.

In the analysis of the quenched tryptophan fluorescence decays we consider RET from tryptophan donors in a cylindrical shaped protein volume to pyrene acceptors located within the protein (interacting with the protein helices) or within a cylindrical shell of detergent molecules (Figure 1). Although it has been determined that the majority of tryptophan donors are located within the transmembrane domain of Band 3 (P.G. Wood, unpublished observations) their precise locations and those of the pyrene acceptors are unknown. Therefore, the analysis presented here should be considered as an approximate one. Probability functions of the tryptophan to pyrene distance were generated by simulating a large number of donors and acceptors with randomly chosen coordinates from which the distance of each donor-acceptor couple was determined. The coordinates of tryptophan residues and pyrene lipids interacting with the protein were randomly generated within a cylindrical protein volume with radius R_p = 3.3 nm and height H_p = 8 nm and those of non-interacting pyrene lipids were generated within a cylindrical shell with radius R_m (see Figure 1). The dimensions of the transmembrane domain of Band 3 are based on recent results of 2D-crystal analysis (Wang et al., 1993; Dolder et al., 1993). R_m was adjusted in the analyses of the fluorescence decays.
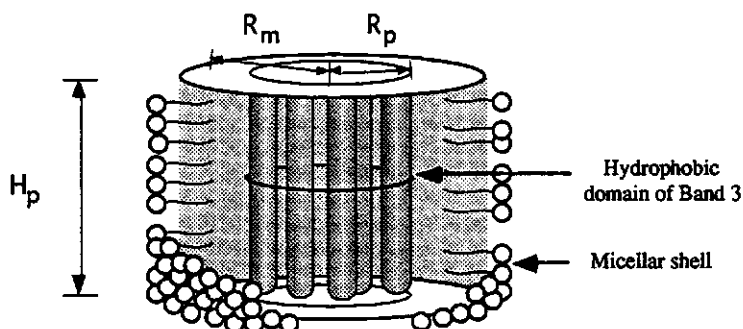
Figure 1. Cylindrical protein shape in cylindrical detergent shell as a simplified model for the hydrophobic domain of Band 3 surrounded by thesit molecules. In the analysis of the quenched fluorescence decays of Band 3 tryptophans, it is assumed that two populations of pyrene lipids contribute to the quenching of the tryptophan fluorescence: First pyrene lipids interacting with the transmembrane helices of Band 3 and second those which are located within the micellar shell.

The shape of the distance probability function ($P(r)$) obtained from simulations depended on the fraction of pyrene lipids associated with Band 3 (β) and on R_m. According to this model the decay of tryptophan fluorescence in presence of pyrene lipids can be described as:

$$f(t) = \sum_{q_b=0}^{q_{max}} \sum_{q_f=0}^{q_{max}} \sum_{i=0}^{i_{max}} \alpha_i \, P_{qb} \, P_{qf} \, exp\left(-t \, \tau_i^{-1}(1 + \sum_{r_{in}=r_{min}}^{r_{max}} q_b \, P(r_{in})\left(\frac{R_o}{r_{in}}\right)^6 + \sum_{r_{out}=r_{min}}^{r_{max}} q_f P(r_{out})\left(\frac{R_o}{r_{out}}\right)^6)\right) \quad (6)$$

Where $P(r_{in})$ and $P(r_{out})$ correspond to the distance probability functions of tryptophan donors within Band 3 with respect to interacting pyrene lipids and pyrene lipids in the micellar shell, respectively. In the analysis a minimum tryptophan and pyrene separation (r_{min}) was assumed 1.3 nm. This assumption corresponds roughly to the centre to centre separation of aligned tryptophan and pyrene moieties and excludes tryptophans and pyrene separated at infinitely small distance from the calculation of RET. The product $P_{qb} P_{qf}$ corresponds to the probability of finding q_b pyrene lipids bound to Band 3 and q_f pyrene lipids in the surrounding micelle (eqs. 4 and 5). Application of this model to multiple experimental decays of tryptophan fluorescence of Band 3 revealed β for each type of pyrene lipid individually and R_m for the micellar radius.

7.3. Results

### 7.3.1. Steady state determined energy transfer efficiency

In order to evaluate the specificity of Band 3 for phosphoinositides the energy transfer efficiency was determined at several concentrations of pyrPC, pyrPI, pyrPIP and pyrPIP$_2$ (Figure 2). Control experiments with unlabelled lipids showed no effect on the tryptophan fluorescence intensity. Within the concentration range used, the quenching efficiency appeared to be linearly proportional with the added pyrene lipid. The most efficient energy transfer is obtained with pyrPIP$_2$, followed by pyrPIP, pyrPI and pyrPC. These differences in quenching efficiency indicate different affinities of the various pyrene lipids with respect to Band 3.
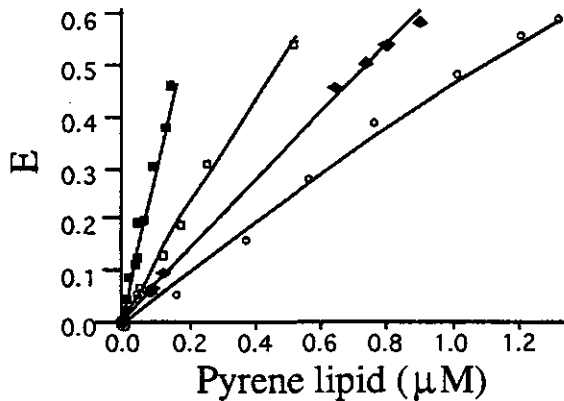
Figure 2. Efficiency of energy transfer (E) from Band 3 tryptophan residues to pyrene-lipids pyrPC(○), pyrPI (◆), pyrPIP (□) and pyrPIP$_2$ (■) versus pyrene-lipid concentration. The efficiency of energy transfer E was calculated from the tryptophan fluorescence in presence and absence of the pyrene lipids, according to Stryer (1978). In this experiment the Band 3 and thesit concentrations were 150 nM and 200 μM, respectively.

7.3.2. *Time-resolved detection of energy transfer*

The MEM-recovered tryptophan fluorescence lifetime distributions of unquenched Band 3 and Band 3 quenched by pyrPIP$_2$ are presented in Figure 3A. As can be expected from a multiple tryptophan protein like Band 3, the decay is complex even in the absence of acceptors. Three major components are present in the lifetime spectrum indicating three major classes of emitters. In the presence of pyrene-lipids the lifetime peaks shift to shorter times, showing that all subclasses are able to interact through dipole-dipole coupling with pyrene lipids. In Figure 3B the first order average lifetime <τ> of Band 3 calculated from the lifetime distributions is plotted versus the mole % of pyrPIP$_2$, pyrPIP, pyrPI and pyrPC in micelles. In agreement with steady-state recovered efficiencies of energy transfer (Figure 2) <τ> is reduced more efficiently by pyrPIP$_2$ than the other lipids. The concentration dependence of <τ> does not show inflection points. The fact that the binding characteristics of phosphoinositides to Band 3 are not affected even when their concentration slightly exceeds that of the protein indicates that the majority of binding locations for PIP$_2$ are still available under these conditions.
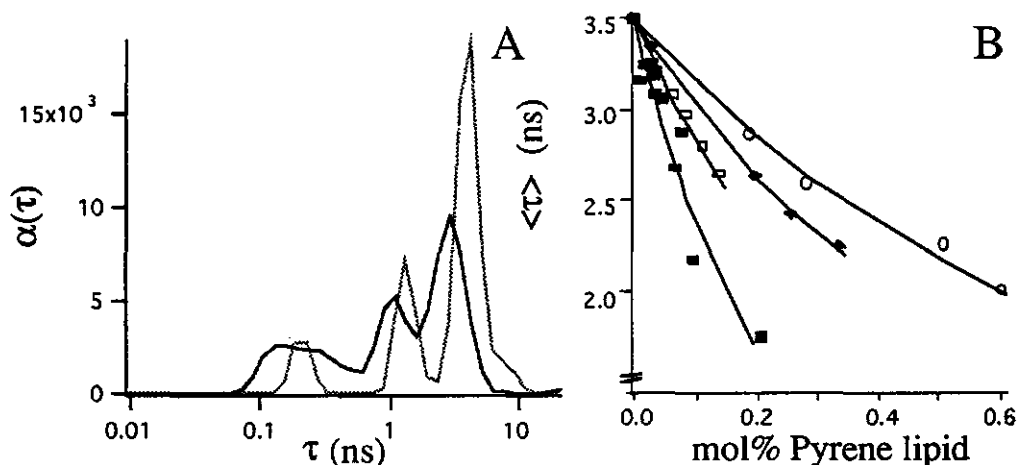

Figure 3A. The lifetime distributions of Band 3 tryptophan fluorescence in absence (----) and presence (—) of 0.2 μM pyrPIP$_2$. **B.** Calculated first order average lifetimes <τ> from fluorescence lifetime distributions of Band 3 tryptophan residues versus the concentration of pyrPC(O), pyrPI (♦), pyrPIP (□) and pyrPIP$_2$ (■) in micelles. In this experiment the Band 3 and thesit concentrations were 150 nM and 200 μM, respectively.

7.3.3. *Relation of quenched decays to the spatial distribution of the pyrene lipid species*

In order to obtain information about the fraction of pyrene lipids interacting with Band 3 (β) and about the spatial distribution of the different pyrene lipid species, the experimental tryptophan fluorescence decays were analysed with the model described in the method section (eq. 5). All fluorescence decay curves (23) obtained from titration of the various pyrene lipids were analysed simultaneously. The adjustable parameters were S_{B3}, R_m and β. Since S_{B3} and

R_m are geometrical properties of the Band 3-micelle system and invariant on either the pyrene lipid or its concentration, these parameters were linked in the analysis of all quenching experiments. β is determined by the affinity of Band 3 for the pyrene lipid and therefore linked over each set of tryptophan fluorescence decays obtained from titration of each individual pyrene lipid. In figure 4A an example is given of a fitted curve through the points of the tryptophanoyl fluorescence decays of Band 3 in presence of 0.2 mole % pyrPIP$_2$ and in absence of pyrene lipid. A global χ^2 of 2.8 was obtained in the analysis. The moderate fit quality may be attributed to invalid assumptions in the model of analysis and to uncertainties in the actual pyrene concentration present in the sample. A very clear trend is, however, observed for the fraction of pyrene lipid associated with Band 3 (β) (see figure 4B). The largest fraction associated with Band 3 is obtained for PIP$_2$ followed by PIP, PI and PC. The optimised value for R_m corresponds to 4.6 nm. The fit quality appeared to be invariant for a wide range of S_{B3} values (1 - 50), indicating that the value of this parameter could not be determined in this analysis.
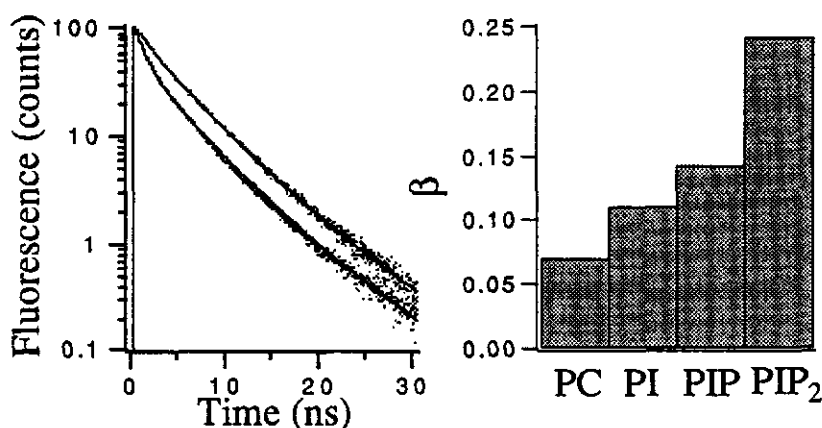
Figure 4A. Experimental decay (dots) and fitted decays (solid lines) of tryptophan fluorescence decay measured in absence of pyrene lipids (upper decay curves) and in the presence of 0.2 mole % pyrPIP$_2$ (lover decay curves). In these experiments the Band 3 and thesit concentrations were 150 nM and 200 μM, respectively. **B.** Histogram of the fraction associated pyrene lipid to Band 3. These β values were obtained from global analysis of the quenched tryptophan fluorescence decays.

In figure 5, the distance probability functions are presented as obtained from simulations with parameter settings used in the analysis (the area of these functions is normalised to unity).
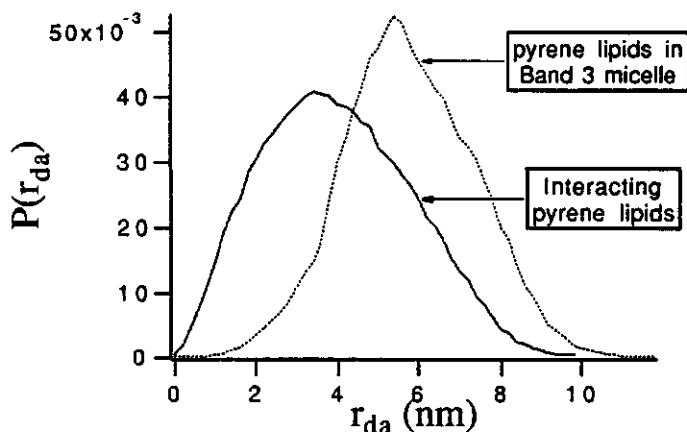
Figure 5. Examples of probability functions of the separation of tryptophan donors and pyrene lipids. These functions describe the probability of finding a pyrene acceptor at a certain distance of a tryptophan donor and were derived from simulations that calculated the distance between randomly positioned tryptophan donors in a cylindrical protein volume and pyrene acceptors random positioned within the protein transhelice region (---) or in a surrounding micellar cylinder with radius 4.6 nm (—).

The distance distribution function of tryptophan residues in the protein cylinder and pyrene lipids in the micellar shell shows a slightly asymmetric profile and a maximum of probability for donor-acceptor distances of 5.5 nm.

7.4. Discussion

This investigation has been focused upon the question whether there is any interaction between Band 3 and the phosphoinositides *in vitro* under non-denaturing conditions. The binding was demonstrated by measuring the quenching of tryptophan fluorescence in Band 3 resulting from radiationless energy transfer to pyrene labelled phosphoinositides in mixed micelles. The quenching efficiency is higher for pyrPIP$_2$ than for pyrPIP > pyrPI > pyrPC. The first order average lifetime $<\tau>$ of Band 3 calculated from the ·lifetime distributions is dependent on the mole % and the species of the pyrene labelled lipid in close agreement with the steady state recovered efficiency of RET. In the analysis, two populations of pyrene lipids were assumed to contribute with different efficiency to the quenching of the tryptophan fluorescence. This two-domain model only moderately fitted the experimental data, which is not suprising since the locations of the tryptophan donors and the geometries of the Band 3 - micellar system are unknown. Despite these uncertainties, the analysis yielded approximate information about the distribution of the pyrene lipids in both populations with respect to the tryptophan donors. From the steady state and time resolved titration experiments it is evident that the affinity of Band 3 for the phosphoinositides decreases from PIP$_2$ > PIP > PI.

The exact cause and possible effects of the interaction between Band 3 and phosphoinositides remains nevertheless unspecified. For the phosphoinositides and PC, we find a positive correlation between their net charges at physiological pH (PIP_2 -4.2; PIP -2.9; PI -1; PC 0) and their potency to act as acceptor of intrinsic Band 3 fluorescence (Abramson et al., 1964; Van Paridon et al., 1986). It is therefore apparent to consider simple electrostatics between the negatively charged lipids and positively charged residues at the protein surface as major driving force for their association to Band 3. Whether this interaction is relevant for any of the biological functions of Band 3 remains to be elucidated.

7.5. References

Abramson, M. B., Katzman, R., Wilson, C. E., & Gregor, H. P. (1964) *J. Biol. Chem.* 239, 4066-4072.

Bartlett, G. R. (1959) *J. Biol. Chem.* 234, 466-471.

Bastiaens, P.I.H., DeBeus, A., Lacker, M., Somerharju, P., Vauhkonen, M., & Eisinger, J.(1990) *Biophys. J.* 58, 665-675.

Bastiaens, P. I. H., Pap, E. H. W., Borst, J. W., Van Hoek, A., Kulinski, T., Rigler, R., & Visser, A. J. W. G. (1993) *Biophys. Chem.* 48, 183-191

Brochon, J. C., Mérola, F., & Livesey, A. K. (1992) in *Synchrotron Radiation and Dynamic Phenomena*, p 435, American Institute of Physics, New York.

Brockerhoff, H. (1986) *FEBS Lett.* 201, 1-4.

Chasan, B., Lukakovic, M. F., Toon, M. R., & Solomon, A. K. (1984) *Biochim. Biophys. Acta* 778, 185-190.

Dale, R.E. & Eisinger, J. (1974) *Biopolymers* 13, 1573-1605.

Dale, R.E., Eisinger, J., & Blumberg, W. E. (1979) *Biophys. J. 26*, 161-194.

Demel, R.A., Van Deenen L.L.M., & Pethica B.A. (1967) *Biochim. Biophys. Acta.* 135, 11-19.

Den Hartigh, J.C., Henegouwen, P.M.P.V., Boonstra, J., & Verkleij, A.J. (1993) *Biochim. Biophys. Acta.* 1148, 249-262.

Dodge, J. T., Mitchell, C., & Hanahan, D. J. (1963) *Arch. Biochem. Biophys.* 120, 119-132.

Dolder, M., Walz, T., Hefti, A., & Engel, A. (1993) *J. Mol. Biol. 231*, 119-132.

Förster, T. (1948) *Ann. Physik.* 2, 55-75.

Gadella, T. W. J., Moritz, J. A., Westerman, J., & Wirtz, K. W. A. (1990) *Biochemistry* 29, 3389-3395.

Gascard, P., Pawelczyk, T., Lowenstein, J.M. & Cohen, C.M. (1993) *Eur. J. Biochem.* 211, 671-681.

Hagelberg, C. & Allan, D. (1990) *Biochem J.* 271, 831-834.

Fung, B.K.K. & Stryer, L. (1978) *Biochemistry* 17, 5241-5248.

Hanicak, A, Maretzi, D., Reimann, B., Pap, E., Visser, A.J.W.G., Wirtz, K.W.A. & Schubert, D. (1994) *FEBS Lett.* Submitted.

Hannun, Y. A., Loomis, C. R., & Bell, R. M. (1985) *J. Biol. Chem. 260*, 10039-10043.

Higashi, T., Richards, C. S., & Uyeda K. (1979) *J. Biol. Chem. 254*, 9542-9550.

Jaynes, E.T. (1968) *Trans. Biomed.* 4, 227-230.

Jennings, M.L. (1989) *Annu. Rev. Biophys. Chem.* 18, 397-430.

Kliman, H. J., & Steck, T. L. (1980) *J. Biol. Chem.* 255, 6314-6321.

Laemmli, U. K. (1970) *Nature (London)* 227, 680-685.

Lee, M. H., & Bell, R. M. (1991) *Biochemistry* 30, 1041-1049.

Livesey, A. K., & Brochon, J. C. (1987) *Biophys. Journal* 52, 693-706.

Low, P. S. (1986) *Biochim. Biophys. Acta* 864, 145-167.

Missiaen, L., Raeymaekers, R., Wuytack, F., Vrolix, M., Desmet, H., & Casteels, R. (1989) *Biochem. J.* 263, 687-694.

Oikawa, K.Lieberman, D.M. and Reithmeier, R.A.F. (1985) *Biochemistry* 24, 2843-2848.

Pap, E. H. W., Bastiaens, P. I. H., Borst, J. W., van den Berg, P. A. W., van Hoek, A., Snoek, G. T., Wirtz, K. W. A. & Visser, A. J. W. G. (1993) *Biochemistry* 32, 13310-13377.

Pappert, G., & Schubert, D. (1983) *Biochim. Biophys. Acta* 730, 32-40.

Passow, H. (1986) *Rev. Physiol. Biochem. Pharmacol.*, 103, 61-203.

Passow, H., & Bamberg, E. (1992) in *The Band 3 Proteins Anion Transporters, Binding Proteins and Senescent Antigens,* Progress in Cellular Research 2, Elsevier Amsterdam

Reithmeier, R.A.F., Lieberman, D.M. Casey, J.R., Pimplikar, S.W., Werner, P.K., See, H. & Pirraglia, C.A. (1989) *Ann. NY. Acad. Sci.*, 574, 75-83.

Rousser, G., Fleischer, S. & Yamamoto A. (1970) *Lipids* 5, 494-496.

Scheuring, U., Kollewe, K., Haase, W., & Schubert, D. (1986) *J. Membr. Biol.* 90, 123-135.

Schubert, D., Poensgen J., & Werner, G. (1972) *Hoppe-Seyler's Z. Physiol. Chem.* 335, 1034-1042.

Schubert, D., & Domnig, B. (1978) *Hoppe-Seyler's Z. Physiol. Chem.* 359, 507-511.

Shaklai, N., Ygerabide, J., & Ranney, H. M. (1977) *Biochemistry* 16, 5593-5597.

Shen, B. W., Josephs R., & Steck, T. L. (1986) *The Journal of Cell Biology* 102, 997-1006.

Somerharju, P. J., & Wirtz, K. W. A. (1982) *Chem. Phys. Lipids* 30, 82-91.

Somerharju, P. J., Virtanen, J. A., Eklund, K. K., Varno, P., & Kinnunen, P. K. J. (1985) *Biochemistry* 24, 2773-2781.

Steinberg, I.Z. (1971) Ann. Rev. Biochem. 40, 83-114.

Strapazon, E., & Steck, T. L. (1977) *Biochemistry* 16, 2966-2971.

Stryer, L. (1978) *Ann. Rev. Biochem.* 47, 819-846.

Van Hoek, A., & Visser, A. J. W. G. (1985) *Analytical Instrumentation* 14, 359-378.

Van Hoek, A., & Visser, A. J. W. G. (1990) *Appl. Optics* 29, 2661-2663.

Van Paridon, P. A., De Kruijff, B., Ouwerkerk, R., & Wirtz, K. W. A. (1986) *Biochim. Biophys. Acta* 877, 216-219.

Verbist, J., Gadella, T. W. J., Raeymaekers, L., Wuytack, F., Wirtz, K. W. A., & Casteels, R. (1991) *Biochim. Biophys. Acta* 1063, 1-6.

Vos, K., Van Hoek, A., & Visser, A. J. W. G. (1987) *Eur. J. Biochem.* 165, 55-63.

Wang, D. N., Kühlbrandt, W., Sarabia, V. E., & Reithmeier, R.A.F. (1993) *EMBO J.* 12, 2233-2239.

Yoon, S. C., Toon, M. R., & Solomon, A. K. (1984) *Biochim. Biophys. Acta* 778, 385-389.

Yu, J., & Steck, T. L. (1975) *J. Biol. Chem.* 250, 9170-9184.

Chapter 8

Quantitative analysis of lipid-lipid and lipid-protein interactions
in membranes by use of pyrene labelled phosphoinositides

Abstract

The lateral and rotational dynamics of pyrene-decanoyl labelled analogues
of phosphatidylinositol-4, 5-biphosphate (PIP$_2$), phosphatidylinositol-4-
phosphate (PIP), phosphatidylinositol (PI) and phosphatidylcholine (PC) were
determined in dioleoylphosphatidylcholine (DOPC) membranes in the absence
and presence of Band 3 protein. In these systems the collision frequency of
pyrene labelled lipids was studied by monitoring the monomeric pyrene
fluorescence yields as a function of their mole fractions in the membranes.
From this dependence the lateral diffusion coefficient and a repulsion factor
between two phosphoinositides could be estimated by applying an extended
form of the Milling Crowd model (Eisinger et al., 1986). The repulsion appeared
to be highly dependent on the amount of negative charge of the lipid
headgroups. From experiments with DOPC vesicles containing Band 3 protein,
the fraction of lipid molecules bound to this protein and the minimum
number of sites possessing affinity for PIP could be determined approximately
by applying a simple two domain model. In this model the effect of lipid-
protein interactions on the dynamical properties of pyrene labelled lipids is
described in terms of lipids interacting directly with the protein surface
separate from lipids in the bulk bilayer. Intramolecular excimer formation of
dipyrene labelled PC, PI and PIP yielded information about the acyl chain
dynamics of lipids surrounding the protein and of lipids in the bulk
membrane. Time-resolved measurements of the pyrene fluorescence anisotropy
decay showed that in membranes of resealed erythrocyte ghost cells the
rotational freedom of pyrene labelled PIP$_2$ is smaller than that of pyrene
labelled PC. In contrast, no significant differences could be detected when these
pyrene lipids were dispersed in DOPC membranes. It is proposed that the non-
random distribution of the phosphoinositides induced by lipid-lipid repulsion
and by protein-lipid attraction affects the phospholipase C catalysed
hydrolysis of the phosphoinositides into second messenger molecules.

8.1 Introduction

Phosphatidylinositol-4, 5-biphosphate (PIP$_2$) and its precursors PIP and PI are
intriguing lipids because of their vital importance in the regulation of cellular
processes. In addition, their highly negative charge (Van Paridon et al., 1986)
results in strong lipid-lipid and lipid-protein interaction forces. There are three
major *myo*-inositol containing lipids, phosphatidylinositol (PI), phos-
phatidylinositol-4-phosphate (PIP) and phosphatidylinositol-4,5-biphosphate
(PIP$_2$) which together comprise only 2-8 % of the total phospholipids present in
mammalian cells (Majerus, 1992).

The phosphoinositides are preferentially located on the cytosolic surface of the plasma membrane (Schmell & Lennarz, 1974; Sekar & Hokin, 1986; Gascard et al., 1991). Extensive studies on phosphoinositide metabolism showed that inositide lipids play a key-role in the signal transduction cascade (Berridge, 1993; Michell, 1992; Sekar & Hokin, 1986). In response to an extracellular signal for instance, receptor stimulation or calcium channel opening, the turnover of the inositides increases dramatically and phosphodiesteric cleavage of phophatidylinositols by phospholipase C yields the intracellular second messengers diacylglycerol (DG) and various water-soluble inositol phosphates. These messengers trigger a wide range of cellular responses. In contrast to their role in cellular signalling, relatively little is known about the physical behaviour of the phosphoinositides in membranes and their interaction with membrane proteins. Evidence has been obtained that there are distinct pools of phosphoinositides within cells which can be divided on a functional basis into pools that can be hydrolysed for signal tranduction purpose and pools that cannot (King et al., 1987; Koréh & Monaco, 1986; Müller et al., 1986; Cubitt et al., 1990; Monaco & Adelson, 1991; Gascard et al., 1989, 1993a). It has, for example, been observed that only 50-60 % of the total phosphoinositides in erythrocyte membranes is accessible for PLC catalysed hydrolysis (Gascard et al., 1989). Discrete regions or domains of phosphoinositides that are maintained by integral membrane proteins may form a basis for this metabolic heterogeneity of phosphoinositides (Gascard et al., 1993a) although direct evidence for such domains is difficult to establish. Besides a second messenger precursor role, other biological functions for PIP_2 have been discussed. So it has been reported that phosphoinositides interact with membrane proteins like the Ca^{2+}-ATPase (Verbist et al., 1991), erythrocyte Band 4.1 (Gascard et al., 1993b; Hagelberg & Allan, 1990), Band 3 protein (Chapter 7) and cytosolic proteins like profilin (Lassing & Lindberg, 1985; Janmey et al., 1987), gelsolin (Janmey & Stossel, 1989; Yin et al., 1988) and protein kinase C (Huang & Huang, 1991; Pap et al., 1993). In addition, these lipids regulate the functioning of the Ca^{2+}-ATPase (Missiaen et al., 1989), EGF receptor (Den Hartigh et al., 1993), protein kinase C (Huang & Huang, 1991; Pap et al., 1993; O'Brain et al., 1987; Lee & Bell, 1991; Chauhan & Brockerhoff, 1988) and the shape of the erythrocyte (Ferrel & Hyestis, 1984).

The aim of this study is to characterise the physical behaviour of phosphoinositides in membranes and their interaction with proteins. To achieve this, phosphoinositides carrying a pyrene decanoyl moiety as fluorescent reporter group were incorporated in vesicles and biological membranes and the lateral and rotational dynamical characteristics of these probe lipids were determined. The excimer experiments provide information on intermolecular electrostatic repulsion of the phosphoinositides and on the effect of protein on the intermolecular collision frequency. Experiments with dipyrene labelled analogues of PC, PI and PIP provided information on the acyl chain dynamics at close proximity of the protein and in bulk lipid and support time-resolved anisotropy experiments of the pyrene labelled PC and PIP_2 in resealed ghost cells and in lipid vesicles.

8.2 Experimental procedures

8.2.1. Materials

1-Palmitoyl-2-(1'-pyrenedecanoyl)-PC (pyrPC) was synthesised from egg yolk PC (Sigma) as described by Somerharju and Wirtz (1982). sn-2-(1'-Pyrenedecanoyl)-PI (pyrPI) was synthesised from yeast PI as described by Somerharju et al., (1985). sn-2-(1'-Pyrenedecanoyl)-PIP (pyrPIP) and sn-2-(1'-pyrenedecanoyl)-PI (pyrPIP$_2$) were synthesised enzymatically from pyrPI using partially purified PI and PIP kinase preparations from bovine brain as described by Gadella et al., (1990). sn-1, 2-(Pyrenyldecanoyl)-PC (DipyrPC) was synthesised by methods described previously (Patel et al., 1979). sn-1, 2-(Pyrenyldecanoyl)-PI (DipyrPI) and (DipyrPIP) were a kind gift of Dr. P. Nieuwenhuizen, University of Utrecht. The experiments were performed using buffer containing 0.5 mM EDTA, 10 mM Tris HCl, 50 mM KCl at pH 8.

8.2.2. Methods

Isolation of Band 3 protein

Band 3 protein was purified as described by Steck and Yu (1975) and Pappert and Schubert (1983) and incorporated into DOPC vesicles by dialysis according to Scheuring et al., (1984)

Incorporation of pyrene labelled lipids into membranes

Membrane vesicles containing pyrene labelled lipids were prepared by mixing the fluorescent lipid with the other lipids in ethanol-DMSO (75:25 v/v) and injecting the mixture in buffer under stirring. The protein enriched vesicles and ghost cell membranes were loaded with pyrene containing lipids by adding small aliquots (max. 2% of sample volume) of pyrene lipid stock solutions in ethanol/DMSO 75:25 (v/v). The pyrene-lipid concentration in the stock solution was measured spectrophotometrically using an extinction coefficient ε = 39700 $M^{-1}cm^{-1}$ at 345 nm in ethanol/DMSO. The samples were incubated overnight at 4°C in an argon saturated atmosphere prior to fluorescence measurements.
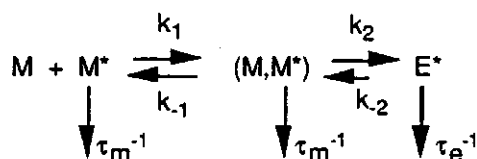
Fluorescence methods

Pyrene emission intensities were monitored on a DMX-1000 steady state spectrofluorometer (SLM Aminco, Urbana, IL, USA). The measurements were corrected for background emission (sample without pyrene lipid) and spectral instrument characteristics. Excitation and emission bandwidths were set at 4 nm. Monomer and excimer emission was detected at 377 nm and 487 nm, respectively. The excitation wavelength was set at 347 nm. The sample holder was thermostated to 20°C.

Fluorescence lifetime and anisotropy decays of samples with probe to lipid molar ratios of 0.005 were measured by use of a time-correlated single photon counting setup as described elsewhere (Pap et al., 1993). The excitation wavelength was 327 nm and the fluorescence emission was selected using a WG 360 cut-off filter and an interference filter at 374.6 nm (Schott, Mainz, Germany). After each measurement the background was measured at one fifth

of the time of sample acquisition. 1,4-bis(2-(5-Phenyloxazolyl))benzene (Eastman Kodak, Rochester, NY, USA) dissolved in ethanol served as reference compound ($\tau = 1.35$ ns) to yield the dynamical instrumental response function of the set-up (Vos et al., 1987). The sample holder was thermostated at 4° C.

Excimer formation in lipid membranes

Pyrene analogues can form excited-state dimers (excimers) between one pyrene molecule in the excited state and one in the ground state (Förster & Kasper, 1955). The rate of excimer formation is determined by the collision frequency of pyrene moieties. Therefore, when pyrene analogues are applied in membranes, their excimer formation can report about lateral organisation and translational mobility of lipids (Galla & Sackmann, 1974; Eisinger et al., 1986; Vauhkonen et al., 1989, 1990; Sassaroli et al., 1990). For lipids containing one pyrene acyl chain the process of excimer formation (M + M* → E*) can be described by the following scheme (Vauhkonen et al., 1990):

$$\mathrm{M + M^*} \underset{k_{-1}}{\overset{k_1}{\rightleftarrows}} \mathrm{(M,M^*)} \underset{k_{-2}}{\overset{k_2}{\rightleftarrows}} \mathrm{E^*}$$

$$\downarrow \tau_m^{-1} \qquad \downarrow \tau_m^{-1} \qquad \downarrow \tau_e^{-1}$$

in which τ_m^{-1} and τ_e^{-1} (in s^{-1}) represent the rate constants for the fluorescence decay of the excited monomer and excimer, respectively. Two dynamic processes govern the excimer formation. First, neighbour formation (M + M* → (M, M*)) which is characterised by the rate constants k_1 and k_{-1}. This process is modelled well with the so-called Milling Crowd (MC) model (Eisinger et al., 1986) which considers lipid probes migrating in a trigonal lattice of lipids by exchanging positions with one of their six nearest neighbours. The rate constant k_1 is related to the frequency of lipids exchanging positions in the membrane matrix (f) and to the number of lipid exchange events required before (M, M*) is formed. Inherent to the trigonal organisation of lipids k_{-1} corresponds approximately to f/2 (Sassaroli et al., 1990; Vauhkonen et al., 1990). Secondly, the reaction leading to formation of E* is governed by the rate of association k_2, and of dissociation k_{-2} which are related to the rotational freedom and dynamics of pyrene acyl chains. In most kinetic considerations k_{-2} is assumed much smaller than τ_e^{-1} and therefore negligible. The overall rate of intermolecular excimer formation of monopyrene lipids (k_{ex}) can be expressed by (Eisinger et al., 1986):

$$k_{ex} = \frac{f}{n} \qquad\qquad\qquad (1)$$

where n corresponds to the average number of lipid exchanges required before an excimer is formed. The parameter n is a function of the probe mole fraction (x), of interaction forces between pyrene lipids and of k_2 (see below, eq. 7).

In principle, both k_2 and f can be estimated from least square fitting of the dependence of the monomeric fluorescence yield (I_m) on the mole fractions of pyrene lipid (Eisinger et al., 1986):

$$\frac{I_m}{I_m^{'}} = \frac{1}{1 + \tau_m\, k_{ex}} \qquad (2)$$

where I'_m corresponds to the monomer intensity obtained at very low mole fraction of pyrene lipid. In practice, however, the quality of the data is such that large errors in the optimised values are obtained resulting in multiple sets of solutions for f and k_2. Therefore it is preferable to determine k_2 in an independent way by using the excimer to monomer fluorescence intensity ratio of lipids containing two pyrene acyl chains (dipyrene lipids) (EM_2) and of monopyrene lipids (EM_1) at the critical mole fraction (x_o) (Vauhkonen et al., 1990). At this critical molar probe ratio, the rate of excimer formation is equal to the monomer decay rate τ_m^{-1} (Sassaroli et al., 1990):

$$k_2 = \frac{EM_2}{EM_1(x_0)}\, \tau_m^{-1} \qquad (3)$$

We have adapted the MC-model for lipid migration by incorporating a lipid-lipid interaction factor (R). In addition, we have derived a statistical description for n which turns out to be a good alternative for the n values obtained from simulations in previous studies (Eisinger et al., 1986; Sassaroli et al., 1990). It is assumed that pyrene lipids that do not repel each other, will be randomly distributed (repulsion factor, R = 1) in the membrane, and exchange positions with randomly chosen nearest neighbours, either occupied by a normal lipid or a probe lipid molecule. The probability of finding a probe molecule at a neighbour position of a certain excited pyrene molecule is equal to the pyrene mole fraction in the membrane (x). When pyrene lipids do repel each other (like in the case of pyrPIP$_2$) the randomness of migration is affected and the probability of finding a probe molecule at a position next to a certain excited probe molecule is equal to xR (with R < 1). Generally, the probability of finding q probe molecules out of s neighbours is binomially distributed according to:

$$P_q = \frac{s!}{q!\,(s-q)!}\left[(x\, R)^q\,(1 - x\, R)^{s-q}\right] \qquad (4)$$

where $(xR)^q\,(1 - xR)^{s-q}$ corresponds to the probability that q neighbours are pyrene lipids and s-q are not, and the binomial term of eq. 4 to the number of ways how q molecules can be rearranged at s positions. From the kinetic scheme it can be derived that the probability that a pyrene surrounded by q neighbouring pyrene lipids will not form an excimer corresponds to:

$$\left(1 - \frac{k_2}{k_2 + k_{-1} + \tau_m^{-1}}\right)^q \qquad (5)$$

After time f^{-1}, the molecules in the matrix will exchange positions with one of their neighbours with new opportunities for excited pyrene probes to meet probe molecules in ground-state and form excimers. For each excited probe, this process will continue until an excimer is formed or de-excitation occurs via alternative pathways. This consideration leads in combination of eqns. 4-5 to the following relation for the probability that an excimer is formed after m steps (note that $k_{-1} \equiv f/2$):

$$P^s(f,k_2,m) = 1 - \left\{ \sum_{q=1}^{s} P_q \left(1 - \frac{k_2}{k_2 + \frac{f}{2} + \tau_m^{-1}} \right)^q \right\}^m \qquad (6)$$

Since the probability that an excimer is formed in the mth step corresponds to $P^s(f,k_2,m) - P^s(f,k_2,m-1)$, n is equal to:

$$n = \sum_{m=1}^{\infty} m \left\{ P^s(f,k_2,m) - P^s(f,k_2,m-1) \right\} \qquad (7)$$

In previous studies the function n was obtained by polynomial fitting to simulated probe migration data (Eisinger et al., 1986; Sassaroli et al., 1990). Eq. 7 is able to fit random walk simulations with high precision for various values of P_e (the probability that two pyrene neighbours form an excimer ($= k_2/(k_2 + f/2 + \tau_m^{-1})$)) and f as is shown in figure 1. However, both our simulations and eq. 7 predict significantly lower n-values than in these previous reports. This discrepancy leads to significant differences in the analysis of excimeric data and therefore remains to be solved.

Two domain model for excimer formation in the presence of Band 3 protein
  The coexistence of proteins in the plane of the biological membrane has several important consequences for in-plane lipid diffusion. Proteins act as simple physico-chemical barriers of lipids. The effect of proteins on the long-range diffusion of lipids has been evaluated by Eisinger et al., (1986). These authors performed simulations with the MC-model in which proteins were considered as lipid-forbidden hexagons in the bilayer. In addition, three effects contribute to a protein induced reduction of the excimer formation of pyrene lipids. 1) Proteins statistically reduce the excimer formation by occupying neighbouring positions of probe lipids and thus affecting the parameter s of eq. 6. 2) Lipids interacting at the protein surface are laterally immobilised and exchange positions with neighbouring lipids only slowly. The exchange frequency of bound lipids (f_b) might be significantly lower than that of lipids in the bulk lipid matrix (f_f). 3) Flexible lipid chains adjacent to proteins will adapt to the protein surface. This will affect the rotational dynamics and angular freedom of the lipid probes. Therefore a k_{2b} for protein bound pyrene lipids has to be defined apart from a k_{2f} for noninteracting pyrene lipids.
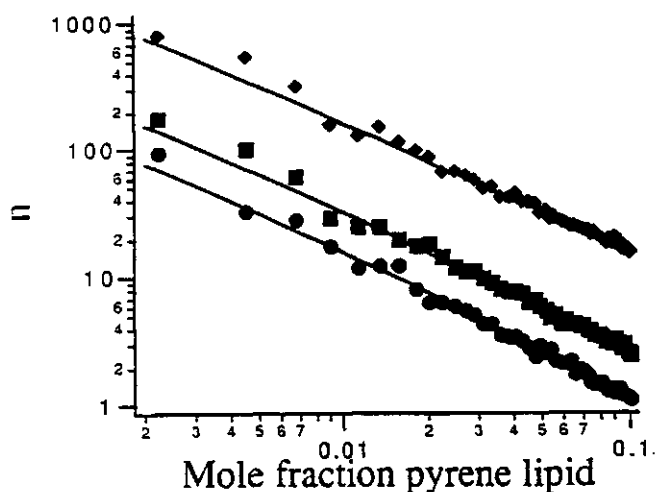
Figure 1 The dependence of the average number of lipid exchange events of an excited pyrene before an excimer is formed (n) on the mole fraction of pyrene probe x in membranes. No repulsive or attractive interaction forces were taken into account (R = 1). The points were obtained from random walk simulations of an excited pyrene lipid in a trigonal lipid matrix containing various mole fractions of nonexcited pyrene lipids. Both excited and nonexcited pyrenes migrated by exchanging positions with one of their randomly chosen six neighbouring lipids. After each relocation of the pyrene lipids, the program tested if an excimer was formed from the number of pyrene neighbours of the excited pyrene and for $P_e = 0.1$ (♦), 0.5 (■) and 1 (●)). The points correspond to the total number of steps taken (50000) divided by the number of events that leads to an excimer. The curves through the points were obtained for the corresponding P_e values with the statistical description of n as described in eq. 7.

In order to include these effects in the description for excimer formation we have to derive the fraction of pyrene lipids adjacent to a protein. We assume that a protein is surrounded by j lipid positions (B) which are occupied either by a pyrene lipid (P) or by a nonlabelled lipid (L). The relative binding constant K of a certain lipid positioned adjacent to the protein is equal to the ratio of the association constants for P and L occupying this position.

$$ L + BP \rightleftarrows P + BL \; ; \qquad K = \frac{K_P}{K_L} = \frac{[L][BP]}{[P][BL]} \qquad (8) $$

The average fractional occupancy (γ) of a protein lipid site with pyrene lipid is a function of the relative concentration of the individual components in this equilibrium:

$$\gamma = \frac{[BP]}{[BP] + [BL]} \qquad (9)$$

Since K is a relative constant, it is independent of the actual concentration of pyrene lipid and protein. Only the protein to lipid molar ratio (ρ) and pyrene mole fraction (x) are relevant parameters. If $K = 1$ (equal interaction forces between the protein surface and the pyrene lipid and unlabelled lipid), the fractional occupancy of a lipid position adjacent to the protein will be equal to x. In case of $K \neq 1$, one can derive an expression for the fractional occupancy from mass balance relationships and eqns. 8 and 9:

$$\gamma = \frac{1}{2(K-1)j\rho}(1 - j\rho + Kj\rho - x(1-K) -$$

$$\sqrt{-4(-1+K)Kj\rho x + (-1 + j\rho - Kj\rho + x - K x)^2}) \qquad (10)$$

From the average number of pyrene lipids per protein or "protein occupancy", $<J>$ ($= \gamma/j$), the fraction of pyrene lipids (v) located next to a protein can be calculated:

$$v = \frac{\langle J \rangle \rho}{x} \qquad (11)$$

Protein hexagons in a trigonal (lipid) matrix have 6 lipid positions with 5 lipid neighbours and j - 6 positions with 4 lipid neighbours. If we neglect the probability that a pyrene lipid molecule is interacting with more than one protein, the following expression for the probability of excimer formation is obtained after m steps in protein-containing membranes:

$$P(f,k_2,m) = 1 - \left\{ \frac{v(j-6)}{j}P^{s=4}(f_b,k_{2b},m) + \frac{v\,6}{j}P^{s=5}(f_b,k_{2b},m) + \right.$$
$$\left. (1-v)\,P^{s=6}(f_f,k_{2f},m) \right\}^m \qquad (12)$$

This equation can be applied to eq. 7 yielding an extended expression for n in protein-containing membranes. For the calculation of k_{ex} (eq. 1), f is divided similarly into a fraction v of protein bound lipids with exchange frequency f_b, and a fraction $(1 - v)$ of lipids in the bulk membrane with exchange frequency f_f.

8.3 Results

8.3.1. Model independent determination of k_2

In order to estimate the rate constant of excimer formation of two neighbouring pyrene moieties (k_2) we performed an experiment with dipyrPC, dipyrPI and dipyrPIP in DOPC vesicles, in DOPC vesicles containing Band 3 protein and in resealed ghost membranes. In each experiment the lipid to probe molar ratio was smaller than 0.005 so that intermolecular excimer formation can be neglected (Somerharju et al., 1985). The ratio of excimer to monomer fluorescence (EM_2) of dipyrPC, dipyrPI and dipyrPIP in these membrane systems are listed in Table 1. As described in the Methods section k_2 is related to the EM value of dipyrene lipids, to the EM_1 value of monopyrene lipids at the critical mole fraction and to the average monomer fluorescence lifetime. The value of the average monomer fluorescence lifetime ($\tau_m = 50$ ns) used in this calculation was obtained independently from fluorescence lifetime measurements. The value of the average lifetime is smaller than the one found in former studies (Sassaroli et al., 1990) which can be explained by the sensitivity of pyrene for oxygen that could still be present in trace amounts in our samples.

Probe/lipid system	EM_2		$EM_1(x_0)$	k_2 $(10^7$ $s^{-1})$
dipyrPC/DOPC	0.226	(0.03)	0.15	3.0
dipyrPI/DOPC	0.221	(0.04)		2.9
dipyrPIP/DOPC	0.245	(0.04)		3.2
dipyrPC/Band 3	0.248	(0.04)	0.16	3.1
dipyrPI/Band 3	0.225	(0.05)		2.8
dipyrPIP/Band 3	0.204	(0.05)		2.6
dipyrPC/ghost	0.241	(0.03)	0.18	2.6
dipyrPI/ghost	0.201	(0.04)		2.2
dipyrPIP/ghost	0.157	(0.02)		1.7

Table 1. The ratio of excimer to monomer fluorescence of dipyrene labelled analogues of PC, PI and PIP in DOPC vesicles, in DOPC vesicles containing Band 3 protein and in resealed ghost cell membranes. The values between parentheses correspond to standard errors of average values obtained from three experiments. The EM_1 value determined for pyrPC was used in the calculation of k_2 of all dipyrene labelled lipids according to eq. 3. This approach is validated by the fact that the EM_1 value at the critical mole fraction is not dependent on dynamic properties. The molar protein-lipid ratio was 1:140 for ghost cell membranes and 1:1000 for the Band 3 protein reconstitutions. The experiments were performed at 20°C.

The calculated k_2 values show some interesting features (Table 1). For dipyrPC, only a 10% reduction of k_2 is observed when the pyrene lipids are dispersed in ghost cell membranes. This indicates that the "microfluidity" experienced by this probe differs only slightly in the different membrane systems. In DOPC

membranes, the k_2 values of the three different dipyrene lipids are approximately equal. The differences in headgroup moieties apparently do not influence the collision frequency of the pyrenes at both acyl chains. A considerable reduction of k_2 value of especially dipyrPIP is observed when dispersed in protein containing membranes. This reduction of k_2 is particularly large in the resealed ghost cell membranes, having relatively high protein content. This implies that phosphoinositides interact to a higher extent with the membrane proteins than dipyrPC and as a consequence experience a more rigid environment.

7.3.2. Monomer fluorescence in DOPC vesicles

The normalised monomer fluorescence emission obtained after titration of various monopyrene lipids in DOPC membranes is given in figure 2. The negatively charged pyrPI and the electrically neutral pyrPC have a similar dependence of the monomer quenching on their mole fraction. The collision frequency of the higher phosphorylated inositide lipids pyrPIP and pyrPIP$_2$, however, is substantially lower at comparable mole fractions in membranes. The relatively bulky headgroup of inositide lipids may contribute to a lower lateral diffusion coefficient. We assume, however, that diffusion of pyrene lipids is mainly dependent on the host lipid matrix and thus the effect of the various probe lipid headgroups on the lipid exchange frequency (f) can be neglected. This approximation holds true only at low mole fractions of pyrene lipid in the membranes. Repulsive electrostatic interactions between the phosphorylated headgroups of the inositides will lower the probability that two pyrene labelled inositide lipids become each others nearest neighbours (and thus there will be an effect on n).
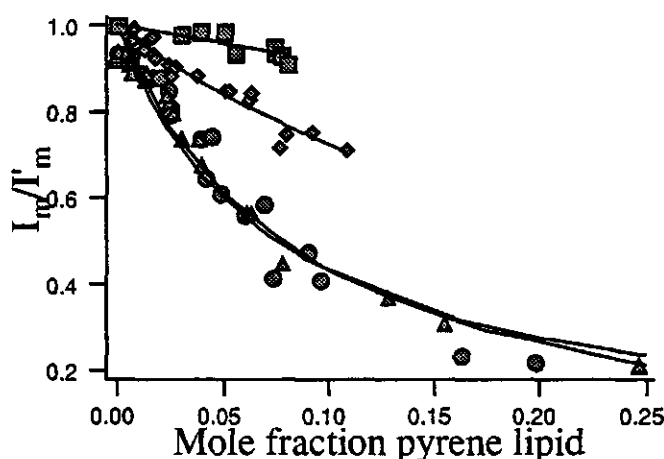

Figure 2 The dependence of the normalised monomeric fluorescence intensity on the mole fraction incorporated pyrene labelled PC (●), PI (▲) PIP (◆) and PIP$_2$ (■) in DOPC vesicles. The curves are the best fits obtained by applying eqs. 2 and 7 to the experimental points giving results listed in Table 2. The experiments were performed at 20°C.

The repulsion factor R between the two pyrene labelled inositide lipids can be estimated by applying the extended MC model to the normalised monomeric yields of the various lipids (see Methods section). In this approach we assume that pyrPC's in a DOPC environment do not repel or attract each other (R = 1). Analysis of the monomeric pyrPC fluorescence with the extended MC model using the value for k_2 obtained from the former dipyrene experiments, yielded optimal fits with a value for f of 10^8 s^{-1}.

| Probe	f (10^8 s^{-1})	D μm^2 s^{-1}	R		SSQ*	Charge
pyrPC	1 (0.85, 1.24)	17.5	1		0.0013	0
pyrPI	1	17.5	1	(0.85-1.24)	0.0034	- 1
pyrPIP	1	17.5	0.3	(0.27-0.33)	0.0005	-2.9
pyrPIP$_2$	1	17.5	0.08	(0.06-0.09)	0.0003	-4.2

Table 2. Values of dynamical (f, D) and repulsive parameters (R) recovered from the analysis of the normalised monomer fluorescence yield of the various pyrene labelled lipids. In the analysis k_2 was fixed to 3.0 10^7 s^{-1} (Table 1). The lateral diffusion coefficient was calculated according to (f $\lambda^2/4$) (Eisinger et al., 1986), where λ corresponds to the lipid-lipid spacing ($\lambda^2 = 70$ nm^2 for DOPC (Demel et al., 1967). The values between the parentheses correspond to the errors at a 67 % confidence level as determined from the dependence of the SSQ on the value of the examined parameter (see Beechem et al., (1991)). The net charge of the lipids at pH 7.4 is given in the last column (van Paridon et al., 1986).

$$*SSQ = \frac{1}{N} \sum_{i=1}^{N} (Data_i - Fit_i)^2 \quad \text{for N datapoints}$$

Application of k_2 and f in analyses of the monomeric data of pyrPI, pyrPIP and pyrPIP$_2$ (figure 2) yielded R values of 1, 0.31 and 0.08, respectively (Table 2). We can thus conclude that a PIP$_2$ lipid prefers more than ten times a neutral lipid neighbour than another PIP$_2$ molecule as neighbour. Therefore, the polyvalent phosphoinositides will be non-randomly distributed in the membrane.

8.3.3. Monomer fluorescence in DOPC vesicles containing Band 3

The dependence of the monomer fluorescence on the mole fraction of mono-pyrene inositide lipids in Band 3 protein reconstituted in DOPC vesicles is given in figure 3. From comparison with figure 2 two major conclusions can be drawn. 1) Band 3 protein reduces the number of intermolecular collisions of the pyrene inositide. 2) The affinity of Band 3 protein for inositides is limited. Multiple sites with high affinity for the pyrene lipids should lead to a sigmoidal dependence of the monomer intensity on the concentration of pyrene lipids added. In other words, even at higher mole fractions of pyrene lipids there are (lipid) positions next to the protein that are not occupied by a pyrene lipid.
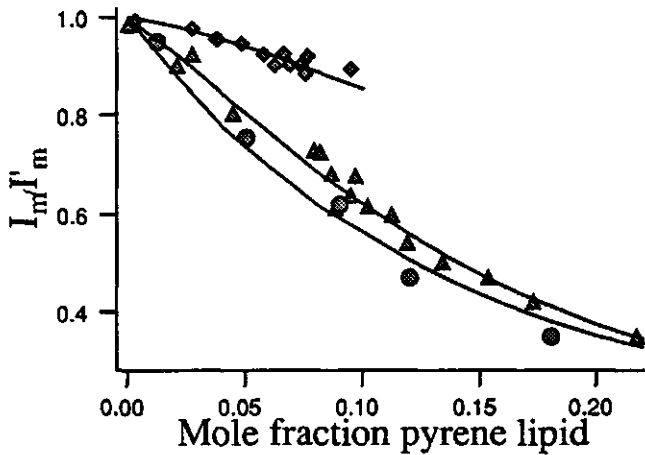
Figure 3. The dependence of the normalised monomeric fluorescence intensity on the mole fraction of incorporated pyrene labelled PC (●), PI (▲) and PIP (◆) in Band 3 protein reconstituted in DOPC vesicles. The curves are the best fits obtained by applying the two domain model to the experimental points (see Methods section). The experiments were performed at 20°C.

As described in the Methods section protein-induced reduction of excimer formation originates from statistical factors and from differences in local order and dynamics of lipids in the vicinity of proteins. The complex relationship for excimer formation in protein-rich membranes is embodied in the model in which many parameters have to be determined. This number can, however, be drastically reduced if the optimised values of the independent analysis of lipids in DOPC are used to obtain both R and f_f. This step is validated by the fact that DOPC was used as a host lipid in both the reconstitution of Band 3 protein and the titration experiments described in figure 2. We thus neglect effects of proteins on the lipid-lipid (electrostatic) interaction forces (R). Since the excimer formation of dipyrPC is hardly affected by the presence of protein (Table 1) its k_2 value is representative for lipids that do not interact with protein (k_{2f}). On the other hand the excimer formation of dipyrPIP is significantly influenced by proteins. The value of the rate constant k_2 will thus represent a mean value composed of dipyrPIP molecules interacting with Band 3 protein and dipyrPIP molecules residing in bulk lipid. Therefore, k_2 can be considered as an upper limit for k_2 of lipids that interact with the protein (k_{2b}). The protein-lipid ratio (PL) is determined chemically (PL = 0.001; see Methods Section) and the size of Band 3 protein in membranes is approximately 66 Å diameter as was determined from electron microscopic analysis of Band 3 crystals (Wang et al., 1993; Dolder et al., 1993). This corresponds to approximately 72 lipids surrounding the protein. When we assume that the fluorescence lifetime is short relative to the mean residence time of a pyrene lipid at the protein surface (f_b = 0) the two-domain model can now be applied to the excimeric data given in figure 3 with only K as constrained adjustable parameter (K ≥ 1). The SSQ searches of these analyses are presented in figure 4. As can be expected for a labelled PC lipid in PC

142

membranes, the average affinity of pyrPC for Band 3 relative to the bulk DOPC is negligible. The SSQ minimum is well defined to a K value of 3, which is in view of the inexact estimates of several parameters in this analysis and the simplicity of the two domain model a satisfying result. For pyrPI and pyrPIP, the optimal K values amounted to 19 and 29, respectively.
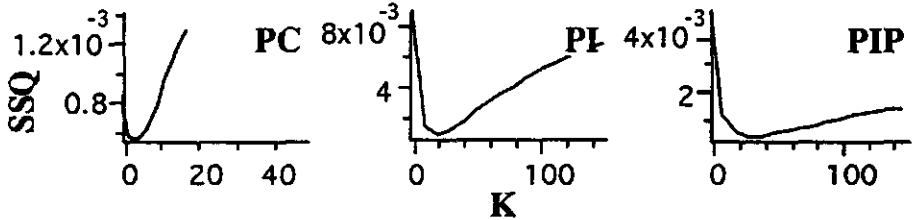
Figure 4. SSQ search of the average relative binding constant K of Band 3 for pyrPC, pyrPI and pyrPIP as obtained by applying the two domain model (see Methods section) to the data of figure 3. In the analysis the parameters f_b and k_b were fixed to 0 s^{-1} and 1.7 10^7 s^{-1} respectively.

These K values are rough indices of the average relative affinity of the pyrene lipids for the Band 3 surface. Based on this analysis one may conclude that the average time that a pyrPIP molecule is located near the Band 3 surface is approximately 30 times longer than that of a DOPC molecule. If one assumes that only a selective number (Q) of the total lipid sites (j) on the Band 3 protein possesses high affinity for pyrPIP (K → ∞), while the remaining surface (j - Q) has no affinity for pyrPIP (K = 1) and one assumes that the interacting pyrPIP lipids do not form excimers (k_b, f_b = 0), a minimal number of affinity sites for pyrPIP can be estimated (Q_{min}) (see figure 5).
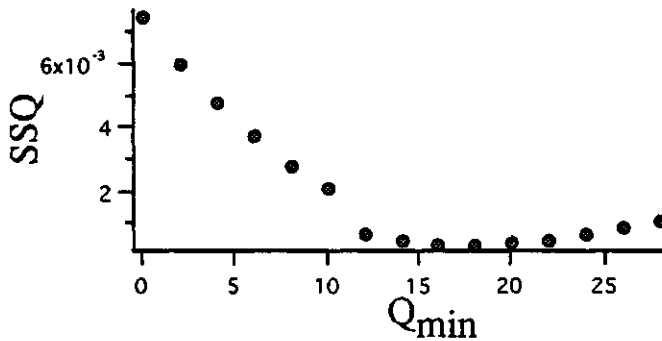
Figure 5. SSQ plot of the analysis of the pyrPIP data in figure 3 as a function of the number of high affinity sites Q. In this two-domain analysis it is assumed that S sites possess high affinity for pyrPIP (K was set to 10^9), while the others (j - Q) do not (K = 1). In order to obtain an absolute minimum, the parameters f_b and k_b were both fixed to 0 s^{-1}.

8.3.4. Rotational dynamics of pyrene labelled lipids in ghost cell membranes

Next to the lateral organisation and dynamics, pyrene probes offer also the possibility to study rotational dynamics by means of fluorescence anisotropy decay. The influence of protein-lipid interactions on the rotational dynamics of the pyrene labelled lipids was characterised further by measuring the polarised fluorescence decays of the lipid probes in resealed ghost cells and in DOPC membranes. From these decays the anisotropy was constructed, which are presented for PIP_2 and PC in figure 6. For this technique, however, the properties of pyrene are not so suitable since the fluorescence lifetime is one order of magnitude longer than the reorientational dynamics of the probe in vesicles (which considerably prolongs the experiment) and, in addition, the theoretical treatment of the rotational motion is extremely complex (Zannoni et al., 1983). Therefore detailed interpretation is omitted and the results are qualitatively described. Some interesting features are nonetheless obtained from these experiments. In DOPC membranes, the fluorescence anisotropy of both $pyrPIP_2$ and pyrPC declines to zero at longer times. This indicates that the rotation of the pyrene chains in these membranes is not restricted on the time scale of the relatively long lifetime. However, in the protein-rich ghost cells, the fluorescence anisotropy of $pyrPIP_2$ has a finite value at longer times indicating that its motion is restricted. In contrast, the pyrPC analogue, is able to rotate free in the membrane. The acyl chain moieties of PIP_2 are apparently interacting with the protein surface and therefore are constrained in their motions.
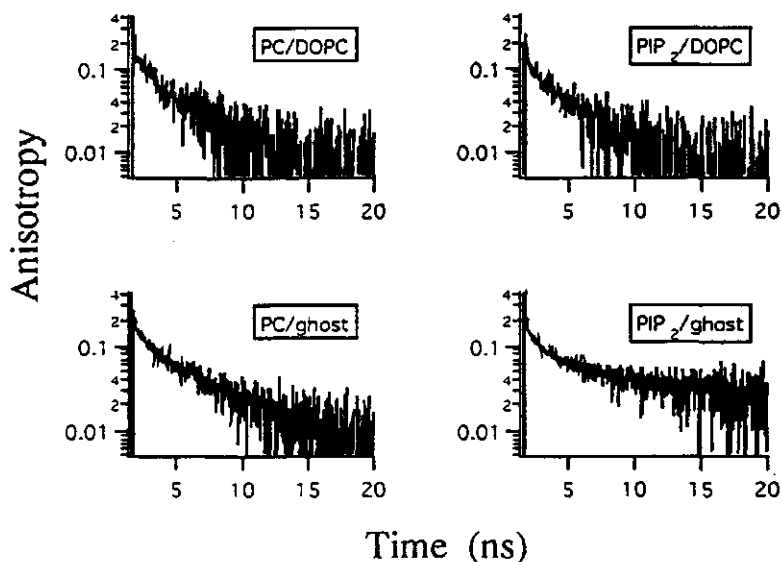

Figure 6. The experimental fluorescence anisotropy decays of pyrPC and $pyrPIP_2$ in DOPC and in erythrocyte ghost cell membranes. The experiment was performed at 4°C.

8.4. Discussion

In this study we have characterised the effect of repulsive electrostatic lipid-lipid forces on the randomness of the distribution of pyrene labelled phosphoinositides in membranes. In addition, the effect of interaction with Band 3 protein on the lateral organisation and dynamic properties of these labelled lipids was evaluated. Registration of excimer formation of pyrene analogues appeared to be very suitable for quantitative analysis of interactions between particular lipid species and between lipids and proteins. From our experiments we conclude that the spatial distribution of polyphosphoinositides in membranes is organised to some extent. A value of 0.09 and 0.33 was obtained for the lipid-lipid repulsion factor R of PIP_2 and PIP. Differences in the lateral organisation of PI and PC in DOPC membranes were not observed. Since R is defined as the probability ratio to find a pyrene lipid or a nonlabelled lipid at a certain position next to a pyrene lipid when present at equal mole fractions, this implies that PIP_2 prefers 11 times more a electrically neutral PC neighbour than one of their own species. For the less phosphorylated inositides PIP and PI this preference is 3 and 1 respectively. This observation thus excludes the possibility of segregated domains of pure phosphoinositides which are PLC accessible or resistant. Such pools with special properties and compositions have been suggested repeatedly in the literature for other (acidic) lipids (Karnovsky et al., 1982; Levin et al., 1985; Wolf et al., 1988).
The excimer experiments in DOPC containing Band 3 protein and in ghost cells indicate that phosphoinositides are located preferentially adjacent to Band 3 (see also Chapter 7). The phosphoryl moieties of the phosphoinositides probably interact electrostatically with positively charged amino acid residues at the protein surface. This observation does not necessarily imply that Band 3 is regulated by the phosphoinositides. Analysis with the two domain model yielded that there are at least 15 sites with affinity for PIP. Therefore, a specific allosteric function of phosphoinositides is not likely, but the relevance of the interactions for the biological function of Band 3 has to be systematically investigated further. From a catalytic point of view of certain enzymes like phospholipase C, the results may have some bearing. The ghost cell membranes used in our experiments consisted of only 140 lipid molecules per integral protein molecule, which is typical for natural membranes (Newton, 1993). Considering this high protein to lipid ratio, the relative binding constant of polyphosphoinositides for abundant proteins like Band 3 protein, and the large differences in protein and lipid molecular surfaces, the majority of the phosphoinositides will be in direct contact with protein surfaces. The non-random distribution of the phosphoinositides and their interactions with membrane proteins like Band 3 might reduce the accessibility of the phosphoinositides for PLC and even be rate limiting for the second messenger production. In light of these observations it is tempting to speculate about the origin of PLC resistant phosphoinositides which are tightly interacting with membrane proteins and form a non-hydrolysable pool of inositides. This speculation agrees well to several observations of other research groups:
1) About 70 % of the PIP and 20 % of the PIP_2 molecules turn over rapidly (Gascard et al., 1989). This difference can be ascribed to a larger fraction of

PIP_2 interacting with protein surfaces. 2) The majority of the PLC sensitive phosphoinositides appears to be newly synthesised and not already present in the membrane. Lassing and Lindberg (1990) observed that stimulation of kinases phosphorylating PI and PIP precedes the activation of receptor-linked PLC. In addition, Gascard and coworkers (1989) observed that newly synthesised molecules of PIP_2 in erythrocytes membranes are initially accessible to PLC, but are subsequently moved towards a PLC resistant pool (which might be protein bound). In addition, recent evidence has been obtained that the PI-transfer protein is required for prolonged PLC activity in permeabilised HL60 cells (Thomas et al., 1993). The authors proposed that the PI-transfer protein is involved in transporting PI from intracellular compartments for conversion to PIP_2 prior hydrolysis by PLC. A different view is given by Gascard and coworkers, who proposed on the basis of an phospholipase A_2 assay, that PLC catalysed hydrolysis of PIP_2 and PIP is facilitated through their interactions with proteins (Gascard et al., 1993). It is however hard to visualise how proteins may enhance the accessibility of the phosphoinositides for PLC.

8.5 References

Beechem, J.M., Gratton, E. Ameloot, M., Knutson, J.R. & Brand, L. (1991) in: *Topics in Fluorescence Spectroscopy* (Lakowicz, J.R. Eds) vol 2., Principles, Plenum Press, New York.

Berridge, M.J. (1993) *Nature,* 361, 315-325.

Chauhan, V.P.S. & Brockerhoff, H. (1988), *Biochem. Biophys. Res. Commun.*, 155, 18-23.

Cubitt, A., Zhang, B. & Gershengorn, C. (1990), *J. Biol. Chem.*, 265, 9707-9714.

Demel, R.A., Van Deenen L.L.M., & Pethica B.A. (1967) *Biochim. Biophys. Acta.* 135, 11-19.

Den Hartigh, J.C., Enhenegouwen, P.M.P.V., Boonstra, J., & Verkleij, A.J. (1993) *Biochim. Biophys. Acta.* 1148, 249-262.

Dolder, M., Walz, T., Hefti, A., & Engel, A. (1993) *J. Mol. Biol.* 231, 119-132.

Eisinger, J., Flores, J., & Petersen, W.P. (1986) *Biophys. J.* 49, 987-1001.

Ferrel, J.E. & Huestis, W.H. (1984) *J. Cell. Biol.* 98, 1992-1998.

Förster, Th., & Kasper K. (1955) *z. Elektrochem.* 59, 976-980.

Gadella, T.W.J., Moritz, A., Westerman, J., Wirtz, K.W.A. (1990) *Biochemistry,* 29, 3389-3395.

Galla, H.J. & Sackman E. (1974) *Biochim. Biophys. Acta* 339, 103-115.

Gascard, P., Journet, E., Sulpice, J.C. & Giraud, F., *Biochem. J.* (1989) 264, 547-553.

Gascard, P., Sauvage, M. Sulpice, JC., & Giraud, F. (1993a) *Biochemistry* 32, 5941-5948.

Gascard, P., Pawelczyk, T., Lowenstein, J.M. & Cohen, C.M. (1993b) *Eur. J. Biochem.* 211, 671-681.

Gascard, P., Tran, D., Sauvage, M., Sulpice, JC., Fukami, K., Takenawa, T., Claret, M., & Giraud, F. (1991) *Biochim. Biophys. Acta* 1069, 27-36.

Hagelberg, C. & Allan, D. (1990) *Biochem J.* 271, 831-834.

Huang, F.L., & Huang K.P. (1991) *J. Biol. Chem.* 266, 8727-8733.

Janmey, P.A., & Stossel T.P. (1989) *J. Biol. Chem.* 264, 4825-4831.

Janmey, P.A., Iida, K., Yin, H.L., Stossel, T.P. (1987) *J. Biol. Chem.* 262, 12228-12236.

Karnovsky, M.J., Kleinfeld, A.M., Hoover, R.L., Klausner, R.D. (1982) *J. Cell. Biol.* 94, 1-6.

King, C.E., Stephens, L.R., Hawkins, P.T., Guy, G.R. & Michell, R.H. (1987) Biochem. J. 244, 209-217.

Koréh, K. & Monaco M.E. (1986) *J. Biol. Chem.* 261, 88-91.

Lassing, I., & Lindberg U. (1985) *Nature* 314, 472-474.

Lassing, I., & U. Lindberg (1990) *FEBS Lett.* 262, 231-233.

Lee, M.H., & R.M. Bell (1991) *Biochemistry* 30, 1041-1049.

Levin, I.W., Thompson, T.E., Barenholz, Y., & Porter, N.A. (1985) *Biochemistry* 24, 6282-6286.

Majerus, P.W. (1992) *Annu. Rev. Biochem.* 61, 225-250.

Michell, R.H. (1992) *Trends Biochem. Sci.* 17, 274-276.

Missiaen, L. Raeymaekers, L. Wuytack, F. Vrolix, M., De Smedt, H. & Casteels, R. (1989) *Biochem. J.* 263, 687-694.

Monaco, ME., & JR. Adelson (1991) *Biochem. J.* 279, 337-341.

Muller, E, Hegewald, H, Jaroszewicz, K, Cumme, G.A. Hoppe, H & Frunder, H. (1986) *Biochem. J.* 235, 775-783.

Newton, A.C. (1993) *Annu. Rev. Biophys. Biomol. Struct.* 22, 1-25.

O'Brain, C.A., Arthur, W.L., & Weinstein, I.B. (1987) *FEBS Lett.* 214, 339-342.

Pap, E.H.W., Bastiaens, P.I.H, Borst, J.W., Berg, van den P., Hoek, A., Snoek, G.T, Wirtz, K.W.A. & Visser, A.J.W.G. (1993) *Biochemistry*, 32, 13310-13317.

Pappert, G. & Schubert, D. (1983) *Biochim. Biophys. Acta* 730, 32-40.

Patel, K.M., Morrisett, J.D., & Sparrow, J.T. (1979) *J. Lipid. Res.* 20, 674-677.

Ruocco, M.J., & Shipley G.G. (1982) *Biochim. Biophys. Acta* 691, 309-320.

Sassaroli, M., Vaukonen, M., Perry, D., Eisinger, J. (1990) *Biophys. J.*, 57, 281-290.

Scheuring, U., Kollewe, K. & Schubert, D. (1984) *Hoppe-Seyler's Z. Physiol. Chem.* 365, 1056-1057.

Schmell, E., & W.J. Lennarz (1974) *Biochemistry* 13, 4114-4121.

Sekar, M.C., & L.E. Hokin (1986) *J. Membrane Biol.* 89, 193-210.

Somerharju P.J. & Wirtz K.W.A. (1982), *Chem. Phys. Lipids* 30, 81-91.

Somerharju, P. J., Virtanen, J. A., Eklund, K. K., Viano, P., & Kinnunen, P. K. J. (1985) *Biochemistry* 24, 2773-2781.

Thomas, G.M.H., Cunningham, E., Fensome, A., Ball, A., Totty, N.F., Truong, O., Justing Hsuan, J. & Cockcroft, S. (1993) *Cell* 74, 919-928.

van Hoek, A., & Visser A.J.W.G. (1985) *Anal. Instrum.* 14, 359-378.

van Paridon, P.A, de Kruijff, B., Ouwekerk R., & Wirtz, K.W.A. (1986) *Biochim. Biophys. Acta.* 877, 216-219.

Vauhkonen, M., Sassaroli, M., Somerharju, P., & Eisinger, J. (1989) *Eur. J. Biochem.* 186, 465-471.

Vauhkonen, M., Sassaroli, M., Somerharju, P., & Eisinger, J. (1990) *Biophys. J.* 57, 291-300.

Verbist, J., Gadella, T.W.J., Raeymaekers, L, Wuytack, F., Wirtz, K.W.A., & Casteels, R. (1991) *Biochim. Biophys. Acta.* 1063, 1-6.

Vos, K., van Hoek A., & Visser, A.J.W.G. (1987) *Eur. J. Biochem.* 165, 55-63.

Wang, D.N., Kuhlbrandt, W., Sarabia, V.E. & Reithmeier, R.A.F. *EMBO J.* 12, 2233-2239

White, D.A. "Form and Function of phospholipids." Ed. Ansell G.B., Dawson, R.M.C. & Hawthrone, J.M., Eds. Amsterdam: Elsevier, 1973. 2nd edition: 445-482.

Wolf, D.E., Libscomb, A.C., & Maynard, V.M. (1988) *Biochemistry*, 27, 860-865.

Yin, H.L., Iida, K., & Janmey P.A. (1988) *J. Cell Biol.* 106, 805-812.

Yu, J. & Steck, T.L. (1975) *J. Biol. Chem.* 250, 9176-9184.

Zannoni, C., Arcioni, A., & Cavatorta, P. (1983) *Chem. Phys. Lipids.* 32, 179-250.

Chapter 9

Summarising discussion

Introduction

Cellular communication is partly mediated through the modulation of protein activity, structure and dynamics by lipids. In contrast to the biochemical aspects of lipid signalling, relatively little is known about the physical properties of the "signal" lipids (lipids involved in cellular signalling) in membranes and their interaction with membrane proteins. Knowledge about these properties contributes to the understanding of the molecular mechanism of intracellular communication. The main objective of this thesis is to evaluate organisational and motional aspects of protein-lipid systems that play a role in this signalling. Fluorescence spectroscopy was employed to distinguish between interacting elements of the protein-lipid binding equilibrium from the non-interacting ones and to reveal their motional properties and characteristics in organisation. The first chapter of this thesis summarises the functional relevance and fundamental mechanisms of protein-lipid interactions and introduces some fluorescopic tools which can be applied in these investigations. In the remaining chapters the biophysical properties of the phosphoinositides phosphatidylinositol (PI), phosphatidylinositol-4-phosphate (PIP) and phosphatidylinositol-4, 5-biphosphate (PIP$_2$) and diacylglycerol (DG) and their relation to protein kinase C (PKC) and Band 3 (an abundant anion exchanging protein in erythrocyte membranes) form a central theme. Three types of binding are evaluated: 1) peripheral membrane binding of proteins, 2) lipids replacing other lipids at the protein surface and 3) lipids which bind to vacant cofactor sites at the protein. By combining complementary fluorescopic techniques, and by refinement of fluorescence data analysis, new aspects of protein-lipid relations have been elucidated which are summarised below. As a model study and introduction for the protein-lipid studies described in this thesis, Chapter 2 considers the association of lysozyme with acidic vesicles. From the experiments it could be concluded that the protein conformation and dynamics of lysozyme are effected when the protein interacts with acidic membranes. Apart from the general interest in protein-lipid interactions, this study demonstrates that a fractional analysis of time-resolved fluorescence and fluorescence anisotropy decay curves can provide accurate binding curves of protein molecules to lipid interfaces.

The interaction of PKC with PS and phosphoinositides and DG

Various aspects of the application of fluorescence anisotropy in the evaluation of lipid motion are introduced in Chapter 3. In that Chapter the motional characteristics of three 1, 6-diphenyl-1, 3, 5-hexatriene (DPH) labelled phosphatidylcholines are compared.

Based on the results of this study the effect of PKC on the reorientational properties of fluorescent analogues of DG and PC have been evaluated using a constrained model of analysis (Chapter 4). It appeared that in membranes DPH-DG experiences a larger motional freedom than DPH-PC, which indicates

that DG induces a lipid packing irregularity. Defects in membrane organisation lead to a partial exposure of hydrophobic regions of phospholipids to aqueous environment and thereby increase the ground state energy of bilayers (Jain & Zakim, 1987). Therefore the activation energy associated with insertion of PKC into the hydrophobic membrane core could be reduced by DG. Three complementary observations provide evidence that PKC is able to interact with PS containing membranes in the absence of calcium:

1) The isotropic rotation of PS containing micelles slows down upon addition of PKC (Chapter 4).

2) Micelles and vesicles containing pyrene labelled lipids quench the tryptophan fluorescence of PKC (Chapter 5).

3) PKC significantly reduces the collision frequency of pyrene labelled PS (Chapter 5).

Addition of calcium results in the binding of PKC to DG (Chapter 6). For this DG-PKC interaction the presence of PS is a prerequisite (Chapters 4, 5, 6). The precise mechanism of this calcium dependence of DG binding remains unclear. Calcium enhances the binding of PKC to PS. As a result of this enhanced PS binding the probability of finding a DG molecule close to PKC may increase since PKC molecules retain longer at the membrane surface. Alternatively, calcium may induce changes in PKC that result in exposure of a shielded lipid cofactor site for DG. As a consequence of the interaction with PKC, the lateral and rotational diffusion and orientational freedom (Chapters 4 and 5) of labelled DG are reduced. The interaction with DG is highly specific, since the motional properties of labelled PC, PS and PI analogues are only moderately effected by PKC (Chapters 4 and 5) and these lipids are not able to quench PKC fluorescence at low concentrations (Chapter 6). However, labelled phosphoinositides PIP and PIP_2 partly mimic the properties of DG. They bind with high affinity to PKC and the acyl chain dynamics of (dipyr)PIP and (dipyr)DG are equally effected by PKC (Chapters 5 and 6). In addition, like is known for DG, only a very limited number of phosphoinositides bind to one PKC molecule (Chapter 6). Double labelling experiments and replacement studies suggest that PIP and DG can bind simultaneously to PKC while PIP_2 and DG cannot (Chapters 5 and 6). In addition, it appeared that only PIP_2 and DG effectively activate PKC. Combined, these results indicate a cofactor role of PIP_2 for PKC.

Although the role of PIP_2 in the activation of PKC has to be established *in vivo*, its properties do fit excellently to a messenger function. Radioactive labelling studies with H-inositol and P-phosphate revealed that the turnover of PIP_2 is extremely rapid and in resting cells its level is low (reviewed by Hokin, 1985). The major part of PIP_2 present at resting conditions, may even be not available for PKC activation. Several studies have shown that the inositol lipids are heterogeneously distributed in the different cellular membranes and that only a small fraction of the total inositol lipid content is available for enzymes like phospholipase C (see for a review Downes & Michell, 1985). Like most other signalling lipids the PIP_2 concentration increases transiently to high levels within seconds after hormone stimulation of cells (Hansen et al., 1986). The dual role of PIP_2 as a DG-precursor and as a direct PKC-activator opens new avenues for the differentiation of signals via the various PKC families. The cell

responses that induce the PLC catalysed hydrolysis of phosphoinositides always result in the co-appearance of DG and calcium. Several PKC-isoforms, however, do no need calcium for their activity. Other lipid cofactors like PIP_2 may function as cofactors for these calcium independent protein kinases. For the calcium dependent protein kinases an inositol triphosphate (IP_3) mediated calcium release would imply the production of DG.
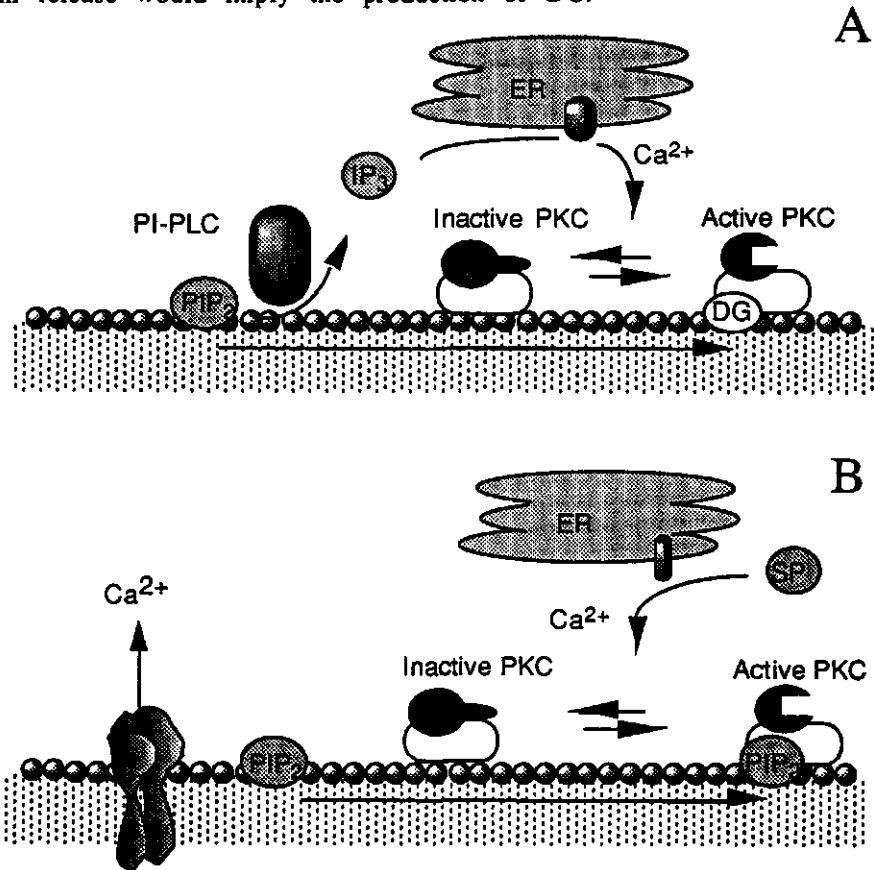
Figure 1. Possible dual role of PIP_2 in the regulation of PKC activity. (A) In the PLC pathway, the hydrolysis of PIP_2 functions as a switch for the activation of PKC, by providing simultaneously the factors required for PKC activity: calcium (via IP_3) and DG. When calcium is released via a sphingosine phosphate (SP) mediated mechanism or imported by calcium channels in the plasma membrane, no DG is produced. In this case (B) PKC may be activated by other lipid cofactors like PIP_2.

When calcium is provided via calcium channels in the plasma membrane or via sphingosine phosphate signalling (Dessai et al., 1992), no DG is released and other lipid activators like PIP_2 can take over the cofactor role. In this DG-independent activation, the temporal availability of calcium in the cytosol is the main switch for PKC activity. In this respect, it would be interesting to know if there are situations in the cell in which the PIP-kinase and (phosphoinositide-specific) phospholipase C activities are uncoupled. In that

case the levels of PIP_2 can be regulated independently from those of DG, which would make the double role of PIP_2 in the regulation of PKC activity even more attractive (Figure 1).

Heterogeneous distribution of phosphoinositides in membranes
In Chapter 7, the interaction of the phosphoinositides with human erythrocyte Band 3 protein was characterised using resonance energy transfer. The efficiency of quenching of the fluorescence from tryptophan residues in the protein by pyrene lipids in the membrane decreased in the order $pyrPIP_2$, pyrPIP, pyrPI and pyrPC indicating different spatial distributions of these lipids with respect to Band 3. Global analysis of the quenched tryptophan fluorescence decays yielded indices for the spatial distributions of the different lipids. It appeared that the charged lipids PIP_2 and PIP spend longer time in the vicinity of Band 3 than PI and PC. In investigations complementary to these protein fluorescence observations, the monomer/excimer fluorescence of pyrene labelled phosphoinositides in DOPC membranes was evaluated in the absence and presence of Band 3 protein (Chapter 8). In combination with theoretical refinements of the model for lipid migration, these experiments revealed estimates for the lateral dynamics and lipid-lipid repulsion in membranes. In addition, the relative binding constants and the minimum number of Band 3 sites possessing affinity for the phosphoinositides could be roughly estimated. Consistent with intuitive expectations the lipid-lipid repulsion appeared highly dependent on the amount of negative charge of the lipid headgroups. Combining these experiments indicates that lipid-lipid repulsion and the Band 3-lipid interactions induce a non-random distribution of the phosphoinositides. This non-random distribution will probably effect the accessibility of the inositol lipids for phospholipase C and for other phosphoinositide dependent proteins like PKC and may result in the functional heterogeneity of the phosphoinositides (Downes & Michell, 1985).

References

Desai, N.N., Zhang, H., Olivera, A., Mattie, M.E. & Spiegel, S. (1992) *J.Biol. Chem.* 267, 23122-23128
Downes, C.P. & Michell, R.H. (1985) In *"Molecular Mechanism of Transmembrane Signalling"* (P. Cohen and M.D. Houslay, eds), 3-56, Elsevier Science Publ., Amsterdam.
Hansen, C.A., Mah, S., & Williamson, J.R. (1986) *J.Biol. Chem.* 261, 8100-8103.
Hokin, L. E. (1985) *Ann. Rev. Biochem.* 54, 205-235.
Jain, M.K. & Zakim, D. (1987) *Biochim. Biophys. Acta* 906, 33-68.

Nederlandse samenvatting

In bepaalde opzichten zou een levende cel kunnen worden vergeleken met een middeleeuwse vestingstad. De stad is een duidelijke eenheid omgeven door een stadsmuur. Diverse stadspoorten en waarnemers zorgen voor interacties met de buitenwereld waardoor de stad niet een geheel geïsoleerde eenheid is. In de vestingstad is het een drukte van belang. Boeren, ridders en knechten lopen schijnbaar doelloos door elkaar. In deze wirwar speelt menselijke communicatie een vitale rol bij het afstemmen van transacties en het dicteren van algemene doelen. Evenzo zijn cellen en cel-organellen zijn begrensde eenheden waarin zich een wirwar van levensprocessen afspelen. Deze eenheden zijn omgeven door een celmembraan welke voornamelijk bestaat uit lipiden, eiwitten en cholesterol. De lipiden en cholesterol zijn van belang bij het handhaven van de celstructuur. Daarnaast hebben enkele speciale lipiden ook een boodschappersfunctie. Eiwitten kunnen ingedeeld worden in meerdere functionele groepen zoals: enzymen (de arbeiders in de cel), kinases (de leidinggevenden), ionkanalen (de portieren), hormoonreceptoren (torenwachters) enzovoort. Dankzij receptoren in de membranen kunnen cellen reageren op signalen (bv. hormonen) uit hun omgeving. Net als gealarmeerde wachters op een stadsmuur hun ontdekkingen doorgaven aan boodschappers die diverse mensen met sleutelfuncties waarschuwden, en uiteindelijk de response bewerkstelligden, induceren geactiveerde receptoren de afbraak van specifieke lipiden tot moleculaire boodschappers die de functie van kinases beïnvloeden. Het doel van het onderzoek in dit proefschrift is om de organisatie en dynamica te beschrijven van eiwit-lipide systemen die betrokken zijn bij de cellulaire communicatie. Centraal staan de fosfoinositiden PI, PIP en PIP_2. Zij zijn van vitaal belang in de regulatie van diverse enzymen die een rol spelen in de handhaving van de celstruktuur en in celgroei. Daarnaast vormen zij de voorlopers van twee zeer belangrijke cellulaire boodschappers: diacylglycerol (DG) en de inositol fosfaten. Eén van de belangrijkste biologische doelen van DG is proteïne kinase C (PKC), een eiwit dat een centrale rol vervult in de regulering van vele cellulaire processen. Inmiddels zijn 12 vormen van PKC geïdentificeerd. De meeste van deze PKC's zijn pas actief als zowel calcium en DG aanwezig zijn in de cel. De relatie tussen de fosfoinositiden, DG, calcium en PKC vormt dan ook een belangrijk thema in dit proefschrift.

Om eiwit-lipide interacties te karakteriseren is een techniek nodig die gebonden en niet gebonden eiwit en lipidecomponenten kan onderscheiden. Fluorescentiespectroscopie is hiervoor zeer geschikt. Het principe van deze techniek kan worden geïllustreerd met de wijzerplaten van sommige horloges die zijn bekleed met een laagje moleculen welke overdag licht absorberen en pas later in het donker weer uitzenden. Het licht uitgezonden door lipiden en eiwitten gelabeld met dergelijke moleculen geeft zeer unieke informatie over interacties tussen eiwit en lipiden. Tevens geeft de verandering van de oriëntatie van het uitgezonden licht (depolarisatie) van gelabelde lipiden en eiwitten zeer gedetailleerde informatie over hun dynamica en bewegingsvrijheid. Voordat fluorescentie methoden succesvol toegepast kunnen worden in eiwit lipide systemen moeten de fluorescentie eigenschappen van

eiwitten en fluorescent gelabelde lipiden worden gekarakteriseerd in eenvoudige systemen. Daarom is in hoofdstuk 2 een model studie uitgevoerd naar de associatie van lysozyme aan negatief geladen membranen. Tevens is in dit hoofdstuk een eenvoudige methode ontwikkeld die de eiwit-lipide interacties nauwkeurig kan kwantificeren uit een reeks van fluorescentie-vervalcurven. In hoofdstuk 3 wordt de dynamica en bewegingsvrijheid van gelabelde lipiden in kunstmatige membranen gekarakteriseerd door de depolarisatie van het uitgezonden licht te bepalen. Aan de ene kant bleek het mogelijk de beweging van gelabelde lipiden zeer gedetailleerd te beschrijven in overeenstemming met studies die zijn uitgevoerd door anderen. Aan de andere kant waren de uitkomsten enigszins in tegenspraak met de verwachte resultaten.

Interactie van protein kinase C met boodschapper lipiden

Gebaseerd op de conclusies van hoofdstuk 3, is de theoretische interpretatie van fluorescentie depolarisatie experimenten in hoofdstuk 4 vereenvoudigd. In deze studie werden de bewegingskarakteristieken van gelabeld DG in aan- en afwezigheid van PKC bepaald. Het bleek dat DG in kunstmatige membranen een grotere bewegingsvrijheid heeft dan PC. Dit duidt erop dat DG de membraan structuur verstoord. Deze verstoring kan de incorporatie van PKC in de membraan die nodig is voor activatie van het eiwit, vergemakkelijken.

Vele onderzoeksgroepen hebben waargenomen dat de binding van PKC aan (negatief geladen) membranen afhankelijk is van calcium. In het onderzoek van dit proefschrift blijkt PKC echter onafhankelijk van calcium te associëren met negatief geladen membranen. Dit resultaat blijkt uit drie verschillende en onafhankelijke observaties:
1) PKC reduceert de rotatiesnelheid van kleine negatief geladen lipide aggregaten (hoofdstuk 4).
2) De fluorescentie van PKC wordt uitgedoofd door negatief geladen membranen met gelabelde lipiden (hoofdstuk 5).
3) PKC heeft een effect op de botsingsfrequentie van gelabelde negatief geladen lipiden in membranen (hoofdstuk 5).
Het membraan-gebonden PKC bindt aan DG wanneer calcium wordt toegevoegd (Hoofdstukken 4, 5 en 6). Deze binding leidt tot een afname van de bewegingsvrijheid en dynamica van DG (hoofdstukken 4 en 5). De affiniteit van PKC voor dit boodschapper lipide is erg hoog in tegenstelling tot die voor andere gelabelde lipiden (PC, PS en PI) (hoofdstukken 4, 5 en 6) waardoor de regulerings-plaats van PKC specifiek DG binden ook al komt dit boodschapper lipide in lage concentraties voor in de membraan. Net als de legerleiding in een stad ook niet geactiveerd mag worden door iedere willekeurige burger is specificiteit in de regulering van PKC van groot belang. Het blijkt echter dat de fosfoinositiden PIP en PIP_2 deels dezelfde bindingseigenschappen als DG hebben. Zij binden met hoge affiniteit aan PKC en activiteitsmetingen van PKC laten zien dat PIP_2 net als DG in staat is dit eiwit te activeren (hoofdstuk 6). Deze resultaten duiden erop dat PIP_2 de juiste eigenschappen heeft om als boodschappermolecuul voor PKC te fungeren. Dit lijkt problematisch omdat DG ontstaat uit de afbraak van PIP_2. Als nu PIP_2 zelf ook PKC activeert is DG eigenlijk overbodig. Dit is echter niet het geval als er specifieke situaties

voorkomen in de cel waarin of PIP$_2$ of DG als activator optreden. Hierover wordt gespeculeerd in hoofdstuk 6 en in de engelstalige samenvatting.

De verdeling van fosfoinositiden in membranen

Zoals de loopsnelheid en de verdeling van boodschappers op een stadsmuur van belang is voor de effectiviteit waarmee een stad kan reageren op de waarnemingen van wachters, is de beweeglijkheid en verdeling van de fosfoinositiden in membranen van groot belang voor een effectieve cellulaire respons. In de hoofdstukken 7 en 8 zijn deze eigenschappen bepaald in membranen die het transmembraaneiwit Band 3 bevatten. Dit Band 3 eiwit heeft een portiersfunctie in de celmembraan van rode bloedcellen.

In Hoofdstuk 7 wordt de effectiviteit van uitdoving van Band 3 fluorescentie door de gelabelde fosfoinositiden bepaald. Het blijkt dat gelabeld PIP$_2$ en PIP de Band 3 fluorescentie veel effectiever uitdoven dan gelabeld PI en PC. Dit duidt erop dat deze sterk gefosforyleerde lipiden zich gemiddeld dichter bij Band 3 bevinden dan PI en PC. Met enige aannamen is de ruimtelijke distributie van de verschillende fosfolipiden ten opzichte van Band 3 bepaald uit de fluorescentievervalcurven van Band 3.

Aansluitend wordt in hoofdstuk 8 de verdeling en dynamica van pyreen gelabelde fosfoinositiden gekarakteriseerd in membranen met en zonder Band 3. Deze experimenten leverden een maat voor de onderlinge repulsie van de geladen fosfoinositiden in membranen en een bindingsconstante van Band 3 voor de verschillende fosfoinositiden. De lipide-lipide repulsie en interacties met Band 3 resulteren in een heterogene distributie van de fosfoinositiden in de membranen. De heterogene verdeling van fosfoinositiden kan hun beschikbaarheid voor de productie van DG en voor fosfoinositide afhankelijke enzymen in belangrijke mate verlagen.

Curriculum vitae

Everard Herman Warner Pap is geboren op 14 mei 1963 te Amersfoort. In 1979 behaalde hij het diploma MAVO (Andreas Mavo te Amersfoort) en in 1981 het diploma HAVO (Farel College te Amersfoort). In datzelfde jaar begon hij aan de nieuwe lerarenopleiding te Utrecht met de vakken Biologie en Natuurkunde. Deze tweedegraads opleiding werd in 1985 met gunstig gevolg afgesloten. In 1986 begon hij met de studie Biologie aan de Landbouw-universiteit te Wageningen. Afstudeervakken werden gevolgd bij de vakgroepen Biochemie (Prof. C. Veeger; toepassing van fluorescentie technieken voor bestudering van protein kinase C- lipide interactie) en Moleculaire Biologie (Prof. A. van Kammen, constructie van een genenkaart van chromosoom 6 van tomaat). De stageperiode is doorgebracht aan het Centrum voor Biomembranen en Lipide Enzymologie te Utrecht (Prof. K.W.A. Wirtz, synthese van fluorescente fosfoinositiden). In 1989 studeerde hij af.

Van december 1989 tot december 1993 is hij als OIO verbonden geweest aan de vakgroep Biochemie van de Landbouwuniversiteit te Wageningen onder leiding van Dr. A.J.W.G. Visser. Zijn onderzoek werd gesubsidieerd door de Stichting voor Biofysica (NWO) en heeft geleid tot de inhoud van dit proefschrift.

Vanaf december 1993 werkt hij aan een onderzoeksproject dat tot doel heeft de functie van proteïne kinase C in de differentiatie van embryonale carcinoma cellen vast te stellen. Dit onderzoek wordt gesubsidieerd door de Stichting Koningin Wilhelmina Fonds en wordt uitgevoerd bij de Vakgroep Biochemie van de Landbouwuniversiteit te Wageningen.

Publications:

Quantitation of the interaction of protein kinase C with diacylglycerol and phosphoinositides by time resolved detection of resonance energy transfer. E.H.W. Pap, P.I.H. Bastiaens, J.W. Borst, P.A.W. van den Berg, A. van Hoek, G.T. Snoek, K.W.A. Wirtz and A.J.W.G. Visser (1993) *Biochemistry* 32, 13310-13317

Fluorescence dynamics of diphenyl-1,3,5-hexatriene-labeled phospholipids in bilayer membranes. E.H.W. Pap, J.J. ter Horst, A.van Hoek and A.J.W.G. Visser (1994) *Biophys. Chem.* 48, 337-351

Reorientational properties of fluorescent analogues of the protein kinase C cofactors diacylglycerol and phorbol ester in vesicles and mixed micelles. E.H.W. Pap, A. van Hoek, M. Ketelaars, J.W. Borst and A.J.W.G. Visser (1994) *J. Biol. Chem.*, submitted.

Parallel probing of lipid and protein properties results in a refined description of protein kinase-C and lipid cofactors interactions. E.H.W. Pap, P.A.W. van de Berg, J.W. Borst and A.J.W.G. Visser (1994) *J. Biol. Chem.*, submitted.

Fluoresence detection of protein kinase C - lipid cofactor interaction. E.H.W. Pap, P.I.H. Bastiaens, J.W. Borst, A. van Hoek and A.J.W.G. Visser (1994) *J. Cell. Biochem.* QZ 310, 91.

The interaction of pyrene labeled diacylglycerol with protein kinase C in mixed micelles. P.I.H. Bastiaens, E.H.W. Pap, J.W. Borst, A. van Hoek, T. Kulinski, R. Rigler, A.J.W.G. Visser (1993) *Biophys. Chemi.* 48, 183-191

Steady-state fluorescence studies on lipase-vesicle interactions. E.W.J. Mosmuller, E.H.W. Pap, A.J.W.G. Visser and J.F.J. Engbersen, (1994) *Biochim. Biophys. Acta* 1189, 45-51

Integration of the classical and molecular linkage maps of tomato chromosome 6. R. Weide, M.F. van Wordragen, R.K. Lankhorst, R. Verkerk, C. Hanhart, T. Liharska, E.H.W. Pap, P. Stam, P. Zabel and M. Koornneef, (1993) *Genetics 135*, 1175 - 1186

Erythrocyte band 3 protein strongly interacts with phosphoinositides A. Hanicak, D.A. Maretzki, B. Reimann, E.H.W. Pap, A.J.W.G. Visser, K.W.A. Wirtz and D. Schubert (1994) *FEBS Lett.* 348 169-172

Band 3 - phosphoinositide interactions revealed by fluorescence spectroscopy. A. Hanicak, E.H.W. Pap, A. van Hoek, D. Schubert & A.J.W.G. Visser (1994) *Biochemistry*, Submitted.

Quantitative analysis of lipid-lipid and lipid-protein interactions in membranes by use of pyrene labelled phosphoinositides E.H.W. Pap, A. Hanicak, A. van Hoek, K.W.A. Wirtz and A.J.W.G. Visser (1994) *Biochemistry*, submitted.

Protein kinase C modulates the motional properties of its lipid cofactor DPH-diacylglycerol.
E.H.W. Pap, J.W. Borst, M. Ketelaars, A. van Hoek and A.J.W.G. Visser. (1994) *Proc. SPIE*, in press.